INSTITUTE OF CELL AND MOLECULAR BIOSCIENCE NEWCASTLE UNIVERSITY

THE RESPONSE OF THE MITOCHONDRIAL PROTEOME AND ROS PRODUCTION TO AGEING AND DIETARY RESTRICTION

Doctor of Philosophy

Amy Bell

2/1/2015

ABSTRACT

The free radical theory of ageing proposes ageing is the result of macromolecules, damaged by free radicals, accumulating in cells over time. Mitochondria are critical to this theory as they are the primary source of the free radical superoxide. This thesis aims to understand the effect of age and dietary restriction (DR) with regard to mitochondrial protein abundance and superoxide generation.

Superoxide production and protein composition was studied from multiple ages in isolated mitochondria from both ad libitum (AL) and DR mice. Superoxide production was assessed by measuring hydrogen peroxide release from multiple electron transport chain (ETC) sites. Mass spectrometry was used to determine the mitochondrial protein composition from mouse liver tissue.

Older mice have increased hydrogen peroxide release from ETC complexes I and III. DR has decreased complex I hydrogen peroxide release in brain, skeletal muscle and liver mitochondria analysed at 15 and 24 months old. DR doesn't prevent but delays the age associated hydrogen peroxide release. Hydrogen peroxide release at the same survival point is not significantly different between AL and DR mice.

The liver mitochondrial proteome is affected by age and DR. Fatty acid metabolism protein abundance increases with age whereas amino acid metabolism protein abundance decreased. Superoxide clearance protein abundance is increased in older and DR liver mitochondria. Catalase had increased abundance in DR mitochondria at 15 and 24 months than at 3 or 36 months old.

In conclusion hydrogen peroxide release, superoxide clearance protein abundance and fatty acid metabolism protein abundance are increased with ageing. The age associated increase in hydrogen peroxide release is delayed in DR mitochondria possibly due to increased abundance of catalase.

ACKNOWLEGEMENTS

I would like to express my appreciation and thanks to my supervisors, Professor Thomas von Zglinicki, Dr Satomi Miwa and Dr Achim Treumann. You have all been extremely understanding during this period. I am so grateful for your support and patience in helping me produce and complete this thesis. I would like to single Dr Satomi Miwa out as a great advisor and teacher. Her help in dissections of tissue and mitochondrial isolation was invaluable. The guidance given by all my collegues at both Newcastle University and NEPAF Proteome Analysis Facility was greatly appreciated. I will only mention a few by name, Glyn Nelson, James Wordsworth, Karen Baty and Sarah Smith, I am very grateful for the help and training you gave me.

The huge volume of mice from which tissue was collected required a large team. Adele Kitching and the other technicians (Liz and Julie) were invaluable in this process. Including the entire team involved in tissue collection: Kerry Cameron; Satomi Miwa; Amy Johnson; Rafal Czapiewski; Laura Wiley; Hannah Gautrey; Claire Kolenda; Craig Parker; Carmen Martin-Ruiz; Clara Correia Melo; Joanna Gorniak; Sabine Langie; Sofia Lisanti.

The mass spectrometry data could not have been obtained without Dougie Lamont, Kenny Beattie and all the staff at FingerPrints Proteomics in the University of Dundee. Thanks for answering all my questions and the quick turnaround of my measurements and data.

I would finally like to thank my family for their continued love and support through this last few years I could not have got to this point without them.

TABLE OF CONTENTS

LIST OF FIGURES

LIST OF EQUATIONS

LIST OF TABLES

LIST OF ABBREVIATIONS

ETC	Electron transport chain
AL	Ad Libitum feeding
DR	Dietary restricted feeding (40%)
PMAL/PMDR	Post-prandial feeding under ad libitum or dietary restricted nutrition
UCP	Uncoupling proteins
BSA	Bovine serum albumin
PM	Pyruvate Malate
Succ	Succinate
Rot	Rotenone
AA	Antimycin A
ATP	Adenosine Triphosphate
Atp A5	Atpenin A5
H_2O_2	Hydrogen peroxide

Myx	Myxathiozol
TERT	Telomerase reverse transcriptase
WT	Wild type (TERT-/- controls)
ROS	Reactive Oxygen Species
mtDNA	Mitochondrial DNA
HRP	Horseradish Peroxidase

CHAPTER 1: INTRODUCTION

1.1. THE FREE RADICAL THEORY OF AGEING

The mechanism by which ageing occurs is still undetermined. Multiple factors have been shown to change with age. Increased age has been associated with impaired protein turnover (Ryazanov and Nefsky, 2002), shortened telomeres (Kim Sh *et al.*, 2002) and increased reactive oxygen species (ROS) levels (Lass *et al.*, 1998).

The free radical theory of ageing was proposed over 60 years ago and remains a popular theory. This theory proposes the constant generation of reactive oxygen species (ROS) and free radicals continually causes molecular damage. The accumulation of molecular damage over time, causing detrimental effects on the function of the cells and therefore the organism as a whole (Harman, 1956). ROS have been linked to carcinogenesis, ageing and other age-related disorders (Andersen, 2004; Trachootham *et al.*, 2009; Shukla *et al.*, 2011)(Haigis and Yankner, 2010)(Mates *et al.*, 1999)

There are multiple sites of ROS production in the cell. (Quinlan *et al.*, 2012)Gross et al showed the endoplasmic reticulum contained enzymes which produce ROS (Gross *et al.*, 2006). The cytochrome P450 catalytic cycle produces ROS, even without substrate (Gonzalez, 2005)(Mari and Cederbaum, 2000). Peroxisomes are an important intracellular source of ROS production as they are the site of beta fatty acid oxidation and D-amino acid oxidation (Boveris *et al.*, 1972; Mueller *et al.*, 2002). NADPH oxidases in the plasma membrane are well documented to be another cellular source of ROS (Lambeth, 2004; Dikalov, 2011; Coso *et al.*, 2012)(Kowaltowski *et al.*, 2009)

The free radical theory of ageing was refined to the mitochondrial theory of ageing in 1972. Mitochondria produce ROS from three complexes; CI, CII and CIII as well as monoamine oxidase and α-ketoglutarate have been shown to produce superoxide (Starkov *et al.*, 2004; Tretter and Adam-Vizi, 2005; Starkov, 2008; Quinlan *et al.*, 2012). Mitochondria are a major source of ROS in the cell with the superoxide produced a by-product of ATP generation when producing energy. The theory suggests that the role mitochondria play in ageing is critical as they are the primary sites of ROS production (Harman, 1956; Harman, 1972).

1.2. STRUCTURE AND FUNCTION OF THE MITOCHONDRIA

Mitochondrial have an unusual structure comprising two membranes, an outer membrane and folded inner membrane which produces cristae. These membranes create two internal compartments, the intermembrane space and the matrix (figure 1.1).

1.2.1. DIFFERENT POPULATIONS OF MITOCHONDRIA EXIST WITHIN TISSUES

Mitochondrial populations from different tissues don't respond in the same way. Tahara et al (2009) show differences in mitochondrial function in mitochondria from different tissues. The oxygen consumption rates, respiration control ratios and hydrogen peroxide release rates are shown to be different between mitochondria isolated from brain, liver, heart, kidney and muscle tissues (Tahara *et al.*, 2009).

The murine brain comprises different cell type and regions. Studying the different regions of the brain has shown different oxygen consumption rates seen in the cortex, straitum and the ventral midbrain (Subramaniam *et al.*, 2014). Liver and muscle mitochondria have been shown to have subpopulations within individual cells (Lanni *et al.*, 1996; Kuznetsov *et al.*, 2006; Hagopian *et al.*, 2013). Liver mitochondria have been divided into three sub-populations based on differential centrifugation force. The heavier mitochondria are larger and have a higher respiration rate than those found in the lighter sub-populations. These populations are possibly a reflection of mitochondrial maturation with the heavier population containing the older and damaged mitochondria (Lanni *et al.*, 1996)(Hagopian *et al.*, 2013).

1.2.2. MITOCHONDRIA HAVE MULTIPLE CELLULAR FUNCTIONS

Mitochondria are essential in energy production for the cell. The complete metabolism of sugars, fatty acids and amino acids all occur within the mitochondria. Mitochondria contain the krebs cycle and the ETC which allow the cell to extract 15 times the energy of glycolysis alone. (McBride *et al.*, 2006).

Multiple signalling pathways are linked to mitochondria. The mitochondria are a primary site of metabolism. The regulation of metabolic processes can occur by

phosphatases, calcium signalling and the continual fission fusion events between mitochondria themselves (Chen and Chan, 2005; Hill and Van Remmen, 2014). The cell cycle and apoptosis have signalling cascades which are affected by signalling from the mitochondria (Alberts *et al.*, 2008).

Mitochondria contain their own circular DNA. A mitochondrion can have multiple copies of DNA within its matrix. Transcription and translation of the mitochondrial DNA occurs within the mitochondria. Mutations within the mitochondrial DNA have been linked to multiple diseases (Alberts *et al.*, 2008).

1.2.3. CHANGES IN CELLULAR ENVIRONMENT HAVE AFFECTS ON THE MITOCHONDRIA

Mitochondrial biogenesis is affected by calcium levels, nitric oxide, oxidative stress, energy requirements and caloric restriction. The differences in the amount of mitochondria can alter the abundance of mitochondrial proteins (Kowaltowski *et al.*, 2009). Calcium content effects mitochondrial ROS release in both directions. The uptake of calcium can reduce ROS production by increasing electron transport due to a lower electron potential. Calcium can however change the citric acid cycle activity, and the formation of NADH increasing ROS (Kowaltowski *et al.*, 2009). Exercise has been shown to increase heat shock protein abundance in muscle cells in mice (McArdle *et al.*, 2001). Heat shock proteins protect against oxidative stress by aiding the localisation of newly synthesised proteins (McArdle *et al.*, 2002).

1.3. REACTIVE OXYGEN SPECIES PRODUCTION IN THE ELECTRON TRANSPORT CHAIN

The electron transport chain (ETC) is the final stage of aerobic respiration and the major site of superoxide production (Vendelbo and Nair, 2011). Figure 1-1 and figure 1-2 shows there are four complexes in the ETC which pump protons into the inner membrane space. Superoxide is the primary product produced at complex I, II (Quinlan *et al.*, 2012) and III in the ETC (St-Pierre *et al.*, 2002; Barja, 2004; Miwa and Brand, 2005). Complex I produced superoxide is released into the matrix, whereas the superoxide produced from complex III is released into the matrix as well as the inter membrane space (St-Pierre *et al.*, 2002; Miwa and Brand, 2003).

Other mechanisms can affect the mitochondria and superoxide production. Fatty acids and uncoupling proteins (UCPs) can alter membrane potential which has been shown to have an effect of ROS production in drosophila (Miwa and Brand, 2003). Membrane potential is affected by uncoupling proteins which increase the proton leak and reduce the protomotive force, and the membrane potential. These uncoupling proteins can be activated by fatty acids (Beck *et al.*, 2007). The production of superoxide from complex I by reverse electron flow is greatly reduced following a small decrease in membrane potential due to mild uncoupling (Miwa and Brand, 2003). Therefore the amount and role of uncoupling proteins could have large effects on the production of ROS and therefore oxidative damage.

The driving of electron transport in the ETC begins with the addition of a substrate which can enter at either complex I or II. Complex I superoxide production can occur from two locations within the complex depending on the substrate present (Treberg *et al.*, 2011). Pyruvate Malate (PM), a complex I linked substrate, produces NADH which is converted to NAD^+ by complex I (Murphy, 2009; Costa *et al.*, 2011). The reaction results in forward electron flow through the ETC producing small amounts of superoxide. The production of superoxide is increased with the addition of rotenone, a complex I inhibitor, which blocks the transfer of electrons causing a 'traffic jam' of electrons. These electrons leak and react with oxygen to produce superoxide which is released into the mitochondrial matrix (figure 1-2A).

Succinate is a complex II linked substrate, which produces $FADH_2$ and results in both forward and reverse flow of electrons in the ETC (Murphy, 2009; Costa *et al.*, 2011). The superoxide production in the presence of a complex II linked substrate is high and originates from complex I via reverse electron flow (Murphy, 2009; Tahara *et al.*, 2009) (figure 1-1B).

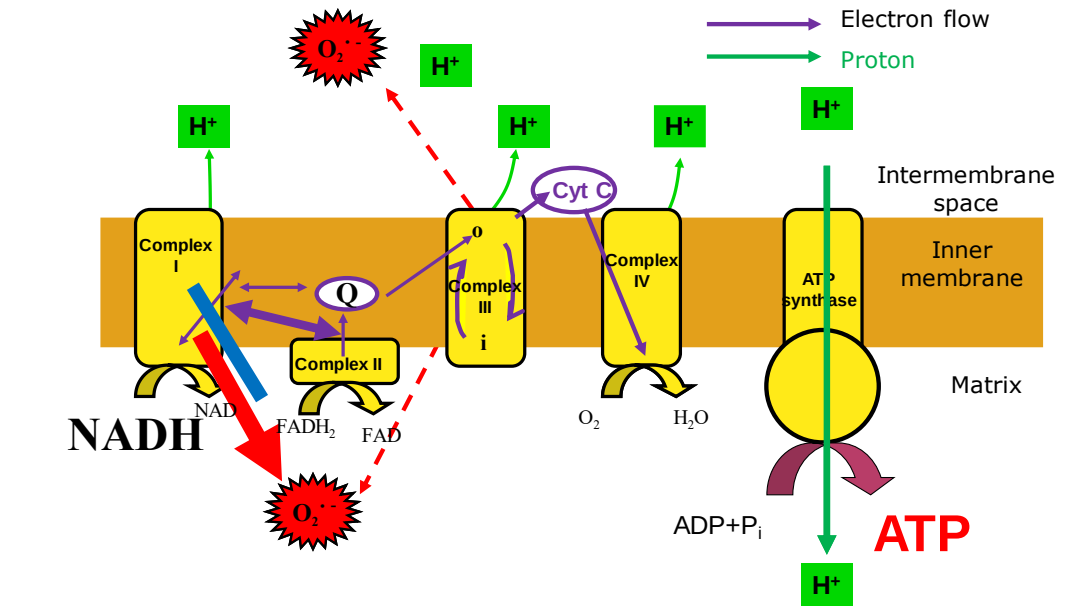

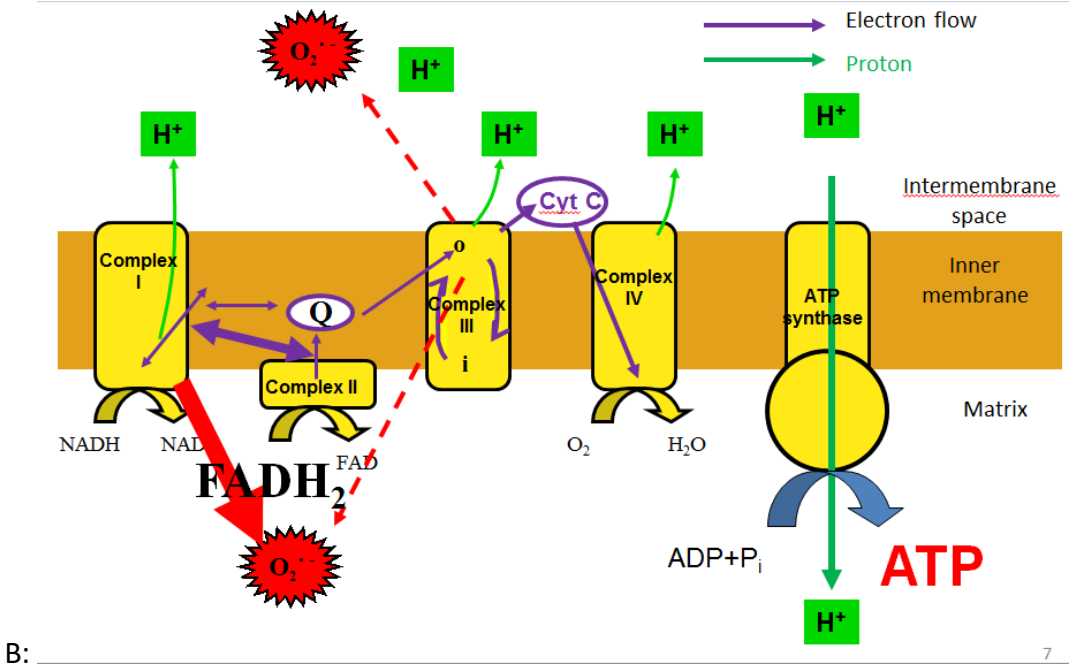

Figure 1-1: Superoxide production from complex I can occur in the presence of both a complex I and a complex II linked substrate. The panels show a simplified diagram of the five complexes of the ETC. In panel A there is a complex I linked substrate present, and a complex I blocker (rotenone). The complex I blockage by rotenone in the presence of forward flowing electrons from the complex I linked substrate causes maximum complex I superoxide production. Panel B has a complex II linked substrate present. Complex II linked substrates produce reverse electron flow causing superoxide release from complex I. Superoxide is released from complex I into the matrix of the mitochondria (Tahara *et al.*, 2009).

Succinate is a complex II linked substrate. In the presence of a complex II linked substrate electrons in the ETC can move in two directions. The electrons can move backwards from complex II to complex I causing reverse flow of electrons and complex I superoxide production. In the presence of succinate and rotenone the electron flow is forward through the ETC. The remaining superoxide production after rotenone block comes from complex III; production can be increased to maximum levels with the addition of Antimycin A (AA), a complex III inhibitor of the o site (Miwa and Brand, 2005; Murphy, 2009). Complex III superoxide is released to both sides of the inner mitochondrial membrane (Muller *et al.*, 2004) (figure 1-2A).

Complex II produces superoxide from the flavin site. Production is higher in complex I and II (St-Pierre *et al.*, 2002). Measuring complex II production requires low concentrations of substrate compared to those added to measure complex I and III (Quinlan *et al.*, 2012) (figure 1-2B).

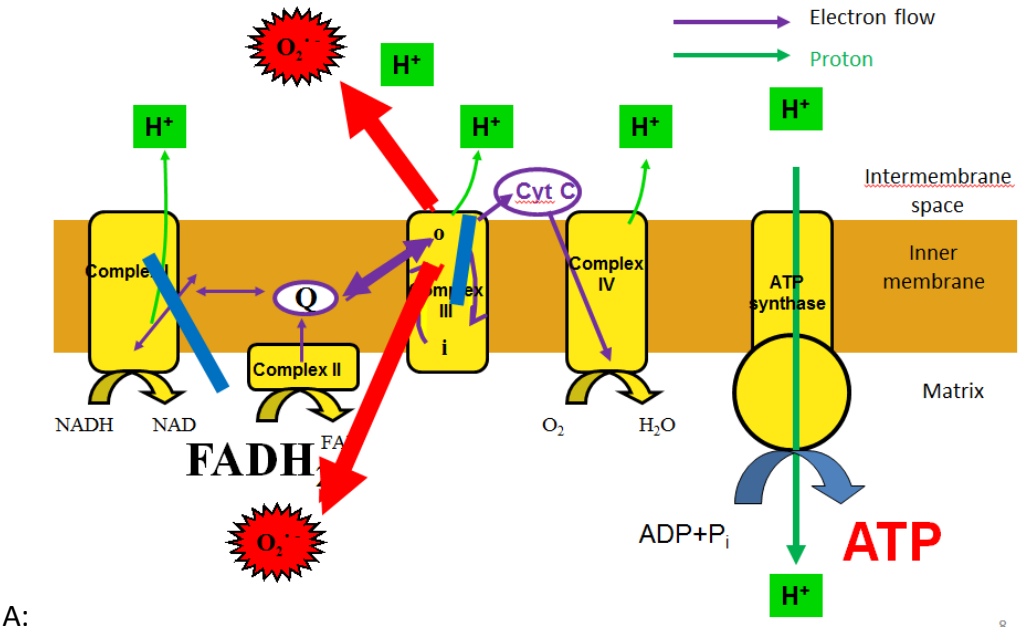

A:

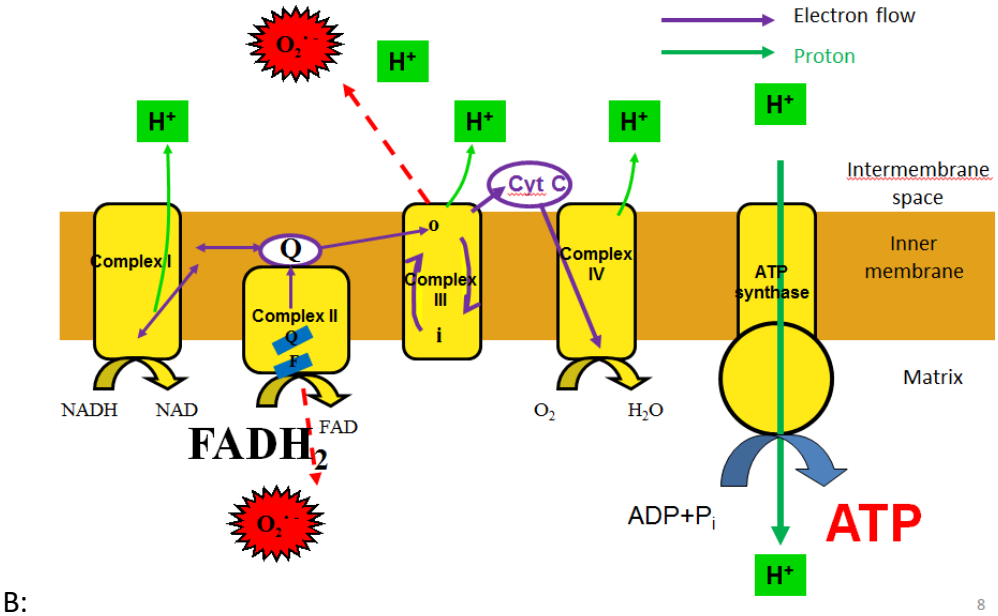

B:

Figure 1-2: In the presence of complex II linked substrates and rotenone complex II and III release superoxide. Two sites of superoxide production are outlined in the above diagrams. A complex II linked substrate and rotenone are present in both panels. In panel A antimycin A blocks complex II producing maximum production of superoxide from complex III. Complex III releases superoxide into the matrix and intermembrane space. Panel B shows the superoxide release from complex II. This can occur in two sites. Site F is the dominant location of superoxide production. Atpenin A5 blocks site$_Q$ and malonate blocks site$_F$ (Tahara *et al.*, 2009).

1.3.1. METHODS AVAILABLE TO MEASURE REACTIVE OXYGEN SPECIES

There are many methods used for the detection of ROS. Reactive oxygen species are normally superoxide, hydrogen peroxide or peroxynitrile. These are transient in nature lasting less than a few seconds and antioxidant mechanisms are well developed to remove them. The short lifespan result in very low levels of steady-state ROS in the cell (Dikalov and Harrison, 2014). Spin traps are one of the earliest methods made available to measure superoxide, these covalently bind the radical to detect it (Finkelstein *et al.*, 1980). These probes are oxidised without binding but have a slow kinetic rate which is less likely to compete effectively with SOD. Spin probes are newer method to detect superoxide which have a quicker kinetic rate and will compete with SOD more effectively (Dikalov *et al.*, 1997; Dikalov and Harrison, 2014).

ROS detection methods were reviewed in Dikalov and Harrison (2014). Chemiluminescent probes including lucigenin, luminol, MCLA and coelenterazine can be used to detect superoxide however none of these are specific to the mitochondria. Dihydroethidium and mitoSOX fluorescent probes have been shown to detect superoxide in the cell and mitochondria respectively. Other fluorescent probes detect hydrogen peroxide which is more stable. Amplex red, dichlorodihydrofluorescein diacetate and other probe which are boronate based can be used to detect hydrogen peroxide (Dikalov and Harrison, 2014). This thesis uses amplex red to detect hydrogen peroxide changes in isolated mitochondria.

Superoxide reacts with superoxide dismutase to produce hydrogen peroxide (McCord and Fridovich, 1969a; McCord and Fridovich, 1969b). Hydrogen peroxide release can be measured to infer superoxide production. Hydrogen peroxide release from isolated mitochondria can be measured effectively by Amplex red (10-acetyl-3,7-dihydroxyphenoxazine). Amplex red reacts in the presence of horseradish peroxidase with hydrogen peroxide in a 1:1 stoichiometry to produce resorufin (Zhou *et al.*, 1997). Resorufin has absorption and fluorescence emission maxima of approximately 571 nm and 585 nm, respectively (Zhou *et al.*, 1997). Monitoring the accumulation of fluorescence resorufin product we can determine the rate of hydrogen peroxide (H_2O_2) release under different conditions.

There are limitations of amplex red as a method of superoxide detection. Superoxide is not directly detected. Superoxide is only detected after conversion to hydrogen peroxide outside of the mitochondria as amplex red cannot cross the mitochondrial membrane (Zhou *et al.*, 1997). Endogenous SOD present within the mitochondrial matrix ensures the conversion of superoxide to H_2O_2 which can then cross the mitochondrial membranes (Galley, 2011).

Mitochondria contain antioxidants. The antioxidants including catalase and glutathione peroxidase convert hydrogen peroxide to water (Beckman and Ames, 1998). Hydrogen peroxide could be cleared by these antioxidants and would not be measured. Hydrogen peroxide would also not be detected is it did not cross the membrane but stayed in the matrix of the mitochondria (Zhou *et al.*, 1997).

1.3.2. REACTIVE OXYGEN SPECIES HAVE BEEN SHOWN TO INCREASE WITH AGE. DIETARY RESTRICTION EXTENDS LIFESPAN AND DECREASES REACTIVE OXYGEN SPECIES

Dietary Restriction (DR) has been shown to increase lifespan, in mammalian models including mice and monkeys (Lass *et al.*, 1998; Colman *et al.*, 2009; Ash and Merry, 2011). A decreased body weight and organ mass in mice has been shown with DR (Drew and Leeuwenburgh, 2003; Drew *et al.*, 2003). ROS production has been shown to increase with age (Lass *et al.*, 1998). Many groups show reduced ROS production in DR mice tissues (Lass *et al.*, 1998; Sanz *et al.*, 2004; Ash and Merry, 2011) This reduction in the rate of oxidative stress has been linked to a reduction in oxidative damage e.g. reduced mtDNA damage, although direct manipulation of oxidative stress has resulted in conflicting results. This has been the mechanism hypothesised as the reason that animals live longer under DR. ROS has been shown to be sensitive to membrane potential (Hansford *et al.*, 1997). Ash and Merry suggested that a reduced membrane potential due to an increased proton leak across the mitochondrial membrane could be the cause of reduced ROS in DR rats (Ash and Merry, 2011). This is consistent which the uncoupling to survive hypothesis proposed by Brand (Brand, 2000). The uncoupling to survive theory has been supported in separate cases. Mitochondria isolated from skeletal muscle the longest living mice had increased

uncoupling and ROS reduction (Harper *et al.*, 2004; Speakman *et al.*, 2004), suggesting an importance of uncoupling in reducing ROS.

1.3.3. RAPAMYCIN TREATMENT AS A DIETARY RESTRICTION MIMETIC

Rapamycin feeding has been shown to increase lifespan under both long-term treatment (Miller *et al.*, 2011) and late-onset treatment (Harrison *et al.*, 2009). Rapamycin inhibits mTOR part of a nutrient sensing pathway activated by growth factor stimuli (Ma and Blenis, 2009). mTORC1 and mTORC2 are both complexes formed by mTOR. mTORC1 appears to be more sensitive to rapamycin. The activation of mTOR has been shown to increase protein synthesis and cell growth while causing a reduction in autophagy (Thomson *et al.*, 2009). The inhibition of the kinase decreases lipid synthesis and promotes the inhibition of growth factors (Clohessy *et al.*, 2012; Fok *et al.*, 2012).

It is thought that rapamycin treatment could be a DR mimetic as both increase lifespan (Kaeberlein and Kennedy, 2009). It has been shown that both rapamycin and DR act through the same mammalian target (Fok *et al.*, 2012). Rapamycin treatment and dietary restriction both cause a decrease in phosphorylation of the ribosomal protein S6 kinase is decreased in both. Reactive oxygen species are shown to decrease in dietary restriction and rapamycin (Ash and Merry, 2011; Shin *et al.*, 2011). There are indications that not all characteristics between rapamycin treatment and dietary restriction are the same. Insulin sensitivity is higher in DR mice a response which is not replicated in rapamycin treated mice (Fok *et al.*, 2012). Fok et al look at differences between mRNA levels of cell cycle proteins none of these are changed, in the same direction, significantly from AL expression (Fok *et al.*, 2012). The release of hydrogen peroxide measured from specific ETC sites would be mirrored between DR and rapamycin treatment if they responded via the same pathways.

1.3.4. TELOMERASE AND MITOCHONDRIAL REACTIVE OXYGEN SPECIES PRODUCTION

Telomeres are tandem repeats at the end of chromosomes, which play an important role in protecting the chromosome (Suh *et al.*, 2002). Normal cell division makes copies of the chromosomes and results in shorter telomeres (Harley *et al.*, 1990). Telomerase

elongates the telomeres to prevent chromosomal instabilities in dividing cells (Haendeler *et al.*, 2003; Haendeler *et al.*, 2009). The lagging strand is replicated during chromosomal replication by initiation using a primer. The final step in chromosomal replication requires removal of the primers. Ligase fills the gaps left by the primer, a process which can't be completed where final primer is attached resulting in shortening the telomeres (Suh *et al.*, 2002).

Telomerase reverse transcriptase protein (TERT) is the catalytic unit of the telomerase enzyme. Telomerase can immortalize cells by maintaining telomere length resulting in continuing growth (Bodnar *et al.*, 1998). Senescence is triggered in response to DNA damage which includes uncapped telomeres. Telomeres are more susceptible to oxidative damage and the repair mechanisms aren't as efficient. Telomeres accumulate damage easily and increase the speed at which they shorten resulting in senescence {Ahmed, 2008 #999}(Passos *et al.*, 2007a; Passos *et al.*, 2007b).

The TERT sequence contains an N-terminal leader sequence which allows for the localisation of telomerase to the mitochondria (Santos *et al.*, 2004). The increase of hydrogen peroxide levels causes an export of telomerase from the nuclei and co-localisation between telomerase and mitochondria (Haendeler *et al.*, 2004; Ahmed *et al.*, 2008; Singhapol *et al.*, 2013). TERT has been shown to have a protective effect in response to oxidative stress in cultured cells. Stress results in the exclusion of telomerase from the nucleus in a reversible manner. Telomerase co-localises with the mitochondria when excluded from the nucleus (Ahmed *et al.*, 2008; Haendeler *et al.*, 2009; Spilsbury *et al.*, 2015). Telomerase expression protects the mitochondria when increased in MRC5 cells. This increased telomerase expression prevents mtDNA damage, reduces superoxide levels and increases antioxidant defences (Ahmed *et al.*, 2008; Haendeler *et al.*, 2009; Spilsbury *et al.*, 2015).

Telomerase is also involved in protecting the activity of the ETC complexes (Haendeler *et al.*, 2009).Mice with mutated TERT has lower respiration and lower complex I activity (Haendeler *et al.*, 2009). Complex I of the ETC is a primary source of superoxide production. Hydrogen peroxide release is measured from specific sites of the electron transport chain will allow us to discover the complexes involved in reduced superoxide.

1.4. THE IMPORTANCE OF QUANTITATIVE PROTEOMICS IN RESEARCH

Proteins are the basis for all cellular processes. Proteins have many functions as enzymes, transporters, signal transducers and structure forming molecules. The versatility in their structure, folding and modification results in a complex and dynamic network of functional proteins. This makes them a desirable target in biological studies to monitor changes in abundance of proteins and modifications within them (Berg *et al.*, 2007).

High-throughput protein identification using automated techniques gave us the ability to study the proteome from an organelle, cell, or tissue. These large scale studies allow for the discovery of multiple pathway changes which interact with each other. High-throughput techniques gave remove the constraints of focusing on a limited number of targets due to elaborate and time-consuming techniques like chromatography and electrophoresis (Reinders and Sickmann, 2009).

1.4.1. DIFFERENT METHODS USED TO QUANTIFY PROTEINS

Quantitative proteomics requires a label on the individual proteins so a comparison can be made to determine changes between samples. Mass spectrometry samples can be labelled using different methods. TMT labelling tags each sample's individual peptides with differently weighted labels. Multiple samples are directly analysed in parallel and separated out by their different tagging with computer analysis after measuring (Okuda *et al.*, 2002; Thompson *et al.*, 2003).

Stable Isotope Labelling with Amino Acids in Cell Culture (SILAC) was developed in the centre for Experimental Bioinformatics. This method requires metabolic labelling of the proteins, prior to digestion of the protein for peptides. This is a different method to TMT labelling which labels the peptides prior to measurements, but similarly directly compares samples in one parallel measurement (Steen and Mann, 2004). Spike-in SILAC method has only one labelled sample, a standard, to which all others are compared. This standard is always the same the protein change in each sample is determined in relation to the standard and then each other (Kim *et al.*, 2002; Geiger *et al.*, 2011).

1.5. MITOCHONDRIAL PROTEOME IS CHANGED WITH AGE AND DIETARY RESTRICTION

ETC complex activity was measured in the gastrocnemus mouse muscle at 10 and 20 months of age. The activity of the four complexes was affected by age and dietary restriction. Complex I, III and IV activity is decreased with age and in 10 month DR. The activity of complexes IV in DR mice became higher than AL at 20 months (Desai *et al.*, 1996).

Comparing three different tissue proteome changes in female rat liver had the highest number of altered proteins (Chang *et al.*, 2007). Bonferroni correction limited the number of significant changes in protein abundance with age and dietary restriction. There were 76% of significantly changed proteins increased with age. These increased proteins included an increase in amino acid metabolism, TCA and respiration proteins suggesting an increase in the need for energy with age. Additional proteins increased with age were chaperone proteins prohibitin and heat shock protein 60. The heat shock protein 60 has been shown to protect against oxidative damage (Chang *et al.*, 2007). However prohibitin stabilises unassembled complex I subunits which causes an oxidative stress increase (Miwa *et al.*, 2014). In the same study dietary restricted mitochondria have a decrease in complex I protein abundance (Miwa *et al.*, 2014).

Novel approaches are continually produced. Complexome profiling is a novel approach using blue native gels to separate large protein complexes (Huang *et al.*, 2009; Heide *et al.*, 2012; Wessels *et al.*, 2013; Miwa *et al.*, 2014; Giese *et al.*, 2015). The mitochondrial ETC complexes are the primary site of superoxide release. Heide et al confirm that these ETC complexes and flavoproteins cluster closely in 2D BN gel electrophoresis (Heide *et al.*, 2012). Complexome profiling allows for the discovery of proteins which are involved in assembling protein complexes. PhB, STOML2 are seen to co-migrate with 28S and 39S mitoribsomal complexes suggesting a role in complex I assembly (Wessels *et al.*, 2013).

Superoxide clearance proteins have been targeted as possible lifespan extension treatments. Overexpression of catalase targeted to the mitochondria caused lifespan extension and attenuation of hydrogen peroxide release in transgenic mice (Schriner *et al.*, 2005). Catalase is increased with age in the brain and dietary restriction has a

higher catalase activity than AL tissues (Sohal *et al.*, 1994). Overexpression of superoxide dismutase has also reduced ROS in cellular models (Lee *et al.*, 2009).

1.5.1. PROTEIN QUALITY CONTROL DETERIATES WITH AGE

Oxidative stress causes protein damage resulting in mitochondrial dysfunction. The maintenance systems which repair protein damage are critical to protect against the ageing process. The increase in free radicals and oxidative stress with age can create mitochondrial dysfunction. The increased oxidative stress increases the likelihood of protein damage leading to mitochondrial function changes (Hamon *et al.*, 2015).

Long-lived mice have a preference for correct ETC complex I matrix arm assembly. The assembly is more efficient in mice with longer lifespan. Correct assembly decreases reactive oxygen species (ROS). In ageing the assembly becomes compromised increasing ROS (Miwa *et al.*, 2014).

Liver protein replacement is reduced in 12 months dietary restriction. Price et al shows an increase in the half-life 85% of liver proteins. The replacement rate is decreased in proteins of the tricarboxylic acid, fatty acid and ATP synthesis metabolism pathways (Price *et al.*, 2012).

1.5.2. MITOCHONDRIAL PROTEIN DEGRADATION PATHWAYS.

Mitochondrial proteins are likely targets for oxidative damage due to the ROS produced by the ETC into the matrix. It is considered that the mitochondrial proteins are degraded internally. This degradation produces free amino acids available for transcription of proteins encoded for in the mitochondrial DNA. Mitochondrial proteins which are moderately damaged can be degraded via the Lon protease pathway {Johnson, 2013 #1230}. Lon protease has been shown to degrade proteins damaged by oxidative stress {Bota, 2002 #1231}. Knockdown of the Lon protease has also been shown to protect against senescence and tumorigenesis {Quiros, 2014 #1233}.

Severe oxidative damage to mitochondrial proteins can cause a decrease in the mitochondrial membrane potential. If the membrane potential of the mitochondria decreases fission of the mitochondria can occur and target the protein for the

lysosome and degradation {Johnson, 2013 #1230}{Twig, 2008 #1234}. Twig et al determined fission events were important for mitophagy. Fission would produce mitochondria which were depolarised and unable to undergo fusion therefore they would be targeted for mitophagy {Twig, 2008 #1235}. The degradation of damaged proteins and mitochondria is important to protect against dysfunction.

1.6. AIMS AND OBJECTIVES OF THE STUDY

The aims of this study were to determine detailed effects of ageing and dietary restriction on changes in hydrogen peroxide production and mitochondrial protein abundance. ROS in the cell is generally a biological derivative of hydrogen peroxide or superoxide (Brown and Borutaite, 2012). Hydrogen peroxide release is examined at multiple ages in addition to the comparison of AL and DR treatments. AL mitochondria were collected at 3, 15, 24 and 30 months with DR collected at 15, 24, 30 and 36 months. 30 month AL mitochondria and 36 month DR mitochondria compares the function at the same survival point (35%) in the mouse lifespan. This timescale is much more detailed than anything previously reported. Lifespan extension mechanisms for example the effect of rapamycin and mechanism which protect against ROS like telomerase were also investigated.

Mitochondria are the primary site of superoxide production and therefore oxidative damage. This suggests the mitochondrial proteome would have the greatest source of proteomic changes to explain the mechanisms of ageing.

The objectives of this thesis is to study the changes in hydrogen peroxide release from different sites of the electron transport chain including:

- Multiple ages in three tissues (Brain, Liver and Skeletal Muscle)
- Long term dietary restriction (DR) in three tissues (Brain, Liver and Skeletal Muscle)
- Dietary restricted mitochondria from three tissues (Brain, Liver and Skeletal Muscle) at multiple ages.
- Dietary restricted mitochondria in three tissues (Brain, Liver and Skeletal Muscle) at two collection times, DR (24hrs after feeding) and postprandial DR (6hrs after feeding)

- A late 35% survival point of AL and DR fed mice in three tissues (Brain, Liver and Skeletal Muscle).
- Short term rapamycin feeding in three tissues (Brain, Liver and Skeletal Muscle)
    - A comparison of short term dietary restriction with short term rapamycin
- The absence of telomerase

I also studied the changes seen in the liver proteome abundance under different conditions including:

- Multiple ages in three tissues (Brain, Liver and Skeletal Muscle)
- Long term dietary restriction (DR) in three tissues (Brain, Liver and Skeletal Muscle)
- Dietary restricted mitochondria from three tissues (Brain, Liver and Skeletal Muscle) at multiple ages.
- Dietary restricted mitochondria in three tissues (Brain, Liver and Skeletal Muscle) at two timepoints, DR (24hrs after feeding) and postprandial DR (6hrs after feeding)
- Late survival points of 35% of AL and DR fed mice in three tissues (Brain, Liver and Skeletal Muscle).

The outline of the proteomics study has male mitochondria of comparable age and treatment studied for their hydrogen peroxide release. A sun diagram depicting the experimental plan is shown in figure 1-3.

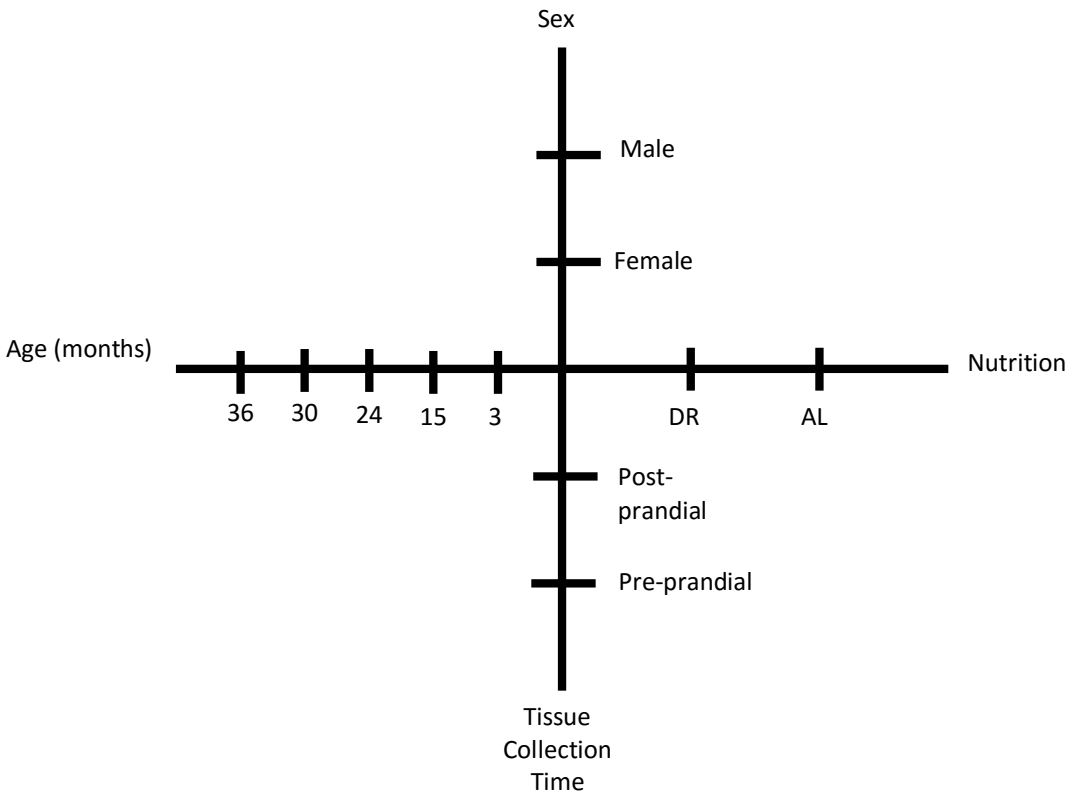

Figure 1-3: The experimental plan for the proteomics study. These are the factors compared in the proteomics study and amplex red study in males only. There are four factors considered (Sex, Nutrition, Age and Time of Culling) each with at least two parameters.

CHAPTER 2: MATERIALS AND METHODS

2.1. ANIMALS

All the work in this thesis complied with the guiding principles for the care and use of laboratory animals and was licensed by the UK Home Office (PPL60/3864). Mice of the same sex were housed in cages (56 cm × 38 cm × 18 cm, North Kent Plastics, Kent, UK) of groups of four to six with an identifying ear notch. Mice were provided with unlimited water, sawdust and paper bedding. Mice were housed at 20 ± 2 C under a 12h light/12h dark cycle with lights on at 7:00 am. Dissections of the mice were carried out in a team this included: Kerry Cameron; Satomi Miwa; Amy Johnson; Rafal Czapiewski; Laura Wiley; Hannah Gautrey; Claire Kolenda; Craig Parker; Carmen Martin-Ruiz; Clara Correia Melo; Joanna Gorniak; Sabine Langie; Sofia Lisanti.

All chemicals are included in table 6-5 in appendix A.

2.1.1. MICE FROM THE DIETARY RESTRICTION STUDY USED FOR MITOCHONDRIAL HYDROGEN PEROXIDE RELEASE ASSAY

A total of 48 C57Bl/6 male mice were purchased from Harlan (Blackthorn, UK) for use in the study focusing on age and dietary restriction. Mice were fed AL diet (CRM (P); Special Diets Services, Witham, UK) until 3 months of age then divided into AL and DR groups. DR mice were fed a 40% restricted diet based on the AL food intake (Cameron, K et al. Longevity & Healthspan 2012). Mice fed an AL diet had tissues collected from 3, 15, 24 and 30 months. Mice fed a DR diet had tissues collected from 15, 24, 30 and 36 months. Brain tissue was collected from mice at all age points. Liver tissue was collected from mice at 3, 24, 30 and 36 months. Skeletal muscle mitochondria were collected from mice at 3, 15, 30 and 36 months. Brain, liver and skeletal muscles from the hind legs were collected and used to obtain mitochondria at these ages for functional hydrogen peroxide release studies as a mark of superoxide and therefore ROS production. Table 6-1 in appendix A summarises additional information on these mice. Pathology, dissection and tissue isolation problems are also detailed in table 6.1.

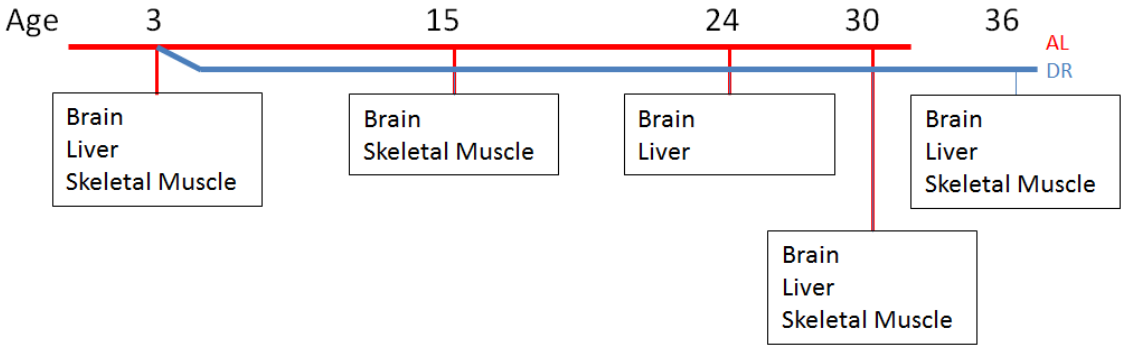

Figure 2-1: Experimental Plan for the long-term dietary restricted study. Mice were culled at 3 months in AL fed mice only; 15, 24 and 30months in both AL and DR mice; and 36 months from DR mice only. The age and dietary treatment is denoted by the coloured lines. AL treated mice are on the red line and DR treated mice are in blue. DR treatment starts at 3 months at this age there is only AL treated mice culled. AL mice have a shorter lifespan so at 36 months only DR mice were available for tissue collection. Amplex red experiments were carried out on tissues collected at each age, the data shown is detailed in the boxes below the time point in the figure.

2.1.2. MICE MITOCHONDRIA OBTAINED FOR HYDROGEN PEROXIDE RELEASE IN TERT KNOCKOUTS AND RAPAMYCIN STUDIES

This study compared the effect of short-term dietary restriction treatment in WT and TERT knockout mice on hydrogen peroxide release from brain mitochondria (strain B6.129S-Tert tm1Yjc/J, Jackson Laboratories) There were four groups of four male 12 month old mice compared. The groups comprised two treatments, ad libitum (AL) fed and 40% dietary restricted (DR) fed groups, for two genotypes, WT and TERT-/-. The dietary restriction was introduced at nine months and maintained for three months until mice were culled, tissues were collected and mitochondria were isolated.

2.1.3. MICE USED TO OBTAIN HYDROGEN PEROXIDE RELEASE FROM SHORT-TERM DIETARY STUDIES

Short-term dietary studies were focused on two areas, dietary restriction was studied including the effects of culling six hours post feeding, and short-term rapamycin treatment. The short-term studies used a mouse strain backcrossed from TERC+/− mice (strain B6.Cg-Terc^{tm1Rdp}/J, Jackson Laboratories). The onset of DR treatments in female mitochondria occurred at 12 months and continued until culling at 15 months. Start controls were mice culled at 12 months obtaining the tissue prior to dietary changes. The short term dietary restriction study had three treatment types for three months, AL, DR and PMDR (Afternoon collected dietary restricted). In AL and DR mice the tissues were collected directly prior to feeding. In PMDR mice the tissues were collected in the afternoon six hours after feeding. DR and PMDR groups were fed a 40% restricted diet compared to the intake of the AL diet. The rapamycin experiment had two treatments control and rapamycin feeding. Rapamycin treatment was studied in two separate experiments. It was started in males at 9 months, and females at 12 months. Control mice had a variation of the AL diet and rapamycin diet has the same basis of the control mice with the addition of 0.067mg rapamycin (Miller *et al.*, 2011; Wilkinson *et al.*, 2012).

2.1.4. MICE USED IN THE LARGE PROTEOMICS STUDY

There were a total of 60 mice used in the large dataset looking at sex, age and dietary restriction. They were from the same strain as those in section 2.1.1 and husbandry

was the same for these mice. The sex, age and treatment for each mouse are detailed in Table 6-3 (appendix A).

2.2. ISOLATION OF MITOCHONDRIA

Mitochondria were isolated by tissue-specific methods as outlined below. The mitochondria for the amplex red assay were immediately resuspended in 200µl of the corresponding isolation medium (detailed below). The mitochondria were used within less than 4h storing them during this period at 4°C. The mitochondrial pellet obtained at the end of the isolation process was snap frozen in liquid nitrogen before storage at -80^{o}C before use for proteomics studies. Mitochondria were isolated by Satomi Miwa unless otherwise stated.

2.2.1. ISOLATION OF MITOCHONDRIA FROM MOUSE BRAIN TISSUE

The mouse brain was dissected and placed in brain isolation medium (250mM Sucrose, 10mM Tris, 0.5mM EDTA pH 7.4 @ 4^{o}C) within 15 seconds of the death of the mouse. The brain was homogenised using a glass homogeniser (Wheaton 15ml Douce tissue grinder) using eight strokes with a loose-fit pestle and centrifuged for 3 minutes at 2000g. The supernatant was centrifuged for 10 minutes at 11400g. The pellet was resuspended in 0.5ml of 3% Ficoll medium (240mM mannitol, 60mM sucrose, 50µM EDTA, 10mM Tris, pH 7.4 @ 4^{o}C, and 6% (w/w) Ficoll (Sigma-Aldrich). This suspension is layered onto 10ml of 6% Ficoll medium and centrifuged at 12500g for 15 minutes. The resultant brown pellet was resuspended in 10ml isolation medium and spun at 12500g for 10 minutes to remove the ficoll.

2.2.2. ISOLATION OF MITOCHONDRIA FROM MOUSE LIVER TISSUE

The liver was dissected from the mouse and cut into smaller pieces. This was washed with liver isolation medium (STE (250mM Sucrose, 5mM Tris, 2mM EGTA pH 7.4 @ 4°C, Sigma)) and homogenised, six strokes with the loose pestle of the glass tissue grinder. The homogenate is centrifuged at 1,050g for 3 minutes. The supernatant is then centrifuged at 11,630g for 10 minutes. This pellet is further purified using density gradient centrifugation (Pagliarini *et al.*, 2008). The pellet is resuspended in 0.5ml isolation medium and carefully layered on top of a stepwise density gradient of 2ml

80%, 6ml 52%, and 6ml 26% Percoll (Sigma). This was centrifuged at 41,100g for 45 min. Mitochondria were collected from the 26%/52% interface, diluted to capacity in a 2ml eppendorf tube with STE, and centrifuged at 11600g for 10 minutes. The supernatant was carefully discarded, and the mitochondria were washed with an additional 2ml STE and re-spun. The resulting pellet was purified mitochondria.

2.2.3. ISOLATION OF MITOCHONDRIA FROM MOUSE SKELETAL MUSCLE TISSUE

Skeletal muscle from the hind legs (quadriceps, biceps femoralis, gastrocnemius) was added to CP1 isolation medium (100mM KCl, 50mM Tris, 2mM EGTA, pH 7.4 @ 4°C, Sigma). It was then minced and chopped then added to CP2 medium [(CP1 isolation medium plus 1mM ATP, 5mM $MgCl_2$, 0.5% fatty acid free BSA (Sigma A3803), Protease (Type VIII Subtilisin A; Sigma, P5380), ph 7.4 @ 4°C] using about 10ml medium per 1g tissue. The muscle CP2 mix is stirred for 1 minute. The tissue was homogenised with a loose pestle in a glass homogeniser and centrifuged for seven minutes at 490g. The supernatant was filtered through two layers of muslin into a new tube and spun for 10 minutes at 10368g. The pellet is resuspended in CP1 and spun for 10 minutes at 11368g. The pellet was flash frozen in liquid nitrogen for proteomics digestion or resuspended in CP1 for hydrogen peroxide production.

2.3. AMPLEX RED ASSAY

Amplex red (Thermo Fisher Scientific) is a non-fluorescent compound which oxidises in the presence of hydrogen peroxide and horseradish peroxidase. The oxidised compound created in the amplex red assay is resorufin which is excited at 450nm and then fluoresces at 490nm. Amplex red reacts with horseradish peroxidase in a 1:1 stoichiometry so as more hydrogen peroxide is made more resorufin is produced and more fluorescence is detected. The volume of hydrogen peroxide can then be calculated from the fluorescence intensity changes when a standard is added.

2.3.1. STANDARD ASSAY CONDITIONS

The release of hydrogen peroxide from isolated mitochondria was determined using an amplex red assay using an Omega FLUOstar using a 96 well black plate. A final

concentration of 0.6mg/ml brain, liver or muscle mitochondria were incubated at 37^{o}C in the assay buffer; 200µl comprising KHE (100mM KCl, 10mM Hepes (pH 7.0), 0.1mM EDTA (pH 7.4 @ 37^{o}C) 1% BSA, All chemical from Sigma), 2U/ml horseradish peroxidase , Sigma, 50µM Amplex Red, 15U/ml SOD, Sigma and 1ug/ml oligomycin, Sigma. The machine was set at an excitation of 544nm and an emission of 590nm to read resorufin fluorescence every 10 seconds. Experimental wells contain the isolation medium and mitochondria. Blank wells contain no mitochondria. Blank wells were used to produce a standard. The standard is an addition made during the assay which comprises of 29.4pmoles of hydrogen peroxide (Sigma). The standard allows for the conversion of resorufin fluorescence to hydrogen peroxide release.

To measure hydrogen peroxide production originating from specific complexes in the ETC, various activators and inhibitors were sequentially added to the reaction mix. The assay, maintained at 37^{o}C, was interrupted after at least two minutes of stable measurements to add these activators and inhibitors and restarted immediately after. These additions can take up to two minutes, this can cause fluctuations in the temperature of the assay. Measurements taken directly after the addition of activators and inhibitors were not used for calculations. Two minutes of incubation at 37^{o}C stabilises the temperature in the wells. Measurements were taken at a stable temperature using consistent rates of fluorescence.

Different methods were used to measure complex II compared to I and III. To measure Complex I and III hydrogen peroxide release, two respiratory substrates were used. Complex I hydrogen peroxide release is determined using 5mM Pyruvate and 5mM Malate (PM, complex I-linked substrate). Rotenone addition (2.5µM, in DMSO Dimethyl Sulfoxide) in the presence of PM inhibits complex I, and stimulates maximum complex I superoxide production. Addition of 4mM Succinate (complex II-linked substrate) gives data on both complex I and III superoxide production. The addition of succinate and rotenone means the electron flow is forward through the ETC. Complex III maximal production is shown by addition of Antimycin A (2.5µM). A further addition of myxothiazol (2.5µM) was made to wells containing succinate, rotenone and antimycin A (all chemicals Sigma).

To measure complex II-linked hydrogen peroxide production (Quinlan et al 2012), mitochondria were incubated with four separate assay buffers. All assay buffers contained an additional 2.5uM rotenone to that outlined in section 2.2.2.1 as a basal buffer. The assay buffers comprised: basal buffer, basal buffer with the addition of 0.4mM Succinate; basal buffer with the addition of 0.4mM Succinate and 1uM Atpenin A5; basal buffer with the addition of 0.4mM Succinate, 1uM Atpenin A5 and 500uM Malonate (all chemicals Sigma). No further additions were made to the assay as it progressed.

Experiments were completed in triplicate for each sample as well as two wells without any mitochondrial suspension which act as a blank control. Results were calculated using fluorescence values, produced after a constant rate has been established from measurements performed every 10 sec over at least two minutes. The SLOPE function in Microsoft Excel was used on each kinetic measurement. This calculation gives us the rate of fluorescence increase. The rate results from the blank wells were subtracted from the rate results from the wells containing mitochondria to remove background fluorescence.

$$b = \frac{\sum (x-\bar{x})(y-\bar{y})}{\sum (x-\bar{x})^2}$$

$\bar{x} = mean\ timepoints$

x = timepoints

b = rate of fluorescence increase per minute

$\bar{y} = mean\ fluorescence$

y = fluorescence values

A hydrogen peroxide standard was created by adding known amounts of hydrogen peroxide to blank wells. The change in fluorescence was determined in the wells with standard addition. This standard allows for the conversion of the rate of mitochondrial fluorescence values to the rate of moles of hydrogen peroxide released.

The fluorescence rate was first determined before substrate addition. This describes the basal release of hydrogen peroxide. All hydrogen peroxide release rates are determined in the presence of PM and PM + Rotenone as well as Succinate, Succinate + Rotenone, Succinate + Rotenone + Antimycin A and Succinate + Rotenone +

Antimycin A + Myxathiozol. The rates of production are determined separately for each substrate and displayed graphically as such. The difference between succinate and succinate + rotenone is calculated to show the reverse flow hydrogen peroxide release from complex I. The rates were calculated for individual wells (technical replicates) any background fluorescence (blank wells) was deducted. Technical replicates were averaged give a value for each mouse.

Complex II hydrogen peroxide release is calculated differently than complex I and III. The mitochondria don't have the activators and inhibitors added in succession. The mitochondria are incubated with the activators and inhibitors from the start of the assay. The different incubation assays are detailed in 2.2.2.1. The results are calculated as rate of hydrogen peroxide release for each well as with complex I and III. The blank results and basal buffer results are subtracted as with complex I and III. The release of hydrogen peroxide is then determined from site IIq and site IIf. Complex IIq release was calculated as the difference between succinate only and succinate + atpenin A5. Complex IIf was calculated as (succinate + atpenin a5) minus (succinate + atpenin a5 + malonate).

Hydrogen peroxide release from liver mitochondria is calculated differently than brain and muscle. The measurements are made in the presence and absence of HRP. The final calculation is the difference between the values in the presence and absence of HRP.

2.3.2. RESORUFIN AS THE TARGET OF THE AMPLEX RED ASSAY

There were problems seen in the detection method used on liver mitochondria. This complication was clouded by the decrease in hydrogen peroxide release after the addition of substrate and other chemicals. Resorufin changes were monitored as a result. The fluorescence of resorufin in the presence of isolated mitochondria was determined using a modified amplex red assay using an Omega FLUOstar spectrophotometer using a 96 well black plate. Firstly incubated at 37^{o}C and monitored was the assay buffer: 200µl of KHE (100mM KCl, 10mM Hepes (pH 7.0), 0.1mM EDTA (pH 7.4 @ 37^{o}C) 1% BSA), 2U/ml horseradish peroxidase, and 200µM Resorufin (Invitrogen). The machine was set at an excitation of 544nm and an emission of 590nm to read fluorescence every 10 seconds. Additions of 0.6mg/ml

brain, liver or muscle mitochondria were incubated with the assay buffer after consistent results were produced. The addition of substrates, hydrogen peroxide and HRP were made as labelled in each experiment separately.

2.3.3. STATISTICAL ANALYSIS

Values are given as either mean ± standard error mean, in cases where n>3, with n being the number of individual experiments, or as mean ± standard deviation if n≤3. Percentage variation is the standard deviation of the values when compared to the mean. Statistical analysis was carried out using the standard t-test in Microsoft Excel 2010 after checking the normality of distribution. The t-test was used to directly compare two separate conditions. Significant values were determined to be $P < 0.05$. ANOVA tests were carried out in sigma plot on data sets involving multiple comparisons, e.g. those related to age. Sigma plot checks for normal distribution and comparable variance. In the case that these conditions were not fulfilled, the ANOVA by ranks was used.

2.4. RESORUFIN ABSORBANCE

Amplex red assay relies on the detection of resorufin fluorescence. The product in the amplex red assay which fluoresces in response to hydrogen peroxide is resorufin. Resorufin absorbs light at 544nM. Absorbance of the reaction medium across the wavelengths 400-700nM was measured using Omega FLUOstar spectrophotometer. Wells were loaded with the same experimental media as in the amplex red assay (2.2.2.1). This reaction media was incubated with either brain mitochondria, liver mitochondria, or no mitochondria. Several conditions were used including substrate, excluding HRP or amplex red. Background levels were determined without mitochondria. Area under the curve was calculated and statistics performed on these numbers.

2.5. PROTEIN CONCENTRATION ASSAY

Protein concentration was determined using the BioRad DC protein concentration assay kit (BioRad). Standards of known protein concentrations (0mg/ml, 0.06mg/ml, 0.125mg/ml, 0.25mg/ml, 0.5mg/ml, 1mg/ml, 2mg/ml) were made using BSA (Sigma).

Mitochondria were measured in a 5% dilution. The standard and the mitochondrial dilutions were combined with reagents A, S and B. The absorbance was read at 750nM after 15 minutes incubation at room temperature. A standard curve was created (figure 2-1). The mitochondrial sample absorbance was compared to the standard curve to determine the protein concentration of the diluted mitochondria. The concentration was then deduced for the mitochondrial sample from its dilution.

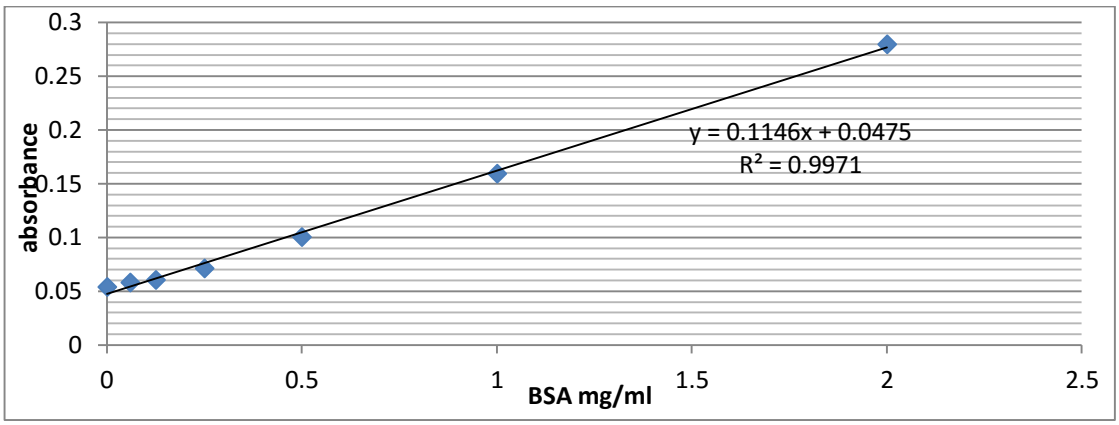

Figure 2-2: An example standard curve produced from the BSA standards with an r^2 value of 0.9971. This standard curve is produced from two replicates of known protein concentrations (0mg/ml, 0.06mg/ml, 0.125mg/ml, 0.25mg/ml, 0.5mg/ml, 1mg/ml, 2mg/ml BSA). A trendline is added with its equation. The curve is used to then obtain accurate protein concentration from the sample absorbance measured.

2.6. ISOLATION OF MITOCHONDRIA FROM MOUSE AML 12 CELLS FOR PROTEOMICS STUDY

Cells were AML12 mouse liver cells (http://www.atcc.org/products/all/CRL-2254.aspx#documentation) and maintained in DMEM/F12 media in 1:1 ratio with the following supplements: 5µl/ml insulin, 5µg/ml transferrin, 5ng/ml selenium and 40ng/ml dexamethasone. Cells were switched to the same type of supplemented media with replacement of FBS with dialyzed FCS (Biowest, France) lysine and arginine labelled with C14 and N13 for SILAC incorporation. SILAC labelled amino acids used were lysine (K8, L-Lysine-2HCl (U13C6, 98%; 15N2, 98%) Cambridge Isotope Lab, Hampshire) and Arginine (R10, L-Arginine; HCl (U-13C6, 98%; 15N4, 98%) Cambridge Isotope Lab). The cells were harvested at 80% confluence and mitochondria were isolated from them using the QuadroMACs separation kit (Miltenyi Biotec). 20 million cells were harvested and resuspended in 2ml of lysis buffer. The cells were lysed using a 27G needle in 5million batches. The mitochondria were labelled with superparamagnetic MACs MicroBeads supplied as part of the kit. The MACs column is attached to a strong magnet this retains all magnetically labelled mitochondria when passed through the column. Removing the column from the magnet allows for elution of the mitochondria (Hornig-Do *et al.*, 2009). Approximately 100µg protein per 10^7 cells was obtained and 3mg isolated mitochondrial protein was collected in total.

2.7. SEPARATION AND DIGESTION OF PROTEINS

2.7.1. ACETONE PRECIPITATION

Mitochondria comprise more than just proteins, to ensure a pure preparation of proteins was used for mass spectrometer analysis acetone precipitation was used (Sigma). 100% acetone stored at -20 ^{o}C is added in a 6:1 ratio with the volume of isolated mitochondria. This was incubated at -20^{o}C overnight. The mixture was centrifuged for 15 minutes at 15,000g at 4^{o}C to remove the acetone. the pellet was allowed to dry before use.

2.7.2. IN SOLUTION DIGEST

Proteins were precipitated from the isolated liver mitochondrial samples were dissolved in 250µl 6M urea (Sigma), 100mM Tris/50mM Ammonium bicarbonate (Sigma). 50µl of this solution was reduced with 2.5µl of reducing agent for 1 hr. The samples were then alkylated in the dark for 1 hour with 10µl of alkylating agent. To consume unreacted iodoacetamide after an hour 10µl of reducing agent was added. 240µl of 50mM ammonium bicarbonate was added to decrease the urea concentration to 1M. 2µg of trypsin was added to each sample and incubated at 37^{o}C overnight. The digest was stopped by adding 100µl of 5% TFA. The samples were cleaned using stagetips. 20µl of each digested sample was combined with 10µl of digested standard. LC-MS/MS analysis was performed at FingerPrints Proteomics laboratories (University of Dundee) and RAW data was returned (performed by Dougie Lamont, Kenny Beattie and FingerPrints Proteomics Staff).

2.7.3. STAGE TIPS

STAGE tips were created with a C18 Empore filter (Sigma) placed in a 10µl pipette tip (Eppendorf). The tip was then used to filter the sample. The sample is filtered using several steps. The STAGE tip has the buffer or sample loaded into the top and a syringe is used to push the buffer over the Empore filter.

The STAGE tip is equilibrated with 10µl acetonitrile then 10µl 0.1% TFA. The sample is then loaded through the STAGE tip twice. The STAGE tip is washed with 0.1% TFA. To elute the sample 10µl of elution buffer (65% Acetonitrile in 0.1% TFA) is added to the STAGE tip to elute the sample into a clean Eppendorf tube.

2.8. INCORPORATION OF HEAVY LABELLED AMINO ACIDS INTO AML12 CELLULAR PROTEINS

2.8.1. 1-DIMENSIONAL GEL ELECTROPHORESIS

To assess the incorporation of heavy labelled isotopes into the AML12 mitochondria, a LC-MS/MS experiment was carried out with a single band from a mitochondrial protein 1-dimensional gel. Isolated liver mitochondria from 2.2.2 were flash frozen in liquid nitrogen and thawed on ice for five repetitions. Acetone precipitation was carried out on the mitochondria to further purify the protins. The dried precipitate was

redissolved in SDS sample buffer, NuPAGE reducing agent, water, 5:1:4 (10µl total volume, Invitrogen), heated to 85°C for five minutes and sonicated for 3 minutes. Samples were separated on a pre-cast 4-12% Bis-Tris gel (NuPAGE) at 180 volts for 90 minutes. Gel was stained using Coomassie Blue (EZBlue, Sigma).

2.8.2. IN GEL DIGEST

To determine SILAC incorporation only a small amount of the gel was needed so only one band was used for an in gel digestion. Gel sections/bands were cut and destained. The gel pieces were then reduced using 10mM DTT (AppliChem) and alkylated in the dark using 50mM Iodoacetamide (Applichem). After washing with ammonium bicarbonate and acetonitrile (Sigma), the gel pieces were incubated at 37°C with 0.2µg trypsin (Promega) in 60µl of 50mM NH_4HCO_3 and 1mM $CaCl_2$ for 18h to digest the proteins. Trypsin was stopped by the addition of 10µl 5% TFA (Trifluoroacetic acid, Sigma). The digested peptides are now in the solution. Further hydrophobic peptides were obtained from the gel by the addition of 20µl 2% TFA/ 60% acetonitrile. 20µl of 100% acetonitrile was added to the gel pieces to elute any remaining peptides. The total solution was then concentrated in a speedvac. The samples were stage tipped to clean the sample. The samples were then acidified using 1% TFA and transferred to MS vials for mass spectrometer analysis. LC-MS/MS analysis was performed, using a 1 hour gradient, on an LTQ XL orbitrap mass spectrometer coupled to an Ultimate 3000 nano HPLC system (Thermo Scientific).

The incorporation of the SILAC label into the standard above a threshold value is fundamental to this method. Unlabelled standard would count as part of the unlabelled sample therefore affecting the quantification of proteins. Therefore determining the incorporation of SILAC into the standard's proteins is vital. Confirmation of fully labelled protein of greater than 95% within the sample is an accepted amount for a spike-in standard (Kim *et al.*, 2002; Geiger *et al.*, 2011). As the heavy labelled amino acids are the only source for new proteins, during mitosis the proteins made in the new cells will contain only heavy labelled amino acids. Therefore mitosis halves the quantity of unlabelled protein. This produces the equation:

$1/(2^n)$ = proteins unlabelled. Where n = number of population doubling

According to the equation after seven population doublings there should be only 1/128 (0.78%) of the cellular protein unlabelled. This is when the incorporation analysis was carried out to ensure more than 95% of the amino acids were labelled. Incorporation was determined by mass spectrometer analysis of a digested protein sample from the cells. The sample was of isolated mitochondria from these cells, as will be used as the standard.

Two protein lists were generated from the one AML12 protein sample. A list containing the SILAC labelled proteins and another of proteins which weren't labelled with SILAC. There were 158 significant proteins found to be fully labelled with SILAC, and 21 which weren't fully labelled. Examining the produced lists can only show which proteins were found with each query result. These lists are more effective in determining SILAC incorporation when analysing the raw data. SILAC incorporation required growing the AML12 cells in media with heavy labelled amino acids which in this case were K8 and R10 (Geiger *et al.*, 2011). Looking in the raw data and using The GPM list as a guide we can find the peak relating to that of the unlabelled peptide. Adding the mass of the heavy labels we can then find the corresponding peak of the peptide containing the labelled protein in this heavier mass range (Craig *et al.*, 2004). Acceptable levels of this unlabelled protein are <5%. The level of incorporation is determined by comparing the mass of the heavy weighted protein with that of the unlabelled protein. Setting the mass spectrometer viewer to monitor the labelled protein at 100%, the percentage of unlabelled protein is calculated as a percentage of the heavy labelled protein. In the analysis performed on the SILAC incorporated samples the levels of labelled protein found in the SILAC labelled mitochondrial proteins were 3% which is well within the threshold for labelling. As further population doubling will further decrease the amount of unlabelled protein the sample is sufficiently labelled to act as a standard for spike in SILAC analysis.

The more divisions that occur more amino acids are incorporated so all mitochondrial protein will be labelled to this standard minimum. 2.5mg of protein will need to be isolated for these experiments to produce enough standard to be spiked in to each sample.

2.8.3. DATA PROCESSING IN MAXQUANT

The raw data files were processed using Max Quant version 1.3.1.5 using the mouse fasta file from May 2013 (www.uniprot.com (Geiger *et al.*, 2013; The UniProt, 2014; UniProt, 2014)). Protein lists were generated using intermediate files produced by MaxQuant. Determination of quantification of the SILAC was also completed in the MaxQuant program.

The proteinGroups.txt file was imported into Microsoft Excel 2010. The data was transformed in Microsoft Excel 2010. The data was logged, then filtered to include only the data present in over 66.6% of samples. The H/L ratio data from the proteins which meet these criteria were transformed in the first transformation step. This resulted in a subtraction of the sample median value from each protein H/L ratio to remove technical variation seen across the dataset. The second transformation step takes the median value of each protein across the samples and subtracts this value from each samples H/L ratio. The resultant value is a comparative amount which can be compared across samples. This comparative value was termed RAAT.

Data is deposited to the ProteomeXchange Consortium (http://proteomecentral.proteomexchange.org) via the PRIDE Partner repository (Vizcaino *et al.*, 2013). MaxQuant parameters (table 6-4) and template files (table 6-2) were attached in appendix A.

2.9. STATISCAL ANALYSIS IN PERSEUS

The transformed data was imported into Perseus a statistical program built to work with large multi-sample SILAC data (Geiger *et al.*, 2013). This program was used to produce random missing values for the mouse samples based on their normal distribution (Geiger *et al.*, 2013). Data program R and Microsoft Excel were both used to produce the figures in section 5.

CHAPTER 3: MITOCHONDRIAL HYDROGEN PEROXIDE RELEASE CHANGES WITH AGE AND DIETARY INTERVENTION

3.1. EXAMINING THREE TISSUES FROM MULTIPLE AGES AND CONDITION REQUIRES AN OPTIMISED METHOD

3.1.1. TECHNICAL VARIATION IS MINIMISED IN THE PROTOCOL

The fluorescence variation in response to the addition of a hydrogen peroxide standard was calculated over three separate days using four wells in five individual amplex red assays. All wells begin as blanks containing reaction medium only. The assay took a measurement every ten seconds, this was paused to add a standard of 29.4pmoles H_2O_2 (3µl) separately into two wells. The increase in fluorescence with the standard addition was measured. Any fluorescence change which occurred due to opening the machine in the blank wells when no addition of hydrogen peroxide was subtracted from the standard. This standard was used to estimate and minimize technical variation.

The mitochondrial experiments carried out in the dietary restriction and ageing study take four hours. Five separate assays of three technical replicates were carried out over four hours. The fluorescence of a standard was checked over a four hour time period to ensure no degradation of either the chemicals used in the reaction medium or the hydrogen peroxide standard.

On day 1 all reagents including hydrogen peroxide were diluted by KHE, for use as a comparable standard, these were used for the full four hours without rediluting the reagents. The high error bars were thought to be a result of poor pipetting technique this was improved on day two reducing the error bars. After the error bars were still high it was considered that hydrogen peroxide may not be stable when diluted in KHE. On day three the hydrogen peroxide was re-diluted between assays. Re-diluting the hydrogen peroxide standard for each experiment reduced the variation over the day's experiments. The coefficient of variation between independent wells decreased from

34% on day 1 to 10% on day 3 (Figure 3-1). This level of technical variation was deemed acceptable and was maintained in all further experiments.

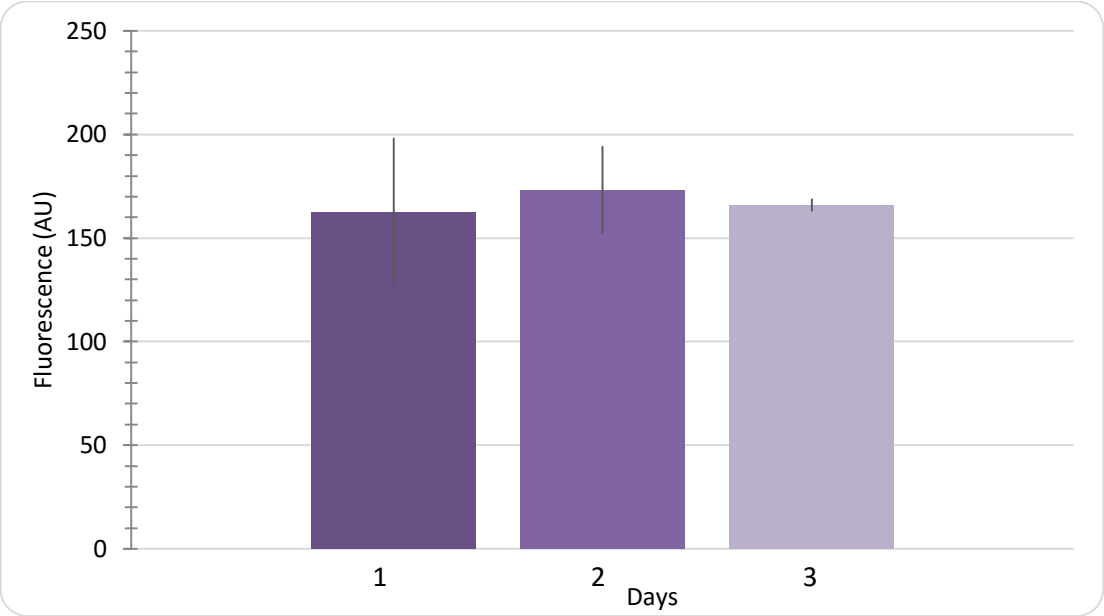

Figure 3-1: Technical variation in fluorescence intensity of a hydrogen peroxide standard. 3µl hydrogen peroxide (29.4pmoles) was added separately to two separate reaction wells in five separate experiments. These experiments were repeated on subsequent days. Data are mean ± standard deviation n=10. Reproducing the usable solutions between experiments and reducing human error decreased technical variation to 10%.

3.1.2. THE TECHNICAL VARIATION USING A BIOLOGICAL SAMPLE

Biological variation exists between mice of the same treatment, age and strain. Technical variation is seen within earlier experiments as shown in Figure 3-2. The mitochondria are re-suspended in isolation medium for use in the amplex red assay. The technical variation obtained from five separate assays with three replicates for each mouse. Figure 3-2 shows the average hydrogen peroxide release from n=5 mice using the assay's averages. The technical variation is higher in biological samples than in the standard as seen in Figure 3-2. This could be due to uneven suspensions in mitochondrial preparations. The disparity in density can re-occur between assays if the mitochondria are kept on ice and stable. Re-suspending the mitochondria between assays is the best way to reduce this. Figure 3-2 also displays the standard deviation from the three mice (biological variation). The standard deviation from biological variation is comparable to the technical variation for each mouse. Progressing with this amount of variation is acceptable. To reduce the variation more replicates are required. Limitations in the amount of mitochondria obtained from the tissues results in optimum technical variation. Minimising the biological variation could be achieved by increasing the number of mice.

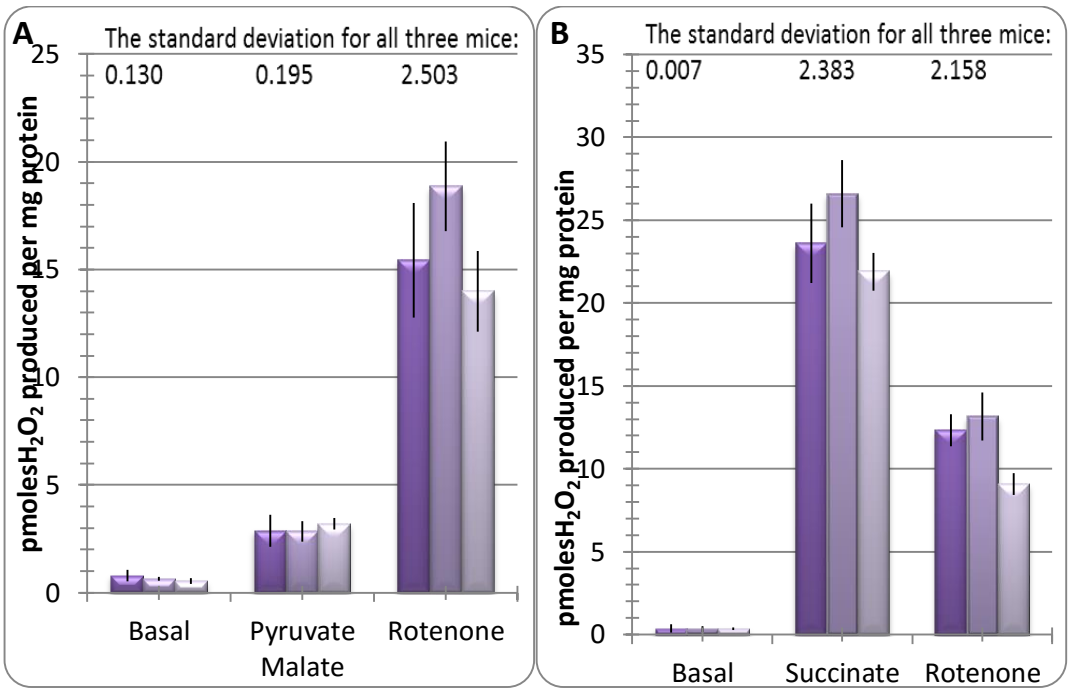

Figure 3-2: Technical Variation is maintained with the use of a mitochondrial sample. Brain mitochondria were incubated with PM (A) and succinate (B) as a substrate. Each bar is a separate mouse, of the same age, treatment and strain, carried out on a separate day. The separate mice are denoted by a lighter purple colour. The separate mice had three technical replicates. The data is displayed as mean ± standard deviation.

3.1.3. OTHER CONTROL EXPERIMENTS TO CONFIRM REACTION MEDIUM COMPOSITION

Rotenone is diluted to concentration in DMSO. DMSO is commonly used to solubilise rotenone and amplex red. DMSO has been shown to preserve plant mitochondria from freezing damage (Dickinson DB, Science 1967). Figure 3-3 confirms that DMSO does not affect the hydrogen peroxide release from the mitochondria. 50uM DMSO was added to the wells after substrate addition to determine whether this would have an effect on hydrogen peroxide production. Figure 3-3 shows 50uM DMSO has no effect on the rate of H_2O_2 production from brain mitochondria.

Mitochondria can be contaminated by free fatty acids from the cytoplasm during the preparation. Free fatty acids play a role in altering the mitochondrial membrane potential. They are known to activate uncoupling proteins (UCP) (Weigle *et al.*, 1998) which can lower the membrane potential of the mitochondria decreasing superoxide production (Miwa and Brand, 2003). Bovine Serum Albumin (BSA) binds free fatty acids preventing UCP activation.

It was shown in figure 3-4 that without BSA there is a statistically significant lower hydrogen peroxide release. The reduced release seen from complex I without BSA is significant in the presence of pyruvate malate and rotenone when complex I is at maximal stimulation. The reduced release is also seen in reverse flow. 0.5mg/ml of BSA was added to all future experiments.

Membrane potential is dependent on the respiratory states. State III respiration (active respiration in the presence of ADP) the membrane potential is lower than that of state IV (without active ATP synthesis). Isolated mitochondria should not contain substrates for the electron transport chain but residual substrates and ADP may remain in the matrix. These residual substrates could be expended during the assay affecting results. Residual substrate would be seen in basal levels of H_2O_2 release. Respiration state II occurs with the addition of substrate. Endogenous ADP will result in state III respiration as opposed to state II. Oligomycin blocks ATP synthase causing state IV respiration. State II and IV are comparable as substrate is present and ATP synthase inactive.

Figure 3-5 shows that the addition of oligomycin has no effect on H_2O_2 release from brain mitochondria when using pyruvate malate as a substrate. There is a significant increase in H_2O_2 release when succinate is used as a substrate and both succinate and rotenone are present. All future experiments contain oligomycin; the addition of oligomycin to the assay medium ensures all hydrogen peroxide release is determined with respiration is at state IV (Hutter *et al.*, 2004).

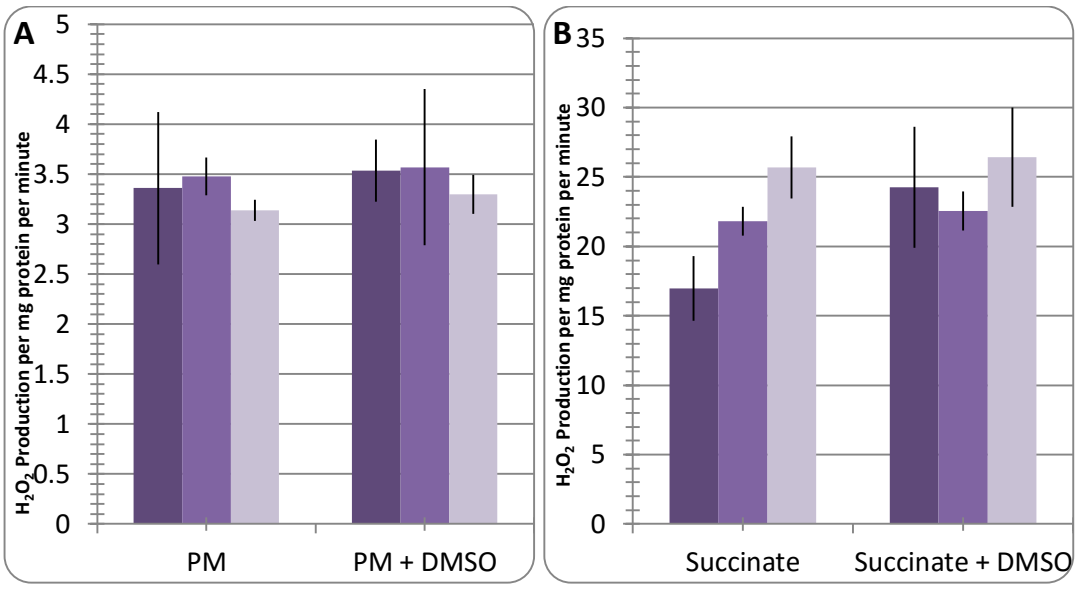

Figure 3-3: DMSO at a concentration of 50uM does not change the rate of hydrogen peroxide release in brain mitochondria. Brain mitochondria were incubated with either PM (A) or Succinate (B), with (right) or without (left) DMSO. Graphs show the results from three independent experiments performed on subsequent days. Each day is denoted by a lighter purple. Each experiment was performed in three technical replicates, and data are mean ± SEM. No significant difference was seen with either a complex I (A) or II (B) substrate (paired t test).

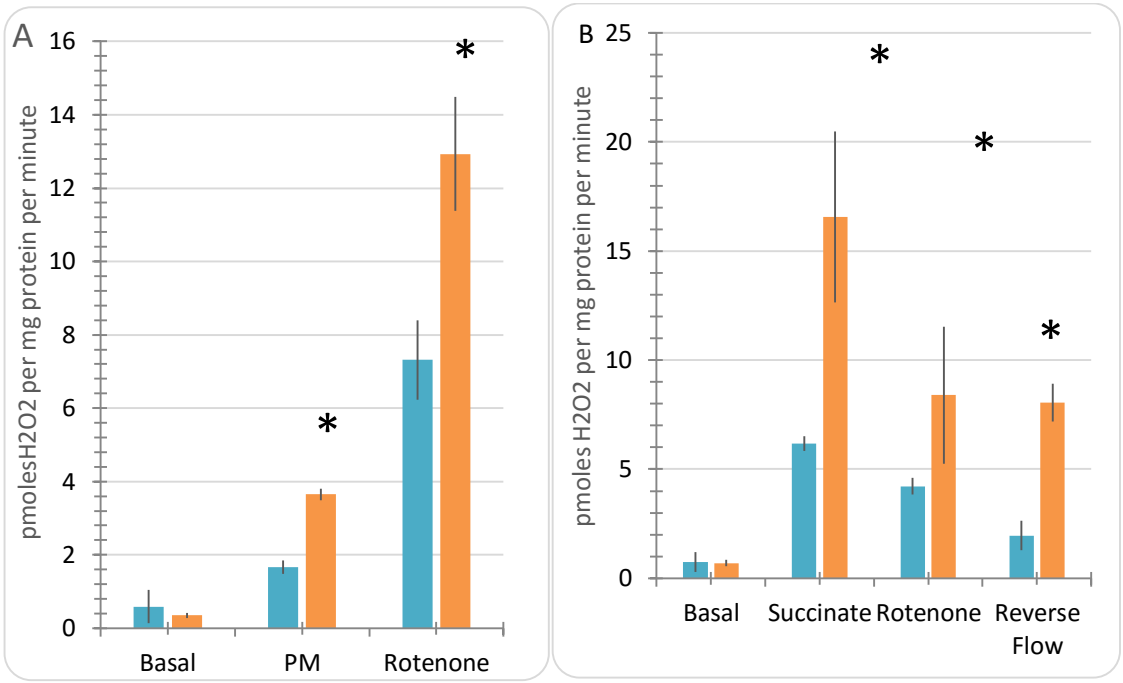

Figure 3-4: The presence of BSA increases hydrogen peroxide release in the presence of both pyruvate malate and succinate. H2O2 release from brain mitochondria in the presence of BSA (0.5mg/ml, orange/right) or its absence (blue/left) with a PM (A) and succinate (B) as a substrate. The bars show the mean of three mice with the same age, strain and treatment. Data is shown as mean ± SEM; * significantly different (t test).

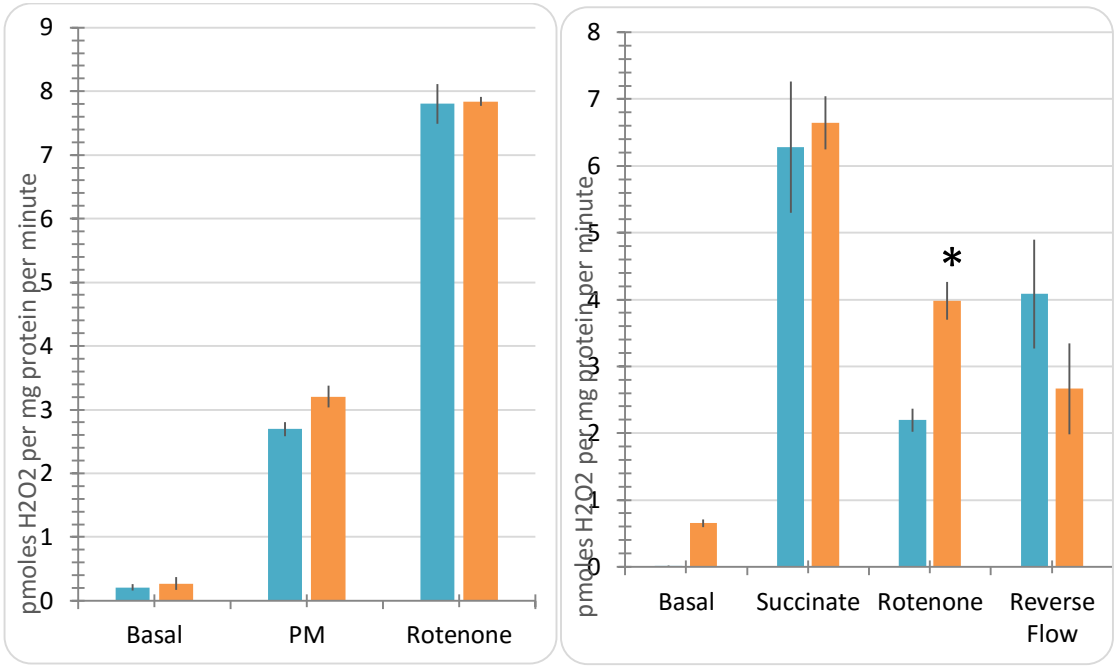

Figure 3-5: Oligomycin increases the release of hydrogen peroxide in brain mitochondria in the presence of succinate and rotenone. Brain mitochondria incubated with pyruvate and malate (A) or succinate (B). The bars display hydrogen peroxide release (pmoles H_2O_2/mg protein/min) in the presence of oligomycin (orange) and absence of oligomycin (blue). The bars are the mean from three mice each with three technical replicates. Data is shown as mean ± SEM; * significantly different (t-test).

3.2. THE MEASUREMENT OF HYDROGEN PEROXIDE PRODUCTION IN PURIFIED LIVER MITOCHONDRIA USING AMPLEX RED

3.2.1. THE LIVER MITOCHONDRIA FLUORESCE DIFFERENTLY IN THE AMPLEX RED METHOD TO BRAIN AND MUSCLE MITOCHONDRIA

Under basal conditions (i.e. in the absence of a respiration substrate), mitochondrial oxygen consumption is negligible and (almost) no superoxide should be produced. This is the case in brain and muscle mitochondria (figure 3-6). However, when studying liver mitochondria with amplex red in the presence of only the reaction medium, there is already a fast increase in fluorescence under 'basal' conditions (figure 3-6). When a respiration substrate (pyruvate + malate, PM) is added, brain and muscle mitochondria generate increased fluorescence in the presence of the catalyst HRP (Figure 3-6), indicating release of hydrogen peroxide. Conversely, in the presence of liver mitochondria this fluorescence rate is lower when a substrate is added (figure 3-6).

To identify possible causes of high basal fluorescence in liver mitochondria, the following questions were experimentally addressed:

Does the fluorescence result from hydrogen peroxide?

Is Amplex red oxidized to resorufin by liver mitochondria?

Is resorufin instable at high hydrogen peroxide concentrations?

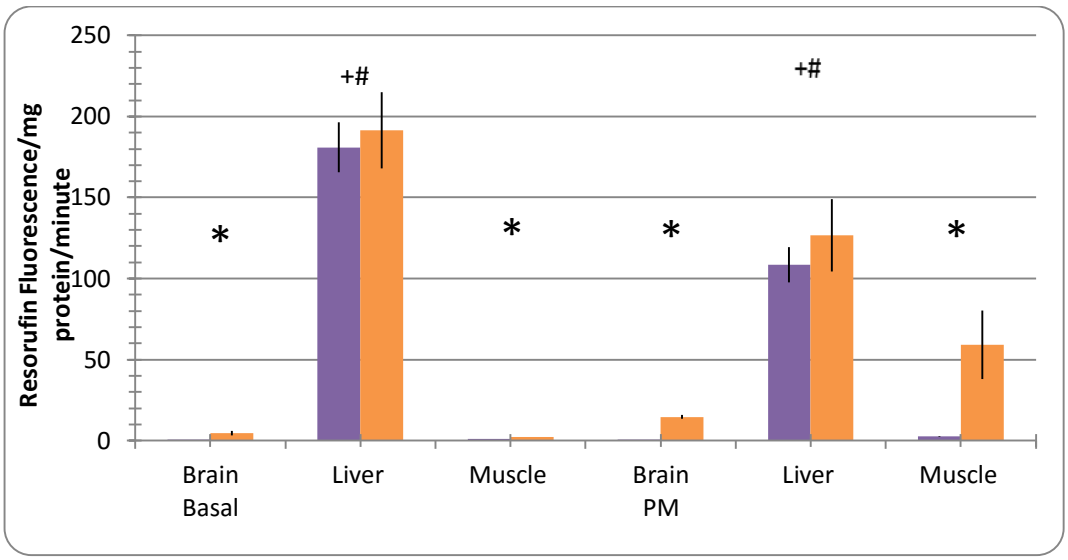

Figure 3-6: Basal fluorescence detection of resorufin is higher in liver mitochondria than brain and muscle mitochondria. The addition of Pyruvate Malate (PM) causes a reduction to the rate of fluorescence Brain, muscle and liver mitochondria are incubated with either assay buffer containing HRP (orange) or excluding HRP (blue). During the assay 'basal' fluorescence was calculated before PM was added. *statistically significant from no HRP, +statistically significant from brain basal, #statistically significant from muscle basal. (t-test)

3.2.2. LIVER MITOCHONDRIA INDUCE STRONG RESORUFIN FLUORESCENCE INDEPENDENTLY FROM HYDROGEN PEROXIDE UNDER BASAL CONDITIONS

The resorufin fluorescence maximum occurs at 585nm. Resorufin has a characteristic absorption spectrum with the absorption maximum at 571nm. To see whether resorufin is generated from amplex red by liver mitochondria, absorption spectra are measured over a wavelength scale of 400-700nm. The assay medium is incubated for five minutes with hydrogen peroxide, liver or brain mitochondria and in the presence or absence of HRP or substrate or both (Figure 3-7). AR with HRP alone or with brain mitochondria in the absence of substrate served as negative controls, while AR + HRP + 98pmoles hydrogen peroxide or brain mitochondria incubated with AR, HRP and substrate were used as positive controls. The absorbance spectra from liver mitochondria + AR with or without substrate and/or HRP are the same as that of resorufin.

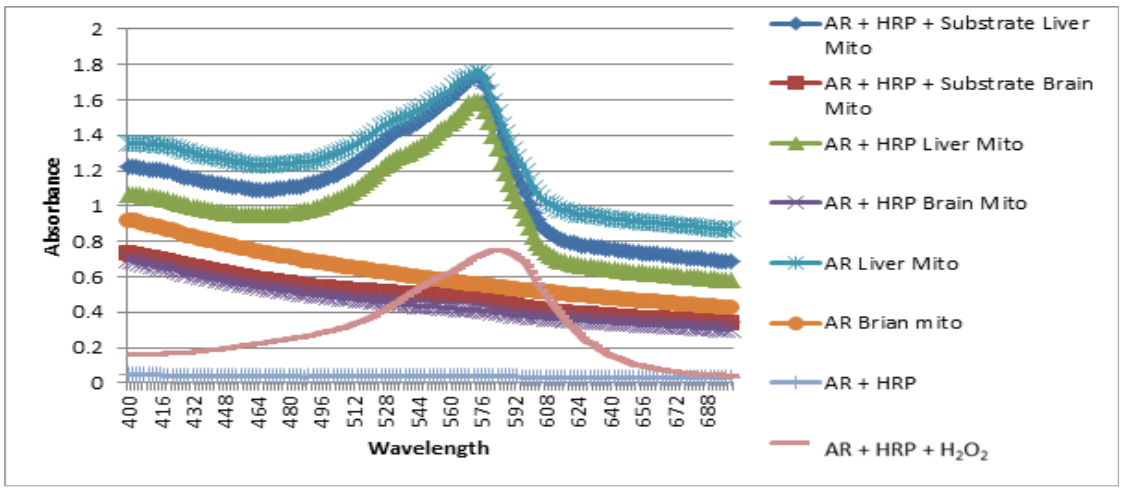

Figure 3-7: The amplex red oxidation product generated by liver mitochondria has the same absorption spectrum as resorufin. The absorbance across a range of wavelengths 400-700nm was measured from amplex red assays using liver and brain mitochondria. The wells were incubated for five minutes prior to detection. Blue, light blue and green traces contain liver mitochondria with and without substrate or HRP. Red, orange and purple traces depict brain mitochondria with and without substrate or HRP. The peaks are smaller in brain mitochondria experiments as less resorufin is produced. The lilac trace (AR+HRP) shows only the reaction medium (negative control). As positive control, 98 nmoles hydrogen peroxide were added to the reaction medium (pink labelled trace, AR + HRP + H2O2).

If the fluorescence generated by liver mitochondria under basal conditions were caused by hydrogen peroxide, it should be inhibitable by catalase added to the reaction medium. Therefore fluorescence was compared in the absence and presence of 1,000U/ml catalase (Votyakova and Reynolds, 2004). In brain mitochondria, basal fluorescence was low, and PM-stimulated fluorescence was strongly suppressed by addition of catalase. However the liver mitochondrial basal production is high as shown before and PM-stimulated fluorescence is unaffected by catalase (figure 3-8).

HRP is the catalyst for the amplex red reaction. If HRP is not present hydrogen peroxide cannot react with amplex red to produce resorufin therefore fluorescence should not occur. The results of which are shown in Figure 3-8. Removing the HRP from the reaction medium completely removes the resorufin signal in brain mitochondria. Completing the reaction without the HRP only removes a small proportion of the fluorescence in liver mitochondria. In liver mitochondria there is no difference in fluorescence signal in the experiments with catalase and without HRP. When there is no HRP in the reaction medium and there is catalase present with liver mitochondria there is no increased suppression with PM addition This suggests that the fluorescence signal does not come from hydrogen peroxide release. If amplex red is removed from the reaction medium there is no fluorescence signal (not shown) suggesting the fluorescence occurs through amplex red by producing resorufin irrespective of hydrogen peroxide addition.

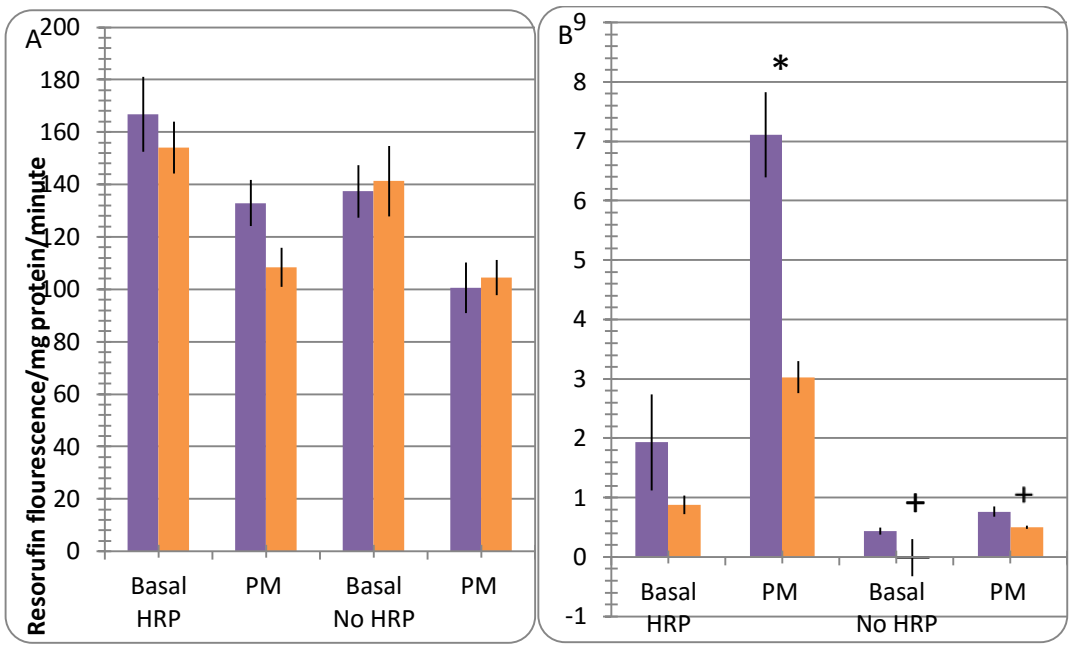

Figure 3-8: Fluorescence generated by liver mitochondria is independent of both catalase and HRP. Liver (A) or brain (B) mitochondria are incubated in assay medium either containing 10^3U/ml (Votyakova and Reynolds, 2004) catalase (orange) or excluding catalase (blue). The presence and absence of HRP is denoted on the x axis. Furthermore substrate addition occurs during the assay and is denoted on the x axis. Results are shown as mean ± SEM calculated from four mice of the same age and strain. * significantly different with catalase addition, + significantly different with HRP absence.

3.2.3. REDUCTION OF RESORUFIN FLUORESCENCE OCCURS IN RESPONSE TO SUBSTRATE ADDITION

To see whether the decrease of fluorescence after substrate addition in liver mitochondria could be due to exhaustion of any reaction component, short and long term kinetic measurements were compared. The kinetic experiments to measure amplex red usually require 30 minutes of measuring time (long term kinetics). Even in brain or muscle mitochondria with their lower amplex red oxidation rate, reduced reduction can be seen over a 60 minute time frame. In liver mitochondria the additions of substrate cause a decreased rate of fluorescence. Mitochondria were incubated with all stimulants and inhibitors for two minutes prior to measuring for only five minutes total these were short kinetics. Brain and liver mitochondria were compared using long and short kinetics in the presence and absence of HRP. Comparing the results from both long and short kinetics no significant differences were seen (Figure 3-9). In the brain there was no amplex red oxidation if HRP was not present. The short kinetic data also showed no amplex red oxidation without HRP. The suppression in fluorescence rate production is not related to an overall decrease in signal with time.

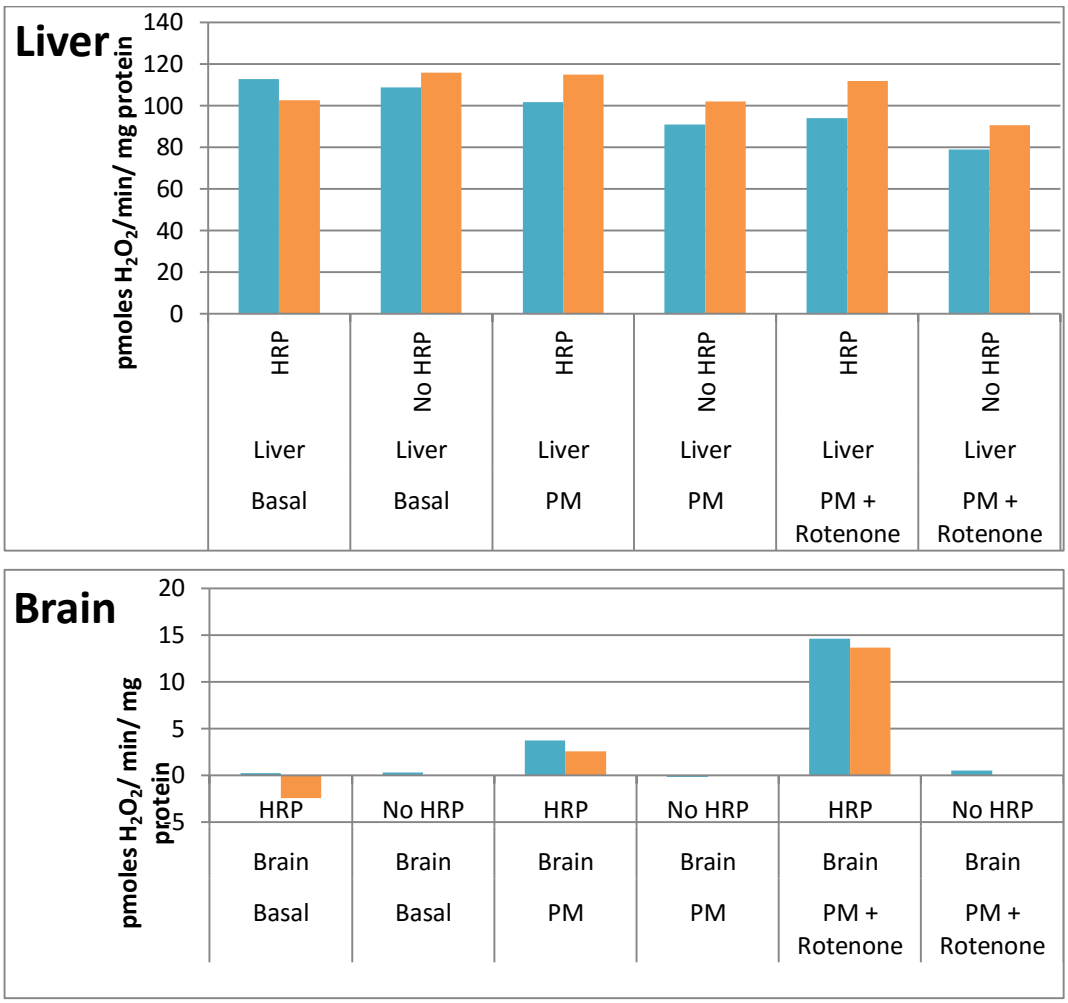

Figure 3-9: Short and long term kinetic data show no difference when measuring hydrogen peroxide release in brain and liver mitochondria. Long kinetics (Blue) were performed as in the materials and methods section, both with and without HRP. The measurements were determined basal, PM only and PM and rotenone. Short kinetics (orange) were carried out incubating the mitochondria with all the stimulants and inhibitors for two minutes prior to measuring for five minutes. Results show mean of three replicates. When comparing the results there are no differences between the measurement techniques.

3.2.4. RESORUFIN CONSUMERS ARE NOT RESPONSIBLE FOR THE LOWER RESORUFIN FLUORESCENCE

As shown in Figure 3-10, liver mitochondria generate higher amounts of a product with fluorescence and absorption characteristics like resorufin from Amplex red even in the absence of substrate and HRP. Surprisingly, with substrate addition the resorufin fluorescence is suppressed. It is unclear how and why the suppression occurs. Resorufin can be reduced into another fluorescent form as well as re-oxidised to reform resorufin. Resorufin can also form resazurin, a non-fluorescent compound, as shown in figure 3-10. It has been shown that resorufin can be reduced to resazurin by high levels of hydrogen peroxide (Towne *et al.*, 2004). In the liver experiments the fluorescence is reduced with substrate addition. It is thus possible that energized liver mitochondria produce so much hydrogen peroxide that resorufin is reduced to resaruzin, resulting in a decrease of fluorescence intensity.

Changes in resorufin fluorescence with hydrogen peroxide addition are shown in figure 3-11. Resorufin fluorescence was monitored over one hour with additions of KHE, succinate, hydrogen peroxide and HRP. As no mitochondria are present in the assay, addition of substrate had no effect. 196pmoles hydrogen peroxide, added at 35 minutes, reduced resorufin fluorescence only when HRP was present as expected.

Figure 3-12 shows the response of resorufin fluorescence in the presence of either liver or muscle mitochondria. After mitochondrial addition substrate was added to determine if mitochondrial release of hydrogen peroxide would result in resorufin consumption. However mitochondrial presence suppresses the effect of added hydrogen peroxide on resorufin. Consequently the high production of hydrogen peroxide has no effect on resorufin fluorescence.

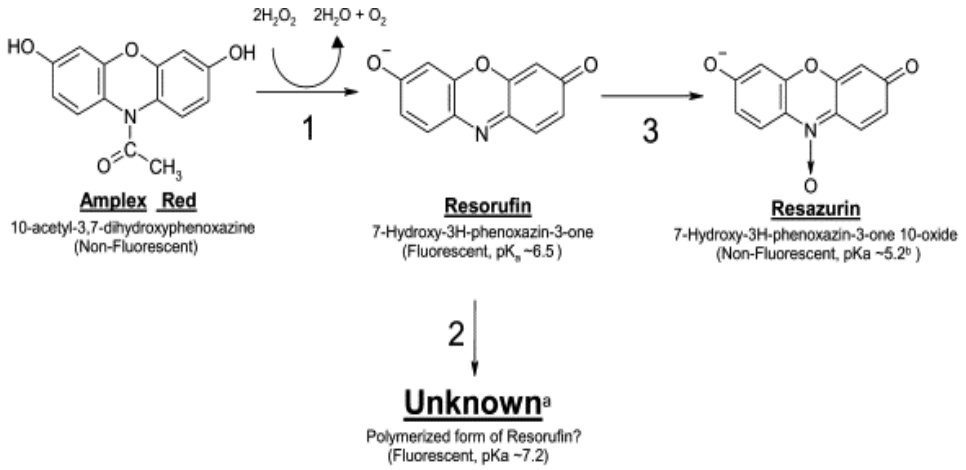

Figure 3-10: The oxidation of amplex red and reduction of resorufin. Amplex red is oxidised to form resorufin in the presence of hydrogen peroxide. Resorufin can be polymerized to form an unknown substance and reduced to form resazurin, a non-fluorescent product. If this was formed the fluorescence would reduce with time without the addition of other stimuli (Towne *et al.*, 2004).

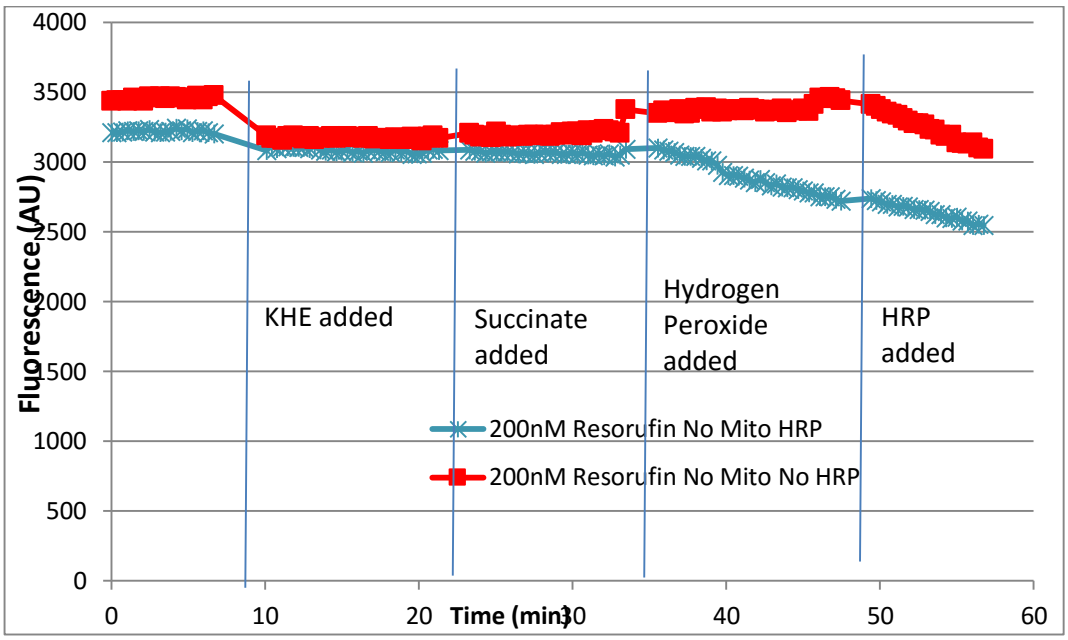

Figure 3-11: Hydrogen peroxide consumes resorufin in the presence of HRP. This graph shows resorufin fluorescence both in the presence (blue) and absence (red) of HRP. At each blue line an addition was made and explained below the traces. 196pmoles of hydrogen peroxide was the third addition. This is the highest amount of hydrogen peroxide the liver mitochondria would produce per minute. This resulted in consummation of resorufin in the presence of HRP only.

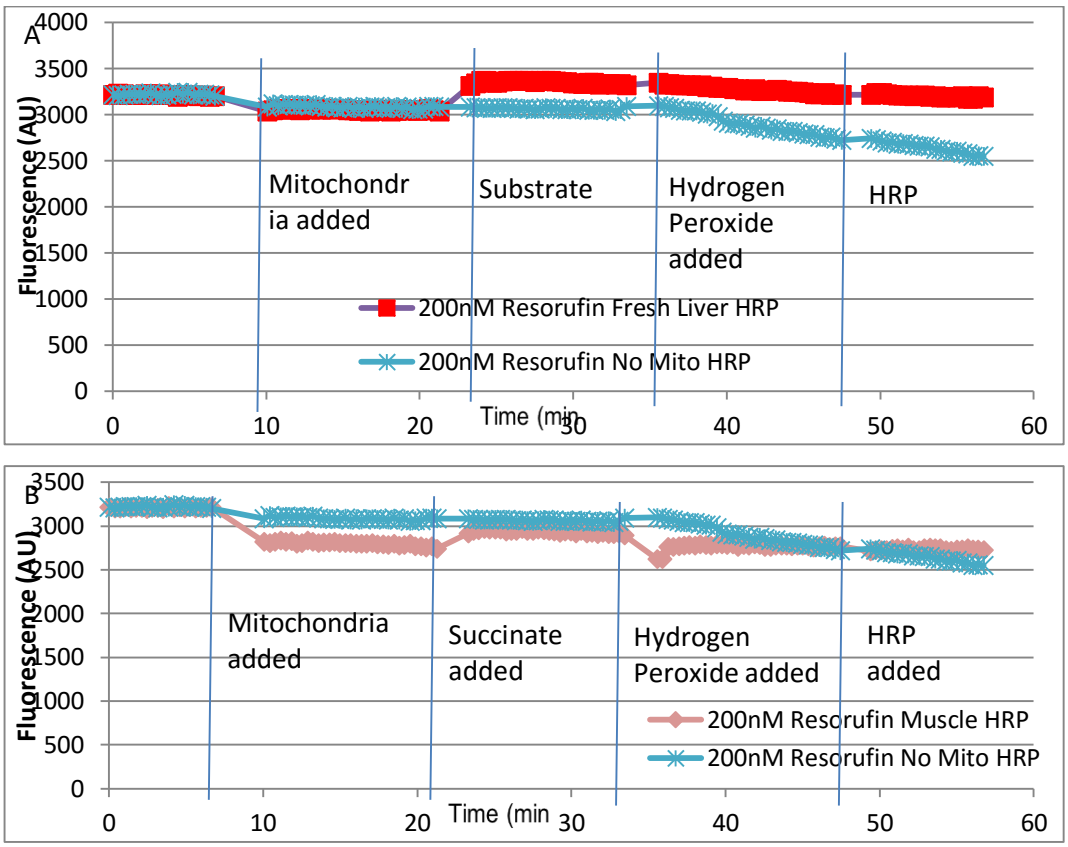

Figure 3-12: Mitochondria have a protective effect on resorufin consumption. Resorufin without mitochondria present is consumed with 196 pmoles hydrogen peroxide added. Resorufin is incubated with and without HRP. In one trace no mitochondria was added blue (A and B). The other trace on each graph has mitochondria added at the first blue line. In red (graph A) liver mitochondria was added to the assay. In pink (graph B) muscle mitochondria was added to the assay. In the presence of 196 pmoles hydrogen peroxide there was no resorufin consummation if mitochondria were present.

3.2.5. THE FLOURESCENCE DECREASE SEEN WITH SUBSTRATE ADDITION IS HRP DEPENDENT

The oxidation of amplex red in the presence of liver mitochondria occurs irrespective of the presence of HRP and substrate. In addition the oxidation is hydrogen peroxide independent. However the addition of a substrate reduces the amount of fluorescence detected from liver mitochondria with or without the presence of HRP in liver mitochondria. In figure 3-13 the HRP was added after substrate addition and compared to the rate of production if it was present prior to the addition. In the presence of a respiration substrate, addition of HRP increases the rate of amplex red oxidation similarly in liver and brain mitochondria. This suggests that the HRP sensitive amplex red signal in the presence of respiration substrate indicates the hydrogen peroxide released by the mitochondria.

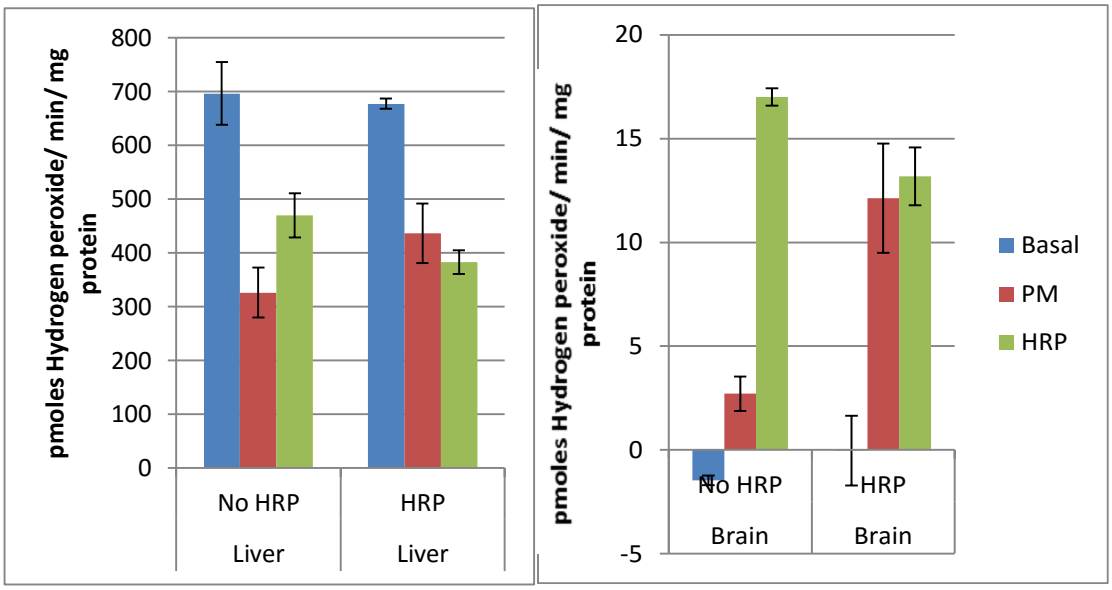

Figure 3-13: The presence of HRP increases hydrogen peroxide release in both liver (left) and brain mitochondria (right) in the presence of PM. Hydrogen peroxide release is measured in basal and substrate only states with and without HRP in liver and brain mitochondria. The addition of HRP is made after substrate addition to wells without HRP (green bars), while those with HRP from the beginning had an addition of KHE made after substrate addition. Results are mean and error bars are standard deviation based on three wells.

Addition of a substrate suppresses the hydrogen peroxide independent oxidation of amplex red. To determine if the suppression is substrate linked, different concentrations of PM were added. In figure 3-14 the rate of oxidation is shown as a percentage of the individual well's corresponding basal rate both with and without HRP. The percentage of oxidation decreases as the concentration of PM added increases. The suppression is higher if there is no HRP in the reaction medium. The increased suppression seen when HRP is absent suggests the presence of a HRP sensitive amplex red signal.

Two substrates are used in the main study to obtain details on the hydrogen peroxide release from specific sites in the ETC. Succinate and Pyruvate malate are the substrates used to dissect these sites out of the ETC. Pyruvate malate and glutamate malate are complex I linked substrate. Whereas succinate is a complex II linked substrate. Studying the effects of both these substrates and glutamate malate allows for the determination of the importance of complex I linked substrates. In figure 3-15 the role of each substrate both combined and individually is compared in the presence and absence of HRP. Glutamate, Pyruvate, Malate and the combinations of Glutamate malate and pyruvate malate show a marked suppression of the signal. Succinate a complex II linked substrate does not show the same degree of suppression.

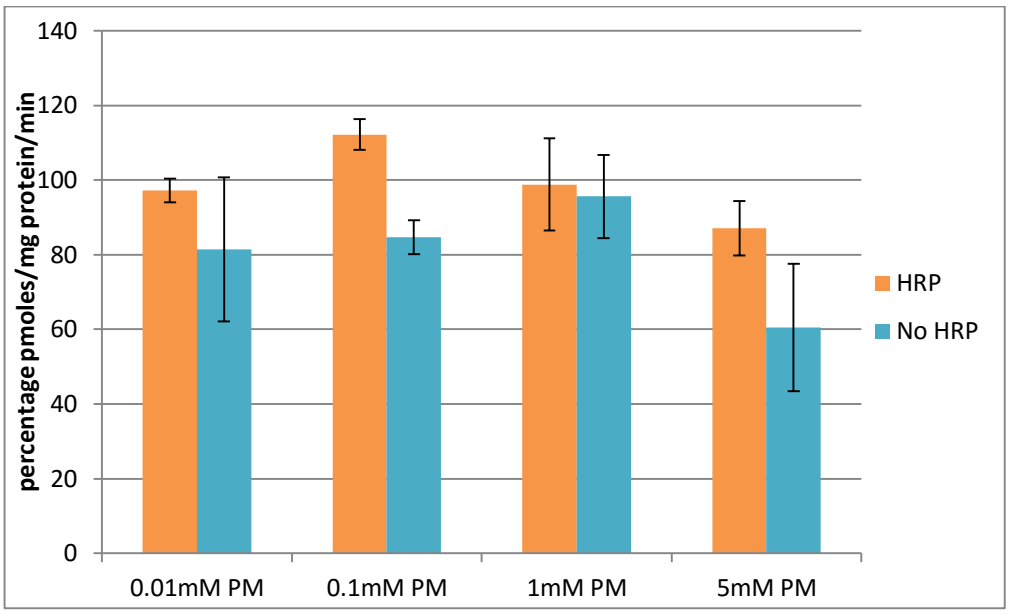

Figure 3-14: The suppression of basal signal is higher if the concentration of PM is higher. The bars show percentage of basal hydrogen peroxide release from liver mitochondria in the presence of HRP (Orange) and absence of HRP (Blue). Four concentrations of PM were added 0.01mM, 0.1mM, 1mM and 5mM (optimal). These experiments were repeated with 5-7 mice three technical replicates each. Mean is shown with error bars denoting standard deviation.

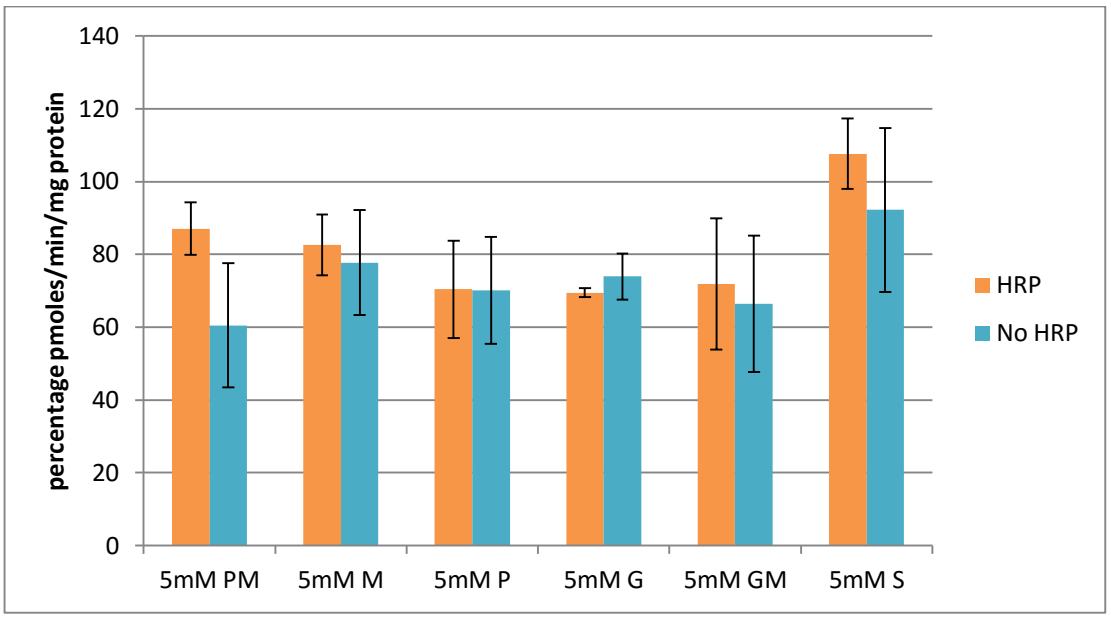

Figure 3-15: Complex I substrates cause more suppression than a complex II linked substrate. Basal rate of hydrogen peroxide release was calculated and the release in the presence of the denoted substrate. These results were used to obtain a percentage, denoting release as a percentage of basal release. S, P, M, G, PM and GM were added in 5mM. Mean of 4-7 replicates error bars showing standard deviation.

Data shown in chapter 3.2.3.3 suggested that the HRP sensitive amplex red signal is due to hydrogen peroxide release from the liver mitochondria. To analyse this further, the effect of myxathiozol on on Amplex Red fluorescence from liver mitochondria was assessed. In the presence of PM, myxathiozol inhibits respiration and oxygen consumption (Thierbach and Reichenbach, 1981b; Thierbach and Reichenbach, 1981a; Porter and Brand, 1995). When respiration is low, superoxide release is low. Accordingly, no HRP sensitive amplex red signal should be produced by liver mitochondria treated with myxathiozol. This is shown in Figure 3-16. The detected fluorescence is comparable in the experiments without HRP and under low superoxide conditions. The rate is significantly higher when HRP and pyruvate malate is present and myxathiozol is absent most likely due to superoxide production causing hydrogen peroxide release from the mitochondria.

I conclude that hydrogen peroxide release from liver mitochondria can be measured by the Ampled red method as the difference between fluorescence rates with and without HRP in the presence of respiration substrate.

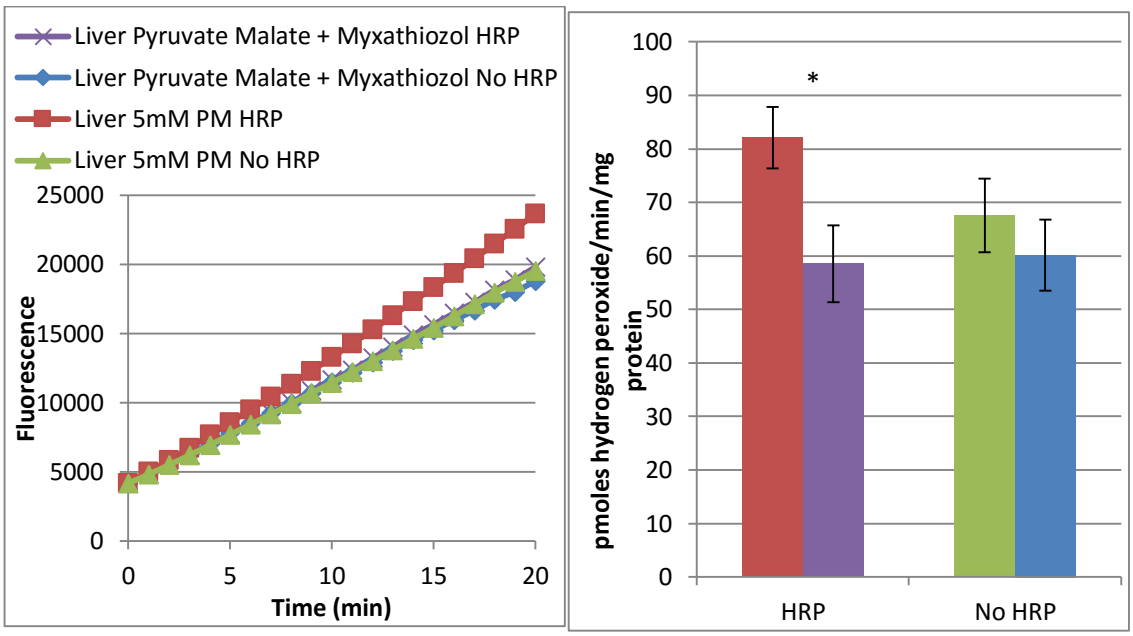

Figure 3-16: Myxathiozol inhibits the HRP-dependent increase of Amplex Red fluorescence from liver mitochondria. On the left the traces show the rate of fluorescence increase. Standardized means from four experiments (± SEM) are shown on the right in corresponding colour laid out in the key above the graph on the left. Measurements were taken with and without HRP, in the presence of a substrate or a substrate and myxathiozol. *=significantly different (t-test)

3.3. CHANGES IN HYDROGEN PEROXIDE RELEASE DURING AGEING AND DIETARY RESTRICTION

3.3.1. CHANGES IN BRAIN MITOCHONDRIA WITH AGE AND DIETARY RESTRICTION

Hydrogen peroxide release increases with age under both AL and DR conditions. In Figure 3-17 an increase with age is seen the presence of PM and rotenone, which indicates the maximum capacity of hydrogen peroxide release from complex I. This increase is significant between 3 and 24 months of age (figure.3-17).

The presence of succinate also shows increased hydrogen peroxide release with age from complex I (Figure 3-18). In AL brain mitochondria there is a significant increase in the presence of succinate between 3 months hydrogen peroxide release and 24 month ages. In the presence of succinate and rotenone as well as succinate, rotenone and antimycin a 24 and 30 months are significantly higher than that of 3 and 15 months. The addition of antimycin a shows the complex III maximal production. These results correlate and the succinate and rotenone result could be a result of the increase from complex III. Figure 3-19 shows an increase in hydrogen peroxide release from reverse flow through complex I between 3 and 15 months, but no further increase with age. Reverse flow shows no differences in hydrogen peroxide release from brain mitochondria in AL treated mitochondria. There is a tendency for all three parameters to improve in the oldest mice. This might be due to a survivor effect.

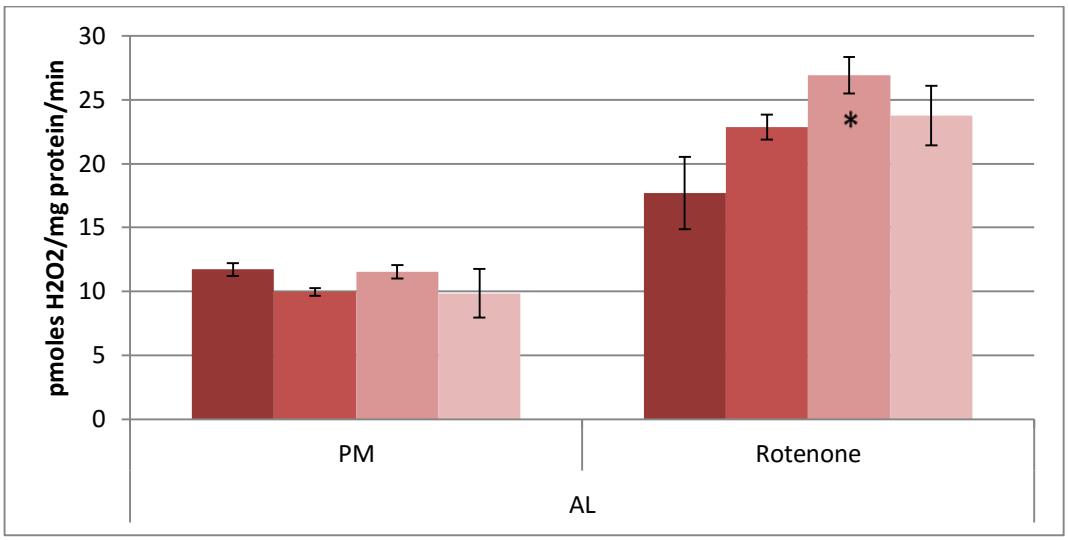

Figure 3-17: Maximum hydrogen peroxide release from complex one in brain mitochondria increases with age. These are the individual rate calculations after basal subtraction in the presence of PM and PM + Rotenone (rotenone) in AL treated brain mitochondria. Hydrogen peroxide release was determined in mice at ages of 3, 15, 24 and 30 months these are denoted by increasingly paler colours. Bars show the mean from n=4-6, with standard error bars displayed. *significantly different from three months (One-way ANOVA).

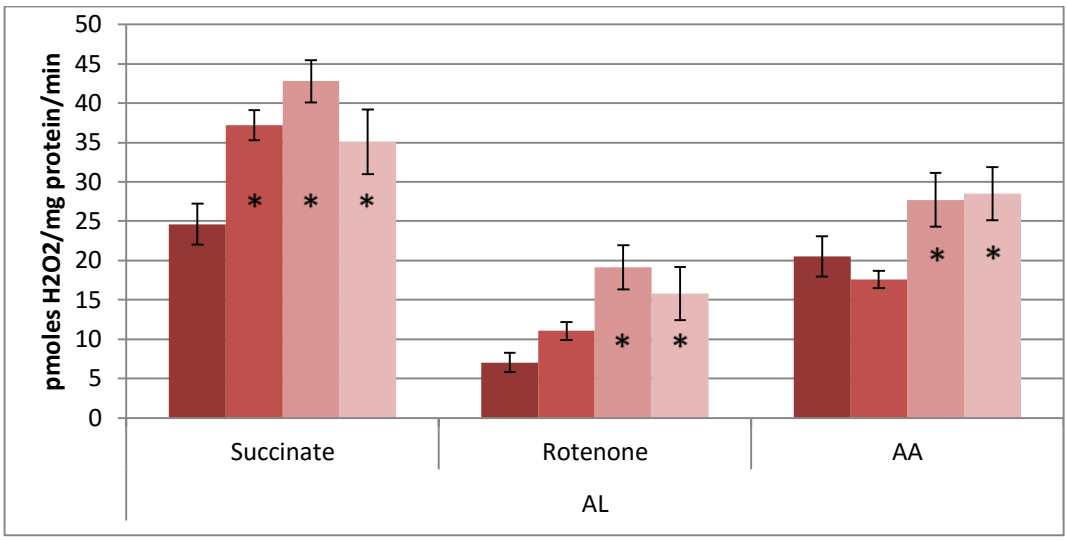

Figure 3-18: The release of hydrogen peroxide from AL brain mitochondria in the presence of a complex two-related substrate increases with age. Hydrogen peroxide release calculated minus basal from AL brain mitochondria in mice at ages of 3 15, 24 and 30 months. The release of hydrogen peroxide is measured in the presence of a complex II linked substrate, succinate. In succession two inhibitors are added; rotenone and antimycin A.. Age is shown in increasingly paler colour. Bars show the mean from n=4-6, with standard error bars displayed. *significantly different from three months.

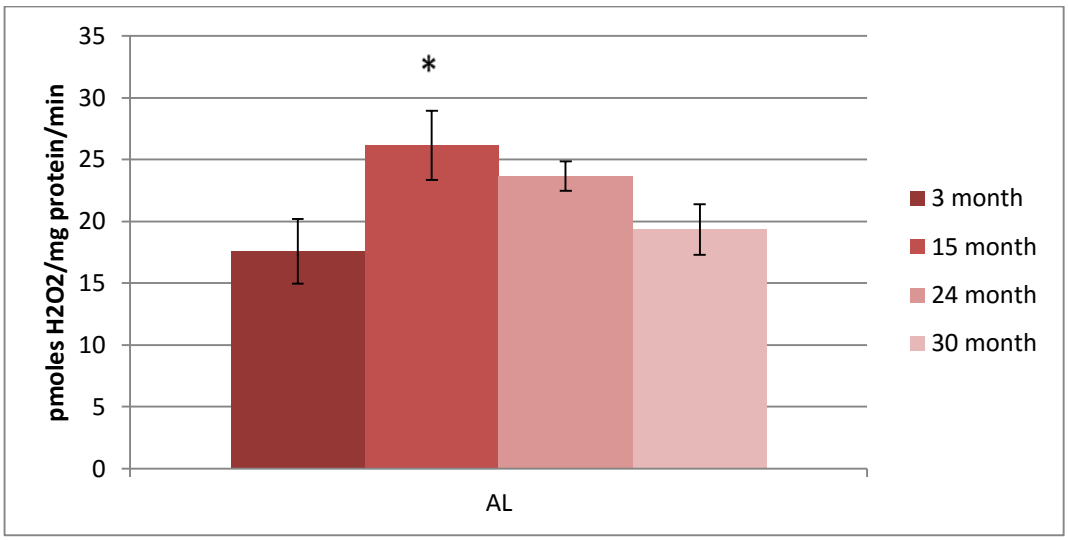

Figure 3-19: Hydrogen peroxide release by reverse flow is only increased between 3 and 15 months in brain mitochondria. Reverse flow of hydrogen peroxide released from AL brain mitochondria in mice at ages of 3 , 15, 24, 30 months. Increasingly paler colour denotes age. Bars show the mean from n=4-6, with standard error bars displayed. * significantly different from three months.

Dietary restriction (to 60% of intake under ad libitum feeding) was induced at 3 months of age. In general, isolated brain mitochondria from DR treated mice show lower hydrogen peroxide release than those from AL mice (figure 3-20, 3-21 and 3-22). The AL and DR values are significantly different at 15 and 24 months for both maximum release from complex I (Figure 3-20), complex II-linked substrate (Figure 3-21) and reverse flow (Figure 3-22), however, the only remaining difference at 30 months of age is in hydrogen peroxide release by reverse flow.

In brain mitochondria from AL mice the predominant increase is between 3 and 15 months. 15-30 month old mitochondria show a plateau effect when fed an AL diet. A DR diet resulted in improved maintenance of a lower level of hydrogen peroxide production up to 24 months of age, although Superoxide release in complex I (Figure 3-20) and complex II (Figure 3-21) linked respiration begins to increase after 15 months of age. The hydrogen peroxide production via reverse flow remains constant up to 30 months under DR (Figure 3-22). However, in very old DR mice (at 36 months, no AL mice were alive at this age) all measured parameters are at least as high as in AL mitochondria from 30 months old mice. In conclusion, the data show that the increase of hydrogen peroxide release with age from brain mitochondria under AL is postponed by DR.

Considering the plateau effect in brain and liver mitochondria the hydrogen peroxide release from complex I in was compared in both groups at 35% survival. 35% survival was determined using the lifespan curves in Figure 3-23. Dietary restriction extends lifespan in the mice, it also delays the effects of increased hydrogen peroxide release a marker of ageing. Mice on an AL diet were at 35% survival at 30 months and therefore we have no 36 month time point for this condition. Dietary restricted mice lifespan was extended so they were at 35% survival at 36 months. Comparing the hydrogen peroxide release in figure 3-24 shows there was no significant difference between these two conditions at 35% survival from reverse flow. There was a significant increase in DR hydrogen peroxide release in the presence of PM and PM and rotenone.

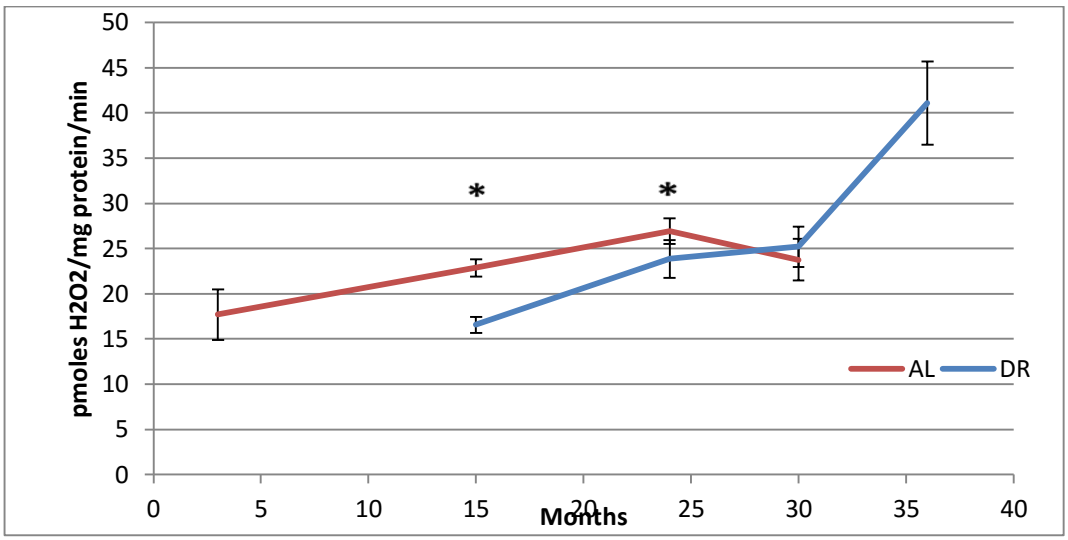

Figure 3-20: Brian mitochondria show decreased hydrogen peroxide release in DR from complex I when in the presence of PM and Rotenone. Maximal stimulation of complex I, PM + Rotenone (rotenone), hydrogen peroxide release from AL (red) and DR (blue) treated brain mitochondria. Hydrogen peroxide release was determined in mice at ages of 3, 15, 24, 30 months. Bars show the mean from n=4-6, with standard error bars displayed. *DR is significantly different from AL (t test).

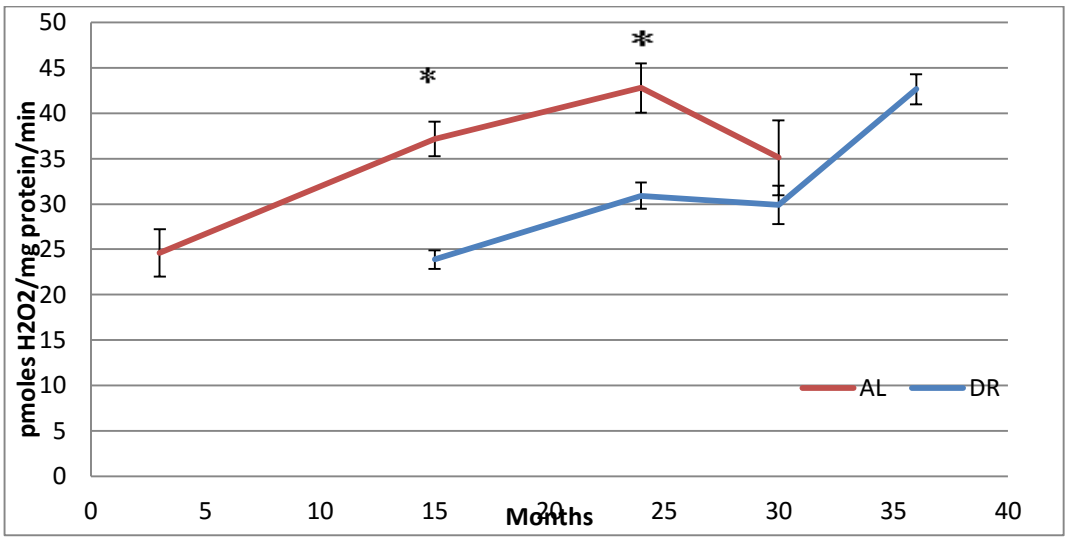

Figure 3-21: The increase of superoxide release from brain mitochondria with age in the presence of the complexII-linked substrate succinate is delayed by DR. In the presence of succinate these are the hydrogen peroxide release values from AL (red) and DR (blue). Values are the mean from n=4-6, with standard error bars displayed. *significantly different from AL.

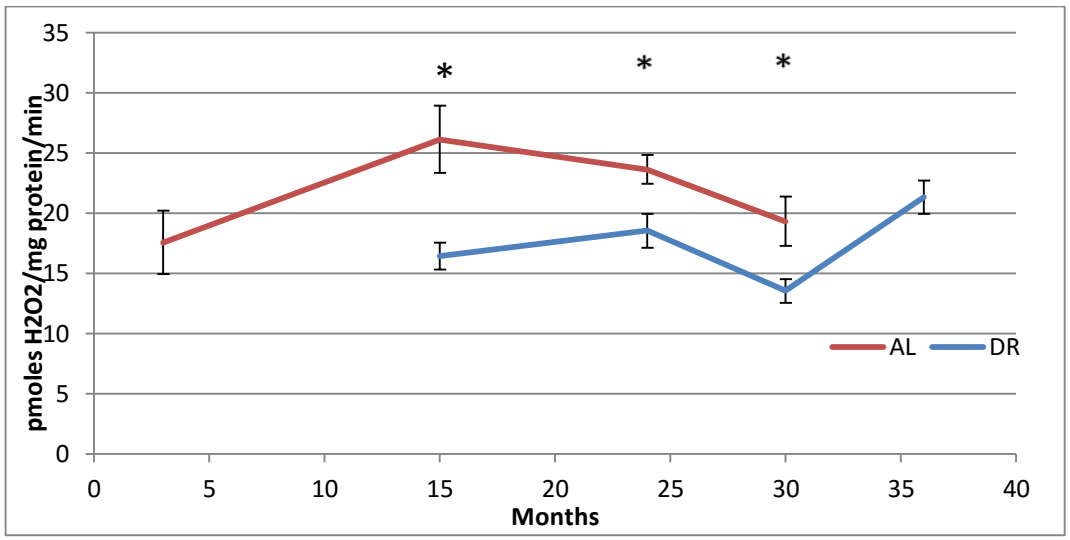

Figure 3-22: There is lower hydrogen peroxide release from reverse flow in DR brain mitochondria up to 30 months of age. Hydrogen peroxide production from muscle mitochondria as a result of reverse flow. Values are calculated after basal subtraction and the mean from n=4-6, with standard error bars displayed. *DR is significantly different from AL.

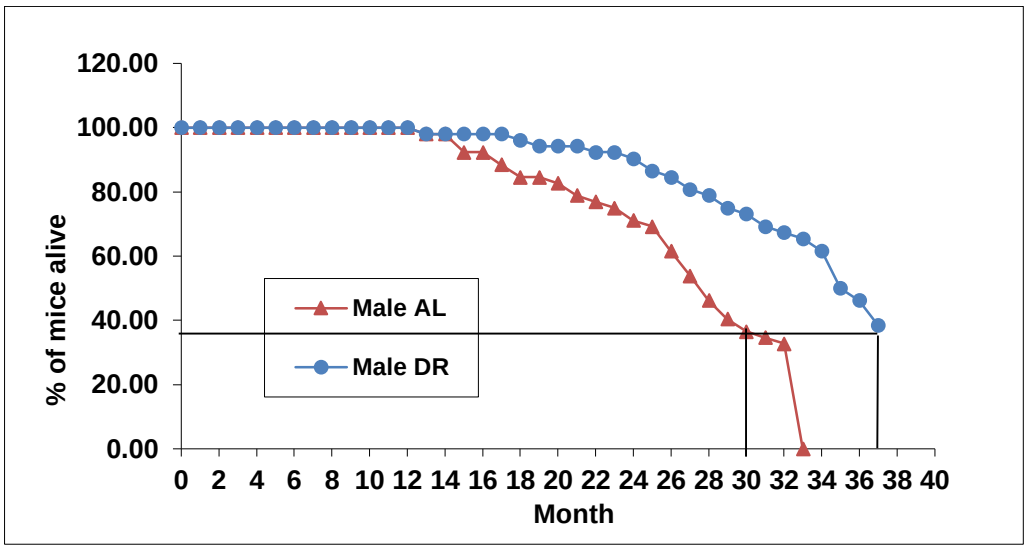

Figure 3-23: The lifespan curves of AL fed and DR males. Marked on the graph is the line at 35% survival this intersects the AL mice at 30 months and the DR mice at 36 months. These age the groups were used to compare the release of hydrogen peroxide.

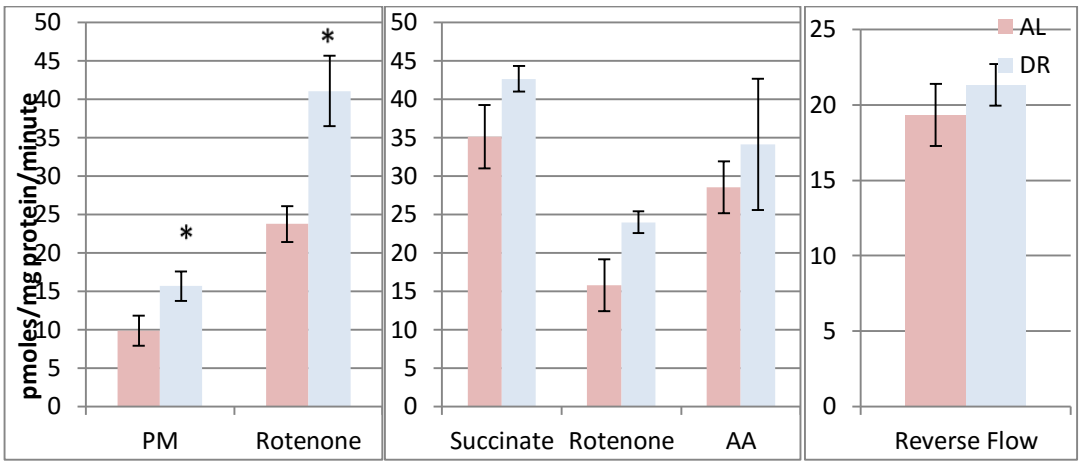

Figure 3-24: There is significantly higher hydrogen peroxide production from DR brain mitochondria in the presence of PM. Comparison of the release of hydrogen peroxide between AL and DR brain mitochondria at the same mouse survival percentage. 30 months from AL mice in red, and 36 months from DR mice in blue. These ages were determined to be 35% survival in each treatment. The left graph display the hydrogen peroxide release from complex I in the presence of PM and after the inhibition of complex I with rotenone. The middle graph shows the hydrogen peroxide release in the presence of complex II substrate succinate. In this graph, rotenone and antimycin A are added as inhibitors. The reverse flow is shown in the graph on the right. The condition added to determine each bar is given beneath. There were four mice per group and standard error is displayed. No significance was determined.

3.3.2. CHANGES IN HYDROGEN PEROXIDE RELEASE IN SKELETAL MUSCLE MITOCHONDRIA

Mitochondria isolated from skeletal muscle of the hind legs produced a higher level of hydrogen peroxide than isolated brain mitochondria from the same animals (compare Figures 3-17, 3-18 and 3-19 with 3-25, 3-26 and 3-27). 24 month old muscle mitochondria are not included in the analysis of muscle mitochondria. The 24 month old mitochondria were damaged during the isolation process and didn't return consistent results. In the presence of PM and rotenone, 30 month old AL muscle mitochondria have significantly higher hydrogen peroxide release than 3 and 15 month old ones. In conclusion the complex I linked hydrogen peroxide release from skeletal muscle mitochondria increases with age.

Succinate only stimulation of muscle mitochondria shows a significant increase with age between all time-points in AL mitochondria. The presence of rotenone in addition to succinate also shows a continuous increase with age in AL mitochondria. Complex III hydrogen peroxide release in AL mitochondria is higher in 15 and 30 month than 3 months (Figure 3-26). Reverse flow is significantly increased with age in muscle mitochondria (Figure 3-27).

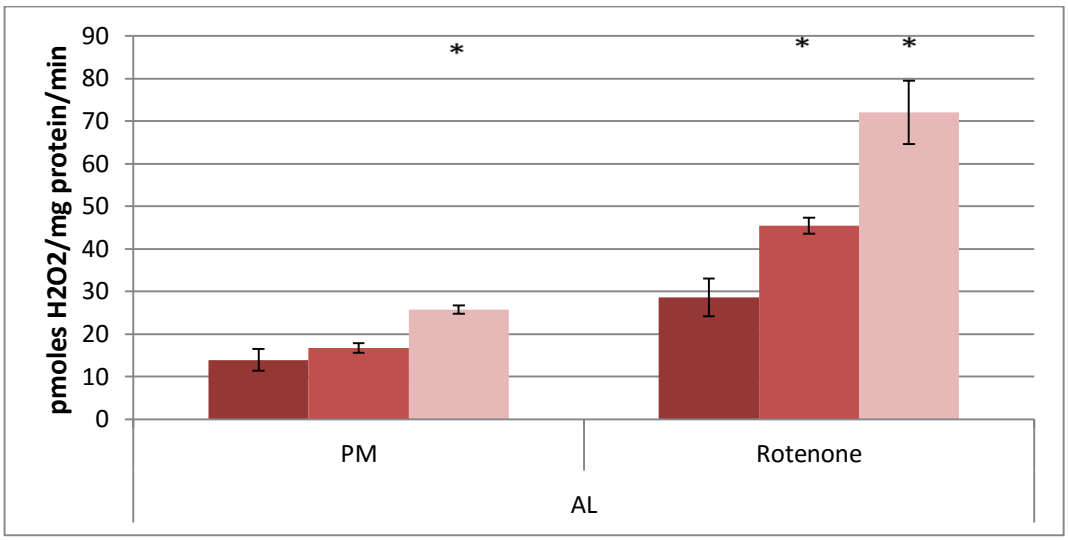

Figure 3-25: There is an increase in hydrogen peroxide release from complex I in AL muscle mitochondria with age. Values are calculated after basal subtraction. Hydrogen peroxide release was determined in mice at ages of 3, 15, 24 and 30 months. Increasing age is shown with increasingly paler colour. Bars show the mean from n=4-6, with standard error bars displayed. *significantly different from three months under the same conditions.

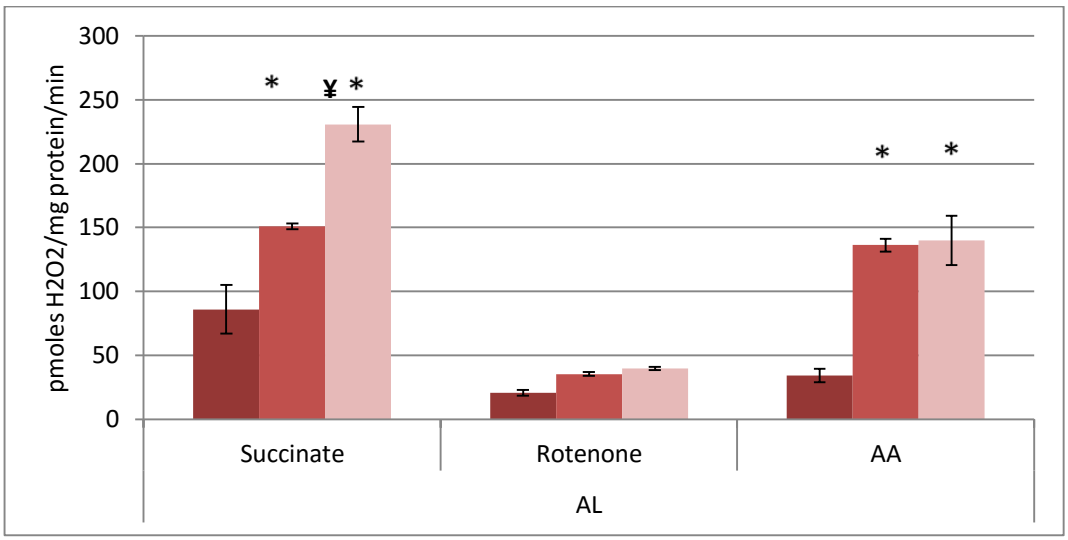

Figure 3-26: Hydrogen peroxide release in the presence of succinate and when both rotenone and antimycin A is present increases with age in muscle mitochondria. The release of hydrogen peroxide is measured in the presence of a complex II linked substrate, succinate. In succession two inhibitors are added rotenone and antimycin a. Increasingly paler red shows different ages; 3, 15, and 30 months. Bars show the mean from n=4-6, with standard error bars displayed. * significantly different from three months. ¥ significantly different from 15 months.

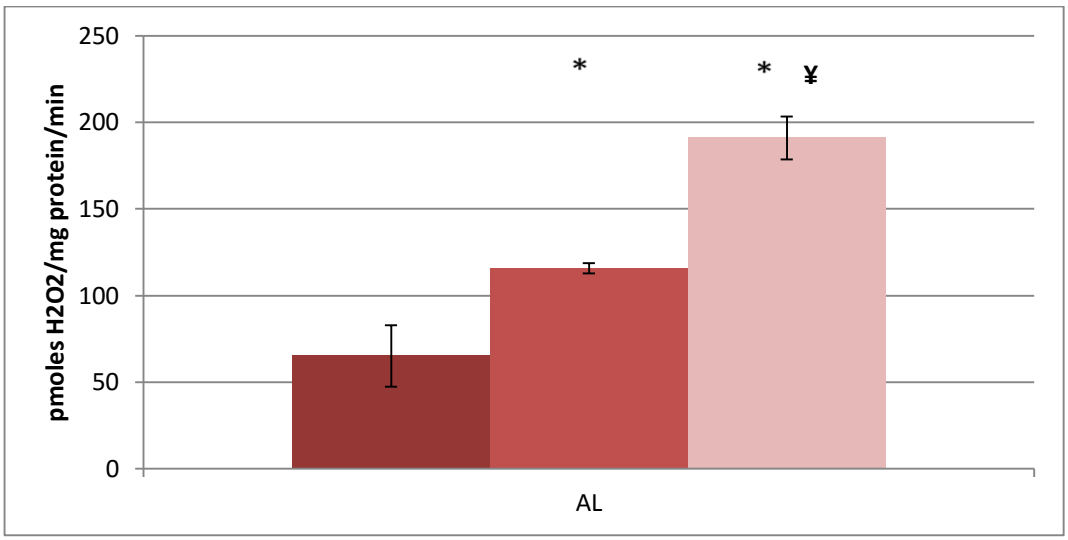

Figure 3-27: Release of hydrogen peroxide via reverse flow increases with age in muscle mitochondria. Hydrogen peroxide release via reverse flow in Al muscle mitochondria. Three ages are shown, 3, 15 and 30 months denoted by paler red colour as age increases. Bars show the mean from n=4-6, with standard error bars displayed. *significantly different from three months and ¥ significantly different from 15 months.

Dietary restriction reduces the hydrogen peroxide release in skeletal muscle mitochondria at 15 and 30 months of age, both in terms of maximum capacity of complex I (Figure.3-28), under respiration with a complex II linked substrate (Figure 3-29) and in reverse flow (Figure 3-30). In conclusion there is a higher hydrogen peroxide release from complex I in AL mitochondria and DR postpones this age-dependent increase.

The plateau effect seen in the Brain and Liver mitochondria is not observed in the skeletal muscle mitochondria. Considering the plateau effect in brain and liver mitochondria, the effect was more obvious at 24 and 30 months rather than 15 and 30 months. Therefore the hydrogen peroxide release from complex I in was compared in both groups of skeletal muscle at 35% survival in figure 3-31. Mice at 35% survival under DR did show no difference from the AL fed mice at the same percentage survival.

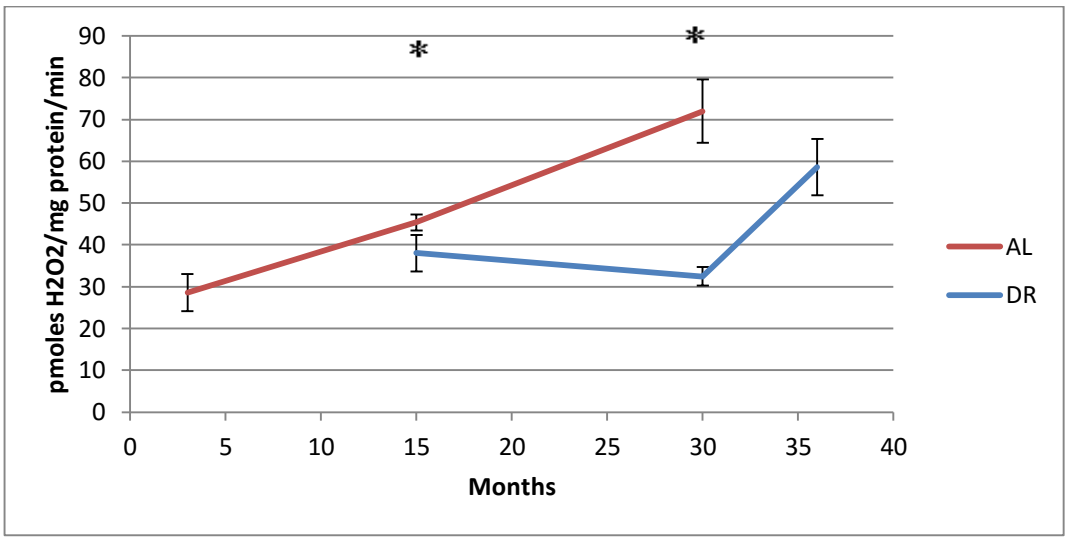

Figure 3-28: The release of hydrogen peroxide from complex I when it is maximally stimulated is significantly lower in DR muscle mitochondria than AL. Maximal stimulation of complex I, PM + Rotenone (rotenone), hydrogen peroxide release from AL (red) and DR (blue). Values are calculated after basal subtraction and the mean is displayed from n=4-6, with standard error bars. *DR is significantly different from AL.

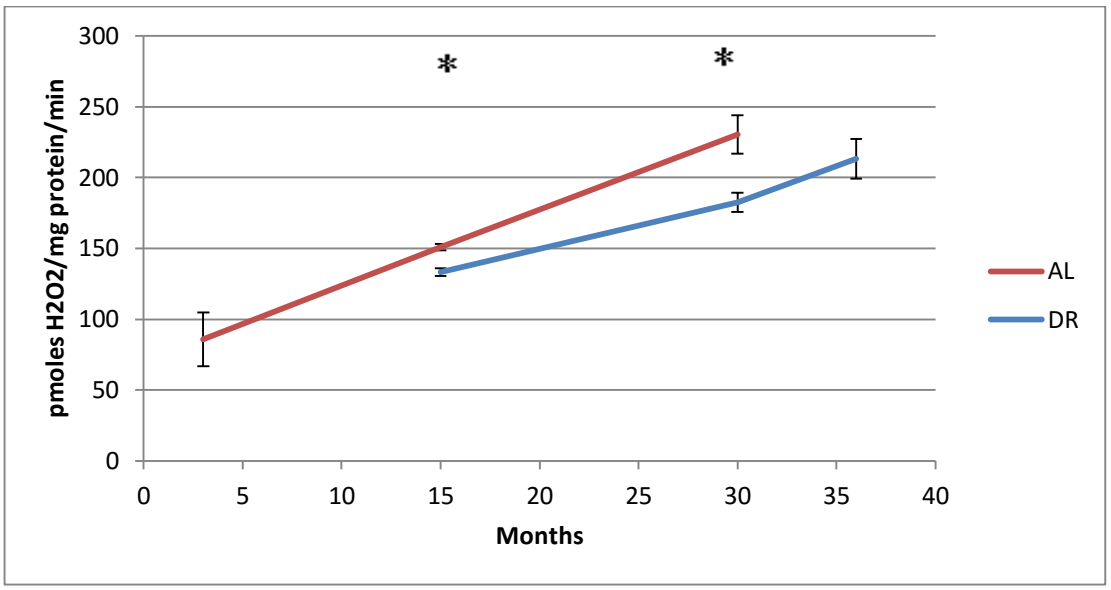

Figure 3-29: The release of hydrogen peroxide in the presence of succinate is significantly lower in DR muscle mitochondria than AL. In the presence of succinate these are the hydrogen peroxide release values from AL (red) and DR (blue). Values are the mean minus basal from n=4-6, with standard error bars displayed. *DR is significantly different from AL.

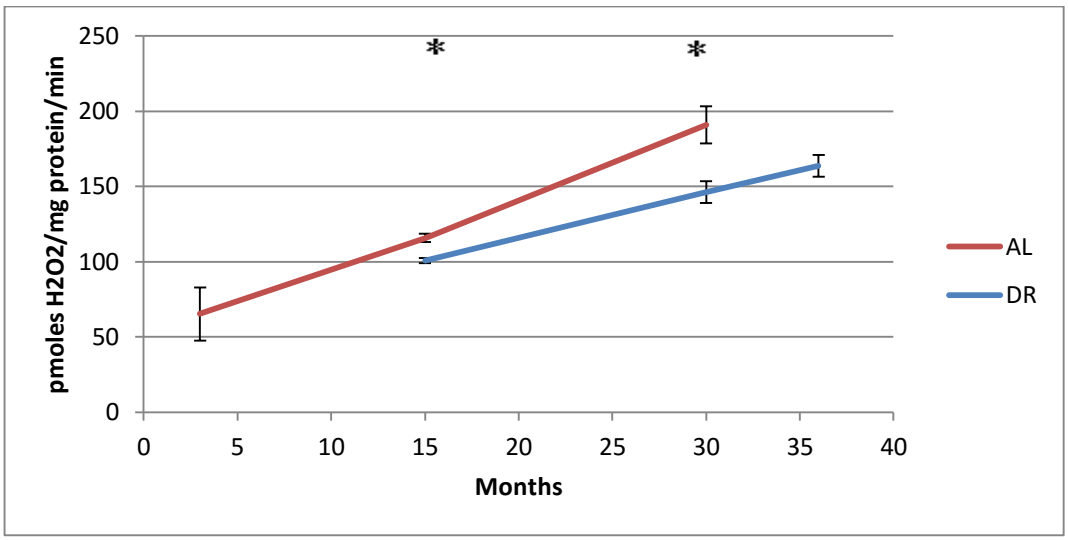

Figure 3-30: The release of hydrogen peroxide from complex I via reverse flow is significantly lower in DR muscle mitochondria than AL muscle mitochondria. Values are reverse flow calculated after basal subtraction and shown is the mean from n=4-6, with standard error bars displayed. *DR is significantly different from AL**.**

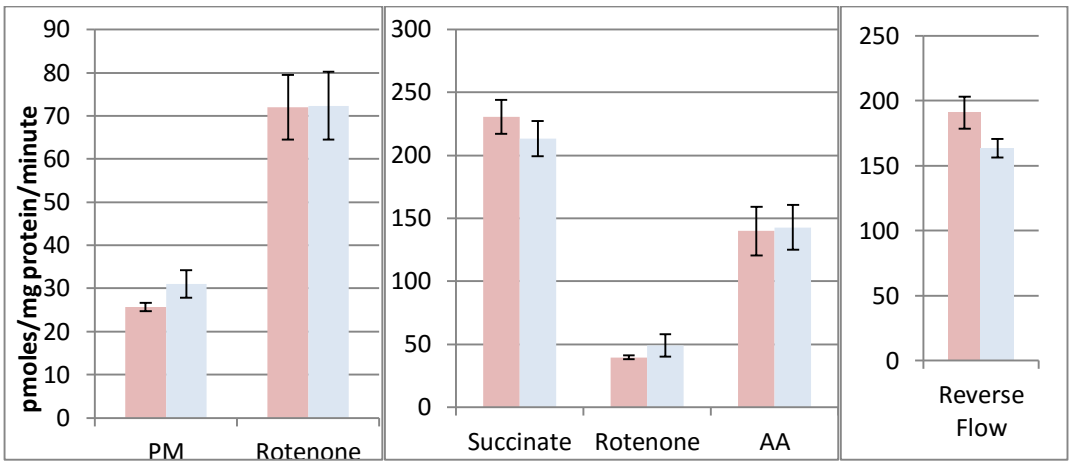

Figure 3-31: There is no significant change between AL and DR at 35% survival. Comparison of the kinetic release of hydrogen peroxide between AL and DR muscle mitochondria at the same mouse survival percentage. 30 months for AL mice in ligh red, and 36 months for DR mice in light blue. These ages were determined to be 35% survival in each treatment. Two substrates were added separately, PM in the left graph, rotenone added as an inhibitor, and succinate in the middle and right graph. Mitochondria in the presence of succinate had two inhibitors added in succession, rotenone and antimycin A. There were four mice per group and standard error is displayed.

3.3.3. THE CHANGE IN HYDROGEN PEROXIDE PRODUCTION IN LIVER MITOCHONDRIA

Hydrogen peroxide release is measured using the corrected method discussed in chapter 3.2. The corrected method is the difference between the presence and absence of HRP and was only used when measuring 3, 24, 30 and 36 month old mitochondria. The liver mitochondria were measured at 15 months but only in the presence of HRP. The corrected data is more accurate so the 15 month data is not included. The rate of hydrogen peroxide release was measured from isolated liver mitochondria from mice fed an AL and a DR diet at 3, 24 and 30 months of age. There is no significant change when only PM is present in AL. In the presence of PM and rotenone AL mitochondria show no significant change with age. In conclusion the complex I linked hydrogen peroxide release doesn't increase with age in liver mitochondria.

Succinate only stimulation of liver mitochondria shows no significant changes with age in AL mitochondria. The presence of rotenone in addition to succinate shows an increase with age in AL mitochondria between 3 and 24 months. Between 3 and 30 months no significant change is seen in liver mitochondria. Complex III hydrogen peroxide release in AL mitochondria is higher in 30 month than 3 months. Reverse flow is unchanged with age in AL liver mitochondria. Complex III is the only specified site of hydrogen peroxide release which is changed with age in liver mitochondria.

There is a plateau effect seen in AL liver mitochondria similar to the brain. 24 month old AL mice have no significant difference to 30 month old AL mice in terms of hydrogen peroxide release. The maximum capacity of complex I to produce superoxide and the release of hydrogen peroxide in the presence of succinate were not significant. This shows the plateau effect of AL fed mice as they are both significantly increased compared to 3 month old mice. In Dietary restricted mice these ages are also not significantly different and the increase is seen at 36 months which is significantly increased rate compared to 24 and 30 months. Comparing both the groups in figure 38 at 35% survival there is no significant difference between the two conditions.

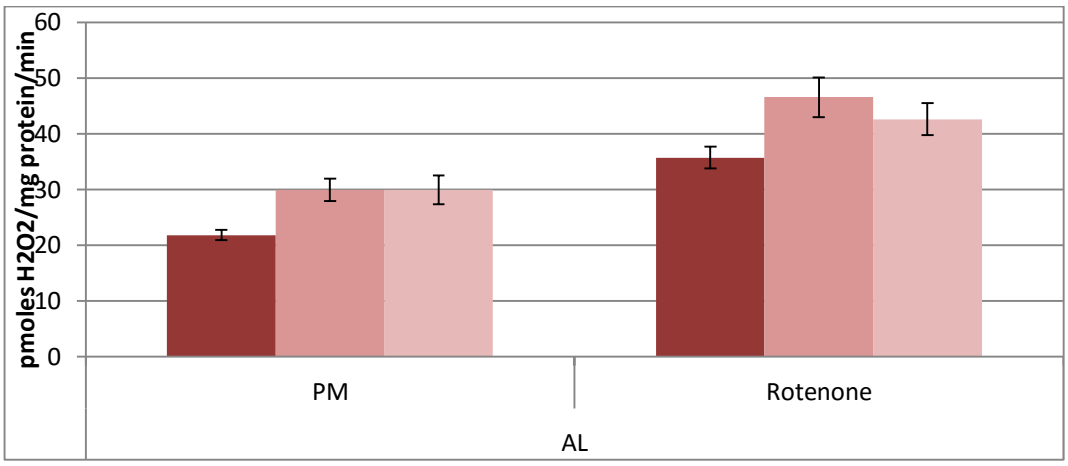

Figure 3-32: The values for corrected release of hydrogen peroxide from liver mitochondria. In the presence of PM and PM + Rotenone these are the hydrogen peroxide release values from AL Liver mitochondria. Hydrogen peroxide release was determined in mice at ages of 3, 24, and 30 months these are denoted by increasingly paler colours. Bars show the mean from n=4-6, with standard error bars displayed. No significant changes.

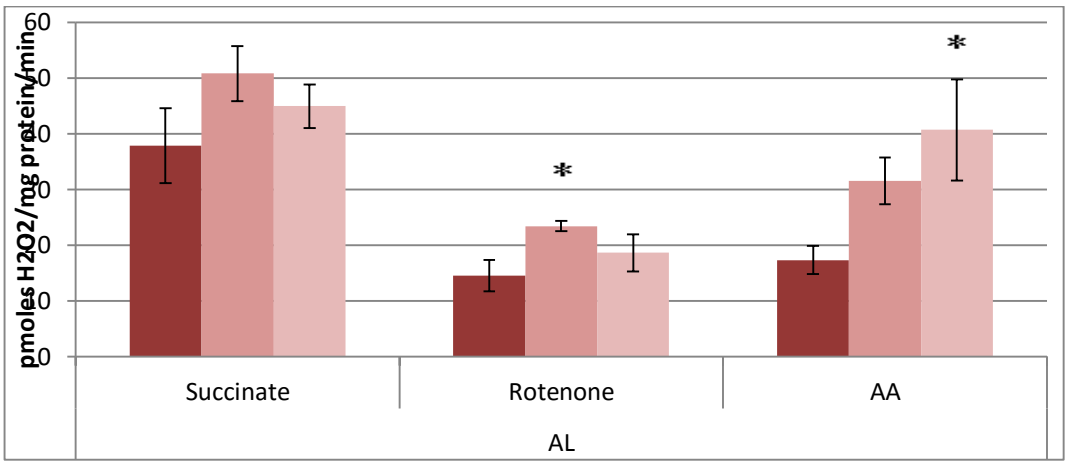

Figure 3-33: The values for corrected release of hydrogen peroxide from liver mitochondria. These are the hydrogen peroxide release values from AL liver mitochondria. Hydrogen peroxide release was determined in the presence of succinate from mice at ages of 3, 24, and 30 months these are denoted by increasingly paler reds. After the addition of succinate in succession two inhibitors are added rotenone, and antimycin a. Bars show the mean from n=4-6, with standard error bars displayed. *significantly different from three months.

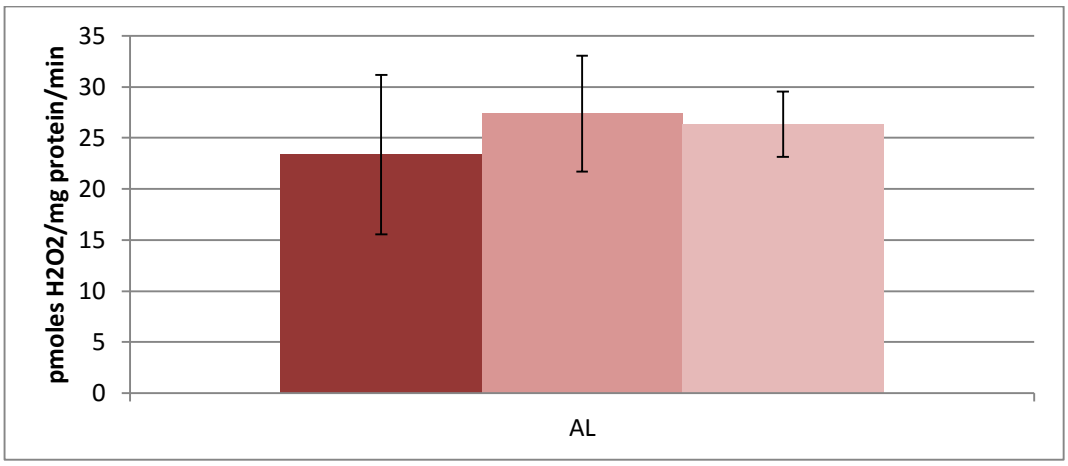

Figure 3-34: The values for corrected reverse flow release of hydrogen peroxide from liver mitochondria. The reverse flow hydrogen peroxide release was determined in mice at ages of 3, 24 and 30 months these are denoted by increasingly paler colours. Bars show the mean from n=4-6, with standard error bars displayed.

Dietary restriction in liver mitochondria shows a decrease in hydrogen peroxide release after onset at 24 and 30 months of age compared with 3 months. Dietary restriction affects liver mitochondria hydrogen peroxide release at 24 and 30 months direct comparison shows a reduced level of release. The maximum capacity of complex I superoxide release as marked by hydrogen peroxide release shows increased levels of production in AL fed mice at both 24 and 30 months (figuren3-35). This is supported by complex II linked respiration which shows increased hydrogen peroxide release at 24 and 30 months in AL (figure 3-36). This increased rate is also predominantly from complex I as the reverse flow shows significantly lower rates of hydrogen peroxide release from complex I at 24 and 30 months (Figure 3-37). In conclusion the decrease in hydrogen peroxide release in DR is a result of complex I changes.

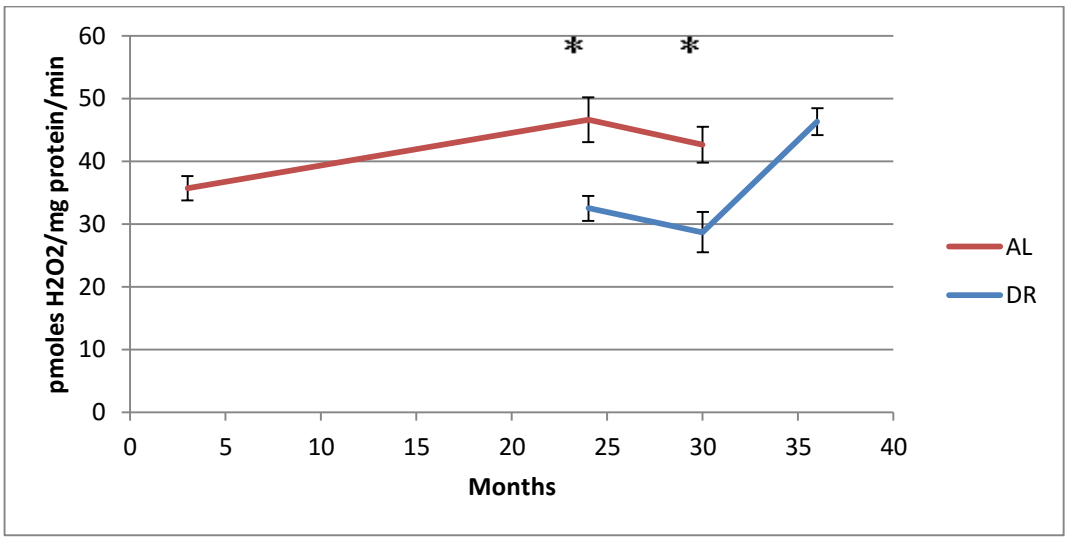

Figure 3-35: The release of hydrogen peroxide in the presence of PM and Rotenone is significantly lower in DR than AL liver mitochondria up to 30 months of age. Maximal stimulation of complex I, PM + Rotenone (rotenone), hydrogen peroxide release from AL (red) and DR (blue). Values show the mean with basal subtracted from n=4-6, with standard error bars displayed. *DR is significantly different from AL.

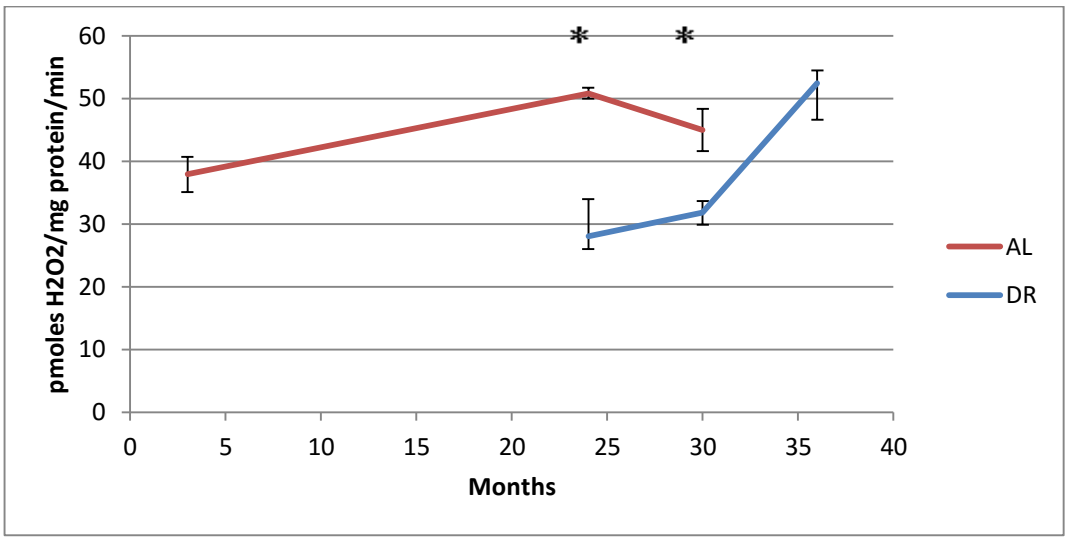

Figure 3-36: The release of hydrogen peroxide release from liver mitochondria is lower in the DR than AL up to 30 months of age. In the presence of succinate these are the hydrogen peroxide release values from AL (red) and DR (blue). Values are the mean with basal subtracted from n=4-6, with standard error bars displayed. *DR is significantly different from AL.

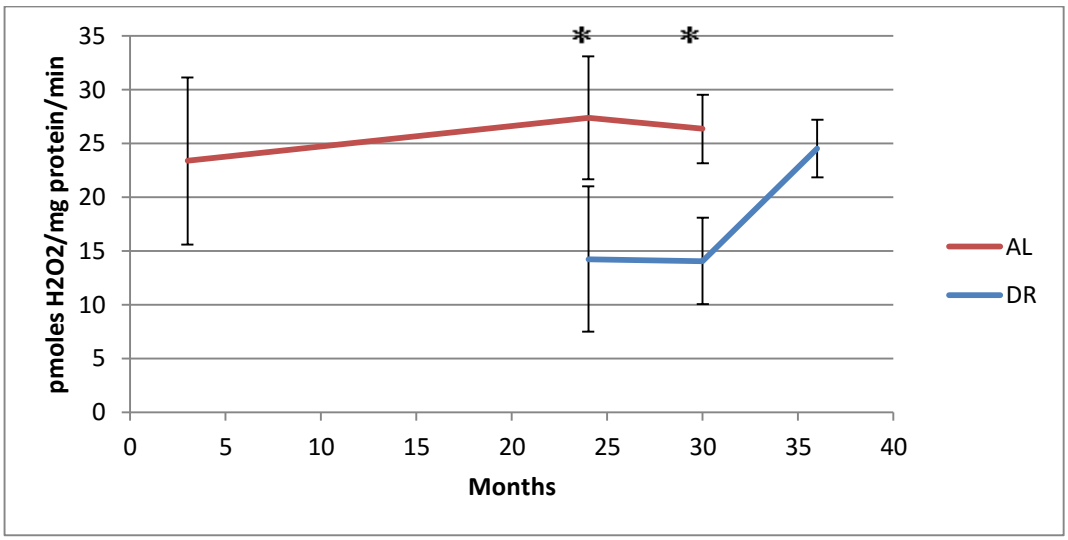

Figure 3-37: Up to 30 months of age there is significantly lower hydrogen peroxide release as a result of reverse flow from DR liver mitochondria compared to AL. The values are the mean with basal subtracted from n=4-6 mice for reverse flow, with standard error bars displayed. *DR is significantly different from AL**.**

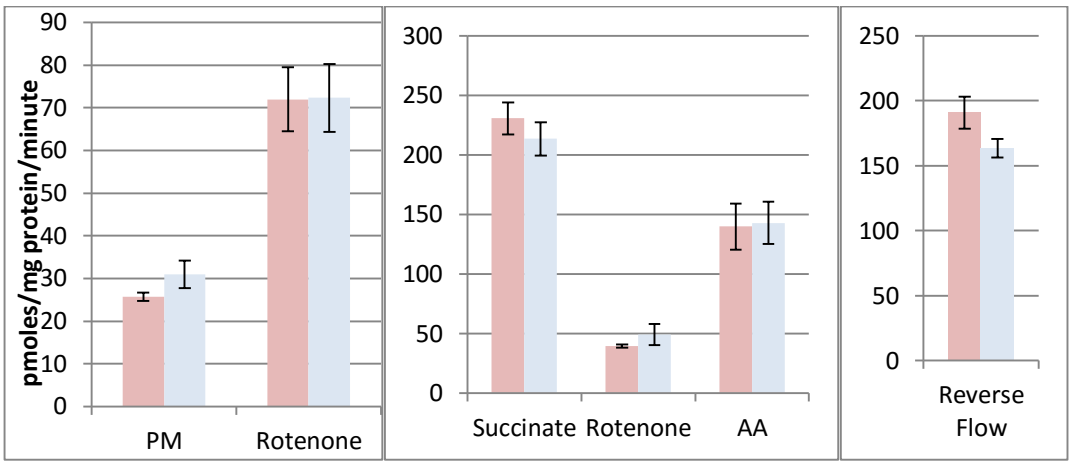

Figure 3-38: There is no significant difference between the hydrogen peroxide release from AL and DR mitochondria at 35% survival. These graphs show the comparison of hydrogen peroxide release between AL and DR brain mitochondria at the same mouse survival percentage. Hydrogen peroxide release was calculated in the presence of PM and rotenone (left), Succinate, rotenone and antimycin A (middle) and the reverse flow was calculated in the final graph. 30 months for AL mice in red, and 36 months for DR mice in blue. These ages were determined to be 35% survival in each treatment. There were four mice per group and standard error is displayed. No significance was determined.

3.3.4. POSTPRANDIAL HYDROGEN PEROXIDE RELEASE IS LOWER THAN THAT OF PREPRANDIAL FROM 30 MONTH OLD MITOCHONDRIA AFTER LONG TERM DIETARY RESTRICTION

In the comparison between AL and DR animals the measurements are always taken at 8am. The DR mice are fed at 8am. Consequently the DR mice haven't eaten for 24 hours prior to measurement. Postprandial states have been shown to decrease ROS in human cells (Sodre *et al.*, 2011). Fasted DR oxidative stress is higher than fed DR oxidative stress (Dani *et al.*, 2010). The differences in oxidative stress suggest fasting could mask the dietary restriction changes. The possibility is that the difference between AL and DR is affected by the increased time without food. The DR mitochondria at 30 months old in this study were compared with DR mitochondria measured six hours after feeding (postprandial - PMDR). 30 months old mice have been treated with DR for 27 months. Figure 3-39, 3-40 and 3-41 outline the rate of hydrogen peroxide production in brain, muscle and liver mitochondria for these conditions.

I have shown in Figure 3-20 that in the presence of only PM normal DR conditions result in no significant difference in brain mitochondria. This doesn't change in PMDR brain mitochondria. Maximum capacity of complex I to produce superoxide is equal in AL and pre-prandial DR mitochondria, but is decreased only in PMDR. In PMDR mitochondria reverse flow is significantly increased compared to DR and is unchanged when compared to AL. Complex III is unchanged in AL, DR or PMDR.

In muscle mitochondria between DR mitochondria showed significantly lower hydrogen peroxide release than AL mitochondria in chapter 3.3.2 analysed by t-test. The same data is analysed here using an ANOVA due to the presence of PMDR a third group. There is no change in AL and DR in the presence of PM only or PM and rotenone when analysed by ANOVA to include the third group. PMDR release of hydrogen peroxide is significantly lower than both AL and DR when only PM is present. PM and rotenone shows a significant decrease in PMDR when compared to AL mitochondria.

As shown before (Figures 3-35-37), In liver mitochondria there is significantly lower hydrogen peroxide release from DR mice compared to AL; this occurs in the presence of PM, PM and rotenone and reverse flow. PMDR mitochondria follow the same trend

as DR mitochondria. PMDR is only lower in DR liver mitochondria when in the presence of PM only. In the presence of PM only, muscle and liver mitochondria have significantly lower hydrogen peroxide release from PMDR than both AL and DR. In brain and muscle mitochondria maximum complex I hydrogen peroxide release is significantly lower from PMDR compared to AL and DR mitochondria. Maximal stimulation of complex I in liver PMDR mitochondria is significantly lower than AL mitochondria only. In muscle and liver mitochondria, postprandial complex I hydrogen peroxide release is lower than preprandial already under basal conditions.

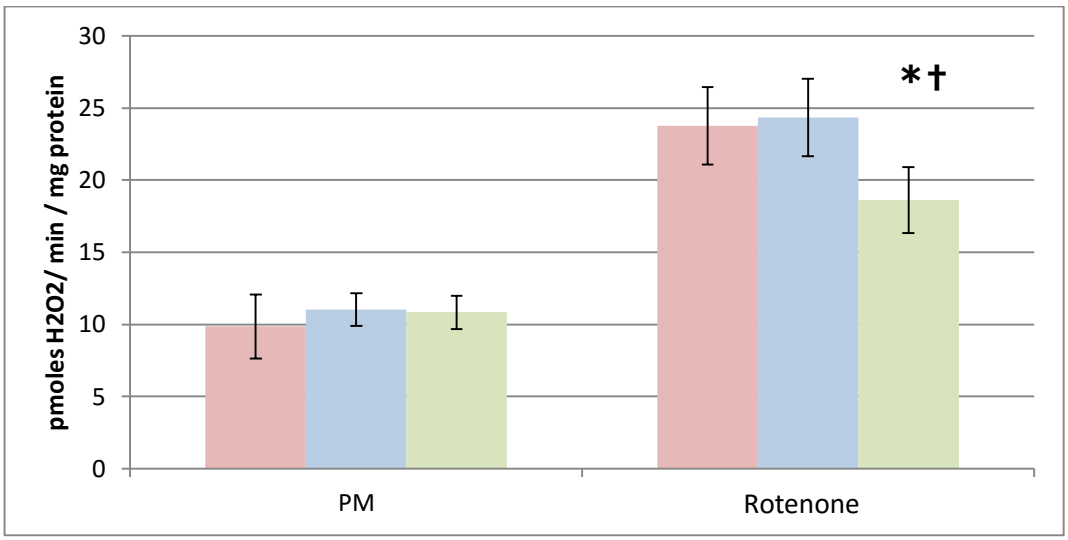

Figure 3-39: PMDR brain mitochondria have significantly lower hydrogen peroxide release capacity than both AL and DR brain mitochondria. The rate of hydrogen peroxide production in brain mitochondria in the presence of a control diet (AL), a dietary restricted diet (DR) and a postprandial DR diet (PMDR). AL (light red) and standard DR (light blue) which are culled prior to feeding were compared to post prandial mice which were culled six hours after being fed (PMDR, light green). The graph shows Pyruvate Malate (PM) as a substrate followed by the further addition of rotenone (PM + ROT). The bars are mean of n=4 mice and show standard error bars. * significantly different from AL. † significantly different from DR.

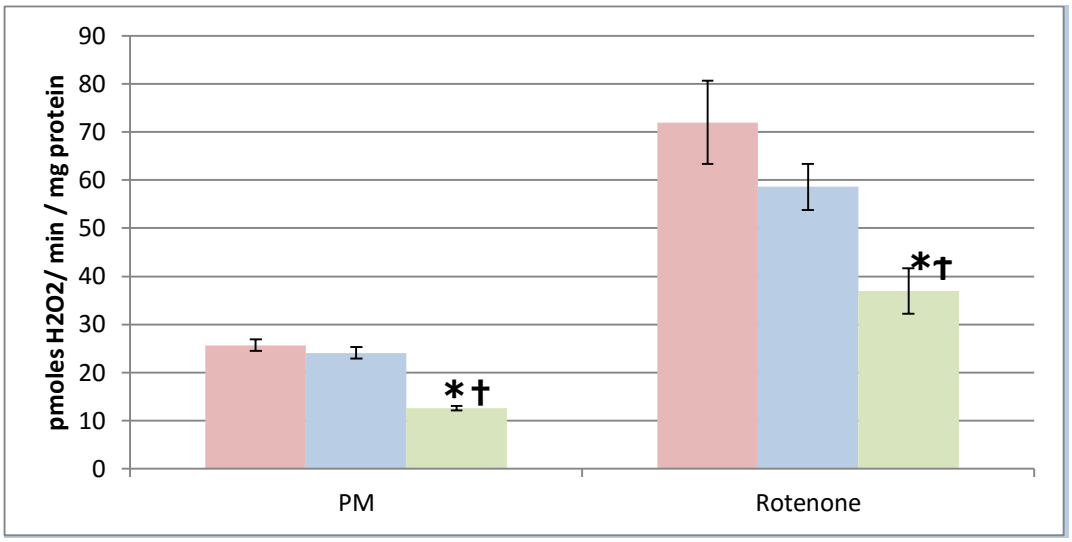

Figure 3-40: PMDR muscle mitochondria have significantly lower hydrogen peroxide release than AL muscle mitochondria. The rate of hydrogen peroxide production in muscle mitochondria in the presence of a control diet (AL) in light red, a dietary restricted diet (DR) in light blue and a postprandial DR diet (PMDR) in light green. The graph shows Pyruvate Malate (PM) as a substrate followed by the further addition of rotenone (PM + ROT). The bars are mean of n=4 mice and show standard error bars. * significantly different from AL. † significantly different from DR.

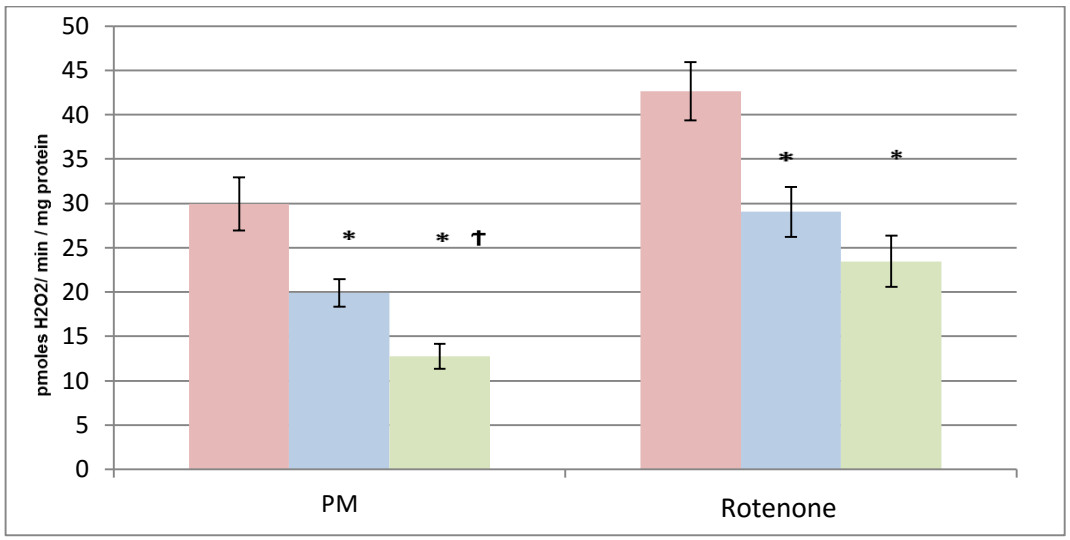

Figure 3-41: PMDR liver mitochondria have significantly lower hydrogen peroxide release than both AL and DR liver mitochondria. The rate of hydrogen peroxide production in liver mitochondria in the presence of a control diet (AL), a dietary restricted diet (DR) and a postprandial DR diet (PMDR). The graph shows Pyruvate Malate (PM) as a substrate followed by the further addition of rotenone (Rotenone). The bars are mean of n=4 mice and show standard error bars. * significantly different from AL. † significantly different from DR.(one-way ANOVA)

3.4. SHORT-TERM DIETARY RESTRICTION AND SHORT-TERM RAPAMYCIN TREATMENT HAVE A SIMILAR EFFECT ON HYDROGEN PEROXIDE RELEASE.

3.4.1. HYDROGEN PEROXIDE RELEASE IS LOWER IN PRE- AND POSTPRANDIAL CONDITIONS AFTER SHORT-TERM DIETARY RESTRICTION

Female mice were fed a short-term dietary restricted diet. The diet was imposed at 12 months and mice were culled and mitochondria obtained at 15 months. The mice which were dietary restricted were culled 24 hours post prandial (DR) or 6 hours post prandial (PMDR).

In brain and muscle mitochondria there was no significant change in hydrogen peroxide release from complex I as a result of reverse flow shown in figure 3-42 and Figure 3-43. When maximum capacity of superoxide release from complex I was stimulated the rate of hydrogen peroxide release was different. In both brain and muscle mitochondria the capacity was diminished significantly in DR mice, and further significantly diminished in PMDR mice.

In liver mitochondria hydrogen peroxide release was lower in DR and further decreased in PMDR when maximum capacity was stimulated shown in Figure 3-44. In the situation when reverse electron flow was stimulated the DR effect was still present reducing the rate of hydrogen peroxide release but this reduction was not furthered in PMDR mitochondria.

Complex III production is measured in the presence of succinate, rotenone and antimycin A. In muscle mitochondria the production from complex III is not significantly different under DR compared with AL (Figure 3-43). Complex III hydrogen peroxide release is decreased in PMDR muscle mitochondria. In liver mitochondria complex III hydrogen peroxide release in decreased under DR and PMDR (Figure 3-44). The release is not significantly different depending on the time at which the DR tissues were collected.

The release of hydrogen peroxide from complex II was measured at two sites site f and site q. Complex IIq (blue) is the difference between succinate and succinate with ATP.

ATP blocks this site and hydrogen peroxide release can be determined from the difference. Succinate with malonate calculates the production from site IIf (red). (Treberg *et al.*, 2011). There were no significant changes in the release from either site in brain mitochondria (figure 3-45). In muscle mitochondria there is less hydrogen peroxide release from site q in DR mitochondria compared to AL (figure 3-46). In the PMDR animals the release of hydrogen peroxide is lower at both sites.

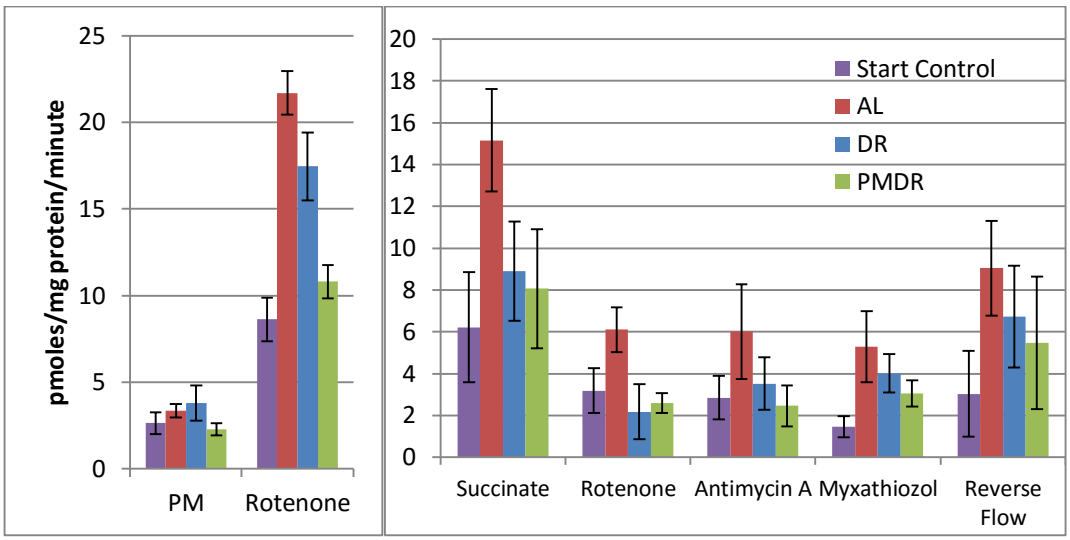

Figure 3-42: The rate of hydrogen peroxide production in brain mitochondria in the presence of a control diet (AL) of a dietary restricted diet (DR). Diet was fed to mice for three months from the age of 12 months. AL (purple) and DR (red) were also compared to post prandial mice which were culled six hours after being fed (green). These mice were to show the effect starvation has on the DR mice. The graph is split in three sections: The addition of Pyruvate Malate (PM) as a substrate followed by the further addition of rotenone; Succinate addition to the mitochondria and the subsequent additions of rotenone, antimycin and myxathiozol; finally the calculation of reverse flow. Standard error is displayed. * = significantly different.

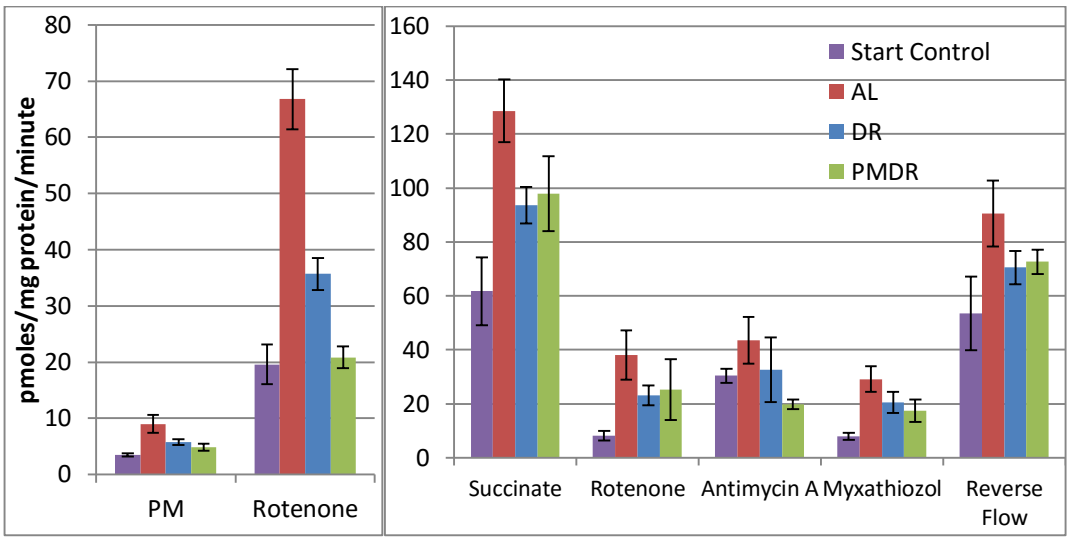

Figure 3-43: The rate of hydrogen peroxide production in muscle mitochondria in the presence of a control diet (AL) of a dietary restricted diet (DR). Diet was fed to mice for three months from the age of 12 months. AL (purple) and DR (red) were also compared to post prandial mice (PMDR) which were culled 6 hours after being fed (green). These mice were to show the effect starvation has on the DR mice. The graph is split in three sections: The addition of Pyruvate Malate (PM) as a substrate followed by the further addition of rotenone; Succinate addition to the mitochondria and the subsequent additions of rotenone, antimycin and myxathiozol; Finally the calculation of reverse flow. Standard error is displayed. * = significantly different.

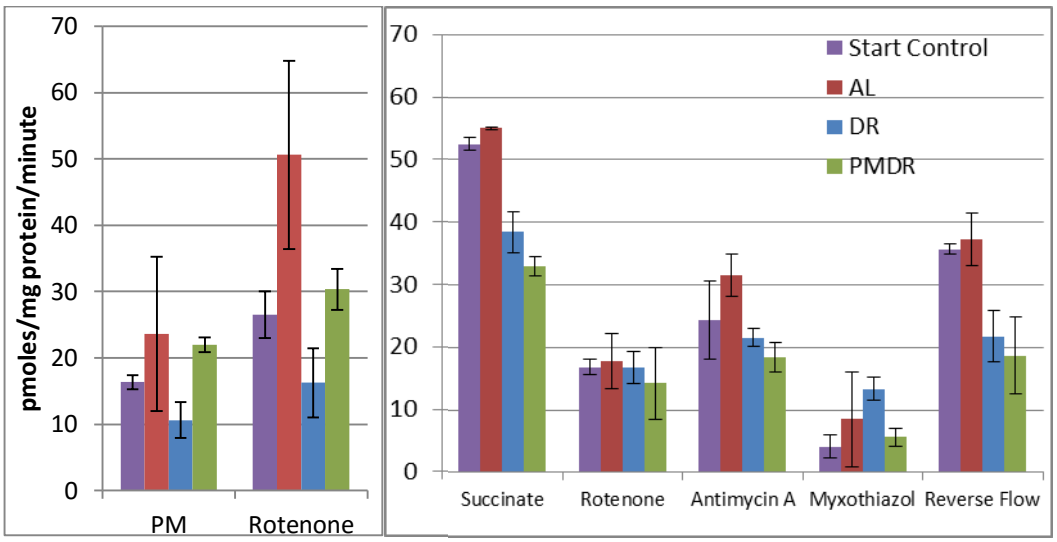

Figure 3-44: The rate of hydrogen peroxide production in liver mitochondria in the presence of a control diet (AL) of a dietary restricted diet (DR). Diet was fed to mice for three months from the age of 12 months. AL (purple) and DR (red) were also compared to post prandial mice which were culled 6 hours after being fed (green). These mice were to show the effect starvation has on the DR mice. The graph is split in three sections: The addition of Pyruvate Malate (PM) as a substrate followed by the further addition of rotenone; Succinate addition to the mitochondria and the subsequent additions of rotenone, antimycin and myxathiozol; Finally, the calculation of reverse flow. Standard error is displayed.

*** = significantly different.**

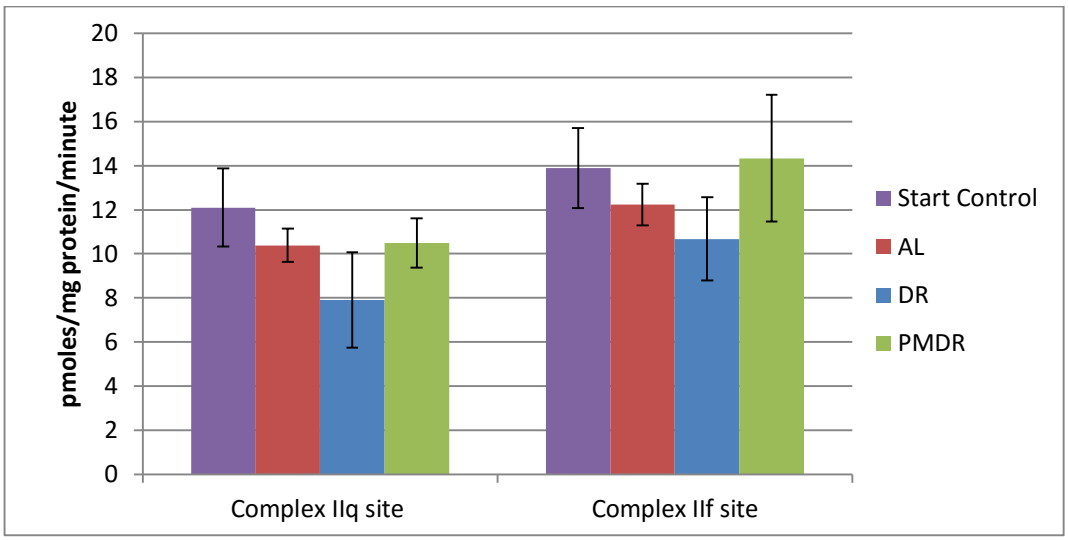

Figure 3-45: The calculated rate of hydrogen peroxide production in brain mitochondria from specific complex II sites. Two sites in complex II had hydrogen peroxide release measured when stimulated. Two ages were compared 12 and 15 months. Start control was measured at 12 months then three different treatments were measured after three months. AL (red) on a normal diet, DR (blue) on a 40% calorie restricted diet and PMDR (green) on a 40% restricted diet and fed prior to tissue collection. Mean values with standard error is displayed.

* significantly different between IIq and IIf.

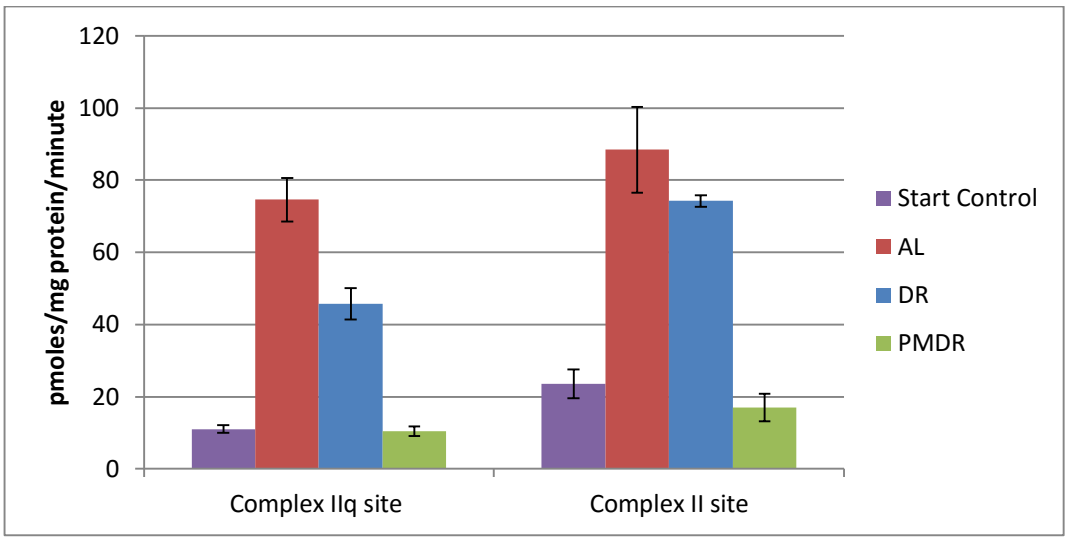

Figure 3-46: The calculated rate of hydrogen peroxide production in muscle mitochondria from specific complex II sites. Hydrogen peroxide release was measured from two complex II sites, IIq and IIf. The measurements were taken at 12 months (start control purple) and 15 months. 15 month old mice had three groups with a different treatment for the three months. AL is normal feeding (red), DR (blue) and PMDR (green) were fed a 40% restricted diet for these three months. DR tissues were collected 24 hours after feeding and PMDR tissue collected 6 hours after feeding. Mean and standard error is displayed.

* significantly different between IIq and IIf.

3.4.2. THREE MONTH RAPAMYCIN FEEDING REDUCES HYDROGEN PEROXIDE RELEASE

Three month rapamycin treatment was studied in both males and females. Female mice were given rapamycin at 12 months and mitochondrial hydrogen peroxide release was compared at 12 month (prior to treatment) and 15 months. In the brain and liver mitochondria no significant difference was seen with rapamycin feeding in complex I hydrogen peroxide production in Figure 3-47 and Figure 3-49. In muscle mitochondria hydrogen peroxide production was reduced from complex I in figure 3-48. This was shown in both the maximum capacity of complex I and the reverse flow through complex I in the presence of succinate.

The hydrogen peroxide production from complex II was unchanged with rapamycin feeding over three months in both brain and muscle shown in figure 3-50 and figure 3-51. In the muscle production from complex IIq and IIf were significantly higher than the production from the starting point mice in figure 3-51.

Male mice were fed for three months with rapamycin prior to being culled at 12 months. Isolated Brain and Liver mitochondria in mice displayed a significantly reduced rate of hydrogen peroxide release from complex I (figure 3-52 and figure 3-53). In liver using either substrate produced significantly lower levels of hydrogen peroxide release. The maximum capacity of complex I to produce superoxide is reduced in both tissues in mitochondria treated with rapamycin (figure 3-53). The hydrogen peroxide release from complex I via reverse flow was also significantly reduced in mitochondria treated with rapamycin.

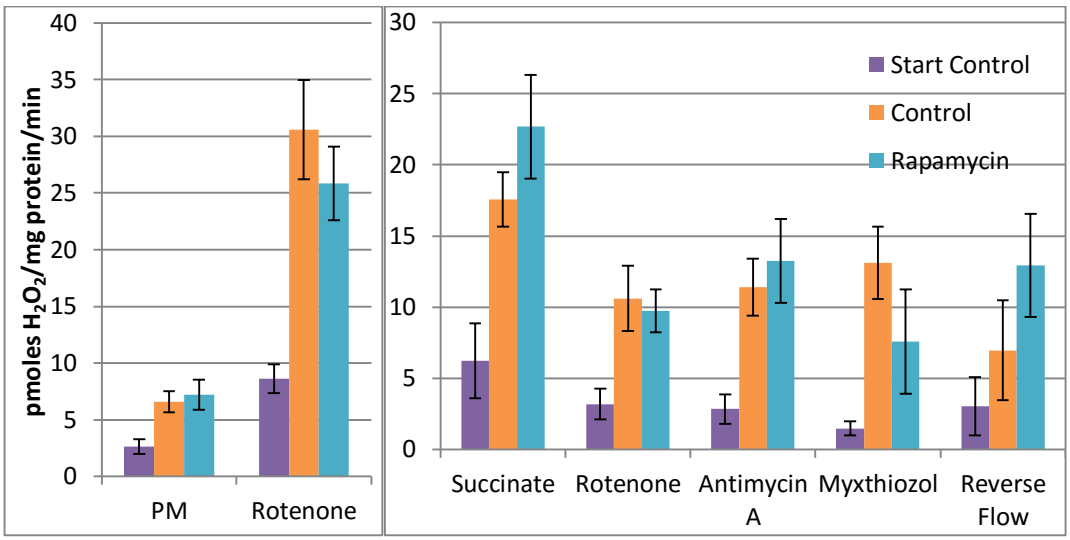

Figure 3-47: The rate of hydrogen peroxide production in brain mitochondria in the presence of a control diet or a rapamycin diet. Control mice data were coloured orange and rapamycin treated mice were blue. Diet was fed to mice for three months from the age of 12 months. The graph is split in three sections: The addition of Pyruvate Malate (PM) as a substrate followed by the further addition of rotenone; Succinate addition to the mitochondria and the subsequent additions of rotenone, antimycin a and myxathiozol; finally the calculation of reverse flow. Standard error is displayed. * significantly different.

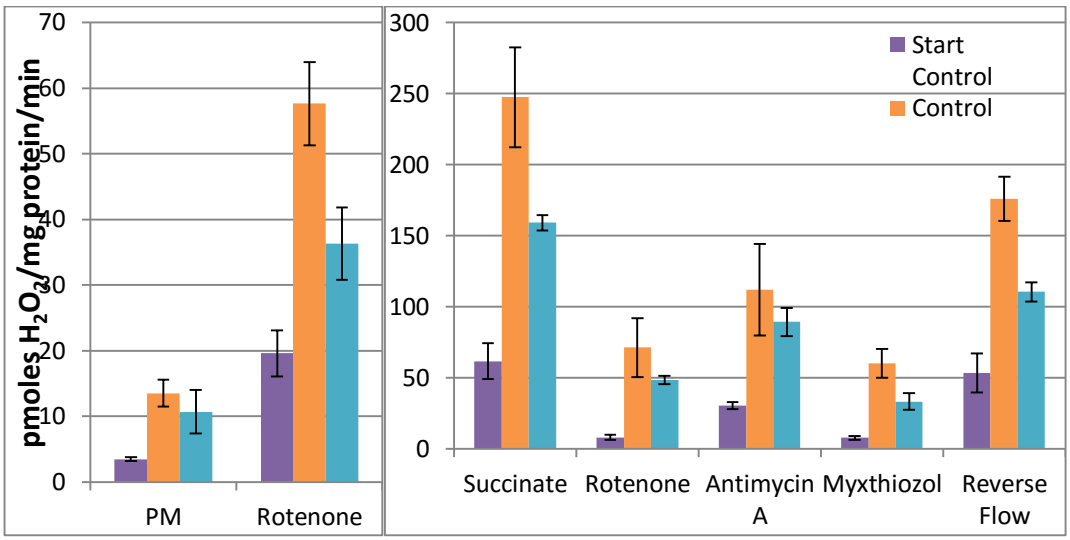

Figure 3-48: The rate of hydrogen peroxide production in muscle mitochondria in the presence of a control diet or a rapamycin diet. Diet was fed to mice for three months from the age of 12 months. The graph is split in three sections: The addition of Pyruvate Malate (PM) as a substrate followed by the further addition of rotenone; Succinate addition to the mitochondria and the subsequent additions of rotenone, antimycin and myxathiozol; Finally the calculation of reverse flow. Standard error is displayed. * significantly different.

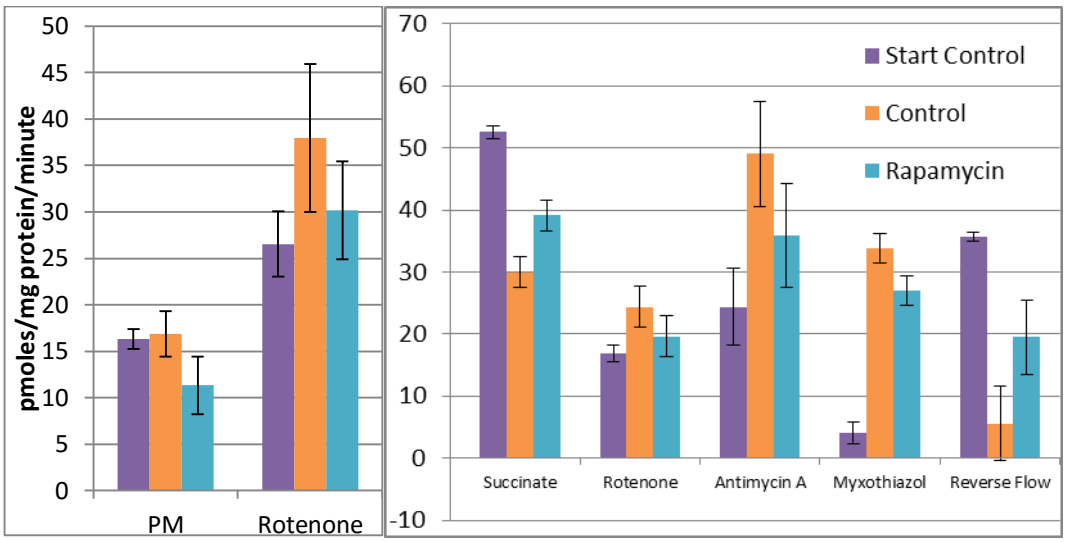

Figure 3-49: The rate of hydrogen peroxide production in liver mitochondria in the presence of a control diet or a rapamycin diet. Diet was fed to mice for three months from the age of 12 months. The graph is split in three sections: The addition of Pyruvate Malate (PM) as a substrate followed by the further addition of rotenone; Succinate addition to the mitochondria and the subsequent additions of rotenone, antimycin and myxathiozol; Finally the calculation of reverse flow. Standard error is displayed. * significantly different.

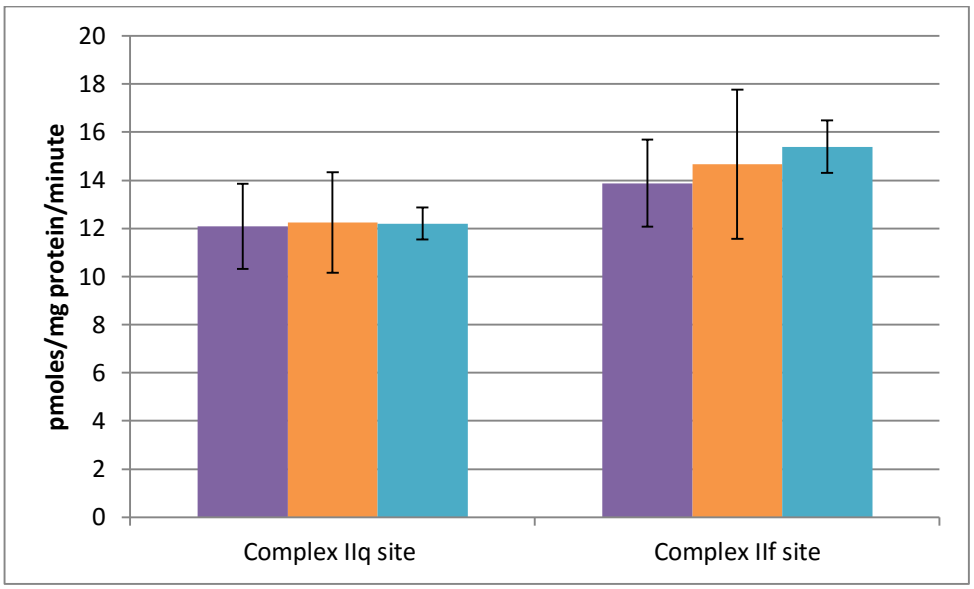

Figure 3-50: The calculated rate of hydrogen peroxide production in brain mitochondria from specific complex II sites. Complex IIq (blue) is the difference between succinate and succinate with atpenin a5. Malonate causes a further block at site IIf the difference seen between succinate with atpenin a5 and succinate with malonate calculates the production from site IIf (red). There are six mouse treatments from which mitochondria were taken: SC is start control these were 12 month mice prior to the short term treatments given. AL is normal feeding form three months from the start control. DR and PF were fed a 40% restricted diet for these three months DR being culled 24 hours after feeding and PF culled six hours after feeding. RC and RAPA relate to rapamycin treatment (RAPA) and it's control diet (RC). Standard error is displayed. * significantly different.

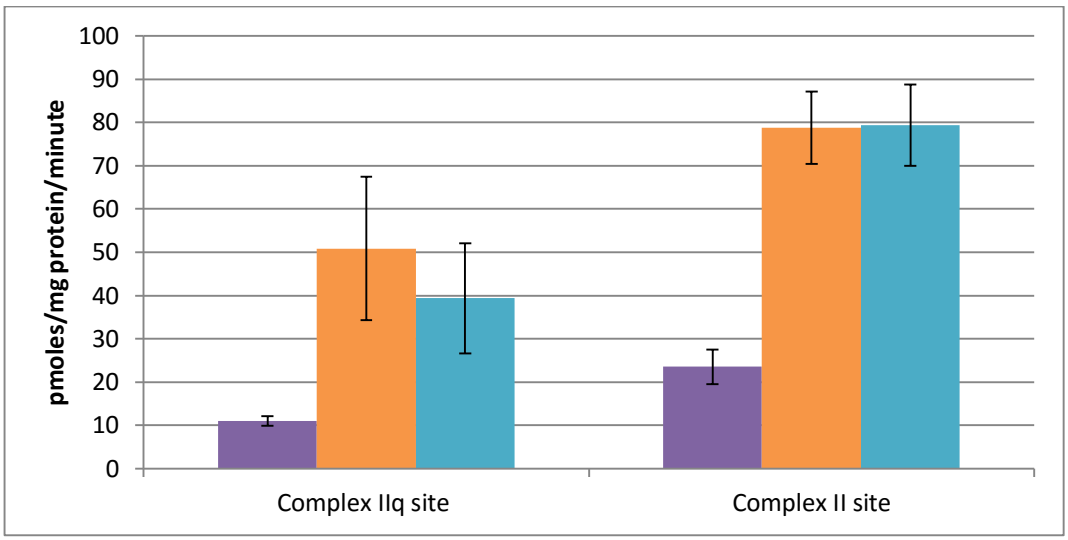

Figure 3-51: The calculated rate of hydrogen peroxide production in muscle mitochondria from specific complex II sites. Complex IIq (blue) hydrogen peroxide release is measured as well as site IIf (red). There are six mouse treatments from which mitochondria were taken: SC is start control these were 12 month mice prior to the short term treatments given. AL is normal feeding form three months from the start control. DR and PF were fed a 40% restricted diet for these three months DR being culled 24 hours after feeding and PF culled 6 hours after feeding. RC and RAPA relate to rapamycin treatment (RAPA) and its control diet (RC). Standard error is displayed. * significantly different.

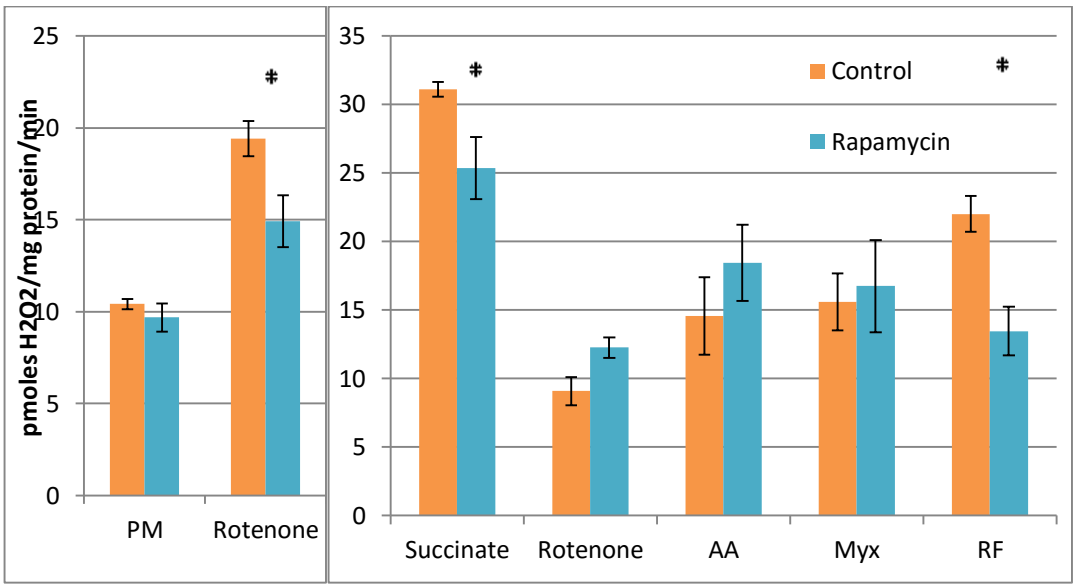

Figure 3-52: Short-term rapamycin feeding in males decreases complex I hydrogen peroxide release from brain mitochondria. On the left measurements in the presence of the complex I linked substrate pyruvate/malate are shown. Right: kinetic measurements of hydrogen peroxide release in the presence of the complex II linked substrate succinate. Mice were fed rapamycin or control diet for 3 months starting at 9 months of age. Mean of each group with standard error is displayed.

* significantly different from control.

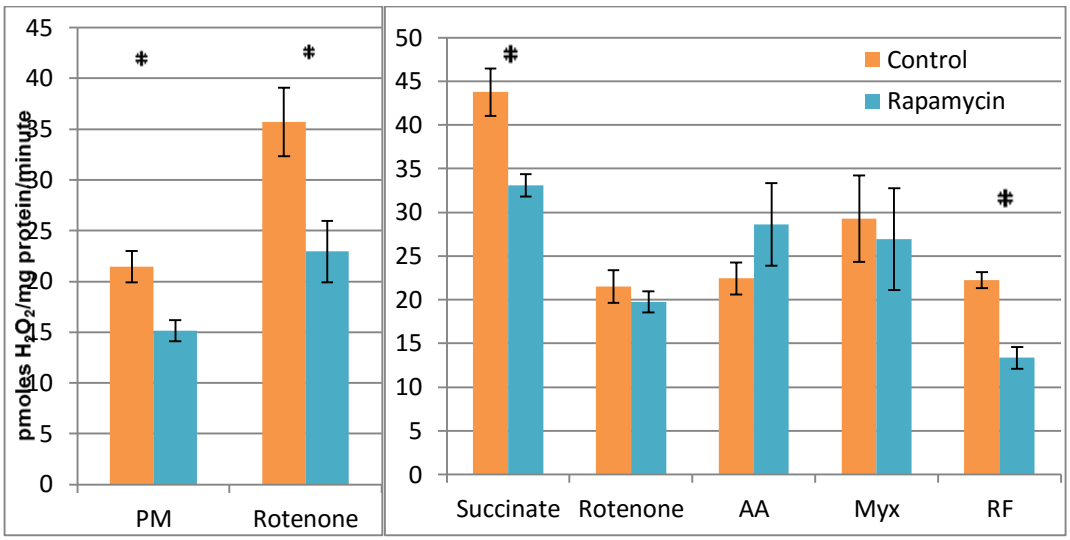

Figure 3-53: In male liver mitochondria treated with rapamycin the hydrogen peroxide release from complex I is significantly lower. Mice were fed rapamycin diet for three months from 9 months of age, mitochondria were isolated at 12 months. The left graph shows the hydrogen peroxide release from mitochondria in the presence of PM and rotenone. The right graph indicates hydrogen peroxide release in the presence of succinate. Mean and standard error is displayed.

* = significantly different from control

In this study when comparing the changes seen in DR and those seen in rapamycin feeding there are no mirroring effects. It was noted that when comparing the studies the rapamycin mice were fed a higher fat content in their diet. This could account for the much higher levels of production determined in the rapamycin and rapamycin control animals than those without these diets. In the experiments shown in Figure 3-42 and Figure 3-44 complex I changes were noted between AL and DR animals the brain and liver respectively. These changes were not present in the rapamycin study in brain (figure 3-47) and liver (figure 3-49). In addition the complex II effects in muscle were not present in the rapamycin mice in figure 3-46 and 3-51. Although the rapamycin control mice had a higher fat content in their diet the rapamycin effect could have been diminished.

When comparing this three month study with the rapamycin feeding seen in the three month TERT-/- study the results are more comparable. These studies were done in mice of the same age and treatment type but there is no starting point data for those in the TERT-/- study. Both brain and liver mitochondria had reduced production of hydrogen peroxide from complex I in response to rapamycin (figures 3-56 and 3-57). This reduction in complex I production was also seen in the 3 month DR mice in figures 3-47 and 3-49.

3.4.3. THE ABSENCE OF TELOMERASE REDUCES HYDROGEN PEROXIDE RELEASE

Telomerase has been shown to have a protective effect of mitochondria reducing superoxide levels and increasing antioxidant defences (Ahmed *et al.*, 2008; Haendeler *et al.*, 2009; Spilsbury *et al.*, 2015). The changes in superoxide release have not been determined from individual sites of the ETC. Here I look at changes in the hydrogen peroxide release from different sites.

Comparing TERT-/- and WT mice shows a lower rate of hydrogen peroxide release from isolated brain mitochondria in TERT-/- at eight months (figure 3-54 and 3-55). However this effect was not seen in the 15 month old TERT-/- mice there was no difference in the release of hydrogen peroxide at complex I maximum capacity shown in figure 3-54. TERT-/- brain mitochondria at 15 months have reduced hydrogen

peroxide release from complex I produced by reverse flow using a complex II linked substrate (figure 3-55).

There was no change with age in WT mice between 8 and 15 months but there was an increase in complex I hydrogen peroxide release in 15 month old mice (figure 3-54). These results suggest that at 8 months telomerase presence increases hydrogen peroxide release. Short age changes without telomerase cause an increase in hydrogen peroxide release which is not seen in WT mitochondria.

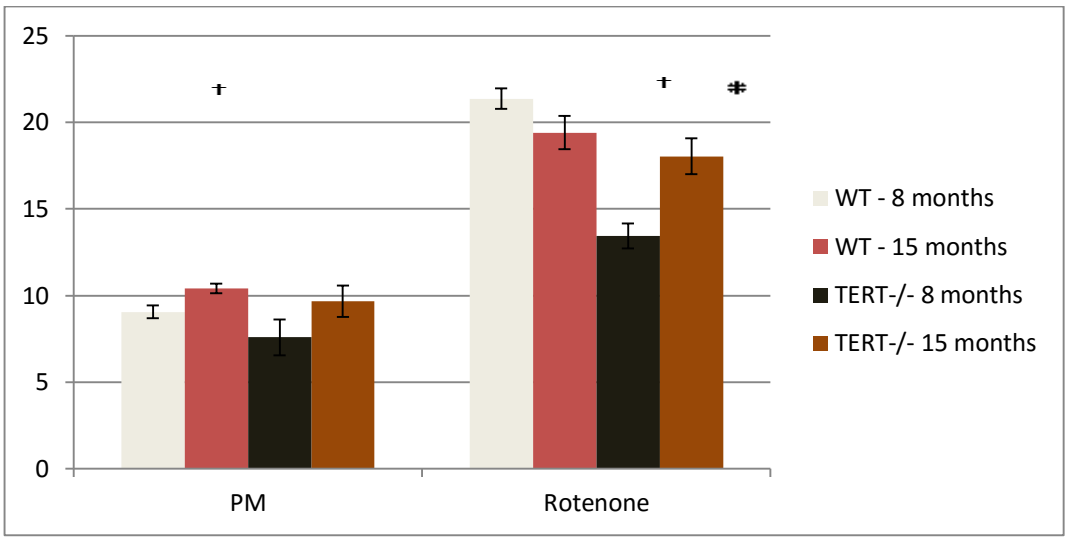

Figure 3-54: Complex I linked hydrogen peroxide release from isolated brain mitochondria from three biological replicates of 8 and 15 month old WT and TERT-/- mice.

*** = Significant from TERT-/- 8 months,**

† = Significantly different from WT – 8 months.

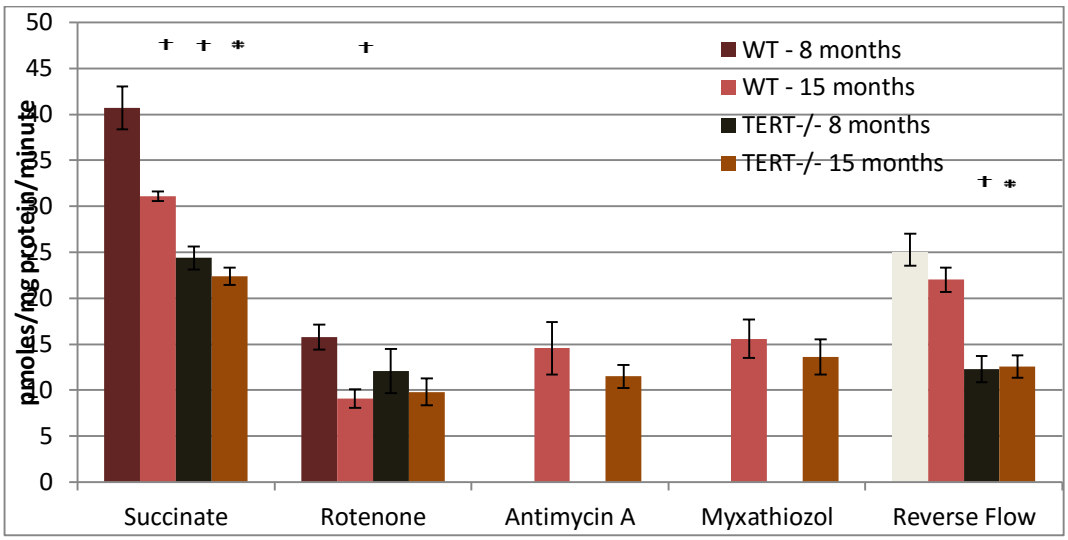

Figure 3-55: Hydrogen peroxide release from isolated brain mitochondria from WT and TERT-/- mice at two different ages using a complex II linked substrate. Mice were either 8 or 15 months old when culled three mice were culled per group. 8 month old mice were only exposed to Succinate and rotenone.

* Significantly different from WT – 15 months,

† significantly different from WT - 8 months.

Rapamycin treatment was also studied in WT and TERT-/- mice. WT mice were fed for three months with rapamycin prior to being culled at 15 months. Isolated brain mitochondria in WT strains of mice displayed a significantly reduced rate of hydrogen peroxide release from complex I. In brain mitochondria (figure 3-56) using either substrate produced significantly lower levels of hydrogen peroxide release. The maximum capacity of complex I to produce superoxide is reduced in both liver and brain tissues in mitochondria treated with rapamycin figure 3-56 and figure 3-57. The hydrogen peroxide release from complex I via reverse flow was also significantly reduced in mitochondria treated with rapamycin.

TERT-/- mice were also treated with rapamycin (figure 3-56 and figure 3-57), only the brain mitochondria were collected from these animals. It was shown that those mice which had also been treated with rapamycin for three months had no change in hydrogen peroxide release than untreated mitochondria with either substrate.

Here there is similarity in the change in hydrogen peroxide release of both DR and Rapamycin treatment with their respective controls. TERT-/- mice have no change in hydrogen peroxide release, therefore TERT is a necessary gene for rapamycin suppression of hydrogen peroxide release.

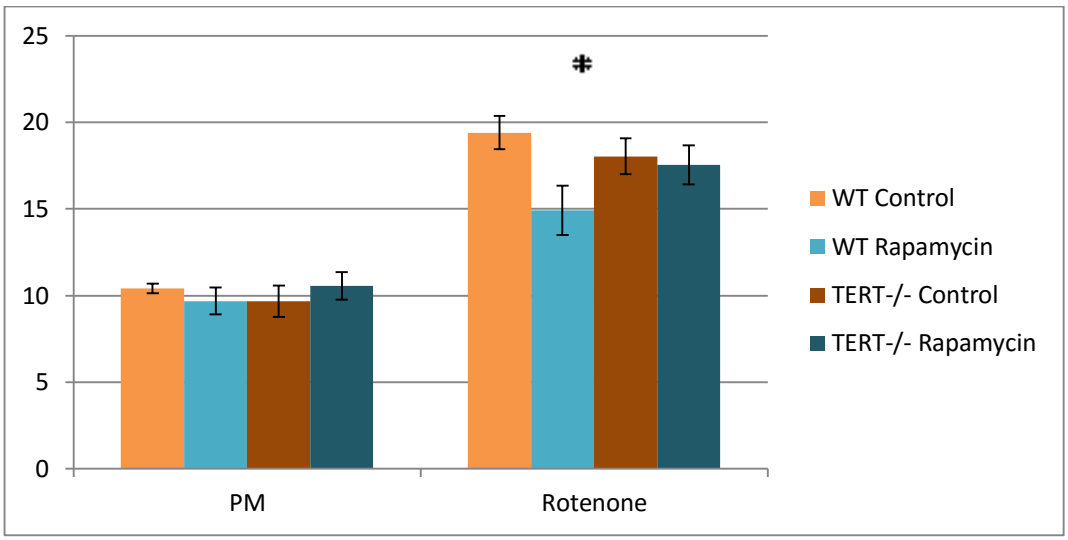

Figure 3-56: Complex I linked hydrogen peroxide release from isolated brain mitochondria in 15 month old mice. Two conditions and treatments are were compared. Isolated brain mitochondria from WT and TERT-/- mice, either on a control diet or with 3 month rapamycin treatment.

* = Significantly different from WT – control. (two-way ANOVA)

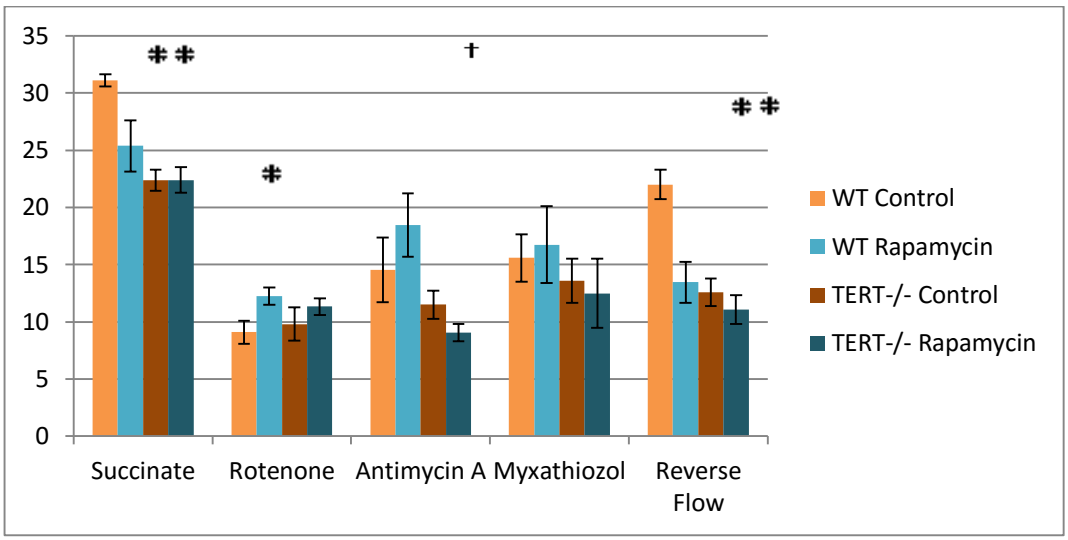

Figure 3-57: Complex II linked hydrogen peroxide release in brain mitochondria of WT and TERT-/- mice, control and 3 months rapamycin treatment in 15 month mice.

*** = Significantly different from WT – control**

† = Significantly different from WT – rapamycin (two-way ANOVA).

3.5. THE INCREASE OF HYDROGEN PEROXIDE RELEASE SEEN WITH AGE CAN BE POSTPONED WITH DIETARY RESTRICTION.

The amplex red method was developed for detecting the hydrogen peroxide release from brain, skeletal muscle and liver mitochondria. Amplex red is a commonly used method for detecting Superoxide or ROS production by way of hydrogen peroxide release from mitochondria. Liver mitochondria were found to respond differently than brain and skeletal muscle mitochondria to the amplex red assay. Amplex red is oxidised to resorufin in the presence of HRP only in the brain and skeletal muscle mitochondria however, in the presence of liver mitochondria resorufin is produced independent from HRP. Hydrogen Peroxide release is calculable using the amplex red assay by monitoring the difference between with and without HRP.

The hydrogen peroxide release was measured from brain, skeletal muscle and liver mitochondria from mice across multiple ages (3, 15, 24 and 30 months) as a marker for superoxide production from the electron transport chain. Hydrogen peroxide was seen to increase with age in brain, skeletal muscle and liver mitochondria from both complex I and complex III. The effects of long-term dietary restriction was studied in the same ages, as well as at 36 months, which is the same survival rate as 30 month AL mice (35%). The dietary restricted mitochondria show reduced hydrogen peroxide release from complex I at 15 months and 24 months in brain, skeletal muscle and liver mitochondria when measured. Dietary restriction has no consistent reduction in complex III production. Hydrogen peroxide release at 36 months is not lower in dietary restricted mitochondria than AL mitochondria at 30 months as is the trend at matched ages.

Thus, the mitochondrial hydrogen peroxide release is not low throughout the lifespan of dietary restricted mice. Hydrogen peroxide release increases with age in dietary restricted mice as well as ad libitum fed mice. The increase in hydrogen peroxide release from mitochondria with age is delayed in DR mice tissue. The low levels of hydrogen peroxide release are maintained for longer in the DR mice tissue compared with that of AL mice tissues. Hydrogen peroxide release at the same survival point in their respective lifespans shows no differences between AL and DR mitochondria. Long-term DR treatment studies mitochondria collected prior to feeding (pre-prandial)

and six hours after feeding (post-prandial). When the mitochondria were collected post-prandially there was a lower hydrogen peroxide release compared to that of DR at 30 months in all tissues.

Short-term dietary changes also show alterations in hydrogen peroxide release. The mitochondria from brain, skeletal muscle and liver show reductions in hydrogen peroxide release in response to dietary restriction. The lower release of hydrogen peroxide is seen whether the mitochondria were collected pre or post prandially. Short-term addition of rapamycin to the diet also causes a reduction in hydrogen peroxide release in male 12 month old brain and liver mitochondria. This reduction was not replicated in female brain and liver mitochondria but was seen in 15 month female skeletal muscle mitochondria.

Telomerase has been shown to be protective against superoxide release and increase antioxidant defences. TERT knockout mice are missing the catalytic unit of telomerase reverse transcriptase, yet they show a decreased level of hydrogen peroxide release. The addition of rapamycin to the diets of these TERT-/- mice show no additional change in hydrogen peroxide release as seen in the controls or earlier rapamycin treatment experiments.

Overall changes to the diet of mice which alter the metabolism of the mice change the production of superoxide from the mitochondria. Short and long-term dietary restriction are shown to alter the protein abundance in fatty acid and amino acid metabolism in Chapter 4, and rapamycin is documented to regulate metabolism. These dietary changes both reduce the release of hydrogen peroxide from brain, liver and muscle mitochondria.

CHAPTER 4: CHANGES IN THE LIVER MITOCHONDRIAL PROTEOME REVEAL POSSIBLE CAUSES OF HYDROGEN PEROXIDE CHANGES WITH AGE AND DR

4.1. PROTEOMICS CAN PROVIDE MORE DETAIL AS TO WHAT OCCURS TO CAUSE THE CHANGES IN LIVER MITOCHONDRIAL FUNCTION SEEN IN AGEING AND DR

Mitochondria are a major source of superoxide in the eukaryotic cell (Chou *et al.*, 2011). Superoxide production occurs mainly at the protein complexes I, II and III in the electron transport chain (ETC) (St-Pierre *et al.*, 2002; Barja, 2004; Miwa and Brand, 2005). It is known that superoxide causes damage to proteins (Harman, 1956). It is likely there are changes in proteome composition in response to increased oxidative stress. The proteome changes occur due to adaptive changes in protein expression in response to the degradation and removal of damaged proteins. To understand a cell and an organism's response to oxidative stress, it is therefore logical to investigate the cellular proteome. This information can complement and add to the observations of changes in superoxide release seen with ageing and dietary restriction (Sohal and Weindruch, 1996; Brand, 2000; Mansouri *et al.*, 2006)(Thesis section 3.4). Protein changes have been shown to change with DR in protein focused studies (Miwa *et al.*, 2008; Chen *et al.*, 2014; Miwa *et al.*, 2014) . However, so far, no large scale study of the mitochondrial proteome has been performed that would take into account different ages, gender and dietary status. In this study I investigate the influence of all these independent variables on the composition of the mitochondrial proteome. Here, I have analysed the proteome from liver mitochondria of twenty groups of three mice each. The liver was chosen as an organ that is rich in mitochondria, central to physiological and biochemical adjustments at an organism level and an early detector of changes in an organism's dietary circumstances. Nine of these groups correlate in diet, age and sex with those used in chapter three to study hydrogen peroxide release from isolated liver mitochondria. There were twenty groups in total. Four dietary treatments (AL, DR, PMAL and PMDR) were investigated. The AL proteome was determined in ages 3, 15, 24 and 30 months in males and females. The DR proteome was determined in ages 15, 24 and 30 in both male and female mice, 36 months in

only male DR mice. PMAL and PMDR are postprandial dietary restriction. Mouse samples were collected 24 hours post-prandially; in alternate day feeding experiments this caused differences in superoxide production (Dani *et al.*, 2010). Here we look at the protein changes in mouse liver mitochondria 24 hours after feeding and 6 hours after feeding. At 15 months in both male and female mice PMAL and PMDR and at 30 months only male PMDR mitochondrial proteomes were investigated.

4.1.1. THE PROTEOMICS METHODOLOGY

Stable Isotope Labelling with Amino Acids in Cell Culture (SILAC) was developed in the centre for Experimental Bioinformatics (CEBI), at the University of Southern Denmark (Ong *et al.*, 2002). Typical SILAC is the biosynthetic labelling of a cell line with heavy amino acids (Mann 2006) followed by a direct relative comparison of peptide peak intensities and subsequently protein concentrations in two samples, one of which is labelled with heavy isotopes and the other one is not. Spike in SILAC (Geiger *et al.*, 2011) requires a biosynthetically heavy labelled complex standard that can be added to multiple samples. A SILAC spike-in method was used to compare a large number of mouse liver mitochondrial samples. We chose the addition of a labelled mouse liver carcinoma mitochondria lysate as an internal standard.

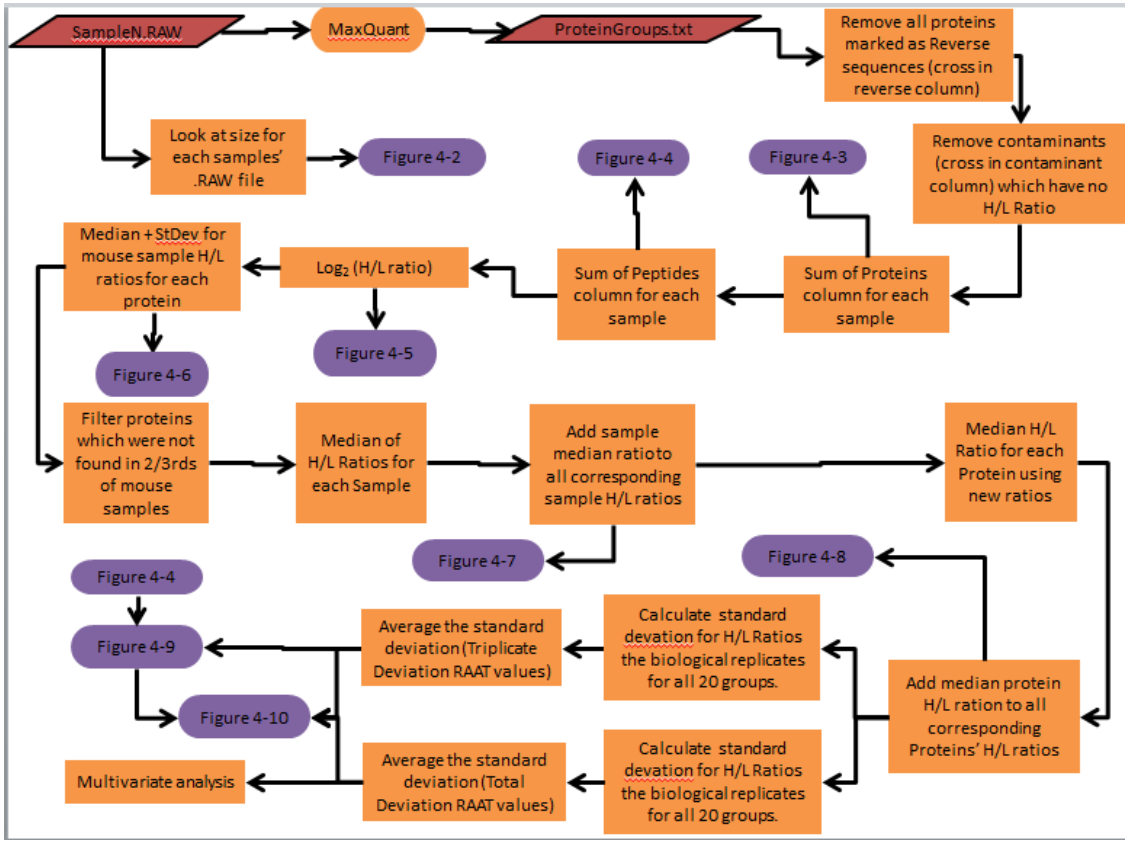

Figure 4-1: Workflows used to produce the figures presented in the proteomics chapter of this thesis. Red parallelograms denote file names. Purple rectangles with rounded ends represent figures in the thesis. Orange rectangles denote computational processes completed in excel or sigma plot unless noted.

4.2. DATA PROCESSING AND NORMALISATION

Data processing and normalisation followed the scheme outlined in Figure 4-1.

4.2.1. QUALITY CONTROL OF THE LCMS DATA

Altogether, just over 1200 proteins were identified in 60 mouse liver mitochondrial samples. To gain a first-hand impression of the overall quality of the dataset, the file sizes of the 60 raw LCMS datasets were compared (Figure 4-2) and found to be roughly equal.

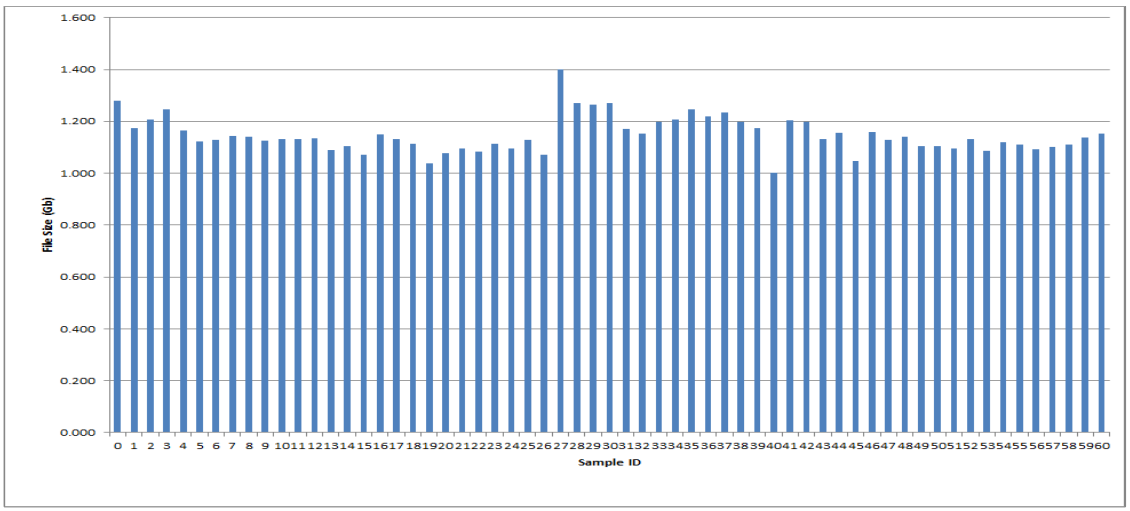

Figure 4-2: Raw data file sizes of all mouse mitochondrial proteomics samples analysed. The y – axis denotes the file size in Gb, whereas the x axis denotes sample ID (Table 6-2)

4.2.2. PROTEIN IDENTIFICATION

Subsequently, proteins were identified using the search engine Andromeda (part of the MaxQuant environment). Prior to counting identified proteins, contaminant proteins (proteins that were of non-murine origin and proteins that did not at all contain heavy isotope standard-labelled peptides) were removed. All samples contained a similar number of proteins (between 342 and 755 proteins per sample). Three samples stand out as having a particularly low number of identified proteins (sample 23 (30m M AL 2, 427 proteins), 35 (30m M PFDR 1, 445 proteins) and 40 (15m M DR 2, 342 proteins))

This is reflected at the peptide level, where variability is much more pronounced than at the protein level, due to the redundancy of the contribution of peptide identifications to specific proteins. The same three samples stand out as having particularly low numbers of identified peptides ((sample 24 (30m M AL 2, 1003 peptides), 35 (30m M PFDR 1, 933 peptides) and 40 (15m M DR 2, 704 peptides)).

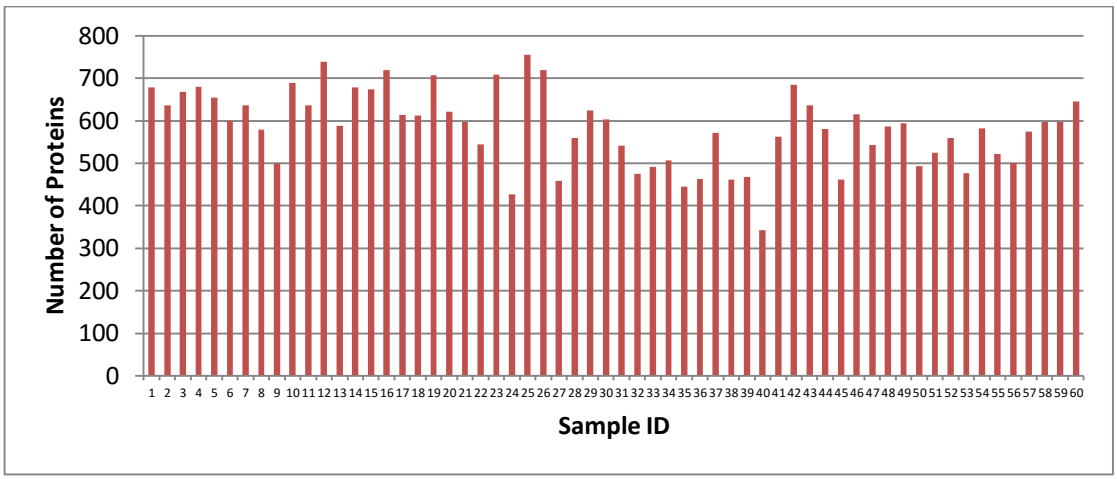

Figure 4-3: Proteins identified in each of the mouse liver mitochondrial samples analysed. Samples 24 and 40 have the lowest number of proteins identified; mouse sample 40 (15m Male DR) had only 342 proteins identified. The y-axis is the number of proteins identified in each mouse sample using the Andromeda search engine at a peptide level FDR rate of 1%. The x axis denotes the sample ID (Table 6-2).

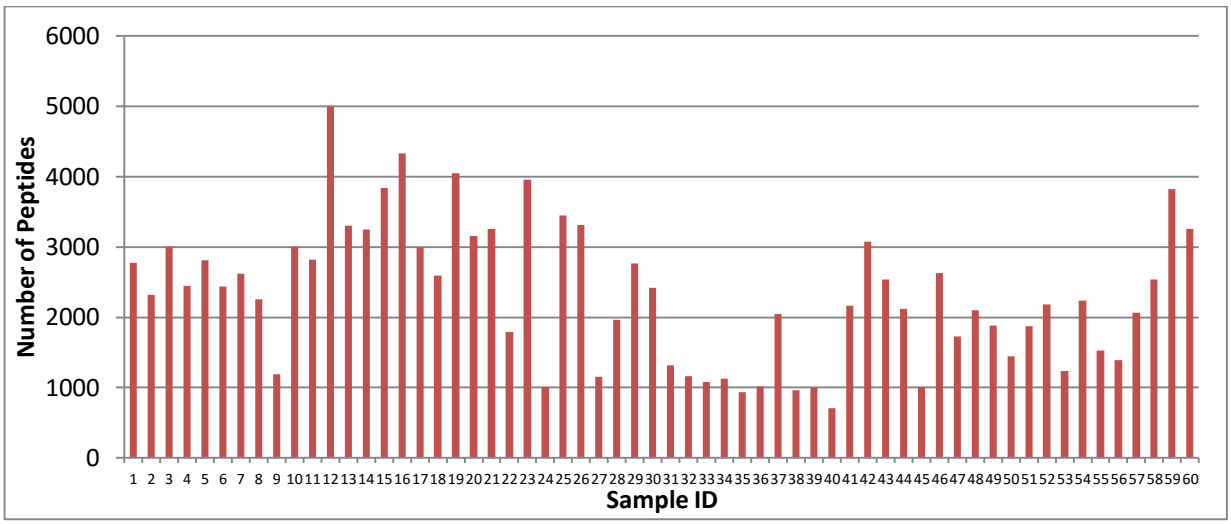

Figure 4-4: Peptides identified in each of the mouse liver mitochondrial samples analysed. There is a range of numbers peptides from 900 in sample 40 to 5000 in sample 12. The mouse sample ID is denoted on the x axis. Peptides were identified using the Andromeda Search engine (FDR rate %1). The x axis denotes the sample ID (Table 6-2).

4.2.3. PROTEIN QUANTITATION

Assessing the result of the protein quantitation indicated that on average in all samples the amount of internal standard proteins was lower than the amount of mouse liver mitochondrial proteins (Figure 4-5). There was considerable variability in the ratio of internal standard protein concentration to sample protein concentrations, in particular samples 34-48 contain lower concentrations of the internal standard. This indicated variation in the amount of internal standard added to the samples and resulted in the necessity of data normalisation as a remedial measure (see section 4.2.4).

The overall reproducibility of the data was assessed by investigating the variability of the ratio of proteins in the carcinoma cell line standard (Heavy) to the same proteins in the liver mitochondrial samples (Light) (H/L ratio, Figure 4-6). It is to be noted that many of the proteins in this figure were only quantifiable in a small number of samples.

Following this, a list of quantifiable proteins was compiled that contains only proteins that were quantifiable in at least two thirds of all samples in the dataset, to ensure that only high quality data entered the quantitative analysis stage of this dataset (Table 6-6 (appendix A)). This list of quantifiable proteins (from here onwards referred to as quantifiable proteins) contained 305 proteins, 232 (76%) of which were found in the mitochondria using at least two methods according to the database mitominer (Smith and Robinson, 2009; Smith *et al.*, 2012) and therefore classed as being mitochondrial. I used the cell part gene ontology (GO) terms to confirm this and 227 of the 305 proteins where labelled with mitochondrion (Ashburner *et al.*, 2000) The other proteins were nevertheless included in the analysis of the dataset, as they co-purified reproducibly with the mitochondrial preparation used in my study.

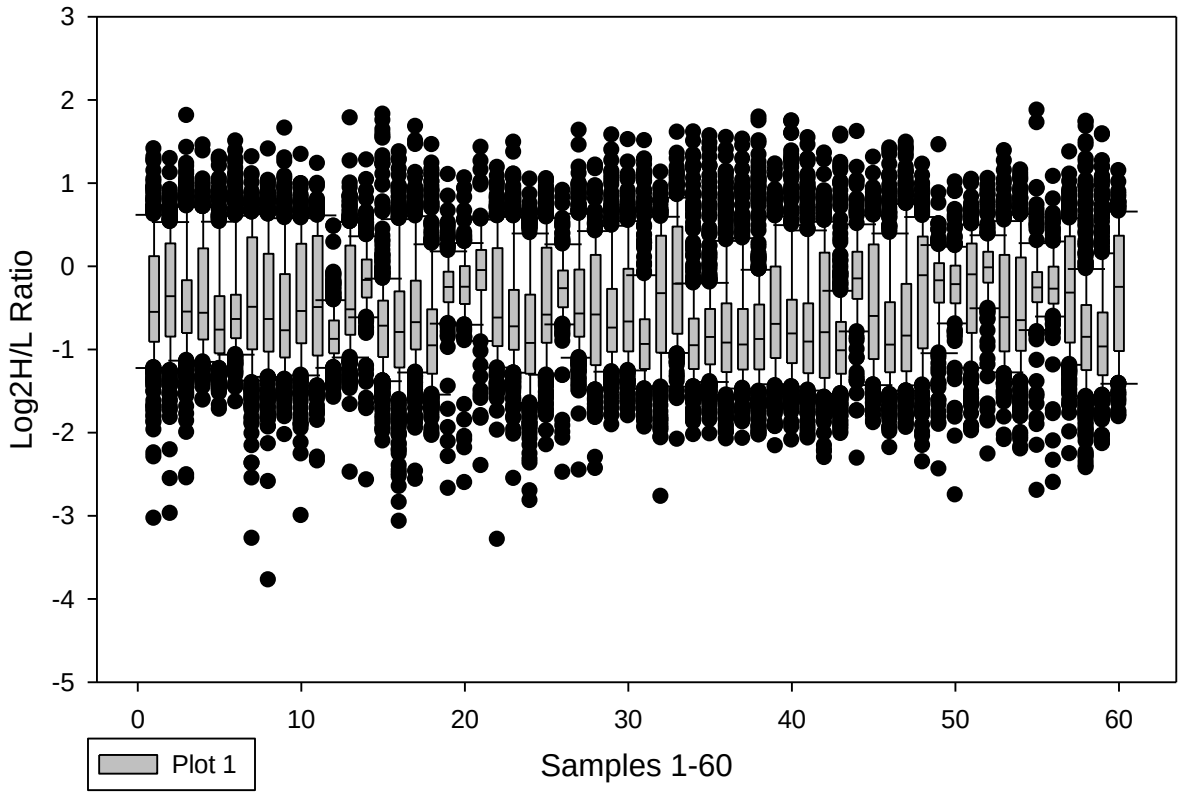

Figure 4-5: Variation in the median log_2 H/L ratio of all quantifiable proteins in mouse liver mitochondria samples. The x axis corresponds to the sample ID (table 6-2). On the y-axis log_2 H/L ratio was denoted. The main cause for the observed variability of the log_2 H/L ratios are differences in the amount of internal standard (heavy labelled mouse hepatocarcinoma proteins) added.

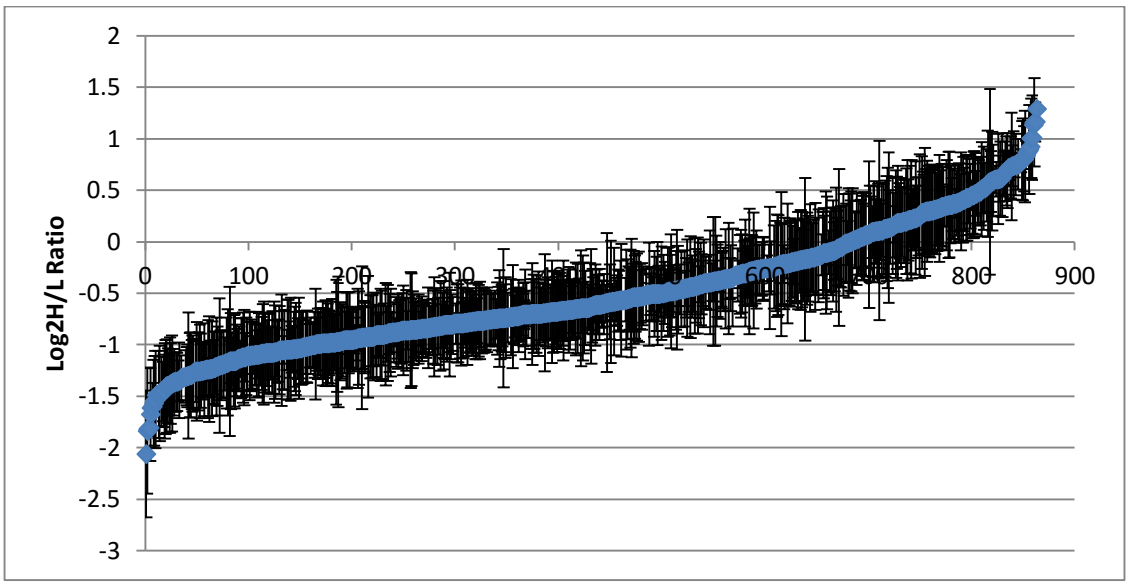

Figure 4-6: The ratio of amount of quantifiable protein in the mouse liver mitochondrial samples to the amount of the same protein in the mouse hepatocarcinoma mitochondria varies over about one order of magnitude but is quite constant for each individual protein in all the mouse samples where it was quantifiable. Median protein concentrations are diamonds and the error bars are the standard deviations of the H/L ratios of the 60 samples. Proteins (on the x axis) are sorted by the H/L (hepatocarcinoma / liver tissue) ratio. The y-axis is the $\log_2$H/L ratio for the proteins. 860 proteins were quantifiable in at least two out of 60 samples and were included in this graph.

4.2.4. DATA NORMALISATION

To account for the variable amounts of internal standard that were added to each sample, the H/L ratios of the 305 quantifiable proteins in each sample were divided by the median H/L ratio for the quantifiable proteins in this sample (Figure 4-7). This normalisation step removes the dependency of the quantitative readout on the amount of internal standard added.

The result of the first transformation is a list of quantifiable proteins for each sample with the H/L ratio indicating the difference between the protein amount in this sample and the amount for the same protein in the internal mouse liver carcinoma cell line mitochondria standard. However, for the purpose of this investigation, it is not interesting, if a protein has been selected for or against in this laboratory cell line. To remove the dependency of the quantitative readout on the internal standard, the H/L ratios after the first transformation for each protein in each sample were divided by the median H/C ratio for this protein in all samples (Figure 4-8). The 2 base log of the resulting value, which will from here onwards be referred to as **R**elative **A**bundance **A**fter **T**ransformation (RAAT value) is solely indicative of a particular mitochondrial protein or peptide's tendency to be more or less abundant in a specific sample when compared to the average of this protein or peptide's abundance in all samples.

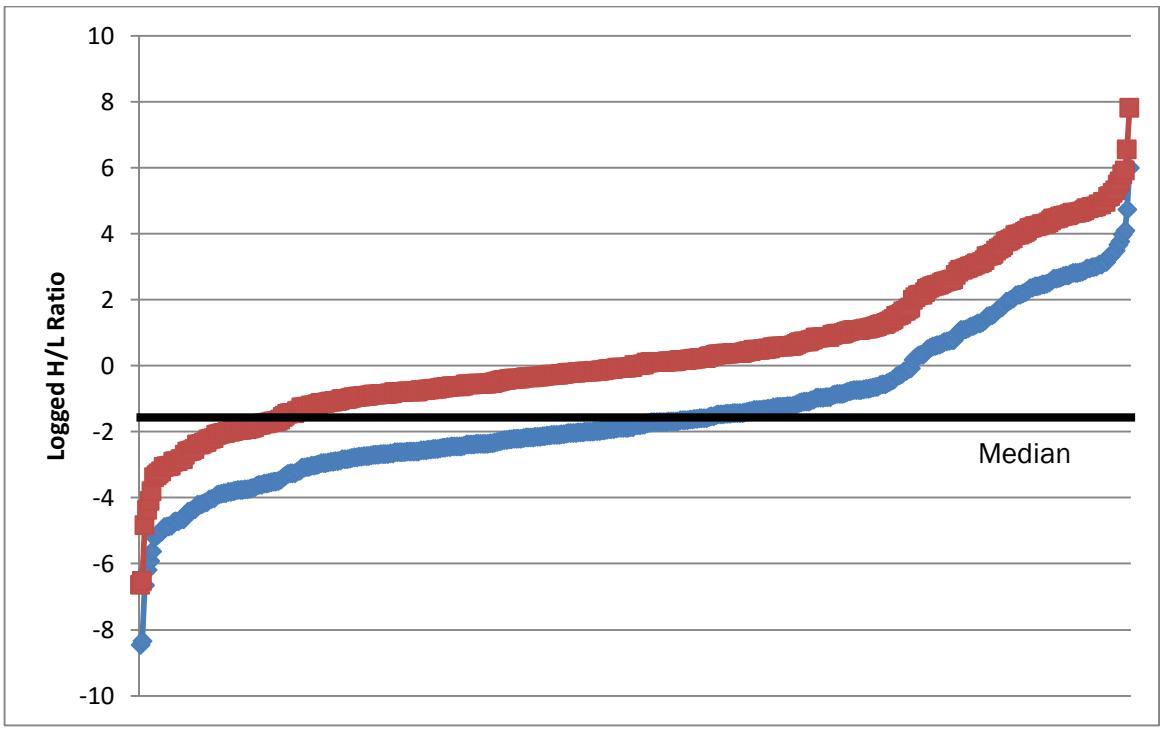

Figure 4-7: The first data normalisation step removes the bias in the data that is caused by the varying amounts of internal standard (mouse hepatocarcinoma mitochondria) added. Blue diamonds represent the median of the H/L ratio (amount of protein in mouse hepatocarcinoma mitochondria divided by the amount of protein in mouse liver mitochondria) for each individual, quantifiable protein in sample 3 (3m Male AL). The 312 proteins that were included in this graph were quantifiable in at least 2/3 of all samples. The same normalisation was carried out for the other 59 samples. Red squares represent the H/L ratios following this transformation step.

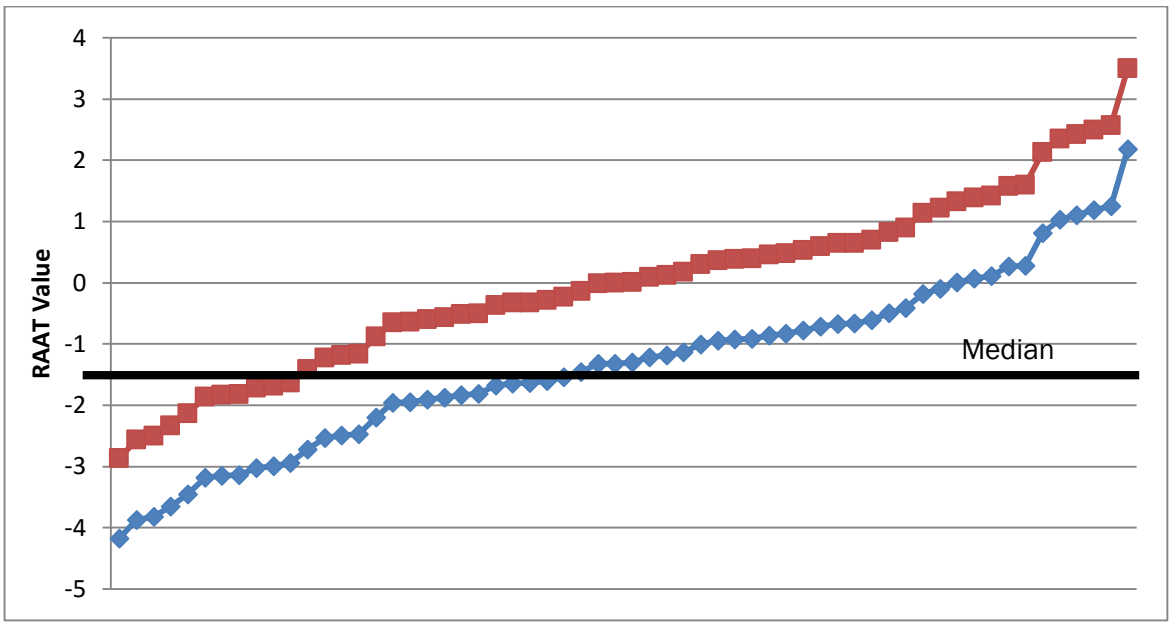

Figure 4-8: The second normalisation step removes the dependence of the quantitation on the internal standard (mouse hepatocarcinoma mitochondria). Blue diamonds represent the median protein H/L ratio for the protein prohibitin 2 (Phb2) in each of 60 individual mouse samples (after the first transformation). Mouse samples are sorted by increasing H/L ratios. Red squares represent RAAT values (Relative Abundance After Transformation) for this protein in each sample. This transformation step was carried out for each individual protein out of 305 quantifiable proteins, resulting in a RAAT value for this protein in all samples where it was quantifiable.

4.3. ANALYSIS OF THE DATA AT THE PROTEOME LEVEL

4.3.1. DIFFERENCES OF RELATIVE PROTEIN AMOUNTS (RAAT VALUES) BETWEEN GROUPS INDICATE THAT THE LARGE SCALE PROTEOMICS EXPERIMENT CONTAINS BIOLOGICALLY RELEVANT INFORMATION

Each mouse group comprises three biological replicates. Mouse groups differ by nutritional status (AL, DR or Post-Prandial), age and sex (see section 1.3.5 for experimental design). The variability of the determination of RAAT values for each individual protein can be assessed by calculating the standard deviation of the RAAT values for this particular protein in one mouse group. The average of these standard deviations over the 20 mouse groups is an overall indicator of the experimental variability of the determination of the RAAT value and will henceforth be referred to as the triplicate standard deviation (Equation 1).

Equation 1. Calculation of the triplicate standard deviation ($SD_{triplicate}$). σ_i represents the standard deviation of the RAAT values of one specific protein in mouse group i prior to shuffling.

$$SD_{triplicate} = \frac{\sum_{i=1}^{20}(\sigma_i)}{20}$$

In order to check, if the protein concentration variability between samples is caused by biological effects or by random fluctuation only, I decided to investigate the random variability in the complete dataset. To do this, the 60 mouse samples were shuffled to create 20 random triplicate groupings. This was followed by the same procedure that was used to calculate the triplicate standard deviation, but the resulting standard deviations (referred to hence as total standard deviation) are calculated from the average of standard deviations for each protein in 20 completely random mouse groups. As a result, it represents the random variability of each protein in the dataset.

Equation 2: Calculation of the total standard deviation (SD_{total}). σ_j represents the standard deviation of the RAAT values of one specific protein in random mouse group j.

$$SD_{total} = \frac{\sum_{j=1}^{20}(\sigma_j)}{20}$$

The triplicate standard deviation $SD_{triplicate}$ is a measure for the reliability of the measurement of the RAAT values permits to assess various aspects of the general reliability of the dataset. When $SD_{triplicate}$ is plotted against the average spectral count for each protein in all mouse groups (Figure 9), it becomes apparent that the reliability of the determination of RAAT values increases with protein concentration (it is generally acknowledged that spectral counts are an approximate measure of protein concentration, (Arike and Peil, 2014)). Two proteins do not conform to this trend (highlighted with red circles in Figure 9). When the identity of these two proteins is checked it turns out that both of them are keratins (keratin 8 and keratin 18) and that the high variability of determination of their concentration is likely to be due to contamination of the samples with human keratins (producing peptides that are identical in sequence to the corresponding murine keratins).

If the variability of the data that were acquired for this study could be entirely explained by random experimental variability, then a plot of the triplicate standard deviations $SD_{triplicate}$ versus the total standard deviations SD_{total} would result in a cloud of points that could be summarised with a regression line with a slope of 1. To test this, one representative random set of SD_{total} was plotted against $SD_{triplicate}$ (Figure 10). Clearly, the slope of a regression curve through the resulting cloud of points deviates from 1, indicating that the dataset contains variability that can only be explained by the grouping of the mouse samples in biological replicates.

To test, if this would be only due to one particular random set of SD_{total}, a Monte Carlo model was employed. SD_{total} was calculated for 1000 randomisation sets derived from the existing dataset and the results of this analysis are shown in the kernel density plot displayed in Figure 11 (the R script employed to do this is in Appendix A). The median slope obtained for all 1000 linear regressions is 1.065 and the probability of obtaining a slope of 1 based on the present data was calculated to be 4.19e-7. This implies that the

distribution of RAAT values in the dataset differs from a random distribution in a statistically highly significant manner.

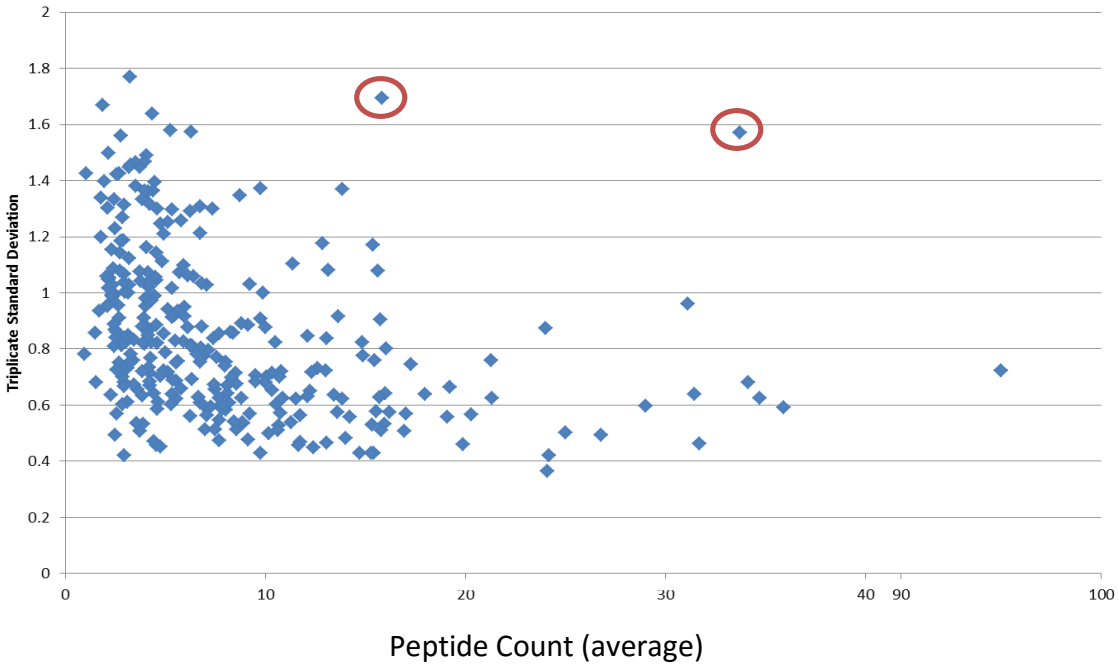

Figure 4-9: Highly abundant proteins yield less noisy quantitation results. Proteins with high peptide counts (highly abundant proteins) have a lower standard deviation of the RAAT value than less abundant proteins (with a lower peptide count). The x-axis represents the median peptide cound for each of 312 quantifiable proteins. The y-axis represents the average standard deviation of the RAAT value for this protein in a group of three biological replicates (mice that received the same treatment).Circled in red are two proteins that don't fit the trend these are keretins 8 and 19.

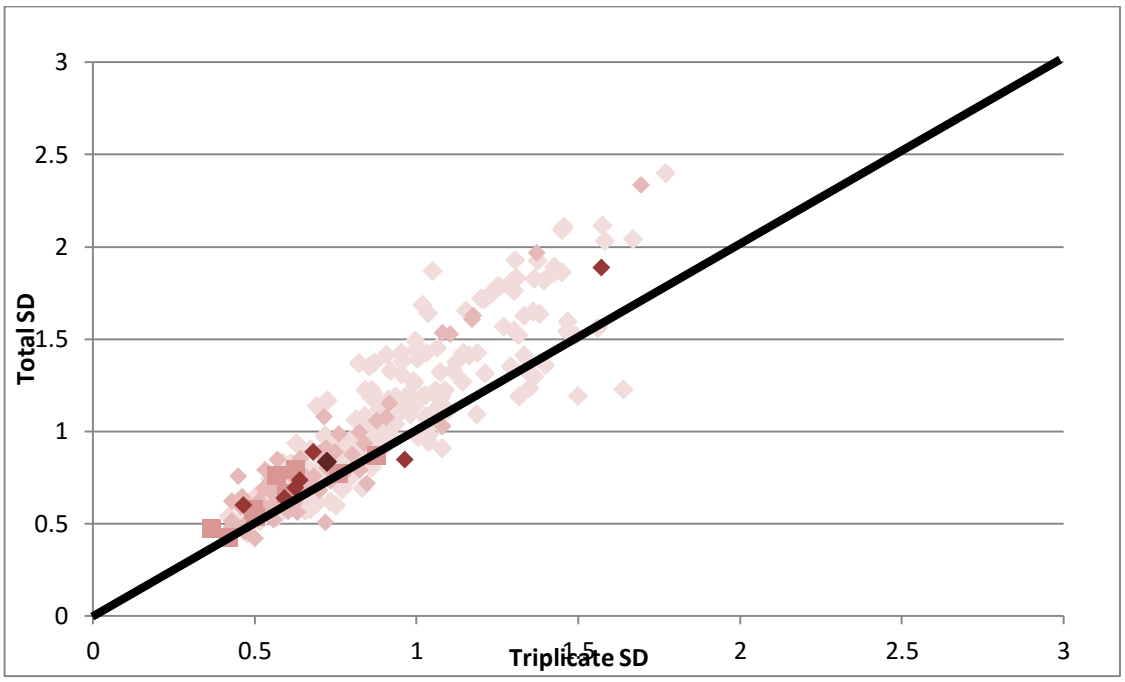

Figure 4-10: Triplicate standard deviation is lower than proteins comparative total standard deviation. On the x axis in triplicate standard deviation determined by avaraging the standard deviation from each of the biological replicate groups. On the y-axis is the total standard deviation determined by averaging twenty randomised groups of three. The proteins displayed an exponential trendline. In the absence of any biological effect, one would expect the two standard deviations to be very similar (black diagonal line). Lower abundant proteins appear to change significantly depending on biological treatment. Peptide count is represented by the shading of the diamonds, a high peptide count having a darker shade of red. Abundant proteins (dark diamonds) tend to have lower triplicate and total standard deviations.

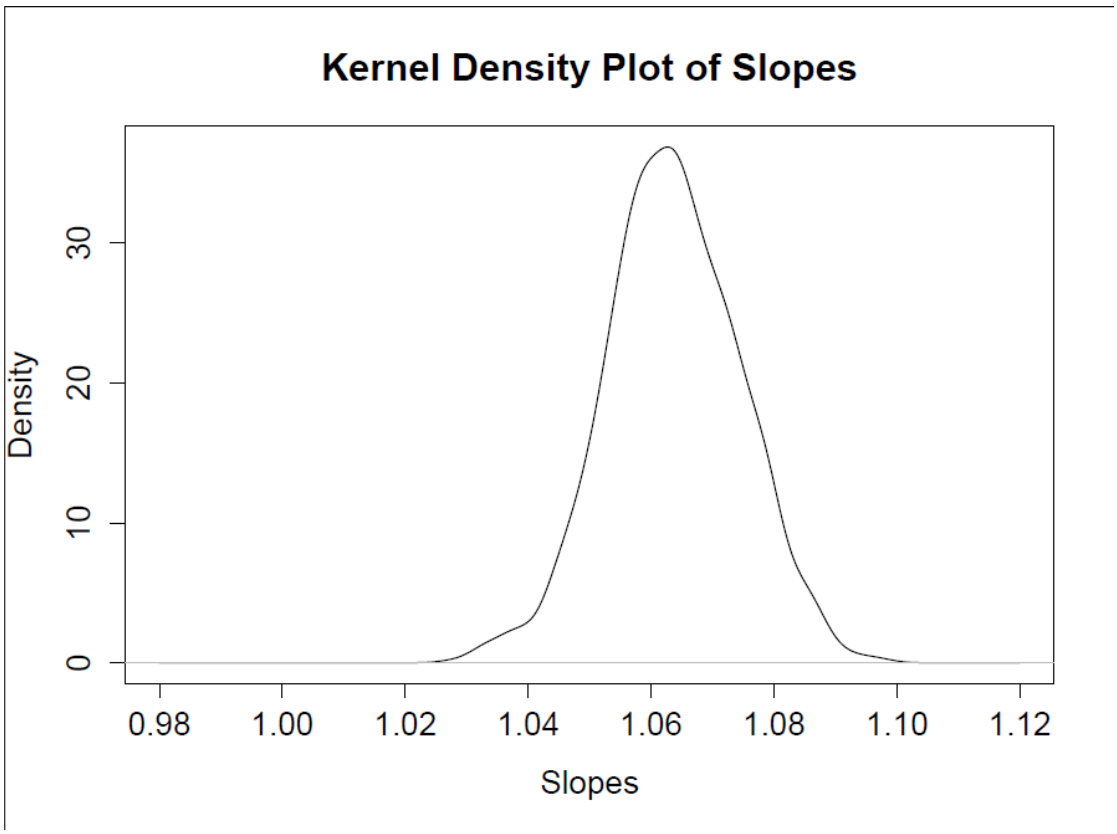

Figure 4-11: The relationship between triplicate SD and total SD has a slope higher than 1 when 1000 randomisations of total standard deviation are completed. This suggests there are significant changes in protein RAAT values with age and treatment within the dataset. This histogram shows the slope from 1000 trend lines. The trend lines are determined from different randomisations of the groupings for calculating total standard deviation. The slope is determined from y=mx, the intercept is set at zero and the slope (m) is calculated for the linear regression trend line which best fits the data (r script in Appendix A).

4.3.2. COMPARISON OF THE INDIVIDUAL SAMPLES

Mice that are very similar to each other are likely to have very similar RAAT values for all of their quantifiable proteins. Biological replicates are therefore likely to have very similar RAAT values and sample groups where ageing or nutritional status have changed the animals' physiology are likely to differ in the RAAT values of the proteins that represent the observed physiological changes.

To see, if the measured RAAT levels reflect the relative concentrations of the proteins and therefore also reflect the physiological status of the individual samples, I have performed to different multivariate statistical analyses to see, if related mouse groups would cluster. The two methods that were chosen here are clustering based on Pearson's correlation coefficients and Principal Component Analysis (Massart, 1997).

The Pearson Correlation Clustering (Figure 4-12) shows that mouse samples can indeed be grouped into clusters that indicate that the distance between individual samples is at least partially determined by biological differences. 60 samples were used in the Pearson correlation clustering. The proteins which weren't determined to be mitochondrial in mitominer (Smith *et al.*, 2012) were excluded for this clustering as they cluster closely and affect the sample clustering. The proteins measured in this study are from isolated mitochondria. None mitochondrial proteins may not be isolated with the mitochondria every time.

Clustering used on the mouse samples show which groups have similar protein RAAT values. Clustering of the samples in figure 4-12 produces an overall trend from young mouse samples on the right to old mouse samples on the left of the right hand side cluster. This cluster also contains high proportion of DR samples on the left. The right hand side of this heatmap has more AL samples. Within these AL samples on the right there is a separation of male (left) and female (right) mice which isn't seen in the other sections of the graph. The post-prandial (PF) mouse samples cluster of opposing sides of the heatmap. It is noticeable that one cluster is essentially formed by samples where a relatively large number of proteins were not quantifiable. This sample cluster is mainly composed of old mice of both sexes on the AL diet. It also contains male mice from the post-prandial (PF) experiment. Six of the samples are 30 months old.

Principle component analysis (PCA) requires a minimum number of non-missing values. Missing values are customary in proteomics research. The missing values can cause problems during data analysis. When calculating the PCA results for this data the missing values became a problem. PCA analysis requires at least two samples which have no missing values, this does not occur in my dataset. As a solution to the missing value problem I would have to exclude many proteins from the analysis. However, missing values are not indicative of an absent protein but can be due to low levels of the protein which weren't measured. In Perseus missing values can be produced to ease the analysis process. The missing values are filled with a random value generated by Perseus for each mouse sample RAAT values (Geiger *et al.*, 2013). These are not used throughout the study as they are not transformed raw data. PCA is an important mathematical tool which requires a more complete dataset and so was used in PCA analysis only.

The sample PCA scores plots in figure 4-13 shows four groups which cluster closely. The mouse samples which are biological replicates should group together. In figure 4-13, not all the biologically analogous mouse samples group together. I coloured the samples by sex (figure 4-13-B), Nutrition separating PMAL and PMDR (figure 4-13-C) and age. There is no grouping seen between male and female mouse samples. The post-prandial mice cluster on the left of component one. Component 2 and 3 remove this grouping. Age is the only condition which shows any grouping within the three components of the principle component analysis. This grouping is seen in the older mouse samples. Samples of 30 and 36 month old group closely together.

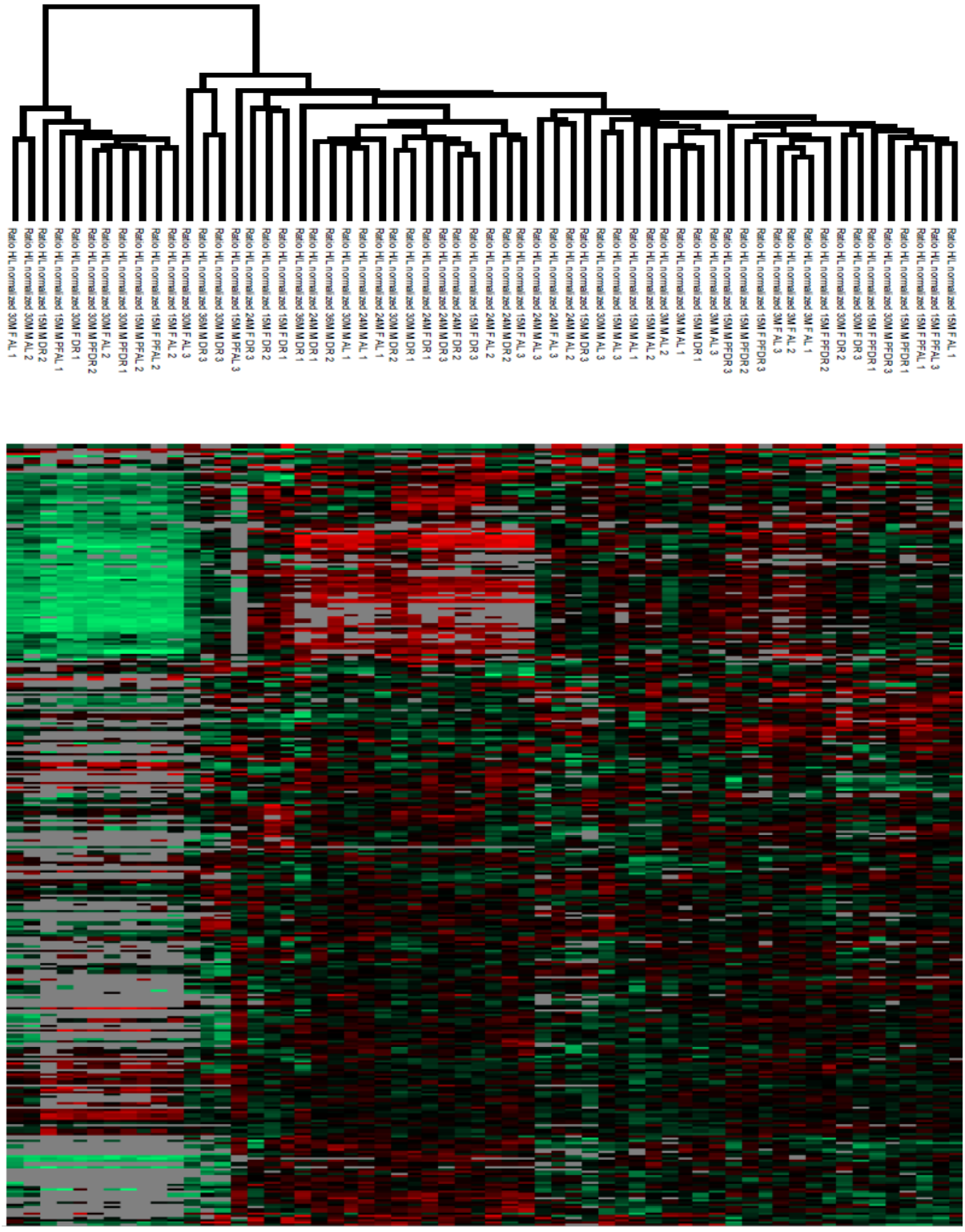

Figure 4-12: Clustering of the individual samples based on the RAAT values for each protein. Individual proteins are coloured red to black to green based on the RAAT value from low to high. Biological replicates which don't cluster closely together suggest a tendency for those groups to have a large triplicate standard deviation.

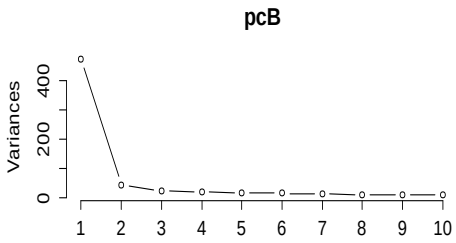

A:

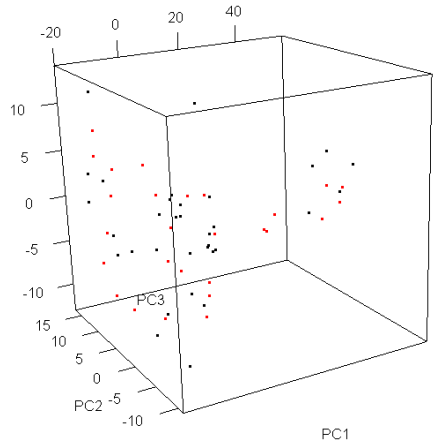

B:

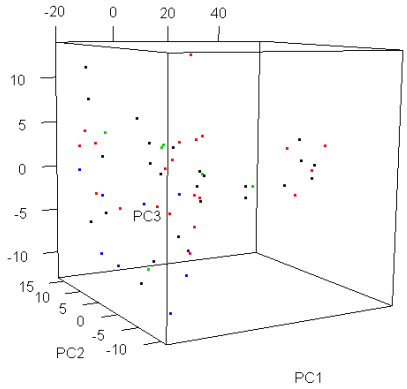

C:

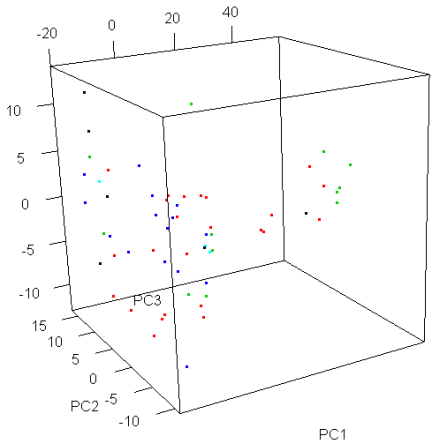

D:

Figure 4-13: PCA shows three distinct groups within the data which are separated by nutrition and age not sex. Principle component analysis scores plot of the 60 samples comparing components 1, 2 and 3. Panel A shows the eiganvalues for each component explaining the cause of data variation. Panel B is coloured to show male in black, and female in red. Panel C is coloured to show AL (black), DR (red), PMAL (green) and PMDR (blue). Panel D is coloured to show age, 3 months (black), 15 months (red), 24 months (blue), 30 months (green) and 36 months (light blue).

4.4. INDIVIDUAL METABOLISM PATHWAY CHANGE WITH AGE AND NUTRITION

The pearson correlation clustering of the proteins was analysed using DAVID (Huang *et al.*, 2007a; Huang *et al.*, 2007b) and uniprot (The UniProt, 2014; UniProt, 2014). The analysis was carried out on protein groupings which have the same heatmap trends in figure 4-12. The groupings were analysed in DAVID against a background of the 305 quantifiable proteins which were in the clustering. Using the annotation clustering offered by DAVID I discovered groupings containing fatty acid enriched clusters and enrichment of branched-chain amino acid degradation. Enrichment of glycolysis was seen in some clusters and was included in further analysis. These pathways were looked at in detail below.

4.4.1. RELATIVE PROTEIN CONCENTRATION OF PROTEINS INVOLVED IN FATTY ACID BIOSYNTHESIS AND CATABOLISM ARE INCREASED WITH AGE

Proteins involved in fatty acid biosynthesis, either from acetyl CoA or triglyeride. Acyl-CoA synthetase family member 2 (Acsf1),2,4-dienoyl-CoA reductase (Decr1),Enoyl-CoA hydratase domain-containing protein 2 (Echdc2),3-ketoacyl-CoA thiolase (Acaa2),Peroxisomal trans-2-enoyl-CoA reductase (Pecr). Protein abundance changes with age as they relate to 3 month old mice are shown in figure 4-14-A. These changes show an increase Echdc2 with age but a decrease in Acsf2. When separating the ageing mice into the two nutritions we see four of the five proteins are increased with age. The proteins increased with age in AL mitochondria are Acaa2, Echdc2, Decr1 and Pecr. Acsf2 is decreased with age. These proteins are unchanged in DR mitochondria (figure 4-14-C) however in Acsf2 is decreased with age in DR mice. DR feeding prevents this increase in Acaa2, Echdc2, Decr1 and Pecr. There are no changes in average RAAT value with the fatty acid biosynthesis pathway between nutrition, collection time and sex irrespective of any other condition.

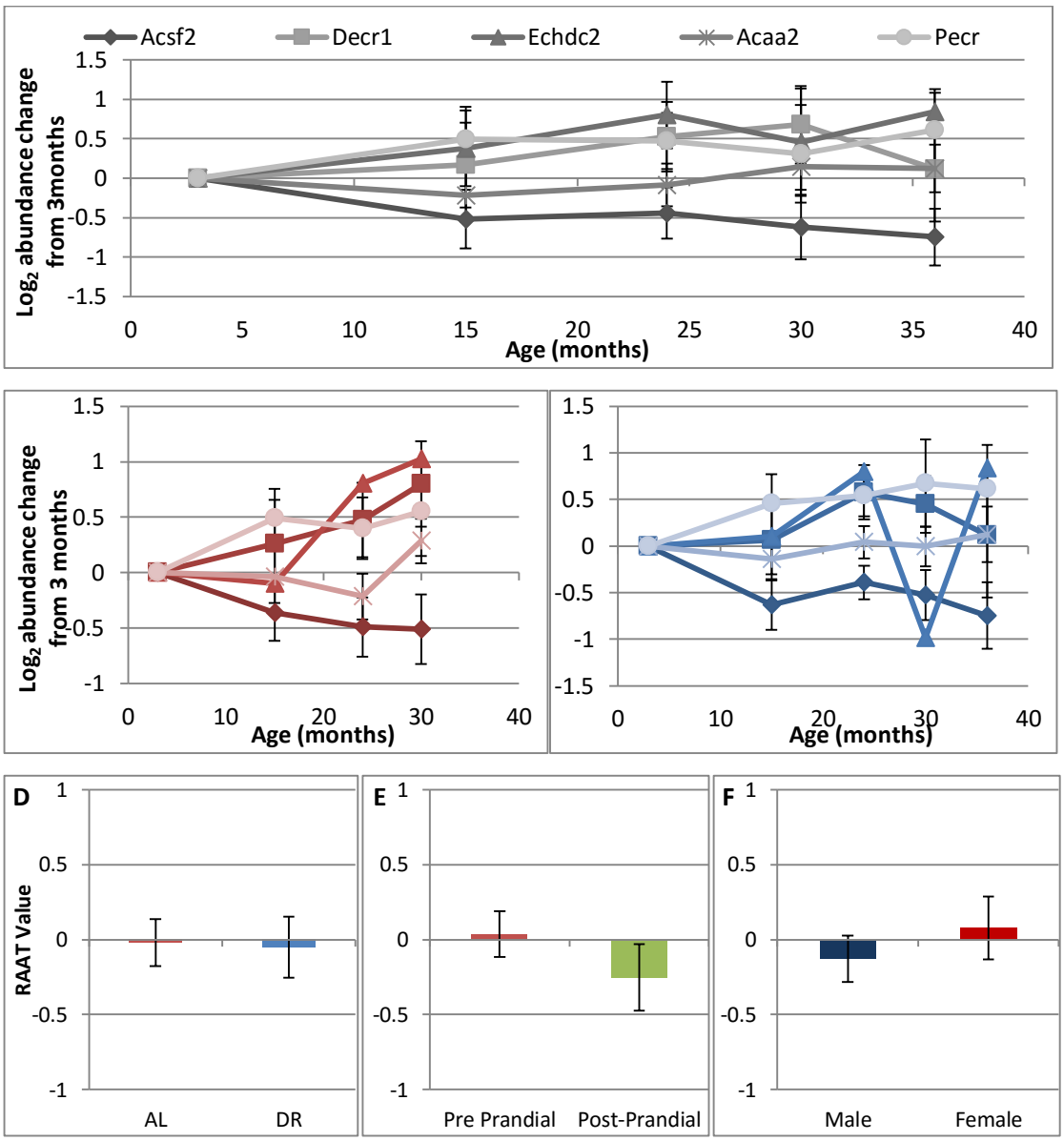

Figure 4-14: The protein concentration of fatty acid biosynthesis proteins is increased with age in AL mice. The change in protein abundance of five quantified proteins which are involved in fatty acid biosynthesis are displayed in the above graph. These proteins are acetyl CoA or triglyeride. Acyl-CoA synthetase family member 2 (Acsf1),2,4-dienoyl-CoA reductase (Decr1),Enoyl-CoA hydratase domain-containing protein 2 (Echdc2),3-ketoacyl-CoA thiolase (Acaa2),Peroxisomal trans-2-enoyl-CoA reductase (Pecr). Panel A, B and C display the same proteins for combined age (in grey, panel A) in red for AL (panel B) and blue for DR (panel C). Panel A has the abundance change from 3 months for each protein at each age without nutrition, collection time or sex differentiation. Panel B and C is the abundance change from 3 months for each protein at each age point B is with AL nutrition, and C is with DR nutrition, from any collection time and either sex. Panel D to F compares the average RAAT value for all four proteins comparing AL and DR (D), pre and post-prandial (E) and male and female (F) irrespective of all other conditions.

Beta-oxidation of fatty acids is the degradation of fatty acids to obtain acetyl CoA for used of the TCA cycle and production of substrate for the electron transport chain. Enoyl-CoA hydratase (Echs1), Carnitine O-palmitoyltransferase 2 (Cpt2), Hydroxyacyl-coenzyme A dehydrogenase (Hadh), Long-chain specific acyl-CoA dehydrogenase (Acadl), Short-chain specific acyl-CoA dehydrogenase (Acads), 3-ketoacyl-CoA thiolase (Hadhb),Very long-chain specific acyl-CoA dehydrogenase (Acadvl), Long-chain-fatty-acid—CoA ligase (Acsl1), Long-chain-fatty-acid--CoA ligase 1 (Acadm) Delta(3,5)-Delta(2,4)-dienoyl-CoA isomerase (Ech1), are the proteins quantified in this study which are involved in this process.

The abundance of the ten proteins linked to beta-oxidation has no strong trend in changes with ageing independent of other conditions. Ageing in AL mitochondria has only one protein with a consistent increase with age (Echs1). In DR mitochondria there is an early decrease in abundance in four of the proteins between 3 and 15 months. These four proteins show an protein abundance then increases with age to 30 months after this initial decrease (Echs1, Acadl, Acadm, and Hadhb). Then there is a drop in the abundance of these four proteins. Acadvl doesn't follow this trend it has a low concentration with age in DR mitochondria.

Fatty-acid beta-oxidation protein abundance is unchanged between colletion time and sex of the mitochondria. Nutritional change causes a change in average RAAT value irrespective of age, collection time or sex.AL mitochondria have a higher protein concentration than DR mitochondria. AL mice weigh more than DR mice; in addition they have a higher amount of fat. DR mitochondria don't have this available resource reducing the use of this pathway.

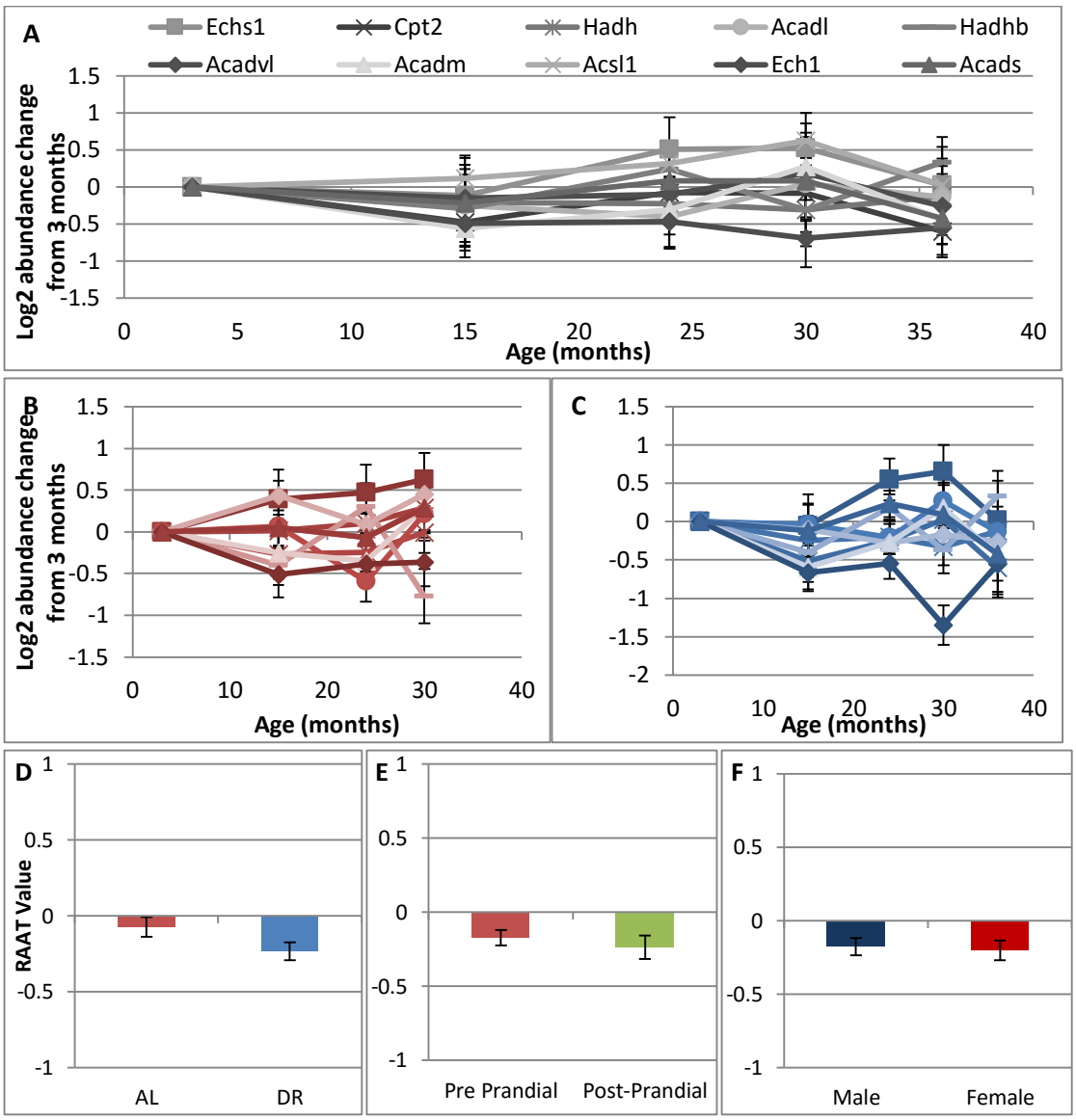

Figure 4-15: The protein concentration of fatty acid beta-oxidation proteins are decreased in DR liver mitochondrial proteomes. The change in protein abundance of fourteen quantified proteins which are involved in fatty acid beta-oxidation are displayed in the above graph. These proteins include: Enoyl-CoA hydratase (Echs1, dark squares), Carnitine O-palmitoyltransferase 2 (Cpt2, dark crosses) Hydroxyacyl-coenzyme A dehydrogenase (Hadh, dark crosses), Long-chain specific acyl-CoA dehydrogenase (Acadl, dark stars), Short-chain specific acyl-CoA dehydrogenase (Acads, dark pluses), Trifunctional enzyme subunit beta (Hadhb, dark dashes), Very long-chain specific acyl-CoA dehydrogenase (Acadvl, light diamonds), 3-ketoacyl-CoA thiolase B (Acaa1b, light squares), Medium-chain specific acyl-CoA dehydrogenase (Acadm, light triangles), Long-chain-fatty-acid--CoA ligase 1 (Acsl1, light crosses). Panel A, B and C display the same proteins for combined age (in grey, panel A) in red for AL (panel B) and blue for DR (panel C). Panel A has the abundance change from 3 months for each protein at each age without nutrition, collection time or sex differentiation. Panel B and C is the abundance change from 3 months for each protein at each age point B is with AL nutrition, and C is with DR nutrition, from any collection time and either sex. Panel D to F compares the average RAAT value for all four proteins comparing AL and DR (D), pre and post-prandial (E) and male and female (F) irrespective of all other conditions.

Ketone bodies are produced by the liver from fatty acids when food intake is low. Three ketone bodies are produced as an alternative to glucose, acetone, acetoacetic acid and beta-hydroxybutaric acid. Four proteins were quantifiable from the synthesis and degradation of ketone bodies pathway in this dataset. These were Acetyl-CoA acetyltransferase (Acat1),D-beta-hydroxybutyrate dehydrogenase (Bdh1),Hydroxymethylglutaryl-CoA lyase (Hmgcl), and Hydroxymethylglutaryl-CoA synthase(Hmgcs2).

The four proteins are compared between AL and DR, pre- and post-prandial and male and female. There was no difference between any of these comparisons. In aging there is no change in three of the proteins however Bdh1 increases with age. When separating age into AL and DR nutritions, Hmgcl is unchanged with age. The other proteins all follow a close trend with an increase in protein abundance with respect to the 3 month concentration between 15 to 30 months. In dietary restricted mitochondrial proteomes the change in protein abundance is only increased in Bdh1. Dietary restriction appears to prevent the ageing increase of three of the ketone bodies but not Bdh1.

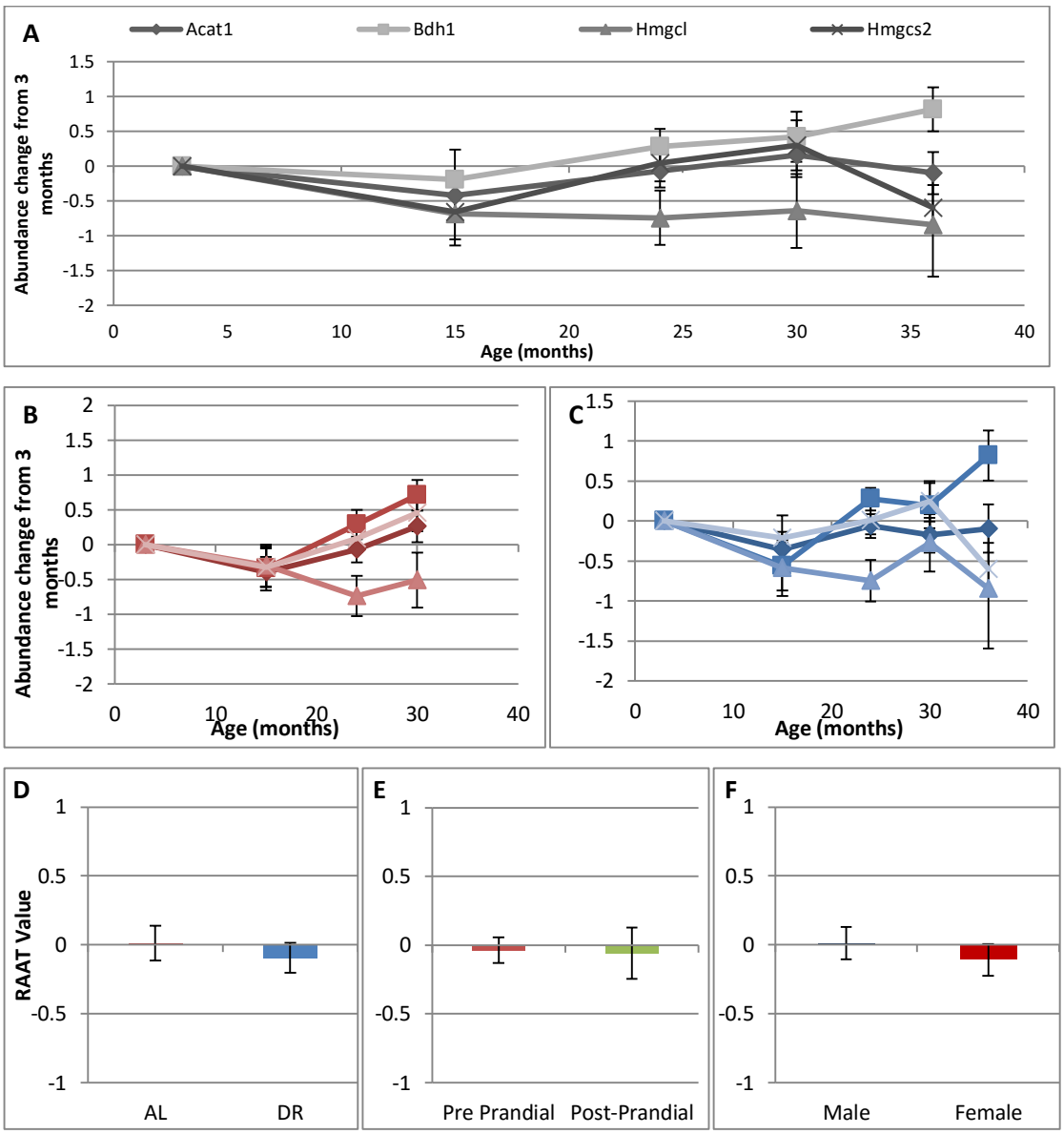

Figure 4-16: The protein concentration of D-beta-hydroxybutyrate dehydrogenase increases with age independent of other conditions. The abundance change in four proteins involved in ketone synthesis and degradation, including for four ketone body synthesis or degradation proteins quantified in this dataset, these were Acetyl-CoA acetyltransferase (Acat1), D-beta-hydroxybutyrate dehydrogenase (Bdh1), Hydroxymethylglutaryl-CoA lyase (Hmgcl), and Hydroxymethylglutaryl-CoA synthase (Hmgcs2). Panel A,B and C display the same proteins in red for AL (panel B) and blue for DR (panel C). Panel A has the Log_2 abundance change from 3 months for each protein at each age without nutrition, collection time or sex differentiation. Panel B is the Log_2 abundance change from 3 months for each protein at each age point for AL nutrition, any collection time and either sex. Panel C is the same Log_2 abundance change from 3 months for each protein at each age point for DR nutrition, all collection times and sexes. Panel D compares the average RAAT value for all three proteins for AL (red) and DR (blue) from all ages and sexes. Panel E compares the average RAAT value from the three proteins for pre- (red) and post-prandial (green) treatments and Panel F shows the average RAAT value from the three proteins for male (blue) and female (red) mice irrespective of age, nutrition or collection.

4.4.2. CHANGES SEEN IN DIFFERENT AREAS OF AMINO ACID METABOLISM WITH DIFFERENT DIETARY TREATMENTS

Groups of amino acids are synthesised using different pathways. Branched chain amino acids, aromatic and nucleophilic amino acids have separate synthesis pathways. The other amino acids are produced with crossover points between individual pathways including the urea cycle, aspartate and asparagine metabolism and glycine, glutamate and histidine metabolism.

Eight amino acid biosynthesis proteins are quantifiable within the urea cycle and glutamate metabolism. These proteins including, Ornithine aminotransferase (Oat), Aspartate aminotransferase (Got2), Glutamate dehydrogenase 1 (Glud1), Glutathione S-transferase kappa 1 (Gstk1) and Amine oxidase (Maob). Three proteins as part of the urea cycle include Argininosuccinate synthase (Ass), Carbamoyl-phosphate synthase (Cps), and Ornithine carbamoyltransferase (Otc). The concentration of the urea cycle proteins increases at 24 months with age independent of nutrition, collection time and sex. There is no change in the other proteins with age. In the urea proteins in AL mitochondria, Ass1 has a large increase with age until 30 months. In the DR mitochondria with age all urea proteins are increased at 24 months and decreased by 30 months of age.

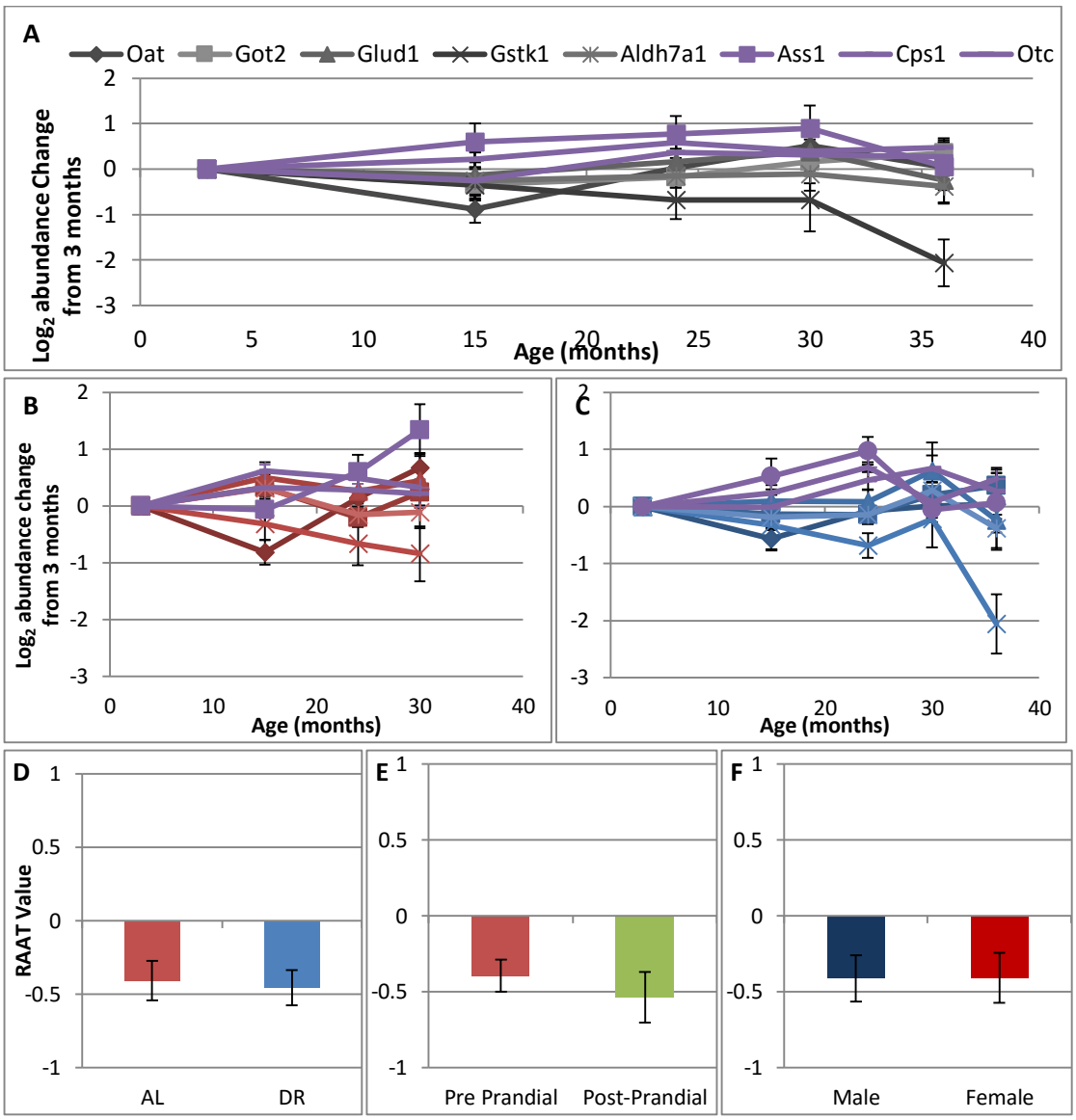

Figure 4-17: The protein concentration of urea amino acid biosynthesis proteins is increased with age. The change in protein abundance of ten quantified proteins which are involved in amino acid biosynthese are displayed in the above graph. Ornithine aminotransferase (Oat), Aspartate aminotransferase (Got2), Glutamate dehydrogenase 1 (Glud1), Glutathione S-transferase kappa 1 (Gstk1), Alpha-aminoadipic semialdehyde dehydrogenase (Aldh7a1) and Amine oxidase (Maob). Three proteins as part of the urea cycle include Argininosuccinate synthase (Ass), Carbamoyl-phosphate synthase (Cps), and Ornithine carbamoyltransferase (Otc) are the quantifiable proteins detected in amino acid biosynthesis. Panel A, B and C display the same proteins for combined age (in grey, panel A) in red for AL (panel B) and blue for DR (panel C). Panel A has the abundance change from 3 months for each protein at each age without nutrition, collection time or sex differentiation. Panel B and C is the abundance change from 3 months for each protein at each age point B is with AL nutrition, and C is with DR nutrition, from any collection time and either sex. Panel D to F compares the average RAAT value for all four proteins comparing AL and DR (D), pre and post-prandial (E) and male and female (F) irrespective of all other conditions.

Branched amino acid degradation proteins were grouped in the clustering. The six proteins in this pathways which have quantifiable results are: 3-mercaptopyruvate sulfurtransferase (Mpst), Protein disulfide-isomerase (P4hb) 3-hydroxyisobutyrate dehydrogenase (Hibadh), 3-hydroxyisobutyryl-CoA hydrolase (Hibch), Methylmalonyl-CoA mutase (Mut), Methylcrotonoyl-CoA carboxylase subunit alpha (Mccc1).

Four of the proteins involved in branched chain amino acid degradation are decreased with age. Three of these are specific to valine degradation. Mccc1 involved in Leucine degradation has no change with age. Mccc1 has no change in AL or DR mitochondria with age. Whereas the other proteins decrease with age in AL mitochondria, in DR mitochondria there is a decrease with age for Mut, Mpst and Hibach. In DR mitochondria P4hb doesn't decrease with age. This is the only protein which has different outcomes between AL and DR.

These proteins have the same average RAAT value in AL and DR mitochondria. There is a lower average RAAT value for the proteins, involved in branched amino acid degradation, if the mitochondria were collected post-prandially. The proteins have a high turnover if they are changed between these two groups. This is the only pathway which has a difference between male and female mice. Female mitochondria have a lower average RAAT value than the male mitochondria.

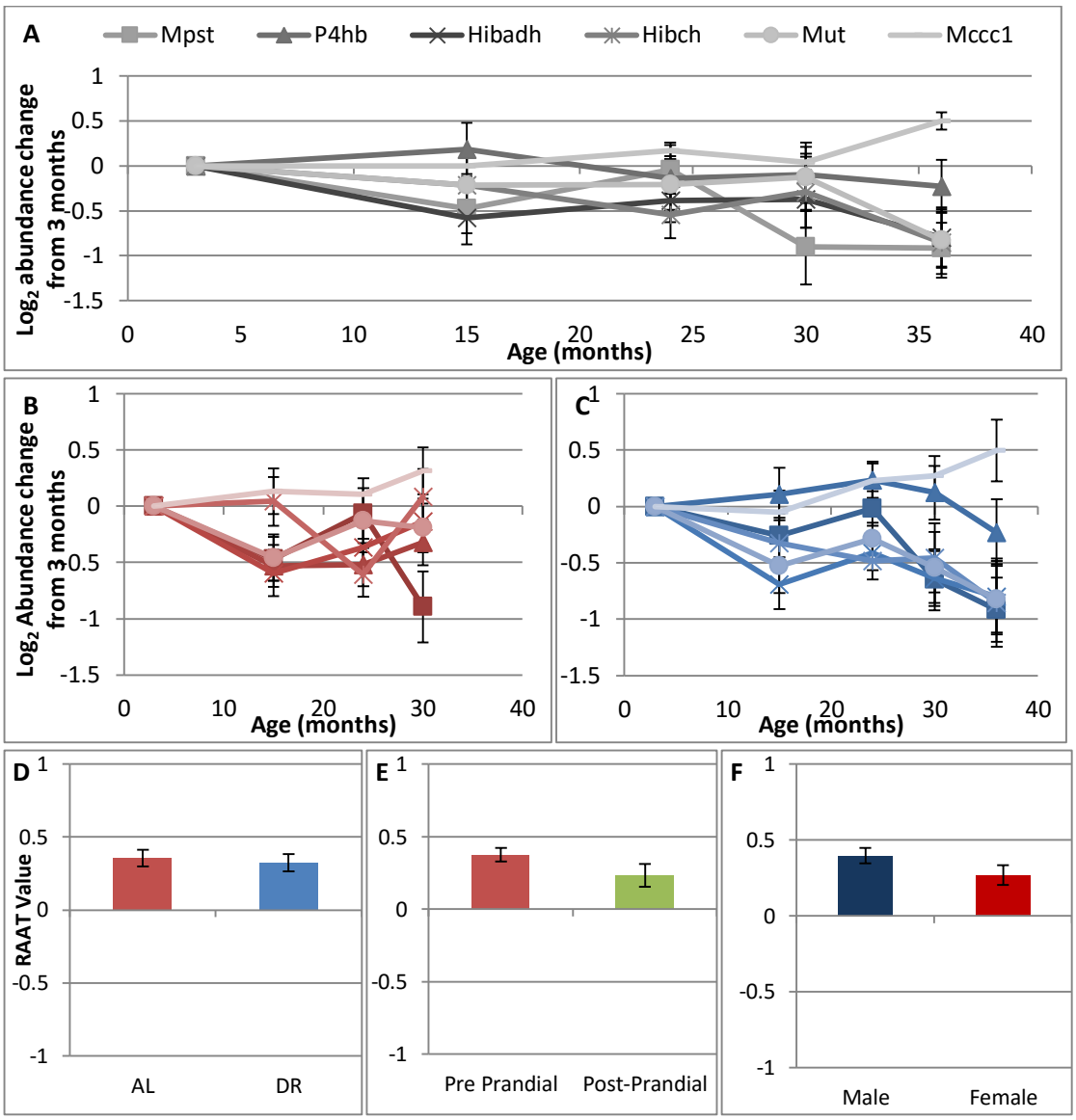

Figure 4-18: The protein concentration of amino acid catabolism proteins is lower in post-prandial mitochondria and female mitochondria irrespective of other conditions. The change in protein abundance of six quantified proteins which are involved in amino acid catabolism are displayed in the above graph. 3-mercaptopyruvate sulfurtransferase (Mpst), Protein disulfide-isomerase (P4hb) 3-hydroxyisobutyrate dehydrogenase (Hibadh), 3-hydroxyisobutyryl-CoA hydrolase (Hibch), Methylmalonyl-CoA mutase (Mut), Methylcrotonoyl-CoA carboxylase subunit alpha (Mccc1) are the quantifiable proteins detected in amino acid catabolism. Panel A, B and C display the same proteins for combined age (in grey, panel A) in red for AL (panel B) and blue for DR (panel C). Panel A has the abundance change from 3 months for each protein at each age without nutrition, collection time or sex differentiation. Panel B and C is the abundance change from 3 months for each protein at each age point B is with AL nutrition, and C is with DR nutrition, from any collection time and either sex. Panel D to F compares the average RAAT value for all four proteins comparing AL and DR (D), pre and post-prandial (E) and male and female (F) irrespective of all other conditions.

4.4.3. PYRUVATE METABOLISM PROTEINS HAVE LOWER CONCENTRATIONS IN POSTPRANDIAL COLLECTED MITOCHONDRIA

Pyruvate metabolism has four proteins which were quantifiable in this study. Three of these proteins are dihydrolipoyl dehydrogenase (Dld) and pyruvate dehydrogenase E1 components (Pdha1 and Pdhb), these proteins are involved in changing pyruvate to acetyl Co A or the reverse. The fourth protein is pyruvate carboxylase (Pcx) which produces oxaloacetate from pyruvate as part of the gluconeogenesis pathway.

Proteins involved in producing acetyl CoA from pyruvate follow a similar trend in figures 4-22-A-C. Ageing changes irrespective of any other condition results in no change with age in these proteins. Separating ageing changes by nutrition produces the same pattern of age changes in both AL and DR. In AL there is decrease in protein abundance compared to 3 month abundance with age in Dld and Pdhb at 15 and 24 months. In DR there is the same abundance change at 15, 24 and 36 months.

Pcx has a different trend to the other three proteins. This protein concentration increases with age irrespective of nutrition, collection time or sex. In AL mitochondria 15 and 24 month old mice have higher Pcx abundance compared to 3 month old mitochondria. In DR mitochondria higher Pcx abundance is seen in 24 and 36 month old mice compared to 3 month old mice. Pcx abundance increases earlier in AL mitochondria, it is higher in 15 month old mice than DR abundance of Pcx, DR abundance doesn't increase until 24 months nutritional restriction delays the abundance increase.

When comparing the conditions directly there is no change within the proteins between AL and DR and male and female. Comparing the pre- and post-prandial conditions reveals these four proteins were reduced in post-prandially collected tissue when compared to pre-prandially collected tissue.

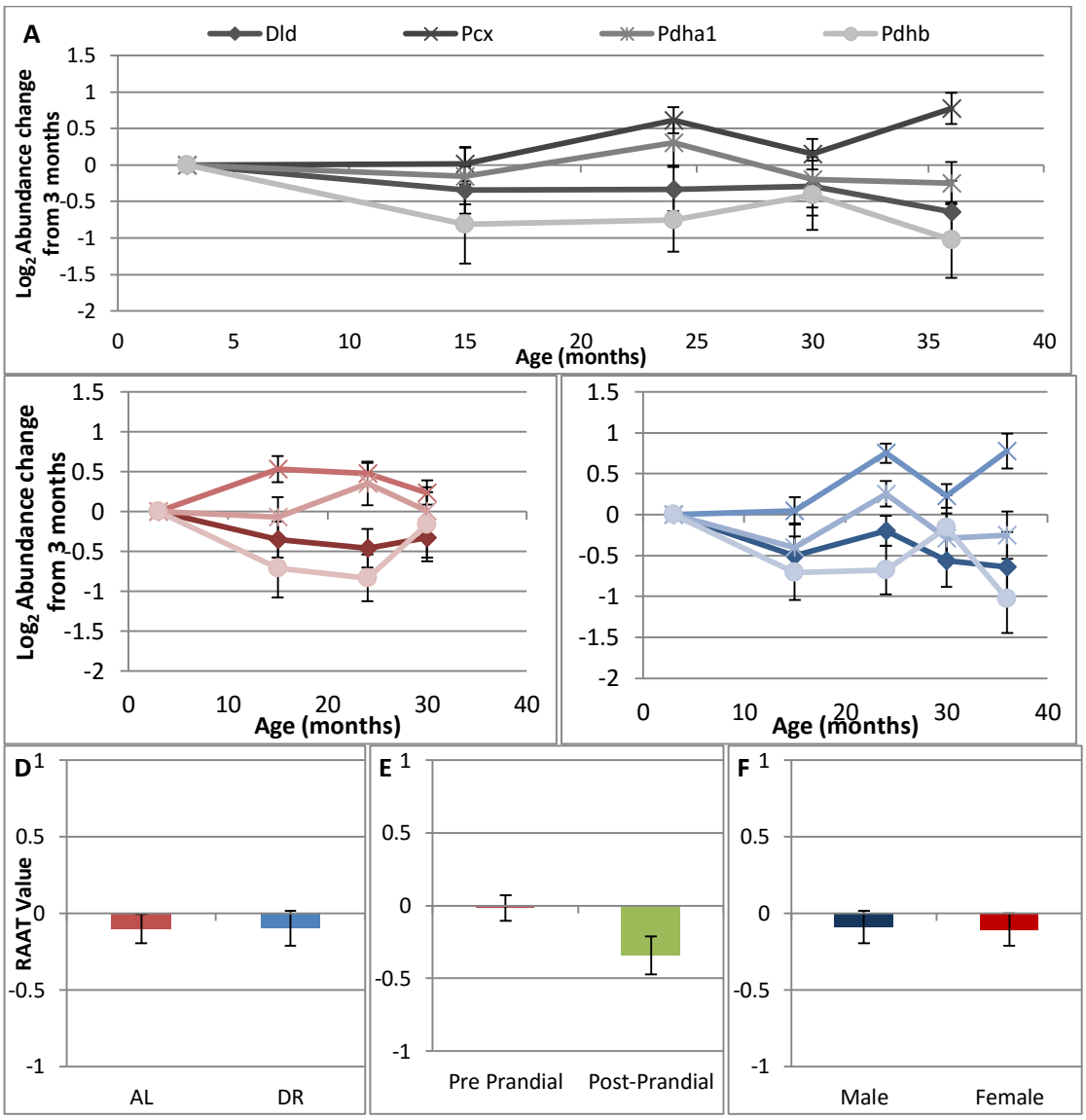

Figure 4-19: The protein concentration of pyruvate metabolism proteins is lower in post-prandial mitochondria. The change in protein abundance of four quantified proteins which are involved in pyruvate metabolism are displayed in the above graph. Dihydrolipoyl dehydrogenase (Dld, Dark diamonds), pyruvate carboxylase (Pcx, dark stars), and two pyruvate dehydrogenase E1 components (Pdha1 (light X) and Pdhb (light circles)) are the quantifiable proteins detected in pyruvate metabolism. Panel A, B and C display the same proteins for combined age (in grey, panel A) in red for AL (panel B) and blue for DR (panel C). Panel A has the abundance change from 3 months for each protein at each age without nutrition, collection time or sex differentiation. Panel B and C is the abundance change from 3 months for each protein at each age point B is with AL nutrition, and C is with DR nutrition, from any collection time and either sex. Panel D to F compares the average RAAT value for all four proteins comparing AL and DR (D), pre and post-prandial (E) and male and female (F) irrespective of all other conditions.

4.4.4. PROTEINS WHICH PROTECT AGAINST SUPEROXIDE HAVE A HIGHER CONCENTRATION IN OLDER AND DIETARY RESTRICTED MICE

Three proteins, mitochondrial superoxide dismutase (Sod2), glutathione peroxidase (Gpx1), and catalase (cat) are involved in clearing superoxide, forming hydrogen peroxide and preventing damage to the cell macromolecules. Glutathione peroxidase and catalase reduce hydrogen peroxide to water. Glutathione peroxidase abundance is unchanged with both age and nutrition. (Mavelli *et al.*, 1982)

Catalase remains unchanged with age independent of nutrition. However, catalase has an increased abundance with age in both AL and DR nutrition, independent of sex and collection time. There is an increased concentration of catalase between 3 and 30 months of age in the AL mitochondrial proteome (Figure 4-20-B). In addition there is an increase in catalase concentration in DR mitochondrial proteomes between 3 and 30 months of age with a decrease in the later 36 month age point (Figure 4-20-C).

The comparisons in panels D-F (Figure 4-20) show there are no independent changes in the three proteins between collection time and sex. The three protein do have an increase in DR mitochondria independent of age, collection time or sex. This change is predominantly in catalase. There is a higher concentration of catalase in DR mitochondria than AL at 15, 24 and 30 month age points in panels B and C of figure 4-20.

Superoxide dismutase removes the radical superoxide by producing hydrogen peroxide (McCord and Fridovich, 1969b). The abundance of the protein doesn't change independently with age, nutrition, collection time or sex. In panel c of figure 4-20 there is a decrease with age between 3 and 36 months. Catalase is the only protein changed which is involved with free radical clearance that is changed with age and nutrition.

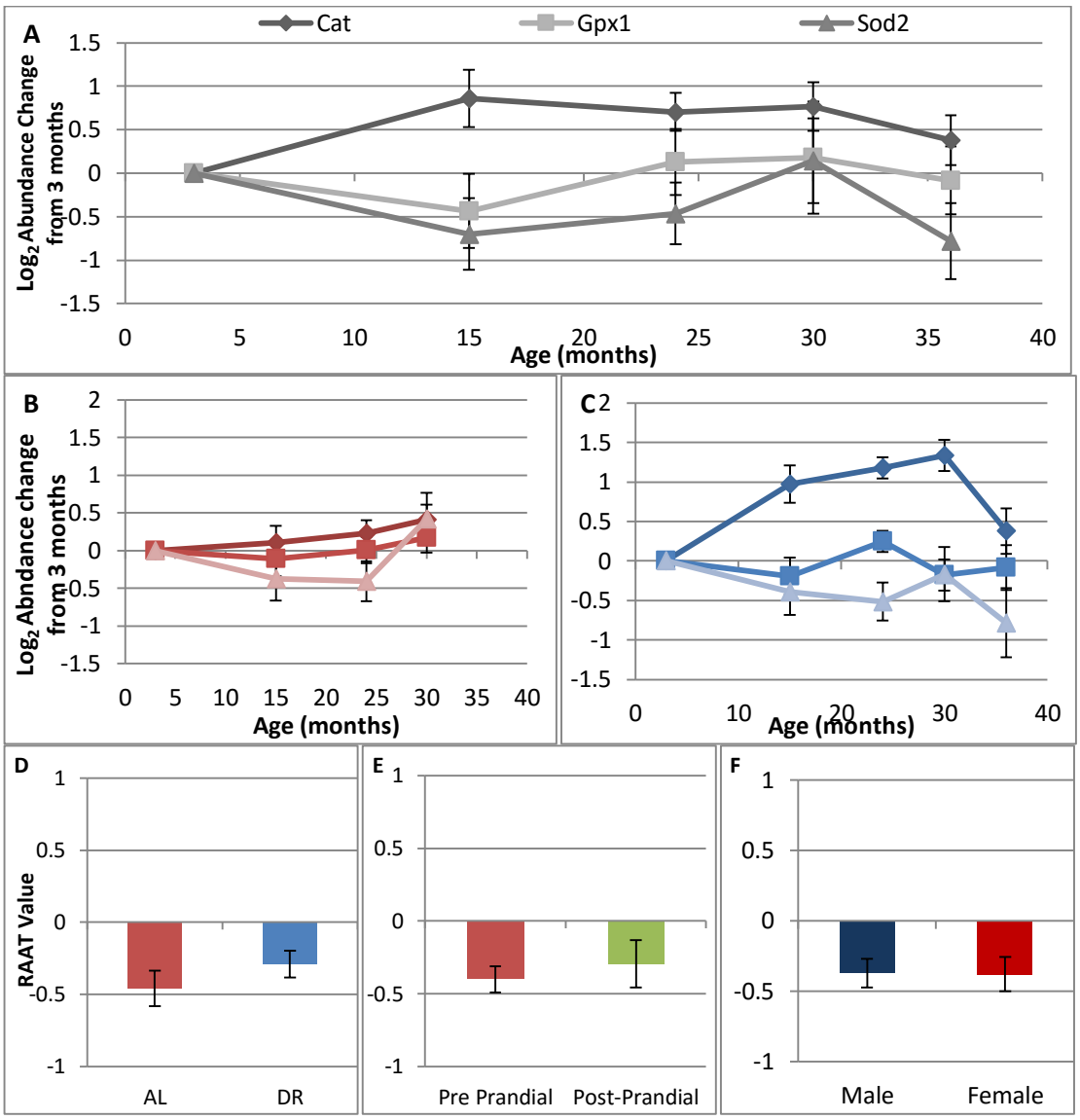

Figure 4-20: The protein concentration of catalase increases with age dependent on nutrition. There is a higher abundance of catalase in DR mitochondria at 15, 24 and 30 months. These panels display the RAAT values for three superoxide clearance proteins quantified in this dataset, catalase (Cat, Dark diamonds), glutathione peroxidase 1 (Gpx1, light squares) and mitochondrial superoxide dismutase (Sod2, Triangles). Panel A and B display the same proteins in red for AL (panel B) and blue for DR (panel C). Panel A has the average RAAT values for each protein at each age without nutrition, collection time or sex differentiation. Panel B is the average RAAT value for each protein at each age point for AL nutrition, any collection time and either sex. Panel C is the same average RAAT value for each protein at each age point for DR nutrition, all collection times and sexes. Panel D compares the average RAAT value for all three proteins for AL (red) and DR (blue) from all ages and sexes. Panel E compares the average RAAT value from the three proteins for pre- (red) and post-prandial (green) treatments and Panel F shows the average RAAT value from the three proteins for male (blue) and female (red) mice irrespective of age, nutrition or collection.

4.5. MITOCHONDRIAL PROTEOME IS ALTERED WITH DIETARY INTERVENTION

Proteomics is a fast developing field which can give a vast amount of information. This study focused on the mitochondrial proteome to better understand the role of ageing and dietary restriction as a lifespan extension model. Four different effects were compared including; sex, age, dietary restriction and tissue collection time (Figure 1-3). The different methodologies accessible for this project determined a spiked SILAC standard in each tissue to be the best method to compare the 60 samples.

A heavy labelled standard was 'spiked in' to 60 samples allowed comparisons to be made between the mouse groups for each protein. Comparisons cannot however be made between levels of the proteins with one sample. Data analysis of proteomics typically involves complicated statistics, and the large amounts of data require the proteins to have very low p-values to achieve statistical significance. The SILAC method used will allow for direct comparisons for all proteins between all samples. The mass spectrometry equipment is not infallible, it may not always detect every peptide. The most abundant peptides are the primary target of the instrument and consequently peptides of lower abundance are not always detected.

The SILAC method required two transformation steps. The first removed any variation of the concentration heavy labelled standard which was added to each sample. The second removed the influence of the mouse carcinoma cell line on the ratio determined by MaxQuant. This resulted in Relative Abundance After Transformation or RAAT values which were directly comparable between samples.

Analysis was started on particular protein functional groups, specific focus was paid to the metabolism pathways as these were the interesting pathways with regard to dietary changes. Proteins were grouped based on type of metabolism and compared between mouse groups. Mouse groups were simplified to compare sex, ageing, diet and collection time effects on protein abundance.

Ageing trends showed that fatty acid metabolism protein abundance was seen to increase with age irrespective of other factors. This trend appears stronger in AL fed mice than DR mice. On the contrary amino acid metabolism decreases with age

irrespective of other factors. Superoxide clearance proteins were shown to increase with age irrespective of any other factors. These proteins also show increased abundance in DR fed mice compared with AL irrespective of age. The abundance of catalase is increased in DR between 15 and 30 months of age yet abundance falls at 36 months. Collection time effects the RAAT values of proteins involved in the amino acid and pyruvate metabolism pathways. When tissues were collected post-prandially amino acid catabolism proteins were lower in abundance irrespective of any other factors. In addition pyruvate metabolism proteins show a decreased abundance when post prandial tissues are collected. Metabolism is altered with age and dietary restriction.

CHAPTER 5: DISCUSSION

5.1. AIMS OF THIS THESIS

Amplex red fluorescence from isolated mitochondria was used to measure hydrogen peroxide release from sites within the electron transport chain. These measurements examined changes with age, under normal and lifespan extension influences including dietary restriction, rapamycin and telomerase presence. The mitochondrial liver proteome was measured under four conditions. These are outlined in section 1.8, figure 1-3 and included ageing, nutrition, sex and time of tissue collection (pre vs post-prandial). The results from these measurements hopefully enlighten us to potential protein changes which cause the functional changes we see with ageing.

Hydrogen peroxide production and proteome composition were measured from up to five age points in isolated mice mitochondria. This is a greater comprehensive coverage of age than has been seen in other studies (Lass *et al.*, 1998; Barja, 2002; Barja, 2004; Ash and Merry, 2011). The first four ageing points were measured with only AL mitochondria (3, 15, 24, and 30 months). Long term dietary restriction was started at 3 months and measured from 15 months until the fifth age point (36 months) which was only reached by the DR mice. AL mice don't survive until 36 months and cannot be measured in 36 months. However we can compare the differences between 30 month AL and 36 month DR mitochondrial hydrogen peroxide release these are the ages when both groups are at 35% survival.

Post-prandial mitochondria will give us an understanding of which proteins have a high turnover. The proteome was measured at 15 and 30 months of age (PMDR), these mitochondria were measured six hours post DR feeding. A control for this group at 15 months was measured PMAL, these mitochondria were measured at 7hrs into the day light cycle. The 30 month old post-prandial mitochondria also used to obtain hydrogen peroxide release from isolated mitochondria. Females have a longer life extension with DR feeding thought to be due to lower oxidant generation (Borras *et al.*, 2007) by looking at the proteome compositional differences between the sexes we might find a reason for the difference in life extension.

5.2. LIVER MITOCHONDRIA REQUIRED AN ALTERED METHOD OF HYDROGEN PEROXIDE DETECTION

Liver mitochondria were measured by a slightly different method to the brain and muscle section 2.3. The brain, muscle and liver mitochondria hydrogen peroxide release are all measured using amplex red. The brain and muscle mitochondria were measured using the traditional method. Liver mitochondria were measured in a slightly different method. The hydrogen peroxide release was measured using amplex red both in and without the presence of HRP. The difference between these values was determined to be the release of hydrogen peroxide from the mitochondria. This method was developed due to a high oxidation of amplex red when no stimulation was presented. This doesn't occur in brain and muscle mitochondria.

Liver mitochondria have a large rate of basal hydrogen peroxide release from mitochondria. These basal levels were measured in the 15 month old AL and DR mice. There was a significantly lower release of H_2O_2 from DR mitochondria at basal levels. This significant reduction is maintained after the addition of substrate and the addition of rotenone and AA. I know from parallel respiration studies that there is no oxygen consumption when there is no substrate present (unpublished data, Satomi Miwa). If there is no oxygen consumption there is no respiratory chain activity. Without respiratory chain activity there is no superoxide production and therefore no hydrogen peroxide release.

The basal fluorescence response in liver mitochondria is complex. The signal is high and in 15 month old male liver mitochondria the addition of a substrate causes a decrease in fluorescence (figure 3-6 and figure 3-13). This decrease implies there is less hydrogen peroxide present to cause fluorescence. The signal would be expected to increase with the substrate addition as in brain mitochondria (figure 3-13). Substrate would activate the electron transport chain and produce superoxide. The production of superoxide would increase the prevalence of hydrogen peroxide increasing fluorescence. The kinetic addition of substrate didn't alter the responses (figure 3-9). The response to substrate occurs irrespective of when the substrate is added. The decrease after substrate addition is the crux of the problem. This removes the ability to subtract the basal level and measure the increase seen after substrate addition.

In liver mitochondrial studies using amplex red this problem is not discussed. Basal (state 1) hydrogen peroxide generation is rarely published as generally this is a negligible value due to the absence of a substrate. The results published for hydrogen peroxide measured by amplex red in mouse liver mimic those I detected without the consideration of the high basal levels (Lopez-Torres *et al.*, 2002). The possibility is these high 'basal' levels are both tissue specific and animal specific.

5.2.1. THE DETECTED FLUORESCENCE IS IN RESPONSE TO RESORUFIN BUT NOT IN RESPONSE TO HYDROGEN PEROXIDE RELEASE

Catalase breaks down hydrogen peroxide into water (Mavelli *et al.*, 1982; Schriner *et al.*, 2005). Catalase reacts with hydrogen peroxide to produce water so hydrogen peroxide can form resorufin and fluorescence. In brain mitochondria catalase almost completely removes the resorufin signal. In liver mitochondria addition of catalase has very little removal of the signal suggesting the signal is not linked to hydrogen peroxide release (figure 3-8). HRP absence removes the catalyst to the amplex red reaction. HRP absence in the amplex red assay with brain mitochondria irradicates the signal completely. Removal of HRP in liver mitochondria has very little effect on the liver hydrogen peroxide release. It is unlikely to be different peroxidases acting as a catalyst as using catalase to remove the hydrogen peroxide should still remove the signal (Votyakova and Reynolds, 2004).

The signal detected in the amplex red assay is resorufin. However the fluorescence signal detected could be another product in the mitochondria which fluoresces in the same area of the spectrum. The absorbance of the fluorescence product in the presence of liver and brain mitochondria occurs in the same range. Both absorbances show a peak at 590nm, the absorbance is higher in the liver mitochondria due to the intensity of the signal (figure 3-7). The addition of hydrogen peroxide to the liver mitochondria well returned a smooth absorbance graph with no second peak so the absorbance is aligned. The fluorescence of hydrogen peroxide only also gives a peak at 590nm further supporting the theory that the basal fluorescence in liver mitochondria is resorufin.

5.2.2. THE SUPPRESSION OF THE FLUORESCENCE IS DEPENDANT ON THE SUBSTRATE AND IT'S CONCENTRATION

Investigating the substrate effect proved that there is a response which occurs in proportion to the addition made. The suppression is dependent on substrate type, and concentration. 5mM of pyruvate malate and 4mM succinate are the optimal concentration for the amplex red assay (figure 3-14 and 3-15). The suppression of hydrogen peroxide release in liver mitochondria is not proportional between with and without HRP. There is greater suppression when HRP is not present. This greater suppression is concluded to be a result of the substrate addition producing superoxide and consequently hydrogen peroxide and resorufin. The type of substrate is also significant. Succinate, a type II linked substrate, has less of a suppressive effect then Complex I linked substrates, pyruvate malate for example.

5.2.3. THE SUPPRESSION OF HYDROGEN PEROXIDE RELEASE FROM MITOCHONDRIA IN THE PRESENCE OF HRP MIMICS THE RESULTS IF HRP IS NOT PRESENT

The difference between with and without HRP is how I have determined hydrogen peroxide release. Addition of a complex I substrate, rotenone and myxathiozol minimises the electron transport chain activity and consequently superoxide production. Figure 3-16 shows an increase in the rate of hydrogen peroxide release when HRP and substrate is present. Suppression of superoxide production results by myxathiozol removes the difference between presence and absence HRP. In addition the suppressed hydrogen peroxide release in equal to the release with substrate but in the absence of HRP. The best method available to determine liver mitochondria superoxide release is to measure the difference in amplex red production from mitochondria with and without the presence of amplex red.

5.3. INCREASED HYDROGEN PEROXIDE RELEASE IS SEEN IN AGEING TISSUES

Hydrogen peroxide production was measured at up to four ages in three tissues in AL mice. This is a much more in depth study of age and oxidative damage. Current studies show an increase in ROS production and superoxide production with age (Sohal *et al.*,

1994; Lass *et al.*, 1998; Dkhar and Sharma, 2010). Complex I superoxide release occurs from two different sites (lambert 2008). Complex I hydrogen peroxide release is increased in both brain and muscle mitochondria with age (section 3.3.1 and 3.3.2).

In the brain it was seen that the function of complex I and III was altered with age. The increase in hydrogen peroxide release which was detected was predominantly from complex I. The maximum capacity of complex I to produce superoxide increased with age. There was also an increase in complex I superoxide release with age under electron reverse flow. The complex III production was increased in the later age points, 24 and 30 months not at 15 months.

Muscle mitochondrial hydrogen peroxide release increases with age form complexes I and III. Increases in hydrogen peroxide release from complex I were seen in both forward and reverse flow with age. The increased reverse flow level is reflected in the higher release of hydrogen peroxide release seen when succinate is present. Complex III maximum capacity was higher in 15 and 30 months.

Liver mitochondria show no increase in hydrogen peroxide production with age as seen in brain and muscle mitochondria. Tissue specificity has been shown in other publications (Tahara *et al.*, 2009). There is no information for the 15 month age group as the problem detected had not shown its full complexity. The hydrogen peroxide release is higher in 24 and 30 months old mice compared with 3 month old mice. This increase was only significant in both maximal complex I stimulated release. This increase in complex I hydrogen peroxide release is not apparent in reverse flow. The age related increase of complex III is in all tissues, however complex I increase is tissue specific to brain and muscle.

5.4. HYDROGEN PEROXIDE RELEASE IS LOWER IN DIETARY RESTRCTED MICE COMPARED WITH AD LIBITUM FED MICE

Dietary restriction is well documented to have lower superoxide than AL fed mice (Sohal *et al.*, 1994; Lass *et al.*, 1998). DR reduced the release of hydrogen peroxide from the mitochondria. This ageing effect seen in AL mice tissues was delayed with dietary restriction. The 15 month old mice show no significant difference in hydrogen peroxide release when compared with 3 month old animals. This suppression is seen in

brain mitochondria. Forward flow complex I release is not significantly different with then of 3 month old animals. Reverse flow from complex I maintains low levels comparative to 3 month old release up until 30 months of age. This effect is also seen in complex III release and is maintained until 24 months old. The same effect does not occur in muscle mitochondria from complex I. At 15 months the release of hydrogen peroxide is significantly higher than that produced at 3 months when forward and reverse flow is occuring. This level of release is significantly lower than that released at 30 and 36 months. This pattern follows complex III production also. The release at 3 months is significantly lower than the DR animal at greater ages. Complex III release also does not increase with age as seen in the brain mitochondria.

Liver mitochondria used a different method this resulted in only uncorrected 15 month old data. The pattern is maintained here at 24 and 30 months of age the release of hydrogen peroxide from complex I, with flow in either direction, is not significantly different than at 3 months old.

A decreased level of ROS production in DR mice has been shown in muscle, heart and liver tissues (Lopez-Torres *et al.*, 2002; Drew *et al.*, 2003). This study looks at older age ranges in DR animals than have been seen previously, so comparisons could be drawn between hydrogen peroxide release at similar survival percentages. Decreased hydrogen peroxide release as a marker of superoxide production in DR mice has been seen in mice up to the age of 30 months, as seen here in liver mitochondria. Most studies compared ageing at two ages, young (3-8 months) and old (24 months). Few studies go up to 30 months old, the data available show an increase in age supporting this data. The effects of DR have also been shown at these ages to be lower than AL mice, with more than two ages to compare a more comprehensive understanding of how the release of hydrogen peroxide changes with age (Lopez-Torres *et al.*, 2002; Drew *et al.*, 2003). Loss of the difference between AL and DR mice at 30months and at 30% survival suggests that the effects of DR are reduced over long term restriction.

The dysfunction of complex I can avoided using dietary restriction until 24 months when there is no improvement compared to AL mice. At 30% survival the mice had similar levels of superoxide production from complex I via reverse flow, though maximum capacity from forward flow was increased in DR brain mitochondria. In

muscle mitochondria the differences in between AL and DR lasted longer. Complex I maximum capacity was increased with age, dietary restriction at ages 15 and 24 months resulted in lower maximum capacities. The data from reverse flow reflected these changes in complex I with age and DR.

Liver mitochondria show the effects of DR most predominantly. There is a large decrease in the hydrogen peroxide release from complex I at 24 and 30 months DR compared with 3 months. At 36 months DR the is a large increase so there is little difference in hydrogen peroxide release at 30% survival in the liver of AL and DR mice. Again the decrease in hydrogen peroxide release in DR and increase with age was seen mainly in complex I production.

The 30 month old mice were compared for AL, DR and PMDR treatments. Dani et al showed that fasted DR (my DR treatment) have higher superoxide levels than fed DR rats (my PMDR treatment –post-prandial) liver mitochondria (Dani *et al.*, 2010). In this study there is a decrease in liver mouse mitochondria from maximal complex I production. Brain and muscle also have significantly lower post-prandial hydrogen peroxide release than pre-prandial hydrogen peroxide release (figure 3-39, 3-40, 3-41).

This comprehensive detail of this study allows the visualisation the delay in ageing which occurs in the DR mice. Again this supports the theory that increased superoxide is linked to complex I dysfunction, and maintained at a lower level for longer with a DR diet. This data was published in Miwa et al (Miwa *et al.*, 2014).

5.4.1. SHORT-TERM DIETARY RESTRICTION

The short term age changes are seen between 12 and 15 months. In the brain as in the main study there is a large increase in both complex I and III hydrogen peroxide release in brain and muscle mitochondria. This increase is not seen in complex I in the liver mitochondria, but there is the increase seen in complex III which agrees with the results seen in the main study. Complex II release has not been measured in relation to age, DR or rapamycin treatment before. This release is most affected in muscle mitochondria with age. There is an increase of superoxide production in both sites of production from complex II (Quinlan *et al.*, 2012).

Short term dietary restriction has been done in late stages of life and shown to extend lifespan (Cameron *et al.*, 2011). In all studied mitochondria complex I hydrogen peroxide release in decreased with DR treatment. These levels show further reduction in the post-fed mice when pyruvate malate is used as a substrate. Liver mitochondria only show the same effect in the reverse flow of mitochondria. These sites of production have different locations in complex one and or sensitive to different conditions which may not be present in short term DR but are with a longer treatment.

Complex III is unchanged between AL and DR in all tissues. In liver and muscle the release of hydrogen peroxide is lower in post fed mice only. Muscle mitochondria also show changes in complex II release of hydrogen peroxide at site q. There is a decrease in the release of hydrogen peroxide with DR treatment which is further decreased in the mice are culled six hours after feeding. Site f shows no difference in release between AL and DR treatments but there is significantly lower release in the post-fed animals (figure 3-46). This has been shown in other studies

5.4.2. SHORT-TERM RAPAMYCIN FEEDING

Rapamycin has been shown to extend lifespan in mice (Anisimov et al., 2011; Chen et al., 2009; Harrison et al., 2009; Miller et al., 2011). Mice treated with rapamycin have also been shown to have less ROS (Tunon *et al.*, 2003). However the breakdown of the site of superoxide production has not been determined. In this study rapamycin reduced the amount of hydrogen peroxide release from complex I in only muscle mitochondria. In liver and brain this is shown in the maximum capacity on complex I and the reverse flow via complex I.

There is no comparison with the effects of DR in liver mitochondria at 15 months. This comparison can be drawn in liver showing that they reflect those in AL and DR mice of the same age. Differences between the WT control and AL mice are seen, these are likely to be due to differences in strain of the mice. Comparing the results from the TERT-/- mice which were treated with rapamycin there was no effect of rapamycin on hydrogen peroxide release on mice.

Only short term feeding of rapamycin have comparable results to those seen in the short term DR treatment. These mice were all obtained from one background and fed

different treatments. The RC and RAPA group were fed a diet with a similar nutritional make up to that of the AL food, with one containing rapamycin and one without. The rapamycin control animals have increased hydrogen peroxide release from complex I in brain and muscle mitochondria. In all three tissues there was an increased hydrogen peroxide release from complex III. There was no change in complex II production. This means while the DR results cannot be directly compared with the rapamycin results the relationship between AL and DR can be compared with that of RC and RAPA treatment. The predominant changes seen with DR treatment are a reduction in complex I release. Only muscle mitochondria replicate these complex I results in both forward and reverse flow. There is an increase in hydrogen production as a result of liver complex I reverse flow with in rapamycin treatment. There is no significant change seen in complex III production in both DR and RAPA when compared with their respective controls.

5.4.3. TERT-/- MICE HAVE LOWER HYDROGEN PEROXIDE RELEASE AT A YOUNG AGE BUT A HIGHER INCREASE WITH AGE

TERT-/- showed a decrease in hydrogen peroxide release at 8 months compared to WT. This decrease was seen in complex I production from both forward and reverse flow of electrons. Looking at the same conditions at 15 months of age there is only a decrease hydrogen peroxide release via reverse flow in TERT-/-. Complex I superoxide release occurs from different sites in the complex for reverse flow compared to forward flow (figure 3-54, 3-55). These differences in release at 15 months could be linked to this. In succinate linked hydrogen peroxide release there is also a decrease with age in the mitochondria. This is not seen in PM linked hydrogen peroxide release.

Rapamycin treatment decreases hydrogen peroxide release in WT mice. In mice without catalytic telomerase the hydrogen peroxide release is unchanged. This suggests rapamycin requires telomerase to cause the hydrogen peroxide release seen with rapamycin treatment (figure 3-56, 3-57).

5.5. OLD AND DIETARY RESTRCTED LIVER SHOW DIFFERENCES IN FUNCTION AND PROTEOME COMPOSITION WHEN COMPARED TO TISSUES FROM YOUNG CONTROLS

Proteome changes were monitored in mouse liver mitochondria from five different age groups. The liver has been seen to have the most changed proteins in a tissue comparative study (Chang *et al.*, 2007). All the groups had male animals and nine of the groups have female animals. 15, 24 and 30 month old mice were either fed a dietary restricted diet (DR) or with unrestricted access to food (AL). This resulted in a very large multidimensional dataset that was mined for differences in the abundance of classes of mitochondrial proteins between different nutritional states and/or during the ageing process (figure 1-3).

5.5.1. FATTY ACID SYNTHESIS AND BETA OXIDATION HAVE NO CHANGE WITH NUTRITION BUT HAVE HIGH TURNOVER OF PROTEINS.

Fatty acids are a source of nutrient. The mitochondria can catabolise the fatty acids to produce acetyl CoA which feeds into the TCA cycle (Alberts *et al.*, 2008). There are two metabolism pathways which synthesize and catabolise fatty acids there is overlap in these proteins. The catabolism pathway for fatty acids is called beta-oxidation, which breaks down fatty acids into acetyl CoA for use in the TCA cycle.

Proteins involved in fatty acid biosynthesis, either from acetyl CoA or triglyeride. There is no change in the total protein abundance between nutrition, tissue collection time and gender differences. In ageing there is a steady increase in Decr1, Pecr and Echdc2. Acaa2 increases at 24 months AL. Acsf2 decreased in both AL and DR with age, this protein is part of an enzyme group which this is the first catalyst in fatty acid metabolism (figure 4-14).

Beta-oxidation of fatty acids is the degradation of fatty acids to obtain acetyl CoA for used of the TCA cycle and production of substrate for the electron transport chain. The abundance of these fatty acid beta oxidation proteins are unchanged with age. Fatty-acid beta-oxidation protein abundance is lower in DR mitochondrial proteomes compared with AL independent of age, collection time or sex (figure 4-15). This has been seen in an early liver proteome study with high significance (Chang *et al.*, 2007). There is no change between protein abundance of fatty acids at different tissue collection times and genders.

Ketone bodies are produced by the liver from fatty acids when food intake is low. The abundance of these enzymes is unchanged between AL and DR, pre- and post-prandial feeding and gender. The four enzymes involved in the synthesis and degradation of ketone bodies act in parallel trends with age in AL mice an initial decrease from 3 to 15 months is highly reproducible with an increase of abundance with age in three of the proteins. In DR ageing only Bdh1 is increased with age (figure 4-16). Fatty acids are increasing used with age in the AL mice,

5.5.2. PROTEINS LINKED TO PYRUVATE METABOLISM HAVE INCREASED ABUNDANCE IN DIETARY RESTRICTED MITOCHONDRIAL PROTEOMES.

Pyruvate metabolism occurs in the mitochondria Pyruvate metabolism proteins have no clear ageing trend between them, even when separated into AL and DR. The protein abundance is unchanged between AL and DR and gender differences. However in post-prandial mitochondria the protein abundance is lower than pre-prandial abundance (figure 4-19).

5.5.3. AMINO ACID METABOLISM

Different groups of amino acids are synthesised using different pathways. Branched chain amino acids, aromatic and nucleophilic amino acids have separate synthesis pathways. The other amino acids are produced with crossover points between individual pathways including the urea cycle, aspartate and asparagine metabolism and glycine, glutamate and histidine metabolism.

There is no change between the protein abundance of enzymes involved in amino acid biosynthesis between AL and DR nutrition (figure 4-17). Post-prandial amino acid biosynthesis proteins have a no change in abundance between pre- and post-prandial protein concentration. Gender shows no abundance change between amino acid proteins either. Proteins involved in the urea cycle are changed with age. In AL and DR mitochondria at 24 months the abundance is higher than 3 months.

A decrease is seen in the protein abundance of branched amino acid catabolism proteins with age in AL mitochondria (figure 4-18). These proteins have a lower abundance in older DR mitochondria. The change is a gradual decrease with age.

Branched chain protein abundance in post-prandial protein mitochondria is lower than that of pre-prandial protein abundance. These proteins are likely to have a high turnover if six hour changes cause alteration of the protein abundance. Gender also has a role in amino acid catabolism protein abundance the protein abundance is lower in female mice irrespective of age, diet and collection time.

5.5.4. THE ABUNDANCE OF REACTIVE OXYGEN SPECIES CLEARING PROTEINS INCREASES WITH AGE ONLY IN AD LIBITUM ANIMALS, INDEPENDENT OF SEX

Superoxide dismutase, glutathione peroxidase, and catalase are quantified proteins in this dataset which are involved in superoxide clearance. Post-prandial feeding and gender have no change in superoxide clearance protein abundance (McCord and Fridovich, 1969b; Mavelli *et al.*, 1982; Schriner *et al.*, 2005).

Increase in the three superoxide clearance proteins with age in the AL mitochondria in both males and females (figure 4-20-B). In DR mice with age and overall age independent of sex, DR and collection time only catalase increases with age (figure 4-20A,C). There is no increase in hydrogen peroxide release from complex I in older liver mitochondria. The increased catalase abundance with age may prevent the hydrogen peroxide increase with age seen in brain and muscle.

Catalase abundance is increased in mitochondria from DR fed mice comparing figures 4-20B and C. In addition there is an increase in superoxide clearance proteins in DR mice compared to AL mice independent of sex, age or tissue collection time. The increase in superoxide clearing proteins in the DR animals correlates with the decrease in hydrogen peroxide release from liver mitochondria which have been dietary restricted. These proteins have been shown to increase with age in brain tissues (Sohal *et al.*, 1994). Catalase overexpression has increases lifespan possibly by a similar mechanism (Schriner *et al.*, 2005). SOD overexpression has reduced superoxide levels in other models (Lee *et al.*, 2009)

CHAPTER 6: APPENDIX A

6.1. TABLES

Age (months)	Nutrition	Mouse ID	Weight (g)	Pathology	Assay Completed			Reason Assay not completed
					Brain	Liver	Skeletal Muscle	
3	AL	Young 1			YES	YES	YES	
3	AL	Young 2			YES	YES	YES	
3	AL	Young 3			YES	YES	YES	
3	AL	Young 4			YES	YES	YES	
15	AL	F4164 NN	49.4		YES	NO	YES	Liver method uneffective
15	AL	F4164 BN	49.7	Liver Growth	YES	NO	YES	Pathology excludes assays
15	AL	F4164 LN	47.4	Pancreatic growth	NO	NO	YES	Pathology altered nutrition
15	AL	F4164 RN	41.1		YES	NO	YES	Liver method uneffective
15	AL	F4164 2RN	40.6		YES	NO	YES	Liver method uneffective
15	AL	F5228 LN	41.5		YES	NO	YES	Liver method uneffective
15	AL	F5228 NN	31.2		YES	NO	YES	Liver method uneffective
15	AL	F5228 RN	37.3		YES	NO	YES	Liver method uneffective
15	DR	F4165 NN	23.3		YES	NO	YES	Liver method uneffective
15	DR	F4165 BN	25.2		YES	NO	YES	Liver method uneffective
15	DR	F4165 LN	26.2		YES	NO	YES	Liver method uneffective

15	DR	F4165 RN	24.7		YES	NO	YES	Liver method uneffective
15	DR	F4165 2RN	27.8		YES	NO	YES	Liver method uneffective
15	DR	F5230 BN	22.5		YES	NO	YES	Liver method uneffective
15	DR	F5230 NN	21.3		YES	NO	YES	Liver method uneffective
15	DR	F5230 RN	22.5		YES	NO	YES	Liver method uneffective
15	DR	F5230 LN	24.2		YES	NO	YES	Liver method uneffective
24	AL	F2921 NN	43.8		YES	YES	YES	
24	AL	F2921 RN	37.2		YES	YES	YES	
24	AL	F2921 BN	37.2		YES	YES	YES	
24	AL	F2921 2RN	39.1		YES	NO	NO	Problem in liver assay and muscle preparation
24	AL	F2921 2LN	33.1	Enlarged Spleen	YES	YES	YES	
24	DR	F2907 2RN	22.5	Prolapse	YES	YES	YES	
24	DR	F2907 2LN	24.7		YES	YES	YES	
24	DR	F2908 2RN	21.9	Blocked gut. Enlarged spleen and kidneys. Dark pancreas	YES	YES	YES	
24	DR	F2910 BN	26.8		YES	NO	NO	Experimental error

24	DR	F2910 2LN	22.4	Blocked gut	YES	YES	YES	
30	AL	F1656 BN	39.88	Seminal Duct abnormal	YES	YES	NO	Low muscle mitochondrial concentration
30	AL	F1657 RN	40.5	Lung Growth	YES	NO	YES	Experimental error
30	AL	F1660 2LN	33.31	Growth under skin	YES	YES	YES	
30	AL	F1660 BN	36.69	Liver Fibrosis	YES	YES	YES	
30	AL	F1659 BN	24.64		YES	YES	YES	
30	PMDR	F1639 RN	26.3		YES	YES	YES	
30	PMDR	F1639 LN	23.2		YES	YES	YES	
30	PMDR	F1639 2LN	27.2		YES	YES	YES	
30	PMDR	F1639 2RN	26.6		YES	YES	YES	
30	DR	F1640 NN	20.3	Liver Fibrosis	YES	YES	NO	Problem in muscle preparation
30	DR	F1640 LN	26.7		YES	YES	YES	
30	DR	F1640 BN	20	Liver Fibrosis	YES	YES	YES	
30	DR	F1640 2LN	24		YES	YES	NO	Problem in muscle preparation
30	DR	F1640 2RN	24.6		YES	YES	YES	
36	DR	F1639 RN	25.8		YES	YES	YES	
36	DR	F1639 LN	26.4		YES	YES	YES	
36	DR	F1639 2LN	22.1		YES	YES	YES	

36	DR	F1639 2RN	23.2		YES	YES	YES	

Table 6-1: Mice used to measure mitochondrial hydrogen peroxide release by the Amplex Red method from the ageing and dietary restriction study. The table includes the mouse age, treatment and body weight at death. It also notes any pathology which could have been the cause of not obtaining or not using the data from particular tissue assays. The table also indicates in which tissues the assay was not performed or not completed (columns on the right).

Name	Fraction	Experiment
AJ-Sample1		3M M AL 1
AJ-Sample2		3M M AL 2
AJ-Sample3		3M M AL 3
AJ-Sample4		15M M AL 1
AJ-Sample5		15M M AL 2
AJ-Sample6		15M M AL 3
AJ-Sample7		15M M DR 1
AJ-Sample8		15M F AL 1
AJ-Sample9		15M F AL 2
AJ-Sample10		15M F DR 1
AJ-Sample11		15M F DR 2
AJ-Sample12		15M F AL 3
AJ-Sample13		15M F DR 3
AJ-Sample14		24M M AL 1
AJ-Sample15		24M M DR 1
AJ-Sample16		24M M DR 2
AJ-Sample17		24M M DR 3
AJ-Sample18		24M F AL 1
AJ-Sample19		24M F AL 2
AJ-Sample20		24M F DR 1
AJ-Sample21		24M F DR 2
AJ-Sample22		24M F DR 3
AJ-Sample23		30M M AL 1
AJ-Sample24		30M M AL 2
AJ-Sample25		36M M DR 1
AJ-Sample26		36M M DR 2
AJ-Sample27		36M M DR 3
AJ-Sample28		30M M AL 3
AJ-Sample29		30M M DR 1
AJ-Sample30		30M M DR 2
AJ-Sample31		30M M DR 3
AJ-Sample32		30M F AL 1
AJ-Sample33		30M F AL 2
AJ-Sample34		30M F DR 1
AJ-Sample35		30M M PFDR 1
AJ-Sample36		30M M PFDR 2
AJ-Sample37		30M M PFDR 3
AJ-Sample38		15M M PFAL 1
AJ-Sample39		15M M PFAL 2
AJ-Sample40		15M M DR 2
AJ-Sample41		15M M PFDR 1
AJ-Sample42		15M M PFDR 2
AJ-Sample43		15M M PFDR 3
AJ-Sample44		15M F PFAL 1
AJ-Sample45		15M F PFAL 2

AJ-Sample46		15M F PFAL 3
AJ-Sample47		15M F PFDR 1
AJ-Sample48		15M F PFDR 2
AJ-Sample49		15M F PFDR 3
AJ-Sample50		15M M DR 3
AJ-Sample51		30M F DR 2
AJ-Sample52		30M F DR 3
AJ-Sample53		30M F AL 3
AJ-Sample54		24M F AL 3
AJ-Sample55		24M M AL 2
AJ-Sample56		24M M AL 3
AJ-Sample57		3M F AL 1
AJ-Sample58		3M F AL 2
AJ-Sample59		15M M PFAL 3
AJ-Sample60		3M F AL 3

Table 6-2: The MaxQuant template denoting the sample ID for each sample number. Fractions were not used on these samples, individual samples were analysed on a long gradient.

Age (months)	Nutrition	Sex	Sample ID	Mouse ID	Pathology
3	AL	M	3M M AL 1	YOUNG 1	
3	AL	M	3M M AL 2	YOUNG 2	
3	AL	M	3M M AL 3	YOUNG 3	
15	AL	M	15M M AL 1	2637 LN	
15	AL	M	15M M AL 2	2637 2RN	
15	AL	M	15M M AL 3	2637 NN	
15	DR	M	15M M DR 1	2630 RN	
15	DR	M	15M M DR 2	2630 LN	
15	DR	M	15M M DR 3	2630 NN	
15	PMAL	M	15M M PFAL 1	2639 2RN	
15	PMAL	M	15M M PFAL 2	2639 LN	
15	PMAL	M	15M M PFAL 3	2639 RN	
15	PMDR	M	15M M PFDR 1	2631 NN	
15	PMDR	M	15M M PFDR 2	2631 LN	
15	PMDR	M	15M M PFDR 3	2631 BN	
24	AL	M	24M M AL 1	2916 2LN	fibrotic liver, cysts on s.gut
24	AL	M	24M M AL 2	2917 BN	cyst on lung. Ingrown teeth so DR phenotype
24	AL	M	24M M AL 3	2917 2RN	
24	DR	M	24M M DR 1	2906 BN	
24	DR	M	24M M DR 2	2906 NN	pancreatic absess
24	DR	M	24M M DR 3	2908 RN	
30	AL	M	30M M AL 1	1646 RN	small lymphoma
30	AL	M	30M M AL 2	1647 2RN	
30	AL	M	30M M AL 3	1649 2LN	calcium deposit in s.int
30	DR	M	30M M DR 1	1642 NN	
30	DR	M	30M M DR 2	1642 2RN	
30	DR	M	30M M DR 3	1642 BN	
30	PMDR	M	30M M PFDR 1	1654 BN	
30	PMDR	M	30M M PFDR 2	1654 2RN	
30	PMDR	M	30M M PFDR 3	1654 2LN	
36	DR	M	36M M DR 1	1666 NN	
36	DR	M	36M M DR 2	1666 BN	
36	DR	M	36M M DR 3	1666 2LN	
3	AL	F	3M F AL 1	YOUNG 1	

3	AL	F	3M F AL 2	YOUNG 2	
3	AL	F	3M F AL 3	YOUNG 3	
15	AL	F	15M F AL 1	2657 LN	
15	AL	F	15M F AL 2	2657 NN	
15	AL	F	15M F AL 3	2657 RN	
15	DR	F	15M F DR 1	2643 2LN	
15	DR	F	15M F DR 2	2643 2RN	
15	DR	F	15M F DR 3	2649 NN	
15	PMAL	F	15M F PFAL 1	2650 NN	
15	PMAL	F	15M F PFAL 2	2650 LN	
15	PMAL	F	15M F PFAL 3	2650 RN	
15	PMDR	F	15M F PFDR 1	2645 NN	
15	PMDR	F	15M F PFDR 2	2645 RN	
15	PMDR	F	15M F PFDR 3	2645 LN	
24	AL	F	24M F AL 1	3104 NN	pancreatic tumour
24	AL	F	24M F AL 2	3104 RN	
24	AL	F	24M F AL 3	3104 BN	cyst on ovary
24	DR	F	24M F DR 1	3093 LN	
24	DR	F	24M F DR 2	3093 RN	couldn't find one ovary
24	DR	F	24M F DR 3	3093 NN	
30	AL	F	30M F AL 1	1695 2LN	
30	AL	F	30M F AL 2	1695 LN	lymphoma
30	AL	F	30M F AL 3	1695 BN	
30	DR	F	30M F DR 1	1698 2RN	lymphoma and kidney tumours
30	DR	F	30M F DR 2	1698 LN	
30	DR	F	30M F DR 3	1698 BN	lymphoma, advanced

Table 6-3: List of mice used in the proteomics ageing and dietary restriction study. The table includes the mouse age, treatment, sex, mouse ID and sample ID.

Parameter	Value
Version	1.3.0.5
Fixed modifications	Carbamidomethyl (C)
Randomize	FALSE
Special AAs	KR
Include contaminants	TRUE
MS/MS tol. (FTMS)	20 ppm
Top MS/MS peaks per 100 Da. (FTMS)	10
MS/MS deisotoping (FTMS)	TRUE
MS/MS tol. (ITMS)	0.5 Da
Top MS/MS peaks per 100 Da. (ITMS)	6
MS/MS deisotoping (ITMS)	FALSE
MS/MS tol. (TOF)	0.1 Da
Top MS/MS peaks per 100 Da. (TOF)	10
MS/MS deisotoping (TOF)	TRUE
MS/MS tol. (Unknown)	0.5 Da
Top MS/MS peaks per 100 Da. (Unknown)	6
MS/MS deisotoping (Unknown)	FALSE
Peptide FDR	0.01
Max. peptide PEP	1
Protein FDR	0.01
Site FDR	0.01
Use Normalized Ratios For Occupancy	TRUE
Apply site FDR separately	TRUE
Min. peptide Length	7
Min. score	0
Min. unique peptides	0
Min. razor peptides	1
Min. peptides	1
Use only unmodified peptides and	TRUE
Modifications included in protein quantification	Oxidation (M);Acetyl (Protein N-term)
Peptides used for protein quantification	Razor
Discard unmodified counterpart peptides	TRUE
Min. ratio count	2
Lfq min. ratio count	2
Site quantification	Use least modified peptide
Re-quantify	TRUE
Keep low-scoring versions of identified peptides	Also between groups
Label-free protein quantification	FALSE
iBAQ	FALSE
iBAQ log fit	TRUE
MS/MS recalibration	FALSE
Match between runs	TRUE
Time window [min]	2
Find dependent peptides	FALSE
Fasta file	C:\Mass Spec Amy\uniprot_mouse_2013_07.fasta

Labeled amino acid filtering	TRUE
Site tables	Oxidation (M)Sites.txt
Cut peaks	TRUE
Randomize	FALSE
Special AAs	KR
Include contaminants	TRUE
RT shift	FALSE
Advanced ratios	FALSE
AIF correlation	0.8
First pass AIF correlation	0.8
AIF topx	50
AIF min mass	0
AIF SIL weight	4
AIF ISO weight	2
AIF iterative	FALSE
AIF threshold FDR	0.01

Table 6-4: The parameters used by MaxQuant to generate protein SILAC data for individual samples from the .RAW file output by the mass spectrometer.

Chemical	Company
Amplex Red	Thermo Fisher Scientific
Sucrose	Sigma
Tris Base	Sigma
EDTA	Sigma
Ficoll	Sigma
EGTA	Sigma
Percoll	Sigma
KCl	Sigma
ATP	Sigma
$MgCl_2$	Sigma
BSA - Bovine Serum Albumin	Sigma
Protease Type VIII Subtilisin A	Sigma
Resorufin	Invitrogen
Hepes	Sigma
SOD	Sigma
Oligomycin	Sigma
DMSO	Sigma
Catalase	Sigma
HRP	Sigma
Pyruvate	Sigma
Malate	Sigma
Succinate	Sigma
Antimycin A	Sigma
Hydrogen peroxide	Sigma
Myxothiazol	Sigma
Atpenin A5	Sigma
Malonate	Sigma
DMEM/F12 Media	Sigma
Insulin	Sigma
Transferrin	Sigma
Selenium	Sigma

Dexamethasone	Sigma
L-Lysine-2HCl (K8)	Cambridge Isotope Lab
L-Arginine-HCl (R8)	Cambridge Isotope Lab
FBS	Sigma
Coomassie Blue	Sigma
DTT	Applichem
Iodoacetamide	Applichem
Acetonitrile	Sigma
Trypsin	Promega
Ammonium Bicarbonate	Sigma
Calcium Chloride	Sigma
TFA - Trifluoroacetic acid	Sigma
Urea	Sigma

Table 6-5: List of chemicals used in this studay and company that they were supplied from.

Protein IDs	Protein names	Gene names
Q99K67	Alpha-aminoadipic semialdehyde synthase, mitochondrial;Lysine ketoglutarate reductase;Saccharopine dehydrogenase	Aass
P61922	4-aminobutyrate aminotransferase, mitochondrial	Abat
Q8VCH0	3-ketoacyl-CoA thiolase B, peroxisomal	Acaa1b
Q8BWT1	3-ketoacyl-CoA thiolase, mitochondrial	Acaa2
Q8K370	Acyl-CoA dehydrogenase family member 10	Acad10
P51174	Long-chain specific acyl-CoA dehydrogenase, mitochondrial	Acadl
P45952	Medium-chain specific acyl-CoA dehydrogenase, mitochondrial	Acadm
Q07417	Short-chain specific acyl-CoA dehydrogenase, mitochondrial	Acads
Q9DBL1	Short/branched chain specific acyl-CoA dehydrogenase, mitochondrial	Acadsb
P50544	Very long-chain specific acyl-CoA dehydrogenase, mitochondrial	Acadvl
Q8QZT1	Acetyl-CoA acetyltransferase, mitochondrial	Acat1
Q99KI0	Aconitate hydratase, mitochondrial	Aco2
Q9QYR9	Acyl-coenzyme A thioesterase 2, mitochondrial	Acot2
Q9R0H0	Peroxisomal acyl-coenzyme A oxidase 1	Acox1
Q9QXD1	Peroxisomal acyl-coenzyme A oxidase 2	Acox2
Q8VCW8	Acyl-CoA synthetase family member 2, mitochondrial	Acsf2
D3Z041	Long-chain-fatty-acid--CoA ligase 1	Acsl1
Q91VA0	Acyl-coenzyme A synthetase ACSM1, mitochondrial	Acsm1
Q8BGA8	Acyl-coenzyme A synthetase ACSM5, mitochondrial	Acsm5
Q7TPR4	Alpha-actinin-1	Actn1
Q8R0N6	Hydroxyacid-oxoacid transhydrogenase, mitochondrial	Adhfe1
A2AS89	Agmatinase, mitochondrial	Agmat

Q3UEG6	Alanine--glyoxylate aminotransferase 2, mitochondrial	Agxt2
Q9Z0X1	Apoptosis-inducing factor 1, mitochondrial	Aifm1
Q9WTP6	Adenylate kinase 2, mitochondrial	Ak2
Q9WTP7	GTP:AMP phosphotransferase, mitochondrial	Ak3
Q9WUR9	Adenylate kinase isoenzyme 4, mitochondrial	Ak4
Q8CG76	Aflatoxin B1 aldehyde reductase member 2	Akr7a2
Q9CZS1	Aldehyde dehydrogenase X, mitochondrial	Aldh1b1
P47738	Aldehyde dehydrogenase, mitochondrial	Aldh2
Q8CHT0	Delta-1-pyrroline-5-carboxylate dehydrogenase, mitochondrial	Aldh4a1
Q8BWF0	Succinate-semialdehyde dehydrogenase, mitochondrial	Aldh5a1
Q9EQ20	Methylmalonate-semialdehyde dehydrogenase [acylating], mitochondrial	Aldh6a1
Q9DBF1	Alpha-aminoadipic semialdehyde dehydrogenase	Aldh7a1
Q3U367	4-trimethylaminobutyraldehyde dehydrogenase	Aldh9a1
Q91Y97	Fructose-bisphosphate aldolase B	Aldob
O09174	Alpha-methylacyl-CoA racemase	Amacr
P07356	Annexin A2;Annexin	Anxa2
P16460	Argininosuccinate synthase	Ass1
Q925I1	ATPase family AAA domain-containing protein 3	Atad3
Q8VDN2	Sodium/potassium-transporting ATPase subunit alpha-1	Atp1a1
O55143	Sarcoplasmic/endoplasmic reticulum calcium ATPase 2	Atp2a2
Q03265	ATP synthase subunit alpha, mitochondrial;ATP synthase subunit alpha	Atp5a1
P56480	ATP synthase subunit beta, mitochondrial	Atp5b
Q91VR2	ATP synthase subunit gamma, mitochondrial;ATP synthase gamma chain	Atp5c1
Q9D3D9	ATP synthase subunit delta, mitochondrial	Atp5d

P56382	ATP synthase subunit epsilon, mitochondrial	Atp5e
Q9CQQ7	ATP synthase subunit b, mitochondrial	Atp5f1
Q9DCX2	ATP synthase subunit d, mitochondrial	Atp5h;Gm10250
Q06185	ATP synthase subunit e, mitochondrial	Atp5i
P97450	ATP synthase-coupling factor 6, mitochondrial	Atp5j
P56135	ATP synthase subunit f, mitochondrial	Atp5j2
Q9CPQ8	ATP synthase subunit g, mitochondrial	Atp5l
Q9DB20	ATP synthase subunit O, mitochondrial	Atp5o
Q3U3J1	2-oxoisovalerate dehydrogenase subunit alpha, mitochondrial	Bckdha
Q6P3A8	2-oxoisovalerate dehydrogenase subunit beta, mitochondrial	Bckdhb
Q80XN0	D-beta-hydroxybutyrate dehydrogenase, mitochondrial	Bdh1
Q8R164	Valacyclovir hydrolase	Bphl
P14211	Calreticulin	Calr
P24270	Catalase	Cat
Q91VT4	Carbonyl reductase family member 4	Cbr4
Q8VCT4	Carboxylesterase 1D	Ces1d
Q9CRB9	Coiled-coil-helix-coiled-coil-helix domain-containing protein 3, mitochondrial	Chchd3
Q8BJ64	Choline dehydrogenase, mitochondrial	Chdh
Q91WS0	CDGSH iron-sulfur domain-containing protein 1	Cisd1
Q5SXR6	Clathrin heavy chain 1	Cltc
Q8R4N0	Citrate lyase subunit beta-like protein, mitochondrial	Clybl
Q9QXT0	Protein canopy homolog 2	Cnpy2
P19783	Cytochrome c oxidase subunit 4 isoform 1, mitochondrial	Cox4i1
P12787	Cytochrome c oxidase subunit 5A, mitochondrial	Cox5a
Q9D881	Cytochrome c oxidase subunit 5B, mitochondrial	Cox5b

Q9DCW5	Cytochrome c oxidase subunit 6A, mitochondrial;Cytochrome c oxidase subunit 6A1, mitochondrial	Cox6a1
P56391	Cytochrome c oxidase subunit 6B1	Cox6b1
Q9CPQ1	Cytochrome c oxidase subunit 6C	Cox6c
P36552	Coproporphyrinogen-III oxidase, mitochondrial	Cpox
Q8C196	Carbamoyl-phosphate synthase [ammonia], mitochondrial	Cps1
P52825	Carnitine O-palmitoyltransferase 2, mitochondrial	Cpt2
Q9CZU6	Citrate synthase, mitochondrial	Cs
Q02248	Catenin beta-1	Ctnnb1
E9Q8Z8	Catenin delta-1	Ctnnd1
P18242	Cathepsin D	Ctsd
P56395	Cytochrome b5	Cyb5a;Cyb5
Q9CQX2	Cytochrome b5 type B	Cyb5b
F2Z456	NADH-cytochrome b5 reductase 3;NADH-cytochrome b5 reductase 3 membrane-bound form;NADH-cytochrome b5 reductase 3 soluble form	Cyb5r3
Q9D0M3	Cytochrome c1, heme protein, mitochondrial	Cyc1
Q9DBG1	Sterol 26-hydroxylase, mitochondrial	Cyp27a1
Q9D172	ES1 protein homolog, mitochondrial	D10Jhu81e
P53395	Lipoamide acyltransferase component of branched-chain alpha-keto acid dehydrogenase complex, mitochondrial	Dbt
O54734	Dolichyl-diphosphooligosaccharide--protein glycosyltransferase 48 kDa subunit	Ddost
Q8BTS0	Probable ATP-dependent RNA helicase DDX5	Ddx5
Q9CQ62	2,4-dienoyl-CoA reductase, mitochondrial	Decr1
Q99LB2	Dehydrogenase/reductase SDR family member 4	Dhrs4
E9QNN1	ATP-dependent RNA helicase A	Dhx9

Q8BMF4	Dihydrolipoyllysine-residue acetyltransferase component of pyruvate dehydrogenase complex, mitochondrial	Dlat
O08749	Dihydrolipoyl dehydrogenase, mitochondrial	Dld
Q9D2G2	Dihydrolipoyllysine-residue succinyltransferase component of 2-oxoglutarate dehydrogenase complex, mitochondrial	Dlst
Q9DBT9	Dimethylglycine dehydrogenase, mitochondrial	Dmgdh
P70245	3-beta-hydroxysteroid-Delta(8),Delta(7)-isomerase	Ebp
O35459	Delta(3,5)-Delta(2,4)-dienoyl-CoA isomerase, mitochondrial	Ech1
Q3TLP5	Enoyl-CoA hydratase domain-containing protein 2, mitochondrial	Echdc2
Q8BH95	Enoyl-CoA hydratase, mitochondrial	Echs1
P42125	Enoyl-CoA delta isomerase 1, mitochondrial	Eci1
Q9WUR2	Enoyl-CoA delta isomerase 2, mitochondrial	Eci2
P10126	Elongation factor 1-alpha 1	Eef1a1
G5E8D6		Efemp2
Q9DBM2	Peroxisomal bifunctional enzyme;Enoyl-CoA hydratase/3,2-trans-enoyl-CoA isomerase;3-hydroxyacyl-CoA dehydrogenase	Ehhadh
P34914	Epoxide hydrolase 2	Ephx2
Q99LC5	Electron transfer flavoprotein subunit alpha, mitochondrial	Etfa
Q9DCW4	Electron transfer flavoprotein subunit beta	Etfb
Q921G7	Electron transfer flavoprotein-ubiquinone oxidoreductase, mitochondrial	Etfdh
Q9DCM0	Protein ETHE1, mitochondrial	Ethe1
Q9CR98	Protein FAM136A	Fam136a
P35550	rRNA 2-O-methyltransferase fibrillarin	Fbl
P46656	Adrenodoxin, mitochondrial	Fdx1
Q61578	NADPH:adrenodoxin oxidoreductase, mitochondrial	Fdxr

P97807	Fumarate hydratase, mitochondrial	Fh
P29391	Ferritin light chain 1;Ferritin light chain 2;Ferritin	Ftl1;Ftl2
Q8BHN3-2	Neutral alpha-glucosidase AB	Ganab
O88986	2-amino-3-ketobutyrate coenzyme A ligase, mitochondrial	Gcat
Q60759	Glutaryl-CoA dehydrogenase, mitochondrial	Gcdh
Q91W43	Glycine dehydrogenase [decarboxylating], mitochondrial	Gldc
Q80Y14	Glutaredoxin-related protein 5, mitochondrial	Glrx5
Q571F8	Glutaminase liver isoform, mitochondrial	Gls2
P26443	Glutamate dehydrogenase 1, mitochondrial	Glud1
Q91XE0	Glycine N-acyltransferase	Glyat
E9QAZ2	Ribosomal protein L15;60S ribosomal protein L15	Rpl15
G3UWG1	Cytochrome c, somatic	Cycs
Q5FW57	Glycine N-acyltransferase-like protein	Gm4952
D3YVN7	Elongation factor Tu;Elongation factor Tu, mitochondrial	Tufm
P08752	Guanine nucleotide-binding protein G(i) subunit alpha-2	Gnai2
E9QKR0	Guanine nucleotide-binding protein G(I)/G(S)/G(T) subunit beta-2	Gnb2
P05202	Aspartate aminotransferase, mitochondrial	Got2
Q64521	Glycerol-3-phosphate dehydrogenase, mitochondrial	Gpd2
P11352	Glutathione peroxidase 1	Gpx1
Q99LP6	GrpE protein homolog 1, mitochondrial	Grpel1
Q9DCM2	Glutathione S-transferase kappa 1	Gstk1
P27661	Histone H2A.x	H2afx
Q9QXE0	2-hydroxyacyl-CoA lyase 1	Hacl1
Q61425	Hydroxyacyl-coenzyme A dehydrogenase, mitochondrial	Hadh

Q8BMS1	Trifunctional enzyme subunit alpha, mitochondrial;Long-chain enoyl-CoA hydratase;Long chain 3-hydroxyacyl-CoA dehydrogenase	Hadha
Q99JY0	Trifunctional enzyme subunit beta, mitochondrial;3-ketoacyl-CoA thiolase	Hadhb
Q99L13	3-hydroxyisobutyrate dehydrogenase, mitochondrial	Hibadh
Q8QZS1	3-hydroxyisobutyryl-CoA hydrolase, mitochondrial	Hibch
Q9D0S9	Histidine triad nucleotide-binding protein 2, mitochondrial	Hint2
P43277	Histone H1.3	Hist1h1d
P22752	Histone H2A type 1	Hist1h2ab
Q8CGP2-2	Histone H2B type 1-F/J/L	Hist1h2bf
P68433	Histone H3.1	Hist1h3a
P62806	Histone H4	Hist1h4a
P38060	Hydroxymethylglutaryl-CoA lyase, mitochondrial	Hmgcl
P54869	Hydroxymethylglutaryl-CoA synthase, mitochondrial	Hmgcs2
O88569	Heterogeneous nuclear ribonucleoproteins A2/B1	Hnrnpa2b1
Q9DCU9	Probable 4-hydroxy-2-oxoglutarate aldolase, mitochondrial	Hoga1
P52760	Ribonuclease UK114	Hrsp12
Q99N15	3-hydroxyacyl-CoA dehydrogenase type-2	Hsd17b10
P51660	Peroxisomal multifunctional enzyme type 2;(3R)-hydroxyacyl-CoA dehydrogenase;Enoyl-CoA hydratase 2	Hsd17b4
P50171-2	Estradiol 17-beta-dehydrogenase 8	Hsd17b8;H2-Ke6
P11499	Heat shock protein HSP 90-beta	Hsp90ab1
P08113	Endoplasmin	Hsp90b1
P20029	78 kDa glucose-regulated protein	Hspa5
P63017	Heat shock cognate 71 kDa protein	Hspa8
P38647	Stress-70 protein, mitochondrial	Hspa9
P63038	60 kDa heat shock protein, mitochondrial	Hspd1

Q64433	10 kDa heat shock protein, mitochondrial	Hspe1
Q8BIJ6	Isoleucine--tRNA ligase, mitochondrial	Iars2
P54071	Isocitrate dehydrogenase [NADP], mitochondrial	Idh2
Q9D6R2	Isocitrate dehydrogenase [NAD] subunit alpha, mitochondrial	Idh3a
Q8CAQ8-2	Mitochondrial inner membrane protein	Immt
P85094	Isochorismatase domain-containing protein 2A, mitochondrial	Isoc2a
Q9JHI5	Isovaleryl-CoA dehydrogenase, mitochondrial	Ivd
Q8CC88	Uncharacterized protein KIAA0564 homolog	Kiaa0564
Q9CPY7	Cytosol aminopeptidase	Lap3
Q7TNG8	Probable D-lactate dehydrogenase, mitochondrial	Ldhd
P48678	Prelamin-A/C;Lamin-A/C	Lmna
P14733	Lamin-B1	Lmnb1
F6TFN2	Lmo7	
Q8CGK3	Lon protease homolog, mitochondrial	Lonp1
Q6PB66	Leucine-rich PPR motif-containing protein, mitochondrial	Lrpprc
Q922Q8	Leucine-rich repeat-containing protein 59	Lrrc59
Q64133	Amine oxidase [flavin-containing] A	Maoa
Q8BW75	Amine oxidase [flavin-containing] B	Maob
Q922Q1	MOSC domain-containing protein 2, mitochondrial	Marc2;Mosc2
Q99MR8	Methylcrotonoyl-CoA carboxylase subunit alpha, mitochondrial	Mccc1
Q3ULD5	Methylcrotonoyl-CoA carboxylase beta chain, mitochondrial	Mccc2
P08249	Malate dehydrogenase, mitochondrial	Mdh2
E9QJW0	Microsomal glutathione S-transferase 1	Mgst1
Q3UW66	Sulfurtransferase;3-mercaptopyruvate sulfurtransferase	Mpst
Q791V5	Mitochondrial carrier homolog 2	Mtch2
P00405	Cytochrome c oxidase subunit 2	Mtco2;mt-Co2

P16332	Methylmalonyl-CoA mutase, mitochondrial	Mut
Q8VDD5	Myosin-9	Myh9
Q9WTI7	Unconventional myosin-Ic	Myo1c
E9Q390	Myoferlin	Myof
Q99LC3	NADH dehydrogenase [ubiquinone] 1 alpha subcomplex subunit 10, mitochondrial	Ndufa10
Q9ERS2	NADH dehydrogenase [ubiquinone] 1 alpha subcomplex subunit 13	Ndufa13
Q9CQ75	NADH dehydrogenase [ubiquinone] 1 alpha subcomplex subunit 2	Ndufa2
Q62425	NADH dehydrogenase [ubiquinone] 1 alpha subcomplex subunit 4	Ndufa4
Q9CPP6	NADH dehydrogenase [ubiquinone] 1 alpha subcomplex subunit 5	Ndufa5
Q9CQZ5	NADH dehydrogenase [ubiquinone] 1 alpha subcomplex subunit 6	Ndufa6
Q9DCJ5	NADH dehydrogenase [ubiquinone] 1 alpha subcomplex subunit 8	Ndufa8
Q9DC69	NADH dehydrogenase [ubiquinone] 1 alpha subcomplex subunit 9, mitochondrial	Ndufa9
Q9CQC7	NADH dehydrogenase [ubiquinone] 1 beta subcomplex subunit 4	Ndufb4
Q91VD9	NADH-ubiquinone oxidoreductase 75 kDa subunit, mitochondrial	Ndufs1
Q9DCT2	NADH dehydrogenase [ubiquinone] iron-sulfur protein 3, mitochondrial	Ndufs3
P52503	NADH dehydrogenase [ubiquinone] iron-sulfur protein 6, mitochondrial	Ndufs6
Q91YT0	NADH dehydrogenase [ubiquinone] flavoprotein 1, mitochondrial	Ndufv1
Q9D6J6	NADH dehydrogenase [ubiquinone] flavoprotein 2, mitochondrial	Ndufv2

Q8C6I5	Cysteine desulfurase, mitochondrial	Nfs1
O55125	Protein NipSnap homolog 1	Nipsnap1
Q61941	NAD(P) transhydrogenase, mitochondrial	Nnt
E9Q5C9		Nolc1
Q9D6Z1	Nucleolar protein 56	Nop56
E9Q7G0		Numa1
P29758	Ornithine aminotransferase, mitochondrial	Oat
Q60597	2-oxoglutarate dehydrogenase, mitochondrial	Ogdh
P11725	Ornithine carbamoyltransferase, mitochondrial	Otc
P09103	Protein disulfide-isomerase	P4hb
P60335	Poly(rC)-binding protein 1	Pcbp1
Q91ZA3	Propionyl-CoA carboxylase alpha chain, mitochondrial	Pcca
Q99MN9	Propionyl-CoA carboxylase beta chain, mitochondrial	Pccb
Q8BH04	Phosphoenolpyruvate carboxykinase [GTP], mitochondrial	Pck2
E9QPD7	Pyruvate carboxylase, mitochondrial	Pcx;Pc
P35486	Pyruvate dehydrogenase E1 component subunit alpha, somatic form, mitochondrial	Pdha1
Q9D051	Pyruvate dehydrogenase E1 component subunit beta, mitochondrial	Pdhb
P27773	Protein disulfide-isomerase A3	Pdia3
Q922R8	Protein disulfide-isomerase A6	Pdia6
Q99MZ7	Peroxisomal trans-2-enoyl-CoA reductase	Pecr
O55022	Membrane-associated progesterone receptor component 1	Pgrmc1
P67778	Prohibitin	Phb
O35129	Prohibitin-2	Phb2
P52480	Pyruvate kinase isozymes M1/M2	Pkm2
E9QMZ5	Plectin	Plec
Q91VA6	Polymerase delta-interacting protein 2	Poldip2

P37040	NADPH--cytochrome P450 reductase	Por
Q91VM9	Inorganic pyrophosphatase 2, mitochondrial	Ppa2
P20108	Thioredoxin-dependent peroxide reductase, mitochondrial	Prdx3
P99029	Peroxiredoxin-5, mitochondrial	Prdx5
Q922Q4	Pyrroline-5-carboxylate reductase 2;Pyrroline-5-carboxylate reductase 1, mitochondrial	Pycr2;Pycr1
P61027	Ras-related protein Rab-10	Rab10
P51150	Ras-related protein Rab-7a	Rab7a
Q5XJF6	Ribosomal protein;60S ribosomal protein L10a	Rpl10a
P47963	60S ribosomal protein L13	Rpl13;Rpl13-ps3
P35980	60S ribosomal protein L18	Rpl18
Q9D8E6	60S ribosomal protein L4	Rpl4
P47911	60S ribosomal protein L6	Rpl6
P14148	60S ribosomal protein L7	Rpl7
D3YU93	60S ribosomal protein L7a	Rpl7a-ps3
Q91YQ5	Dolichyl-diphosphooligosaccharide--protein glycosyltransferase subunit 1	Rpn1
Q99PL5	Ribosome-binding protein 1	Rrbp1
Q9EP69	Phosphatidylinositide phosphatase SAC1	Sacm1l
Q8BGH2	Sorting and assembly machinery component 50 homolog	Samm50
Q99LB7	Sarcosine dehydrogenase, mitochondrial	Sardh
P32020	Non-specific lipid-transfer protein	Scp2
Q8K2B3	Succinate dehydrogenase [ubiquinone] flavoprotein subunit, mitochondrial	Sdha
Q9CQA3	Succinate dehydrogenase [ubiquinone] iron-sulfur subunit, mitochondrial	Sdhb
Q8VIJ6	Splicing factor, proline- and glutamine-rich	Sfpq
Q99JR1	Sideroflexin-1	Sfxn1
Q91V61	Sideroflexin-3	Sfxn3

Q9CZN7	Serine hydroxymethyltransferase	Shmt2
Q9QZD8	Mitochondrial dicarboxylate carrier	Slc25a10
Q9QXX4	Calcium-binding mitochondrial carrier protein Aralar2	Slc25a13
Q8VEM8	Phosphate carrier protein, mitochondrial	Slc25a3
P48962	ADP/ATP translocase 1	Slc25a4
P51881	ADP/ATP translocase 2	Slc25a5
Q9D8T7	SRA stem-loop-interacting RNA-binding protein, mitochondrial	Slirp;1810035L 17Rik
Q6P4T2		Snrnp200
P09671	Superoxide dismutase [Mn], mitochondrial	Sod2
E9Q447	Spectrin alpha chain, brain	Spna2;Sptan1
Q62261-2	Spectrin beta chain, brain 1	Sptbn1
Q9R112	Sulfide:quinone oxidoreductase, mitochondrial	Sqrdl
Q8R2K3	Single-stranded DNA-binding protein, mitochondrial	Ssbp1
Q9D8L3	Translocon-associated protein subunit delta	Ssr4
Q99JB2	Stomatin-like protein 2	Stoml2
Q9Z2I9	Succinyl-CoA ligase [ADP-forming] subunit beta, mitochondrial	Sucla2
Q9WUM5	Succinyl-CoA ligase [ADP/GDP-forming] subunit alpha, mitochondrial	Suclg1
Q9Z2I8	Succinyl-CoA ligase [GDP-forming] subunit beta, mitochondrial	Suclg2
Q8R086	Sulfite oxidase, mitochondrial	Suox
Q921I1	Serotransferrin	Tf;Gm20425
P62075	Mitochondrial import inner membrane translocase subunit Tim13	Timm13
Q9D880	Mitochondrial import inner membrane translocase subunit TIM50	Timm50
Q9WVA2	Mitochondrial import inner membrane translocase subunit Tim8 A	Timm8a1

P62077	Mitochondrial import inner membrane translocase subunit Tim8 B	Timm8b
P39447	Tight junction protein ZO-1	Tjp1
Q61029	Lamina-associated polypeptide 2, isoforms beta/delta/epsilon/gamma	Tmpo
E9Q7Q3	Tpm3;Tpm3-rs7	
Q9CQN1	Heat shock protein 75 kDa, mitochondrial	Trap1
P52196	Thiosulfate sulfurtransferase	Tst
P68373	Tubulin alpha-1C chain	Tuba1c
P99024	Tubulin beta-5 chain	Tubb5
P0CG50	Polyubiquitin-C	Ubc
Q63886	UDP-glucuronosyltransferase 1-1	Ugt1a1
P25688	Uricase	Uox
Q9CQB4	Cytochrome b-c1 complex subunit 7	Uqcrb
Q9CZ13	Cytochrome b-c1 complex subunit 1, mitochondrial	Uqcrc1
Q9DB77	Cytochrome b-c1 complex subunit 2, mitochondrial	Uqcrc2
Q9CR68	Cytochrome b-c1 complex subunit Rieske, mitochondrial	Uqcrfs1
P99028	Cytochrome b-c1 complex subunit 6, mitochondrial	Uqcrh
Q9CQ69	Cytochrome b-c1 complex subunit 8	Uqcrq
Q60932	Voltage-dependent anion-selective channel protein 1	Vdac1
Q60930	Voltage-dependent anion-selective channel protein 2	Vdac2
P20152	Vimentin	Vim

Table 6-6: A list of the 305 quantifiable proteins identified in the whole dataset. The proteins were found in two thirds of samples and used for the normalisation of the dataset. Protein ID, Protein Name and the related Gene Name is included as information about the protein.

6.2. R SCRIPTS

6.2.1. GENERATING SLOPES FROM TRIPLICATE AND TOTAL STANDARD DEVIATIONS

Calculating either the triplicate standard deviation of the individual protein or the total standard deviation uses the following r script.

```
calcProteinSD.01 <-  function(protein, triplicate=TRUE){
#  This function calculates the triplicate standard deviation if triplicate = TRUE (default setting) for 60 samples from a dataset.If triplicate is false it randomly orders the samples to generate total standard deviation for a 60 sample dataset.
   SC <-  12
#First 11 columns
   resultVec <-  numeric(0)
   if(triplicate){
      proteinVec <-  1:60
#If triplicate is TRUE ensures the columns are ordered 1-60 in groups of biological replicates    } else {
      proteinVec <-  sample(1:60,60,replace=F)
#This function randomly orders the 60 samples if triplicate is false
   }
   for(mouse in seq(1,60, by=3)){
      RAAT <-  sapply(protein, function(x){as.numeric(x[1])})
      RAAT1 <-  RAAT[sC+proteinVec[mouse]]
      RAAT2 <-  RAAT[sC+proteinVec[mouse]+1]
      RAAT3 <-  RAAT[sC+proteinVec[mouse]+2]
#Standard deviation is calculated if each group has three RAAT values for the protein otherwise no standard deviation for the group is calculated
      if(!is.na(RAAT1)){
         if(!is.na(RAAT2)){
            if(!is.na(RAAT3)){
               sampErr <-  sd(c(RAAT1,RAAT2,RAAT3))
               resultVec <-  append(resultVec, sampErr)
```

```
            }
        }
    }

  }
  proteinTripSD <- mean(resultVec)
#The standard deviations are averaged to obtain one for each protein
  proteinTripSD
}
```

The following script generates a vector of each proteins standard deviaition (either total or triplicate) for all the proteins.

```
makeProtSDVec <- function(data,triplicate){

# This script generates a vector containing the average standard deviation for each protein in the dataset using the calcProteinSD.01 script.
    resultVec <- numeric(0)
    for(i in (c(1:310))){

# In the data each protein is a row and there are 310 proteins, this function produces the standard deviation for each protein.
          a <- calcProteinSD.01(data[i,],triplicate)
          resultVec <- append(resultVec,a)

# The vector is appended for each row so the final vector has 310 values
    }
    resultVec
}
```

The following script generates 1000 iterations of a slope comparison to compare final values.

```
get1000slopes <- function(data){
```

```
# This script generates 1000 values for the slope of the
trendline, if the intercept is zero, when triplicate standard
deviation and total standard deviation are plotted as a
scattergraph.
     print("calculating triplicate SDs")
     protein_tripl <- makeProtSDVec(data, triplicate = TRUE)

# This section generates a vector of the triplicate standard
deviation (samples grouped as biological replicates) for each
protein.
     resultVec <- numeric(0)
     for(i in 1:1000){

# Generates the following section 1000 times
          sprintf("Calculating total SD %d",i)
          protein_total <- makeProtSDVec(data, triplicate =
FALSE)

# This section generates a vector of the total standard
deviation (samples grouped randomly) for each protein. Random
grouping changes in each i iteration
          slope <-
getProtSDVecSlope(protein_tripl,protein_total)

# Generates the slope when the triplicate vector and this i's
total vector is compared.
          resultVec <- append(resultVec, slope)

# Appends the slope vector with the additional slope after each
iteration so the final vector contains 1000 values
     }
     resultVec
}
```

This generates a single slope from a triplicate vector and a random total vector.

```
getProtSDVecSlope <- function(protein_tripl,protein_total){
```

```
#This script finds the slope of the linear regression of a
scattergraph of triplicate standard deviation compared with
total standard deviation when the intercept is zero.
     model <- lm(protein_total ~ 0 + protein_tripl)
     slope <- as.numeric(model[1][1])
     slope
}
```

REFERENCES

Ahmed, S., Passos, J. F., Birket, M. J., Beckmann, T., Brings, S., Peters, H., Birch-Machin, M. A., von Zglinicki, T. and Saretzki, G. (2008) 'Telomerase does not counteract telomere shortening but protects mitochondrial function under oxidative stress', *J Cell Sci*, 121(Pt 7), pp. 1046-53.

Alberts, B., Wilson, J. H. and Hunt, T. (2008) *Molecular biology of the cell*. 5th edn. New York: Garland Science.

Andersen, J. K. (2004) 'Oxidative stress in neurodegeneration: cause or consequence?', *Nat Med*, 10 Suppl, pp. S18-25.

Arike, L. and Peil, L. (2014) 'Spectral counting label-free proteomics', *Methods Mol Biol*, 1156, pp. 213-22.

Ash, C. E. and Merry, B. J. (2011) 'The molecular basis by which dietary restricted feeding reduces mitochondrial reactive oxygen species generation', *Mech Ageing Dev*, 132(1-2), pp. 43-54.

Ashburner, M., Ball, C. A., Blake, J. A., Botstein, D., Butler, H., Cherry, J. M., Davis, A. P., Dolinski, K., Dwight, S. S., Eppig, J. T., Harris, M. A., Hill, D. P., Issel-Tarver, L., Kasarskis, A., Lewis, S., Matese, J. C., Richardson, J. E., Ringwald, M., Rubin, G. M. and Sherlock, G. (2000) 'Gene ontology: tool for the unification of biology. The Gene Ontology Consortium', *Nat Genet*, 25(1), pp. 25-9.

Barja, G. (2002) 'Endogenous oxidative stress: relationship to aging, longevity and caloric restriction', *Ageing Res Rev*, 1, pp. 397-411.

Barja, G. (2004) 'Free radicals and aging', *Trends Neurosci*, 27(10), pp. 595-600.

Beck, V., Jaburek, M., Demina, T., Rupprecht, A., Porter, R. K., Jezek, P. and Pohl, E. E. (2007) 'Polyunsaturated fatty acids activate human uncoupling proteins 1 and 2 in planar lipid bilayers', *FASEB J*, 21(4), pp. 1137-44.

Beckman, K. B. and Ames, B. N. (1998) 'The free radical theory of aging matures', *Physiol Rev*, 78(2), pp. 547-81.

Berg, J. M., Tymoczko, J. L., Stryer, L. and Stryer, L. (2007) *Biochemistry*. 6th edn (1 vols). New York: W.H. Freeman.

Bodnar, A. G., Ouellette, M., Frolkis, M., Holt, S. E., Chiu, C. P., Morin, G. B., Harley, C. B., Shay, J. W., Lichtsteiner, S. and Wright, W. E. (1998) 'Extension of life-span by introduction of telomerase into normal human cells', *Science*, 279(5349), pp. 349-52.

Borras, C., Gambini, J. and Vina, J. (2007) 'Mitochondrial oxidant generation is involved in determining why females live longer than males', *Front Biosci*, 12, pp. 1008-13.

Boveris, A., Oshino, N. and Chance, B. (1972) 'The cellular production of hydrogen peroxide', *Biochem J*, 128(3), pp. 617-30.

Brand, M. D. (2000) 'Uncoupling to survive? The role of mitochondrial inefficiency in ageing', *Exp Gerontol*, 35, pp. 811-820.

Brown, G. C. and Borutaite, V. (2012) 'There is no evidence that mitochondria are the main source of reactive oxygen species in mammalian cells', *Mitochondrion*, 12(1), pp. 1-4.

Cameron, K. M., Golightly, A., Miwa, S., Speakman, J., Boys, R. and von Zglinicki, T. (2011) 'Gross energy metabolism in mice under late onset, short term caloric restriction.', *Mechanisms of ageing and development*, 132, pp. 202-9.

Chang, J., Cornell, J. E., Van Remmen, H., Hakala, K., Ward, W. F. and Richardson, A. (2007) 'Effect of aging and caloric restriction on the mitochondrial proteome', *J Gerontol A Biol Sci Med Sci*, 62(3), pp. 223-34.

Chen, H. and Chan, D. C. (2005) 'Emerging functions of mammalian mitochondrial fusion and fission', *Hum Mol Genet*, 14 Spec No. 2, pp. R283-9.

Chen, Y., Hagopian, K., Bibus, D., Villalba, J. M., Lopez-Lluch, G., Navas, P., Kim, K. and Ramsey, J. J. (2014) 'The influence of dietary lipid composition on skeletal muscle mitochondria from mice following eight months of calorie restriction', *Physiol Res*, 63(1), pp. 57-71.

Chou, J. L., Shenoy, D. V., Thomas, N., Choudhary, P. K., Laferla, F. M., Goodman, S. R. and Breen, G. a. M. (2011) 'Early dysregulation of the mitochondrial proteome in a mouse model of Alzheimer's disease.', *Journal of proteomics*, 74, pp. 466-79.

Clohessy, J. G., Reschke, M. and Pandolfi, P. P. (2012) 'Found in translation of mTOR signaling', *Cell Res*, 22(9), pp. 1315-8.

Colman, R. J., Anderson, R. M., Johnson, S. C., Kastman, E. K., Kosmatka, K. J., Beasley, T. M., Allison, D. B., Cruzen, C., Simmons, H. A., Kemnitz, J. W. and Weindruch, R. (2009) 'Caloric restriction delays disease onset and mortality in rhesus monkeys', *Science*, 325(5937), pp. 201-4.

Coso, S., Harrison, I., Harrison, C. B., Vinh, A., Sobey, C. G., Drummond, G. R., Williams, E. D. and Selemidis, S. (2012) 'NADPH oxidases as regulators of tumor angiogenesis: current and emerging concepts', *Antioxid Redox Signal*, 16(11), pp. 1229-47.

Costa, R. A., Romagna, C. D., Pereira, J. L. and Souza-Pinto, N. C. (2011) 'The role of mitochondrial DNA damage in the citotoxicity of reactive oxygen species', *J Bioenerg Biomembr*, 43(1), pp. 25-9.

Craig, R., Cortens, J. P. and Beavis, R. C. (2004) 'Open source system for analyzing, validating, and storing protein identification data', *J Proteome Res*, 3(6), pp. 1234-42.

Dani, D., Shimokawa, I., Komatsu, T., Higami, Y., Warnken, U., Schokraie, E., Schnolzer, M., Krause, F., Sugawa, M. D. and Dencher, N. A. (2010) 'Modulation of oxidative phosphorylation machinery signifies a prime mode of anti-ageing mechanism of calorie restriction in male rat liver mitochondria', *Biogerontology*, 11(3), pp. 321-34.

Desai, V. G., Weindruch, R., Hart, R. W. and Feuers, R. J. (1996) 'Influences of age and dietary restriction on gastrocnemius electron transport system activities in mice.', *Archives of biochemistry and biophysics*, 333, pp. 145-51.

Dikalov, S. (2011) 'Cross talk between mitochondria and NADPH oxidases', *Free Radic Biol Med*, 51(7), pp. 1289-301.

Dikalov, S., Skatchkov, M., Fink, B. and Bassenge, E. (1997) 'Quantification of superoxide radicals and peroxynitrite in vascular cells using oxidation of sterically hindered hydroxylamines and electron spin resonance', *Nitric Oxide*, 1(5), pp. 423-31.

Dikalov, S. I. and Harrison, D. G. (2014) 'Methods for detection of mitochondrial and cellular reactive oxygen species', *Antioxid Redox Signal*, 20(2), pp. 372-82.

Dkhar, P. and Sharma, R. (2010) 'Effect of dimethylsulphoxide and curcumin on protein carbonyls and reactive oxygen species of cerebral hemispheres of mice as a function of age', *Int J Dev Neurosci*, 28(5), pp. 351-7.

Drew, B. and Leeuwenburgh, C. (2003) 'Method for measuring ATP production in isolated mitochondria: ATP production in brain and liver mitochondria of Fischer-344 rats with age and caloric restriction', *Am J Physiol Regul Integr Comp Physiol*, 285(5), pp. R1259-67.

Drew, B., Phaneuf, S., Dirks, A., Selman, C., Gredilla, R., Lezza, A., Barja, G. and Leeuwenburgh, C. (2003) 'Effects of aging and caloric restriction on mitochondrial energy production in gastrocnemius muscle and heart', *Am J Physiol Regul Integr Comp Physiol*, 284(2), pp. R474-80.

Finkelstein, E., Rosen, G. M. and Rauckman, E. J. (1980) 'Spin trapping of superoxide and hydroxyl radical: practical aspects', *Arch Biochem Biophys*, 200(1), pp. 1-16.

Fok, W. C., Zhang, Y., Salmon, A. B., Bhattacharya, A., Gunda, R., Jones, D., Ward, W., Fisher, K., Richardson, A. and Perez, V. I. (2012) 'Short-Term Treatment With Rapamycin and Dietary Restriction Have Overlapping and Distinctive Effects in Young Mice', *J Gerontol A Biol Sci Med Sci*.

Galley, H. F. (2011) 'Oxidative stress and mitochondrial dysfunction in sepsis', *Br J Anaesth*, 107(1), pp. 57-64.

Geiger, T., Velic, A., Macek, B., Lundberg, E., Kampf, C., Nagaraj, N., Uhlen, M., Cox, J. and Mann, M. (2013) 'Initial quantitative proteomic map of 28 mouse tissues using the SILAC mouse', *Mol Cell Proteomics*, 12(6), pp. 1709-22.

Geiger, T., Wisniewski, J. R., Cox, J., Zanivan, S., Kruger, M., Ishihama, Y. and Mann, M. (2011) 'Use of stable isotope labeling by amino acids in cell culture as a spike-in standard in quantitative proteomics', *Nat Protoc*, 6, pp. 147-157.

Giese, H., Ackermann, J., Heide, H., Bleier, L., Drose, S., Wittig, I., Brandt, U. and Koch, I. (2015) 'NOVA: a software to analyze complexome profiling data', *Bioinformatics*, 31(3), pp. 440-1.

Gonzalez, F. J. (2005) 'Role of cytochromes P450 in chemical toxicity and oxidative stress: studies with CYP2E1', *Mutat Res*, 569(1-2), pp. 101-10.

Gross, E., Sevier, C. S., Heldman, N., Vitu, E., Bentzur, M., Kaiser, C. A., Thorpe, C. and Fass, D. (2006) 'Generating disulfides enzymatically: reaction products and electron

acceptors of the endoplasmic reticulum thiol oxidase Ero1p', *Proc Natl Acad Sci U S A*, 103(2), pp. 299-304.

Haendeler, J., Drose, S., Buchner, N., Jakob, S., Altschmied, J., Goy, C., Spyridopoulos, I., Zeiher, A. M., Brandt, U. and Dimmeler, S. (2009) 'Mitochondrial telomerase reverse transcriptase binds to and protects mitochondrial DNA and function from damage', *Arterioscler Thromb Vasc Biol*, 29(6), pp. 929-35.

Haendeler, J., Hoffmann, J., Diehl, J. F., Vasa, M., Spyridopoulos, I., Zeiher, A. M. and Dimmeler, S. (2004) 'Antioxidants inhibit nuclear export of telomerase reverse transcriptase and delay replicative senescence of endothelial cells', *Circ Res*, 94(6), pp. 768-75.

Haendeler, J., Hoffmann, J., Rahman, S., Zeiher, A. M. and Dimmeler, S. (2003) 'Regulation of telomerase activity and anti-apoptotic function by protein-protein interaction and phosphorylation', *FEBS Lett*, 536(1-3), pp. 180-6.

Hagopian, K., Soo Hoo, R., Lopez-Dominguez, J. A. and Ramsey, J. J. (2013) 'Calorie restriction influences key metabolic enzyme activities and markers of oxidative damage in distinct mouse liver mitochondrial sub-populations', *Life Sci*, 93(24), pp. 941-8.

Haigis, M. C. and Yankner, B. A. (2010) 'The aging stress response', *Mol Cell*, 40(2), pp. 333-44.

Hamon, M. P., Bulteau, A. L. and Friguet, B. (2015) 'Mitochondrial proteases and protein quality control in ageing and longevity', *Ageing Res Rev*.

Hansford, R. G., Hogue, B. A. and Mildaziene, V. (1997) 'Dependence of H2O2 formation by rat heart mitochondria on substrate availability and donor age', *J Bioenerg Biomembr*, 29(1), pp. 89-95.

Harley, C. B., Futcher, A. B. and Greider, C. W. (1990) 'Telomeres shorten during ageing of human fibroblasts', *Nature*, 345(6274), pp. 458-60.

Harman, D. (1956) 'Aging: a theory based on free radical and radiation chemistry', *J Gerontol*, 11(3), pp. 298-300.

Harman, D. (1972) 'The biologic clock: the mitochondria?', *J Am Geriatr Soc*, 20(4), pp. 145-7.

Harper, M. E., Bevilacqua, L., Hagopian, K., Weindruch, R. and Ramsey, J. J. (2004) 'Ageing, oxidative stress, and mitochondrial uncoupling', *Acta Physiol Scand*, 182(4), pp. 321-31.

Harrison, D. E., Strong, R., Sharp, Z. D., Nelson, J. F., Astle, C. M., Flurkey, K., Nadon, N. L., Wilkinson, J. E., Frenkel, K., Carter, C. S., Pahor, M., Javors, M. A., Fernandez, E. and Miller, R. A. (2009) 'Rapamycin fed late in life extends lifespan in genetically heterogeneous mice', *Nature*, 460(7253), pp. 392-5.

Heide, H., Bleier, L., Steger, M., Ackermann, J., Drose, S., Schwamb, B., Zornig, M., Reichert, A. S., Koch, I., Wittig, I. and Brandt, U. (2012) 'Complexome profiling identifies

TMEM126B as a component of the mitochondrial complex I assembly complex', *Cell Metab*, 16(4), pp. 538-49.

Hill, S. and Van Remmen, H. (2014) 'Mitochondrial stress signaling in longevity: a new role for mitochondrial function in aging', *Redox Biol*, 2, pp. 936-44.

Hornig-Do, H. T., Gunther, G., Bust, M., Lehnartz, P., Bosio, A. and Wiesner, R. J. (2009) 'Isolation of functional pure mitochondria by superparamagnetic microbeads', *Anal Biochem*, 389(1), pp. 1-5.

Huang, D. W., Sherman, B. T., Tan, Q., Collins, J. R., Alvord, W. G., Roayaei, J., Stephens, R., Baseler, M. W., Lane, H. C. and Lempicki, R. A. (2007a) 'The DAVID Gene Functional Classification Tool: a novel biological module-centric algorithm to functionally analyze large gene lists', *Genome Biol*, 8(9), p. R183.

Huang, D. W., Sherman, B. T., Tan, Q., Kir, J., Liu, D., Bryant, D., Guo, Y., Stephens, R., Baseler, M. W., Lane, H. C. and Lempicki, R. A. (2007b) 'DAVID Bioinformatics Resources: expanded annotation database and novel algorithms to better extract biology from large gene lists', *Nucleic Acids Res*, 35(Web Server issue), pp. W169-75.

Huang, K. Y., Filarsky, M., Padula, M. P., Raftery, M. J., Herbert, B. R. and Wilkins, M. R. (2009) 'Micropreparative fractionation of the complexome by blue native continuous elution electrophoresis', *Proteomics*, 9(9), pp. 2494-502.

Hutter, E., Renner, K., Pfister, G., Stockl, P., Jansen-Durr, P. and Gnaiger, E. (2004) 'Senescence-associated changes in respiration and oxidative phosphorylation in primary human fibroblasts', *Biochem J*, 380(Pt 3), pp. 919-28.

Kaeberlein, M. and Kennedy, B. K. (2009) 'Ageing: A midlife longevity drug?', *Nature*, 460(7253), pp. 331-2.

Kim, H. R., Kim, Y. J., Kim, H. J., Kim, S. K. and Lee, J. H. (2002) 'Telomere length changes in colorectal cancers and polyps', *J Korean Med Sci*, 17(3), pp. 360-5.

Kim Sh, S. H., Kaminker, P. and Campisi, J. (2002) 'Telomeres, aging and cancer: in search of a happy ending', *Oncogene*, 21(4), pp. 503-11.

Kowaltowski, A. J., de Souza-Pinto, N. C., Castilho, R. F. and Vercesi, A. E. (2009) 'Mitochondria and reactive oxygen species', *Free Radic Biol Med*, 47(4), pp. 333-43.

Kuznetsov, A. V., Troppmair, J., Sucher, R., Hermann, M., Saks, V. and Margreiter, R. (2006) 'Mitochondrial subpopulations and heterogeneity revealed by confocal imaging: possible physiological role?', *Biochim Biophys Acta*, 1757(5-6), pp. 686-91.

Lambeth, J. D. (2004) 'NOX enzymes and the biology of reactive oxygen', *Nat Rev Immunol*, 4(3), pp. 181-9.

Lanni, A., Moreno, M., Lombardi, A. and Goglia, F. (1996) 'Biochemical and functional differences in rat liver mitochondrial subpopulations obtained at different gravitational forces', *Int J Biochem Cell Biol*, 28(3), pp. 337-43.

Lass, A., Sohal, B. H., Weindruch, R., Forster, M. J. and Sohal, R. S. (1998) 'Caloric restriction prevents age-associated accrual of oxidative damage to mouse skeletal muscle mitochondria', *Free Radic Biol Med*, 25(9), pp. 1089-97.

Lee, S., Van Remmen, H. and Csete, M. (2009) 'Sod2 overexpression preserves myoblast mitochondrial mass and function, but not muscle mass with aging.', *Aging cell*, 8, pp. 296-310.

Lopez-Torres, M., Gredilla, R., Sanz, A. and Barja, G. (2002) 'Influence of aging and long-term caloric restriction on oxygen radical generation and oxidative DNA damage in rat liver mitochondria', *Free Radic Biol Med*, 32, pp. 882-889.

Ma, X. M. and Blenis, J. (2009) 'Molecular mechanisms of mTOR-mediated translational control', *Nat Rev Mol Cell Biol*, 10(5), pp. 307-18.

Mansouri, A., Muller, F. L., Liu, Y., Ng, R., Faulkner, J., Hamilton, M., Richardson, A., Huang, T.-T., Epstein, C. J. and Van Remmen, H. (2006) 'Alterations in mitochondrial function, hydrogen peroxide release and oxidative damage in mouse hind-limb skeletal muscle during aging.', *Mechanisms of ageing and development*, 127, pp. 298-306.

Mari, M. and Cederbaum, A. I. (2000) 'CYP2E1 overexpression in HepG2 cells induces glutathione synthesis by transcriptional activation of gamma-glutamylcysteine synthetase', *J Biol Chem*, 275(20), pp. 15563-71.

Massart, D. L. (1997) '[Medical and pharmaceutical applications of principle component analysis]', *Verh K Acad Geneeskd Belg*, 59(4), pp. 287-325.

Mates, J. M., Perez-Gomez, C. and Nunez de Castro, I. (1999) 'Antioxidant enzymes and human diseases', *Clin Biochem*, 32(8), pp. 595-603.

Mavelli, I., Rigo, A., Federico, R., Ciriolo, M. R. and Rotilio, G. (1982) 'Superoxide dismutase, glutathione peroxidase and catalase in developing rat brain', *Biochem J*, 204(2), pp. 535-40.

McArdle, A., Pattwell, D., Vasilaki, A., Griffiths, R. D. and Jackson, M. J. (2001) 'Contractile activity-induced oxidative stress: cellular origin and adaptive responses', *Am J Physiol Cell Physiol*, 280(3), pp. C621-7.

McArdle, A., Vasilaki, A. and Jackson, M. (2002) 'Exercise and skeletal muscle ageing: cellular and molecular mechanisms', *Ageing Res Rev*, 1(1), pp. 79-93.

McBride, H. M., Neuspiel, M. and Wasiak, S. (2006) 'Mitochondria: more than just a powerhouse', *Curr Biol*, 16(14), pp. R551-60.

McCord, J. M. and Fridovich, I. (1969a) 'Superoxide dismutase. An enzymic function for erythrocuprein (hemocuprein)', *J Biol Chem*, 244(22), pp. 6049-55.

McCord, J. M. and Fridovich, I. (1969b) 'The utility of superoxide dismutase in studying free radical reactions. I. Radicals generated by the interaction of sulfite, dimethyl sulfoxide, and oxygen', *J Biol Chem*, 244(22), pp. 6056-63.

Miller, R. A., Harrison, D. E., Astle, C. M., Baur, J. A., Boyd, A. R., de Cabo, R., Fernandez, E., Flurkey, K., Javors, M. A., Nelson, J. F., Orihuela, C. J., Pletcher, S., Sharp,

Z. D., Sinclair, D., Starnes, J. W., Wilkinson, J. E., Nadon, N. L. and Strong, R. (2011) 'Rapamycin, but not resveratrol or simvastatin, extends life span of genetically heterogeneous mice', *J Gerontol A Biol Sci Med Sci*, 66(2), pp. 191-201.

Miwa, S. and Brand, M. D. (2003) 'Mitochondrial matrix reactive oxygen species production is very sensitive to mild uncoupling', *Biochem Soc Trans*, 31(Pt 6), pp. 1300-1.

Miwa, S. and Brand, M. D. (2005) 'The topology of superoxide production by complex III and glycerol 3-phosphate dehydrogenase in Drosophila mitochondria', *Biochim Biophys Acta*, 1709(3), pp. 214-9.

Miwa, S., Jow, H., Baty, K., Johnson, A., Czapiewski, R., Saretzki, G., Treumann, A. and von Zglinicki, T. (2014) 'Low abundance of the matrix arm of complex I in mitochondria predicts longevity in mice', *Nat Commun*, 5, p. 3837.

Miwa, S., Lawless, C. and von Zglinicki, T. (2008) 'Mitochondrial turnover in liver is fast in vivo and is accelerated by dietary restriction: application of a simple dynamic model', *Aging Cell*, 7(6), pp. 920-3.

Mueller, S., Weber, A., Fritz, R., Mutze, S., Rost, D., Walczak, H., Volkl, A. and Stremmel, W. (2002) 'Sensitive and real-time determination of H2O2 release from intact peroxisomes', *Biochem J*, 363(Pt 3), pp. 483-91.

Muller, F. L., Liu, Y. and Van Remmen, H. (2004) 'Complex III releases superoxide to both sides of the inner mitochondrial membrane', *J Biol Chem*, 279(47), pp. 49064-73.

Murphy, M. P. (2009) 'How mitochondria produce reactive oxygen species', *Biochem J*, 417(1), pp. 1-13.

Okuda, K., Bardeguez, A., Gardner, J. P., Rodriguez, P., Ganesh, V., Kimura, M., Skurnick, J., Awad, G. and Aviv, A. (2002) 'Telomere length in the newborn', *Pediatr Res*, 52(3), pp. 377-81.

Ong, S. E., Blagoev, B., Kratchmarova, I., Kristensen, D. B., Steen, H., Pandey, A. and Mann, M. (2002) 'Stable isotope labeling by amino acids in cell culture, SILAC, as a simple and accurate approach to expression proteomics', *Mol Cell Proteomics*, 1(5), pp. 376-86.

Pagliarini, D. J., Calvo, S. E., Chang, B., Sheth, S. A., Vafai, S. B., Ong, S. E., Walford, G. A., Sugiana, C., Boneh, A., Chen, W. K., Hill, D. E., Vidal, M., Evans, J. G., Thorburn, D. R., Carr, S. A. and Mootha, V. K. (2008) 'A mitochondrial protein compendium elucidates complex I disease biology', *Cell*, 134(1), pp. 112-23.

Passos, J. F., Saretzki, G., Ahmed, S., Nelson, G., Richter, T., Peters, H., Wappler, I., Birket, M. J., Harold, G., Schaeuble, K., Birch-Machin, M. A., Kirkwood, T. B. and von Zglinicki, T. (2007a) 'Mitochondrial dysfunction accounts for the stochastic heterogeneity in telomere-dependent senescence', *PLoS Biol*, 5(5), p. e110.

Passos, J. F., Saretzki, G. and von Zglinicki, T. (2007b) 'DNA damage in telomeres and mitochondria during cellular senescence: is there a connection?', *Nucleic Acids Res*, 35(22), pp. 7505-13.

Porter, R. K. and Brand, M. D. (1995) 'Mitochondrial proton conductance and H+/O ratio are independent of electron transport rate in isolated hepatocytes', *Biochem J*, 310 (Pt 2), pp. 379-82.

Price, J. C., Khambatta, C. F., Li, K. W., Bruss, M. D., Shankaran, M., Dalidd, M., Floreani, N. A., Roberts, L. S., Turner, S. M., Holmes, W. E. and Hellerstein, M. K. (2012) 'The effect of long term calorie restriction on in vivo hepatic proteostatis: a novel combination of dynamic and quantitative proteomics', *Mol Cell Proteomics*, 11(12), pp. 1801-14.

Quinlan, C. L., Orr, A. L., Perevoshchikova, I. V., Treberg, J. R., Ackrell, B. A. and Brand, M. D. (2012) 'Mitochondrial complex II can generate reactive oxygen species at high rates in both the forward and reverse reactions', *J Biol Chem*, 287(32), pp. 27255-64.

Reinders, J. and Sickmann, A. (2009) *Proteomics : methods and protocols*. Dordrecht [etc.]: Humana Press.

Ryazanov, A. G. and Nefsky, B. S. (2002) 'Protein turnover plays a key role in aging', *Mech Ageing Dev*, 123, pp. 207-213.

Santos, J. H., Meyer, J. N., Skorvaga, M., Annab, L. A. and Van Houten, B. (2004) 'Mitochondrial hTERT exacerbates free-radical-mediated mtDNA damage', *Aging Cell*, 3(6), pp. 399-411.

Sanz, A., Caro, P. and Barja, G. (2004) 'Protein restriction without strong caloric restriction decreases mitochondrial oxygen radical production and oxidative DNA damage in rat liver', *J Bioenerg Biomembr*, 36(6), pp. 545-52.

Schriner, S. E., Linford, N. J., Martin, G. M., Treuting, P., Ogburn, C. E., Emond, M., Coskun, P. E., Ladiges, W., Wolf, N., Van Remmen, H., Wallace, D. C. and Rabinovitch, P. S. (2005) 'Extension of murine life span by overexpression of catalase targeted to mitochondria', *Science*, 308(5730), pp. 1909-11.

Shin, Y. J., Cho, D. Y., Chung, T. Y., Han, S. B., Hyon, J. Y. and Wee, W. R. (2011) 'Rapamycin reduces reactive oxygen species in cultured human corneal endothelial cells', *Curr Eye Res*, 36(12), pp. 1116-22.

Shukla, V., Mishra, S. K. and Pant, H. C. (2011) 'Oxidative stress in neurodegeneration', *Adv Pharmacol Sci*, 2011, p. 572634.

Singhapol, C., Pal, D., Czapiewski, R., Porika, M., Nelson, G. and Saretzki, G. C. (2013) 'Mitochondrial telomerase protects cancer cells from nuclear DNA damage and apoptosis', *PLoS One*, 8(1), p. e52989.

Smith, A. C., Blackshaw, J. A. and Robinson, A. J. (2012) 'MitoMiner: a data warehouse for mitochondrial proteomics data', *Nucleic Acids Res*, 40(Database issue), pp. D1160-7.

Smith, A. C. and Robinson, A. J. (2009) 'MitoMiner, an integrated database for the storage and analysis of mitochondrial proteomics data', *Mol Cell Proteomics*, 8(6), pp. 1324-37.

Sodre, F. L., Paim, B. A., Urban, A., Vercesi, A. E. and Faria, E. C. (2011) 'Reduction in generation of reactive oxygen species and endothelial dysfunction during postprandial state', *Nutr Metab Cardiovasc Dis*, 21(10), pp. 800-7.

Sohal, R. S., Ku, H. H., Agarwal, S., Forster, M. J. and Lal, H. (1994) 'Oxidative damage, mitochondrial oxidant generation and antioxidant defenses during aging and in response to food restriction in the mouse', *Mech Ageing Dev*, 74(1-2), pp. 121-33.

Sohal, R. S. and Weindruch, R. (1996) 'Oxidative stress, caloric restriction, and aging', *Science*, 273, pp. 59-63.

Speakman, J. R., Talbot, D. A., Selman, C., Snart, S., McLaren, J. S., Redman, P., Krol, E., Jackson, D. M., Johnson, M. S. and Brand, M. D. (2004) 'Uncoupled and surviving: individual mice with high metabolism have greater mitochondrial uncoupling and live longer', *Aging Cell*, 3(3), pp. 87-95.

Spilsbury, A., Miwa, S., Attems, J. and Saretzki, G. (2015) 'The Role of Telomerase Protein TERT in Alzheimer's Disease and in Tau-Related Pathology In Vitro', *J Neurosci*, 35(4), pp. 1659-74.

St-Pierre, J., Buckingham, J. A., Roebuck, S. J. and Brand, M. D. (2002) 'Topology of superoxide production from different sites in the mitochondrial electron transport chain', *J Biol Chem*, 277(47), pp. 44784-90.

Starkov, A. A. (2008) 'The role of mitochondria in reactive oxygen species metabolism and signaling', *Ann N Y Acad Sci*, 1147, pp. 37-52.

Starkov, A. A., Fiskum, G., Chinopoulos, C., Lorenzo, B. J., Browne, S. E., Patel, M. S. and Beal, M. F. (2004) 'Mitochondrial alpha-ketoglutarate dehydrogenase complex generates reactive oxygen species', *J Neurosci*, 24(36), pp. 7779-88.

Steen, H. and Mann, M. (2004) 'The ABC's (and XYZ's) of peptide sequencing', *Nat Rev Mol Cell Biol*, 5(9), pp. 699-711.

Subramaniam, S. R., Vergnes, L., Franich, N. R., Reue, K. and Chesselet, M. F. (2014) 'Region specific mitochondrial impairment in mice with widespread overexpression of alpha-synuclein', *Neurobiol Dis*, 70, pp. 204-13.

Suh, D., Oh, Y. K., Ahn, B., Hur, M. W., Kim, H. J., Lee, M. H., Joo, H. S. and Auh, C. (2002) 'Comparative binding of antitumor drugs to DNA containing the telomere repeat sequence', *Exp Mol Med*, 34(5), pp. 326-31.

Tahara, E. B., Navarete, F. D. and Kowaltowski, A. J. (2009) 'Tissue-, substrate-, and site-specific characteristics of mitochondrial reactive oxygen species generation', *Free Radic Biol Med*, 46, pp. 1283-1297.

The UniProt, C. (2014) 'UniProt: a hub for protein information', *Nucleic Acids Res*.

Thierbach, G. and Reichenbach, H. (1981a) 'Myxothiazol, a new antibiotic interfering with respiration', *Antimicrob Agents Chemother*, 19(4), pp. 504-7.

Thierbach, G. and Reichenbach, H. (1981b) 'Myxothiazol, a new inhibitor of the cytochrome b-c1 segment of th respiratory chain', *Biochim Biophys Acta*, 638(2), pp. 282-9.

Thompson, A., Schafer, J., Kuhn, K., Kienle, S., Schwarz, J., Schmidt, G., Neumann, T., Johnstone, R., Mohammed, A. K. and Hamon, C. (2003) 'Tandem mass tags: a novel quantification strategy for comparative analysis of complex protein mixtures by MS/MS', *Anal Chem*, 75(8), pp. 1895-904.

Thomson, A. W., Turnquist, H. R. and Raimondi, G. (2009) 'Immunoregulatory functions of mTOR inhibition', *Nat Rev Immunol*, 9(5), pp. 324-37.

Towne, V., Will, M., Oswald, B. and Zhao, Q. (2004) 'Complexities in horseradish peroxidase-catalyzed oxidation of dihydroxyphenoxazine derivatives: appropriate ranges for pH values and hydrogen peroxide concentrations in quantitative analysis', *Anal Biochem*, 334(2), pp. 290-6.

Trachootham, D., Alexandre, J. and Huang, P. (2009) 'Targeting cancer cells by ROS-mediated mechanisms: a radical therapeutic approach?', *Nat Rev Drug Discov*, 8(7), pp. 579-91.

Treberg, J. R., Quinlan, C. L. and Brand, M. D. (2011) 'Evidence for two sites of superoxide production by mitochondrial NADH-ubiquinone oxidoreductase (complex I).', *The Journal of biological chemistry*, 286, pp. 27103-10.

Tretter, L. and Adam-Vizi, V. (2005) 'Alpha-ketoglutarate dehydrogenase: a target and generator of oxidative stress', *Philos Trans R Soc Lond B Biol Sci*, 360(1464), pp. 2335-45.

Tunon, M. J., Sanchez-Campos, S., Gutierrez, B., Culebras, J. M. and Gonzalez-Gallego, J. (2003) 'Effects of FK506 and rapamycin on generation of reactive oxygen species, nitric oxide production and nuclear factor kappa B activation in rat hepatocytes', *Biochem Pharmacol*, 66(3), pp. 439-45.

UniProt, C. (2014) 'Activities at the Universal Protein Resource (UniProt)', *Nucleic Acids Res*, 42(Database issue), pp. D191-8.

Vendelbo, M. H. and Nair, K. S. (2011) 'Mitochondrial longevity pathways', *Biochim Biophys Acta*, 1813(4), pp. 634-44.

Vizcaino, J. A., Cote, R. G., Csordas, A., Dianes, J. A., Fabregat, A., Foster, J. M., Griss, J., Alpi, E., Birim, M., Contell, J., O'Kelly, G., Schoenegger, A., Ovelleiro, D., Perez-Riverol, Y., Reisinger, F., Rios, D., Wang, R. and Hermjakob, H. (2013) 'The PRoteomics IDEntifications (PRIDE) database and associated tools: status in 2013', *Nucleic Acids Res*, 41(Database issue), pp. D1063-9.

Votyakova, T. V. and Reynolds, I. J. (2004) 'Detection of hydrogen peroxide with Amplex Red: interference by NADH and reduced glutathione auto-oxidation', *Arch Biochem Biophys*, 431(1), pp. 138-44.

Weigle, D. S., Selfridge, L. E., Schwartz, M. W., Seeley, R. J., Cummings, D. E., Havel, P. J., Kuijper, J. L. and BeltrandelRio, H. (1998) 'Elevated free fatty acids induce

uncoupling protein 3 expression in muscle: a potential explanation for the effect of fasting', *Diabetes*, 47(2), pp. 298-302.

Wessels, H. J., Vogel, R. O., Lightowlers, R. N., Spelbrink, J. N., Rodenburg, R. J., van den Heuvel, L. P., van Gool, A. J., Gloerich, J., Smeitink, J. A. and Nijtmans, L. G. (2013) 'Analysis of 953 human proteins from a mitochondrial HEK293 fraction by complexome profiling', *PLoS One*, 8(7), p. e68340.

Wilkinson, J. E., Burmeister, L., Brooks, S. V., Chan, C.-C., Friedline, S., Harrison, D. E., Hejtmancik, J. F., Nadon, N., Strong, R., Wood, L. K., Woodward, M. a. and Miller, R. a. (2012) 'Rapamycin slows aging in mice.', *Aging cell*, 11, pp. 675-82.

Zhou, M., Diwu, Z., Panchuk-Voloshina, N. and Haugland, R. P. (1997) 'A stable nonfluorescent derivative of resorufin for the fluorometric determination of trace hydrogen peroxide: applications in detecting the activity of phagocyte NADPH oxidase and other oxidases', *Anal Biochem*, 253(2), pp. 162-8.